

ABSTRACT

Title of Document: PERFORMANCE ENHANCEMENT OF HEAT EXCHANGER COOLERS WITH EVAPORATIVE COOLING

Sahil Popli, 2014

Directed By: Professor Reinhard Radermacher,
Department of Mechanical Engineering

Air or water cooled heat exchangers (HX) are typically utilized as condensers or coolers for air-conditioning, refrigeration or process cooling applications in both commercial and industrial sector. However, air cooled heat exchanger performance degrades considerably with rise in ambient air temperature and water cooled coolers require considerable pumping power, a cooling tower and may consume a significant amount of water which may come from fresh water sources. Evaporative cooling offers a unique solution to this problem, where a small amount of wetting water evaporates on HX surface to boost performance in high ambient air temperature conditions.

In this study, several evaporative cooling technologies were applied to three wavy-fin HXs to quantify capacity enhancement ratio (CER) and air-side pressure drop penalty ratio ($PR_{\Delta Pa}$) compared to respective dry case baseline values. Effect of varying wetting water flow rate, air velocity, fin spacing, hydrophilic coatings, spray orientation and inlet air temperature and relative humidity was investigated on hybrid heat exchanger performance. Several new performance comparison parameters were defined to compare different evaporative cooling approaches.

Deluge cooling achieved overall highest CER but at a $PR_{\Delta Pa}$ that was similar in magnitude to the CER. This limitation was found to be inherent to the nature of wetting water distribution method itself. Although front spray cooling tests indicated $PR_{\Delta Pa} \sim 1$, front spray evaporative cooling technology was found to have up to 23-75 % lower CER at 60-100% lower $PR_{\Delta Pa}$ compared to deluge cooling. In order to understand the wetting behavior a novel visualization method was proposed and implemented, which consisted of borescope assisted flow mapping of water distribution within the HX core as a function of air velocities and wetting water flow rates. It was found that up to 85% of HX volume remained dry during front spray cooling which accounted for lower capacity enhancement and deluge cooling forms non-uniform and thick water film which causes bridging and increased $PR_{\Delta Pa}$. A larger component level testing with HX size similar to commercial units allowed to identify constraints of different evaporative cooling methods, which would not be possible if tests were performed at a smaller segment or fin level.

A novel spray cooling technology utilizing internal jet spray cooling within HX volume was both proposed and implemented and a provisional patent # 61/782,825 was obtained. Compared to front spray cooling at a given spray rate, internal spray cooling could either achieve up to 35% higher HX cooler capacity, or obtain same HX cooler capacity at approximately three times lower air-side pressure drop. Alternatively, at same air-side pressure drop wetting water savings of up to 68-97% are achieved. Internal spraying combines advantages of conventional technologies and overcomes the drawbacks, by getting CER of approx. 3.8, without film carryover and at $PR_{\Delta Pa}=1$, while getting maximum wetting uniformity. Intermittent cooling combined with internal spraying could reduce water consumption as evaporative cooling sustains though the brief period when spray is

turned off. Thus, potential for significant energy and water savings, targeted cooling, and retrofit design offers significant commercialization opportunity for future hybrid evaporative coolers. Discussions are underway for the inclusion of this technology into product line up of a leading HX manufacturing company. .

PERFORMANCE ENHANCEMENT OF HEAT EXCHANGER COOLERS WITH
EVAPORATIVE COOLING

By

Sahil Popli

Dissertation submitted to the Faculty of the Graduate School of the
University of Maryland, College Park, in partial fulfillment
of the requirements for the degree of
Doctor of Philosophy
2014

Advisory Committee:

Professor Reinhard Radermacher, Chair

Research Professor Yunho Hwang

Professor Jungho Kim

Professor Marino DiMarzo

Associate Professor Peter B. Sunderland (Dean's representative)

© Copyright by

Sahil Popli
2014

Dedicated to my parents and my adorable niece Bani.

Acknowledgements

My journey in CEEE started with an online course I was fortunate enough to take under Professor Reinhard Radermacher in Spring 2008. He introduced me to the world of energy system and sparked an interest in research which culminated in admission to the PhD program at University of Maryland. In addition to financially supporting my work Prof. Radermacher has been a constant source of inspiration through his passion for work and lateral approach to problem solving.

I am very thankful to my immediate advisor Prof. Yunho Hwang for his continued support as my immediate advisor. I also am also grateful to the committee members Prof. Jungho Kim, Prof. Marino diMarzo and Prof. Peter Sunderland for serving on my dissertation committee and providing valuable comments which helped improve this dissertation.

A very special thanks to Jan Muehlbauer, who I always felt was more of a colleague and friend rather than my lab manager. He is eager to teach and emphasizes on learning best lab practices. Many thanks also to Vikrant Aute for his guidance on the plethora of topics we have discussed.

I am very thankful to Guntner for funding a portion of this work and to the intern students Michael, Ulrich and Franz who helped build/improve my test setup.

My colleagues, Magnus Eisele, Daniel Leighton and Ali were kind enough to share their knowledge in the lab, and Hang Tao and Long were prompt in helping out with CEEE's software packages. Countless hours have been spent learning from each other's projects through discussions with my lab mates especially, Daniel Spencer, Daniel Bacellar, Bracha, Viren, SuXin and Mangie. Friends outside CEEE who have provided their generous support include Ravi, Heather and Camli. I also want to express my appreciation for my girlfriend Emily Chimiak who supported me immensely in the critical thesis writing and re-writing phase.

My cousin Rajnesh, his wife Rashi and my adorable niece Bani, deserve a special mention for their loving support especially through a particularly tough time. They have been my home away from home in New York. Finally I would like to thank my parents and brother who have been always encouraging and patient during my graduate studies.

Table of Contents

Acknowledgements	iii
Table of Contents	iv
List of Tables.....	viii
List of Figures	xi
Nomenclature	xvii
Chapter 1 Need for hybrid cooling and literature review	1
1.1 Introduction	1
1.2 Methods of condenser cooling	2
1.3 Need for hybrid evaporative cooling	8
1.4 Thermodynamics of evaporative cooling	10
1.5 Evaporatively cooled heat exchangers: Market overview.....	14
1.6 Literature review: Overview of experimental studies	17
1.7 Summary of literature review and research gaps	31
1.8 Research objectives	35
1.9 Dissertation outline	36
Chapter 2 Experimental test facility	38
2.1 Introduction	38
2.2 Air side loop	40
2.2.1 Air-side instrumentation.....	41
2.2.2 Air nozzle sizing.....	43
2.2.3 Axial fan sizing	44
2.2.4 Air mixer and settling means.....	45
2.3 Process fluid loop	46
2.4 Wetting water loop	47
2.5 Heat pump loop	52
2.6 Measuring instrumentation and equipment sizing	54
2.6.1 Process fluid and wetting water-side measuring instrumentation	55

2.7 Test heat exchanger geometry and test matrix	56
2.8 Data acquisition system.....	60
2.9 Uncertainty analysis	64
2.10 Data reduction	65
Chapter 3 Experimental results: Dry cooling	
3.1 Introduction	68
3.2 Effect of hydrophilic coating	68
3.3 Effect of fin spacing	72
3.4 Effect of inclination angle	74
3.5 Summary	81
Chapter 4 Experimental results: Deluge cooling	83
4.1 Introduction	83
4.2 Wetting water distributor design	83
4.3 Performance comparison of deluge and air cooling.....	85
4.4 Effect of hydrophilic coating.....	90
4.5 Effect of fin spacing	92
4.6 Effect of flow-configuration.....	94
4.7 Visualization of deluge wetting water distribution	96
4.8 Summary	99
Chapter 5 Experimental results: Spray cooling	101
5.1 Introduction	101
5.2 Spray nozzle selection.....	101
5.3 Front spray cooling.....	109
5.3.1 Effect of fin spacing	115
5.3.2 Effect of hydrophilic coating.....	117
5.3.3 Effect of ambient air temperature.....	118
5.4 Effect of spray configuration.....	122
5.5 Performance comparison of spray and deluge cooling	129

5.6 Summary	132
5.7 Spray cooling capacity enhancement improvement constraints.....	133
Chapter 6 Internal spray cooling technology development.....	136
6.1 Introduction and problem definition	136
6.2 Technology development process	137
6.3 Comparison of novel and conventional evaporative cooling technologies	143
6.3.1 Internal spray cooling - 2 spray tubes	143
6.3.2 Internal spray cooling - 5 spray tubes	146
6.4 Summary	152
Chapter 7 Wetting water flow visualization	154
7.1 Conventional visualization.....	154
7.2 Need for better visualization method	155
7.3 Novel visualization method.....	156
7.3.1 Removal of bottom air flow guide plate.....	156
7.3.2 Partitioned water collection tray.....	157
7.3.3 Borescope assisted visualization	158
7.4 Results and discussion.....	161
7.5 Summary	172
Chapter 8 Conclusions	174
8.1 Dry case HX performance.....	174
8.2 Deluge evaporative cooling.....	175
8.3 Front spray evaporative cooling.....	176
8.4 Internal jet spray evaporative cooling	177
8.5 Enhanced air-side visualization.....	179
Chapter 9 List of contributions and future work.....	182
9.1 Major contributions	182

9.2 List publications	184
9.3 Future work	185
Appendix 1-Internal jet spray cooling 2-spray tubes	188
Appendix 2-Internal jet spray cooling 5-spray tubes	192
Appendix 3-Review of simulation/modeling studies on direct evaporative cooling of HXs.....	197
References	201
Glossary of terminology.....	210

List of Tables

Table 1.1	Overview of commercially available evaporatively cooled condenser/coolers.	14
Table 1.2	Summary of experimental studies on evaporative cooling of finned heat exchanger coils utilized as condensers or fluid coolers.	18
Table 1.3	Major findings of experimental studies on evaporative cooling of finned heat exchanger coils utilized as condensers or fluid coolers.	21
Table 1.4	Breakup of published experimental studies on wetted heat exchangers based on fin geometry.	25
Table 1.5	Major findings of experimental studies on air cooled HX coils utilized as condensers or fluid coolers where air is evaporatively precooled.	27
Table 1.6	Overview of simulation/modeling studies on direct evaporative cooling of heat exchangers.....	29
Table 2.1	Main sources of air-side pressure drop and their expected contribution to total ΔP_{duct}	44
Table 2.2	Water quality parameters before and after reverse osmosis (RO) treatment.	49
Table 2.3	Systematic errors of measuring instruments.	54
Table 2.4	Geometric specifications of herringbone wavy-fin HXs.	56
Table 2.5	Experimental test matrix for three wavy-fin RTHXs.	59
Table 2.6	Air, refrigerant and wetting water parameters for testing wavy-fin RTHXs.	60
Table 2.7	Minimum and maximum total uncertainty in experimental measurement of key calculated variables.	65
Table 3.1	Performance of uncoated wavy-fin heat exchangers set at 20° from vertical in dry cooling conditions at approximately $T_{a,in}=28^{\circ}\text{C}$, $\text{RH}_{a,in} = 45\%$ and $\omega_{a,in}= 0.0106 \text{ kg}_w/\text{kg}_a$	69
Table 3.2	Performance of three wavy-fin HXs set at 20° from vertical in dry cooling conditions at $T_{a,in} =37^{\circ}\text{C}$	70
Table 3.3	Test-matrix for studying effect of HX angle of inclination on heat transfer rate.	74
Table 4.1	Wetting water distributor designs considered for this Study along with their advantages and disadvantages.	84
Table 4.2	Test summary for deluge cooled uncoated wavy fin RTHX with 2.4 mm fin spacing at approximately $T_{a,in}= 28^{\circ}\text{C}$, $\text{RH}_{a,in} = 45\%$ and $\omega_{a,in}= 0.0106 \text{ kg}_w/\text{kg}_a$	86
Table 4.3	Test summary for deluge cooled hydrophilic coated wavy fin RTHX with 2.4 mm fin spacing at approximately $T_{a,in}= 28^{\circ}\text{C}$, $\text{RH}_{a,in} = 45\%$ and $\omega_{a,in}= 0.0106 \text{ kg}_w/\text{kg}_a$	87

List of Tables (cont'd)

Table 4.4	Test summary for deluge cooled uncoated wavy fin RTHX with 3.0 mm fin spacing at approximately $T_{a,in} = 28^{\circ}\text{C}$, $\text{RH}_{a,in} = 45\%$ and $\omega_{a,in} = 0.0106 \text{ kg}_w/\text{kg}_a$	88
Table 4.5	Dry case capacity and ΔP_a of HX with F_p 3mm before and after removing bottom frame at approximately $T_{a,in} = 28^{\circ}\text{C}$, $\text{RH}_{a,in} = 45\%$ and $\omega_{a,in} = 0.0106 \text{ kg}_w/\text{kg}_a$	98
Table 5.1	Spray rates utilized by experimental studies in published literature. ...	102
Table 5.2	Commercially available spray nozzles, along with their geometry, spray pattern, droplet size range and minimum spray rates for water. [Spray Systems, 2013].	104
Table 5.3	Spray nozzles selected for the current study along mean droplet size and flow rate range.	108
Table 5.4	Test summary for spray cooled uncoated wavy fin RTHX with $F_p = 2.4 \text{ mm}$	111
Table 5.5	Test summary for spray cooled hydrophilic coated wavy fin RTHX with $F_p = 2.4 \text{ mm}$ at approximately $T_{a,in} = 28^{\circ}\text{C}$, $\text{RH}_{a,in} = 45\%$ and $\omega_{a,in} = 0.0106 \text{ kg}_w/\text{kg}_a$, and wetting water flow rate 8, 3.8 and 2.2 g/s.	112
Table 5.6	Test summary for spray cooled uncoated wavy fin RTHX with $F_p = 3.0 \text{ mm}$	113
Table 5.7	Test summary for front spray cooled hydrophilic coated wavy fin RTHX with $F_p = 2.4 \text{ mm}$ at approximately $T_{a,in} = 37^{\circ}\text{C}$, $\text{RH}_{a,in} = 45\%$ and $\omega_{a,in} = 0.0179 \text{ kg}_w/\text{kg}_a$, and wetting water flow rate 8, 3.8 and 2.2 g/s.	120
Table 5.8	Test summary for front spray cooled uncoated wavy fin RTHX with $F_p = 2.4 \text{ mm}$ at approximately $T_{a,in} = 37^{\circ}\text{C}$, $\text{RH}_{a,in} = 45\%$ and $\omega_{a,in} = 0.0179 \text{ kg}_w/\text{kg}_a$, and wetting water flow rate 8, 3.8 and 2.2 g/s.	122
Table 5.9	Test summary for top spray cooled hydrophilic coated wavy fin RTHX with $F_p = 2.4 \text{ mm}$ at approximately $T_{a,in} = 28^{\circ}\text{C}$, $\text{RH}_{a,in} = 45\%$ and $\omega_{a,in} = 0.0106 \text{ kg}_w/\text{kg}_a$, wetting water flow rate 8, 3.8 and 2.2 g/s.	123
Table 5.10	Test summary for top spray cooled hydrophilic coated wavy fin RTHX with $F_p = 2.4 \text{ mm}$ at approximately $T_{a,in} = 37^{\circ}\text{C}$, $\text{RH}_{a,in} = 45\%$ and $\omega_{a,in} = 0.0179 \text{ kg}_w/\text{kg}_a$, and wetting water flow rate 8, 3.8 and 2.2 g/s.	124
Table 7.1	Percentage mass fraction of wetting water in different tray sections and percentage wetted fin area, and HX capacity for deluge and spray cooling at 2.5 m/s air velocity.	161
Table 7.2	Evaporation rate and its contribution to HX capacity enhancement for deluge, front spray and internal jet spray cooling at 2.5 m/s air velocity, at approximately $T_{a,in} = 28^{\circ}\text{C}$, $\text{RH}_{a,in} = 45\%$ and $\omega_{a,in} = 0.0106 \text{ kg}_w/\text{kg}_a$	171

List of Tables (cont'd)

Table A1.1	Test summary for internal intermittent jet spray cooled hydrophilic coated wavy fin RTHX with $F_p=2.4$ mm at approximately $T_{a,in}=28^\circ\text{C}$, $RH_{a,in}$ 45% and $\omega_{a,in}= 0.0106$ using 2 spray tubes.	188
Table A1.2	Test summary for internal continuous jet spray cooled hydrophilic coated wavy fin RTHX with $F_p=2.4$ mm at approximately $T_{a,in}=28^\circ\text{C}$, $RH_{a,in}$ 45% and $\omega_{a,in}= 0.0106$ using 2 spray tubes.	191
Table A2.1	Test summary for internal continuous jet spray cooled hydrophilic coated wavy fin RTHX with $F_p=2.4$ mm approximately $T_{a,in}=28^\circ\text{C}$, $RH_{a,in}$ 45% and $\omega_{a,in}= 0.0106$ using 5 spray tubes.	192
Table A2.2	Test summary for internal intermittent jet spray cooled hydrophilic coated wavy fin RTHX with $F_p=2.4$ mm at approximately $T_{a,in}=28^\circ\text{C}$, $RH_{a,in}$ 45% and $\omega_{a,in}= 0.0106$ using 5 spray tubes.	193
Table A2.3	Test summary for internal intermittent jet spray cooled hydrophilic coated wavy fin RTHX with $F_p=2.4$ mm at approximately $T_{a,in}=28^\circ\text{C}$, $RH_{a,in}$ 45% and $\omega_{a,in}= 0.0179$ using 5 spray tubes.	196
Table A3.1	Major findings of simulation/modeling studies on direct evaporative cooling of heat exchangers	197

List of Figures

Figure 1.1	Overview of condenser or process HX cooling technologies utilized by typical commercial and industrial systems.	3
Figure 1.2	Condenser cooling technology and their water withdrawal rate within the power plant sector in US [Avery, et al., 2011].	8
Figure 1.3	Source of condenser cooling water utilized for power plants within US [Avery, et al., 2011].	9
Figure 1.4	Humidity ratio and dry bulb temperature of air at different state points during dry and evaporative cooling.	10
Figure 1.5	T-s diagram for dry and evaporative cooled condenser.	12
Figure 2.1	Overview of the test setup placed in environmental chamber.	38
Figure 2.2	Leveling the HX in test section.	39
Figure 2.3	Plastic sheet is used to ensure collection of wetting water into the wetting water tank.	39
Figure 2.4	Schematic of air-side loop in test setup.	40
Figure 2.5	Thermocouple grid and RH sensor installed at air outlet in test duct. ..	41
Figure 2.6	RH Sensor installed in air duct.	42
Figure 2.7	Differential pressure measurement across test HX.	42
Figure 2.8	Flow path of wetting water to drain.	43
Figure 2.9	Air-mixer attached to polypropylene sheet, ready to be mounted in test section.	45
Figure 2.10	Settling means mounted prior to air nozzles.	46
Figure 2.11	Schematic of process fluid and wetting water loop in test facility.	46
Figure 2.12	Summary of conventional and proposed wetting water distribution methods tested for evaporatively cooled wavy fin HXs	48
Figure 2.13	Deluge evaporative cooling (a) top view (b) side view.	48
Figure 2.14	Front spray evaporative cooling (a) side view (b) top view.	50
Figure 2.15	Top spray evaporative cooling (a) side view (b) top view.	51
Figure 2.16	Overview of heat pump loop of experimental test setup.	53
Figure 2.17	Wavy-fin RTHX (a) and (b) side view of test HX, (c) coil circuitry, (d) wavy-fins, (e) deluge cooling wetting water distributor, (f) wavy-fin RTHX placed in experimental test section.	58
Figure 2.18	Front panel of LabView graphical user interface (GUI).	61
Figure 2.19	PID controller for process fluid and wetting water loop in LabView GUI.	61
Figure 2.20	Heat pump operating parameters displayed in LabView GUI.	62
Figure 2.21	PID controller for electronic expansion valve (EEV) in heat pump loop.	63

List of Figures (cont'd)

Figure 2.22	Calculated propagated uncertainty of each calculated variable in EES.	64
Figure 3.1	Capacity of coated and uncoated wavy-fin heat exchanger as a function of HX frontal air velocity in dry conditions at $RH_{a,in} = 45 \pm 2\%$, and $T_{a,in}$ $= 28^\circ\text{C}$ and 37°	71
Figure 3.2	ΔP_a of coated and uncoated wavy-fin heat exchanger as a function of HX frontal air velocity in dry conditions at $RH_{a,in} = 45\%$, and $T_{a,in} = 28^\circ\text{C}$ and 37°C	71
Figure 3.3	Capacities of uncoated wavy-fin heat exchangers with Fp 2.4 mm and 3.0 mm as a function of HX frontal air velocity in dry conditions at $RH_{a,in} =$ 45% , and $T_{a,in} = 28^\circ\text{C}$	72
Figure 3.4	ΔP_a of uncoated wavy-fin heat exchangers with Fp 2.4 mm and 3.0 mm as a function of HX frontal air velocity in dry conditions at $RH_{a,in} = 45\%$, and $T_{a,in} = 28^\circ\text{C}$	73
Figure 3.5	Effect of HX capacity on HX angle of inclination at different air velocities and $T_{a,in}$ varying from 5°C to 45°C at 10°C fluid inlet temperature difference (ITD).	75
Figure 3.6	CFD Fluent predicted HX frontal velocity profile and air-side pressure drop for an empty duct.	78
Figure 3.7	CFD predicted velocity profile at $V_a = 2.25$ m/s at 0° HX inclination with vertical.	79
Figure 3.8	CFD predicted velocity profile at $V_a = 2.25$ m/s at 21° HX inclination with vertical.	80
Figure 3.9	CFD predicted velocity profile at $V_a = 2.25$ m/s at 40° HX inclination with vertical.	80
Figure 4.1	Wetting water distributor-Design1.....	84
Figure 4.2	Two-way overflow distributor.....	84
Figure 4.3	Multiple two-way overflow distributor.....	84
Figure 4.4	Wavy fin HX capacity as a function of ΔP_a under dry and deluge evaporative cooling at approximately $T_{a,in} = 28^\circ\text{C}$, $RH_{a,in} = 45\%$ and $\omega_{a,in} =$ 0.0106 kg _w /kg _a	85
Figure 4.5	CER and $PR_{\Delta P_a}$ of wavy-fin RTHXs using deluge evaporative cooling at approximately $T_{a,in} = 28^\circ\text{C}$, $RH_{a,in} = 45\%$ and $\omega_{a,in} = 0.0106$ kg _w /kg _a	89
Figure 4.6	Contribution of deluge water evaporation to overall heat exchanger capacity at approximately $T_{a,in} = 28^\circ\text{C}$, $RH_{a,in} = 45\%$ and $\omega_{a,in} = 0.0106$ kg _w /kg _a	90
Figure 4.7	Effect of hydrophilic coating on % capacity enhancement and % ΔP_a enhancement of deluged wavy-fin RTHX at approximately $T_{a,in} = 28^\circ\text{C}$, $RH_{a,in} = 45\%$ and $\omega_{a,in} = 0.0106$ kg _w /kg _a	91

List of Figures (cont'd)

Figure 4.8	Effect of decreasing fin spacing from 2.4 mm to 3 mm on percentage capacity enhancement and % ΔP_a enhancement of deluged wavy-fin RTHXs at approximately $T_{a,in} = 28^\circ\text{C}$, $RH_{a,in} = 45\%$ and $\omega_{a,in} = 0.0106 \text{ kg}_w/\text{kg}_a$	93
Figure 4.9	Effect of flow configuration on HX capacity of deluged uncoated wavy-fin RTHX with $F_p = 2.4 \text{ mm}$ at approximately $T_{a,in} = 28^\circ\text{C}$, $RH_{a,in} = 45\%$ and $\omega_{a,in} = 0.0106 \text{ kg}_w/\text{kg}_a$	94
Figure 4.10	Effect of flow configuration on HX capacity enhancement ratio of deluged uncoated wavy-fin RTHX with $F_p = 2.4 \text{ mm}$ at approximately $T_{a,in} = 28^\circ\text{C}$, $RH_{a,in} = 45\%$ and $\omega_{a,in} = 0.0106 \text{ kg}_w/\text{kg}_a$	95
Figure 4.11	Effect of flow configuration on evaporation rate of deluged uncoated wavy-fin RTHX with $F_p = 2.4 \text{ mm}$ at approximately $T_{a,in} = 28^\circ\text{C}$, $RH_{a,in} = 45\%$ and $\omega_{a,in} = 0.0106 \text{ kg}_w/\text{kg}_a$	95
Figure 4.12	Typical HX installation configuration in the air duct with bottom and side frame of HX marked.	97
Figure 4.13	HX installed with bottom frame removed to aid visualization.	97
Figure 4.14	Visualization of wetting water distribution in depth of RTHX (3.0 mm fin spacing) in deluge cooling conditions.	98
Figure 5.1	Projected spray pattern for hollow and full cone spray nozzles on HX face.	106
Figure 5.2	Low momentum droplets falling short of heat exchanger.	107
Figure 5.3	Spray droplet size as a function of pintle type nozzle discharge pressure [Spray Systems, 2013].	108
Figure 5.4	HX capacity as a function of ΔP_a under dry and front spray cooling conditions.	110
Figure 5.5	CER and $PR_{\Delta P_a}$ of wavy-fin RTHXs using front spray evaporative cooling at approximately $T_{a,in} = 28^\circ\text{C}$, $RH_{a,in} = 45\%$ and $\omega_{a,in} = 0.0106 \text{ kg}_w/\text{kg}_a$	114
Figure 5.6	Comparison of spray cooling capacity enhancement ratios and ΔP_a penalty ratios of uncoated wavy-fin RTHXs with fin spacing of 2.4 mm (Coil 1) and 3 mm (Coil 3) respectively at approximately $T_{a,in} = 28^\circ\text{C}$, $RH_{a,in} = 45\%$ and $\omega_{a,in} = 0.0106 \text{ kg}_w/\text{kg}_a$	115
Figure 5.7	Effect of increasing fin spacing (from 2.4 mm to 3 mm) on HX capacity and airside pressure drop at approximately $T_{a,in} = 28^\circ\text{C}$, $RH_{a,in} = 45\%$ and $\omega_{a,in} = 0.0106 \text{ kg}_w/\text{kg}_a$	116
Figure 5.8	Comparison of spray cooling capacity enhancement ratios and air-side ΔP penalty ratios of coated and uncoated wavy-fin RTHX with fin spacing of 2.4 mm at approximately $T_{a,in} = 28^\circ\text{C}$, $RH_{a,in} = 45\%$ and $\omega_{a,in} = 0.0106 \text{ kg}_w/\text{kg}_a$	117

List of Figures (cont'd)

Figure 5.9	Effect of hydrophilic coating on percentage capacity and airside ΔP enhancement/reduction at approximately $T_{a,in} = 28^\circ\text{C}$, $RH_{a,in} = 45\%$ and $\omega_{a,in} = 0.0106 \text{ kg}_w/\text{kg}_a$	118
Figure 5.10	Effect of inlet air temperature on capacity enhancement ratio of front spray cooled hydrophilic coated wavy- fin HX.	119
Figure 5.11	Capacity enhancement ratio for front and top spray configurations at at approximately $T_{a,in} = 37^\circ\text{C}$, $RH_{a,in} = 45\%$ and $\omega_{a,in} = 0.0179 \text{ kg}_w/\text{kg}_a$ for hydrophilic coated wavy- fin HX.	125
Figure 5.12	Capacity enhancement ratio for front and top spray configurations at at approximately $T_{a,in} = 28^\circ\text{C}$, $RH_{a,in} = 45\%$ and $\omega_{a,in} = 0.0106 \text{ kg}_w/\text{kg}_a$ for hydrophilic coated wavy- fin HX.	126
Figure 5.13	Percentage reduction of wavy-fin HX capacity for top sprayed coils compared to front spraying in similar conditions at approximately $T_{a,in} = 28^\circ\text{C}$, $RH_{a,in} = 45\%$ and $\omega_{a,in} = 0.0106 \text{ kg}_w/\text{kg}_a$	127
Figure 5.14	Percentage enhancement of wavy-fin HX capacity for top sprayed coils compared to front spraying in similar conditions at approximately $T_{a,in} = 37^\circ\text{C}$, $RH_{a,in} = 45\%$ and $\omega_{a,in} = 0.0179 \text{ kg}_w/\text{kg}_a$	127
Figure 5.15	Unevaporated spray droplets deposited on visualization section plate at air outlet of experimental setup.	128
Figure 5.16	Comparison of CER per unit $PR_{\Delta P}$ for front spray, top spray and deluge cooling of wavy fin HXs with $T_a = 28^\circ\text{C}$ and 37°C	130
Figure 5.17	Comparison of CER per unit wetting water flow rate for front spray, top spray and deluge cooling of wavy fin HXs with $T_a = 28^\circ\text{C}$ and 37°C	130
Figure 5.18	Deluged and dry coil showing bridging between fin surfaces.	131
Figure 5.19	Spray cooling capacity enhancement improvement constraints.	134
Figure 5.20	Wetting water distribution in depth of RTHX (3.0 mm fin spacing) in front spray and deluge cooling conditions at approximately $T_{a,in} = 28^\circ\text{C}$, $RH_{a,in} = 45\%$ and $\omega_{a,in} = 0.0106 \text{ kg}_w/\text{kg}_a$	135
Figure 6.1	Different spray cooling nozzle configurations.	136
Figure 6.2	Schematic representation of permeable spray tubing (isometric view).	138
Figure 6.3	Novel method using two passes of tubing which spray in a 360° radius along the length of the heat exchanger; red dots indicate example spray tube locations.	139

List of Figures (cont'd)

Figure 6.4	Schematic of spray cooling spray tube positions on HX frame (side view).	141
Figure 6.5	Uniform spray pattern obtained from plastic tube with holes in all directions.	142
Figure 6.6	Sealed end of spray tubes using copper tube plug.	142
Figure 6.7	Hydrophilic coated HX capacity enhancement using deluge, front spray and internal spray cooling with 2 spray tubes at approximately $T_{a,in}=28^{\circ}\text{C}$, $\text{RH}_{a,in} = 45\%$ and $\omega_{a,in}= 0.0106 \text{ kg}_w/\text{kg}_a$	143
Figure 6.8	Hydrophilic coated HX capacity enhancement using front spray and internal spray cooling with 2 spray tubes at approximately $T_{a,in}=28^{\circ}\text{C}$, $\text{RH}_{a,in} = 45\%$ and $\omega_{a,in}= 0.0106 \text{ kg}_w/\text{kg}_a$	145
Figure 6.9	HX capacities as a function of wetting water flow rate for continuous and intermittent internal spray cooled HX ($V_a= 1.5 \text{ m/s}$; 2 spray tubes) at approximately $T_{a,in}=28^{\circ}\text{C}$, $\text{RH}_{a,in} = 45\%$ and $\omega_{a,in}= 0.0106 \text{ kg}_w/\text{kg}_a$	145
Figure 6.10	Hydrophilic coated HX capacity enhancement using deluge, front spray and internal spray cooling with 5 spray tubes at approximately $T_{a,in}=28^{\circ}\text{C}$, $\text{RH}_{a,in} = 45\%$ and $\omega_{a,in}= 0.0106 \text{ kg}_w/\text{kg}_a$	147
Figure 6.11	Hydrophilic coated HX capacity using deluge, front spray and internal spray cooling with 5 spray tubes at approximately $T_{a,in}=28^{\circ}\text{C}$, $\text{RH}_{a,in} = 45\%$ and $\omega_{a,in}= 0.0106 \text{ kg}_w/\text{kg}_a$	147
Figure 6.12	Comparison of front and internal spray cooling.	148
Figure 6.13	HX capacities as a function of wetting water flow rate for front spray, continuous and internal spray cooled HX ($V_a= 1.5 \text{ m/s}$; 5 spray tubes) at approximately $T_{a,in}=28^{\circ}\text{C}$, $\text{RH}_{a,in} = 45\%$ and $\omega_{a,in}= 0.0106 \text{ kg}_w/\text{kg}_a$	149
Figure 6.14	Hydrophilic coated HX capacity and CER using front, top and internal spray cooling with 5 spray tubes at approximately $T_{a,in}=37^{\circ}\text{C}$, $\text{RH}_{a,in} = 45\%$ and $\omega_{a,in}= 0.0179 \text{ kg}_w/\text{kg}_a$	150
Figure 6.15	Hydrophilic coated HX capacity and CER using front, top and internal spray cooling with 5 spray tubes at approximately $T_{a,in}=28^{\circ}\text{C}$, $\text{RH}_{a,in} = 45\%$ and $\omega_{a,in}= 0.0106 \text{ kg}_w/\text{kg}_a$	151
Figure 7.1	Conventional visualization; (a, b) front/back view, (c) side view, (d) bottom side view.	154
Figure 7.2	Typical HX installation in air duct with (a) bottom and (b) side support frame of HX.	156
Figure 7.3	HX installed with bottom frame removed.....	156
Figure 7.4	Partitioned collection tray design concept in modified test setup.	157

List of Figures (cont'd)

Figure 7.5	Partitioned collection tray placed underneath HX with each partition sealed to prevent air bypass between HX fins and flexible seal, (b) test setup ready for visualization measurements.	158
Figure 7.6	(a) Borescope inserted into HX through view point; (b) and (c) view-points for visualization.	160
Figure 7.7	Flow map for deluge cooling at wetting water flow rate of (a) 166 g/s; (b) 80 g/s; (c) 15 g/s.	162
Figure 7.8	Wetting profile for front spray cooling flow rate (a) 8 g/s; (b) 3.8 g/s.	163
Figure 7.9	HX capacity as a function of evaporation rate for deluge, spray cooling at 2.5 m/s air velocity.	164
Figure 7.10	HX capacity as a function of fin area wetted for deluge, front spray and internal jet spray cooling at 2.5 m/s air velocity at approximately $T_{a,in}=28^{\circ}\text{C}$, $\text{RH}_{a,in} = 45\%$ and $\omega_{a,in}= 0.0106 \text{ kg}_w/\text{kg}_a$	165
Figure 7.11	Mass of wetting water measured in different sections of bottom split tray as a function of tray section number for deluge, front spray and internal jet spray cooling at 2.5 m/s air velocity at approximately $T_{a,in}=28^{\circ}\text{C}$, $\text{RH}_{a,in} = 45\%$ and $\omega_{a,in}= 0.0106 \text{ kg}_w/\text{kg}_a$	165
Figure 7.12	HX capacity as a function of evaporation rate for deluge, front spray and internal jet spray cooling at 2.5 m/s air velocity at approximately $T_{a,in}=28^{\circ}\text{C}$, $\text{RH}_{a,in} = 45\%$ and $\omega_{a,in}= 0.0106 \text{ kg}_w/\text{kg}_a$	167
Figure 7.13	Generic evaporative cooling performance plot.	169
Figure 7.14	Test data obtained for three wavy-fin HXs plotted on evaporative cooling performance plot at approximately $T_{a,in}=28^{\circ}\text{C}$, $\text{RH}_{a,in} = 45\%$ and $\omega_{a,in}= 0.0106 \text{ kg}_w/\text{kg}_a$	169

Nomenclature

Abbreviations

COP	Coefficient of performance	(-)
CER	Capacity enhancement ratio ($\dot{Q}_{\text{wet}}/\dot{Q}_{\text{dry}}$)	(-)
CISC	Continuous internal spray cooling	(-)
FPI	Fins per inch	(-)
FSC	Front spray cooling	(-)
HTC	Heat transfer coefficient	(W/m ² /K)
HVAC	Heating, ventilation, and air-conditioning	(-)
IISC	Intermittent internal spray cooling	(-)
ITD	Inlet temperature difference	(-)
MTC	Mass transfer coefficient	(kg/m ² /s)
PID	Proportional-integral-derivative	(-)
PR	Penalty ratio	(-)
RO	Reverse osmosis	(-)
RH	Relative humidity	(-)
RTD	Resistance temperature detectors	(-)
RTHX	Round tube heat exchanger	(-)
VFD	Variable frequency drive	(-)
WUI	Water utilization index	(-)

Parameters

F_p	Fin spacing	(mm)
\dot{m}	Mass flow rate	(kg/s)
h	Enthalpy	(kJ/kg)
$PR_{\Delta Pa}$	Air-side pressure drop penalty ratio ($\Delta P_{wet}/\Delta P_{dry}$)	(-)
ρ	Density	(kg/m ³)
P	Pressure	(Pa)
\dot{Q}	Heat transfer rate	(kW)
T	Temperature	(°C)
\dot{v}	Volume flow rate	(m ³ /s)
v	Velocity	(m/s)
ω	Humidity ratio	(kg _w /kg _a)

Subscripts

a	air	(-)
c	condenser	(-)
dry	dry cooling capacity	(kW)
eb	energy balance	(-)
evap	evaporative cooling capacity	(kW)
expt	experimental	(-)
in	inlet stream	(-)
lat	latent component of HX capacity	
out	outlet stream	(kW)

P	pressure	(Pa)
pf	process fluid	(-)
sens	Sensible component of HX capacity	(kW)
tot	total	(-)
ww	wetting water	(-)

Chapter 1 Need for hybrid cooling and literature review

1.1 Introduction

Round tube-and-fin heat exchangers (RTHX) are widely used as condensers or coolers in power generation, air-conditioning, refrigeration and process cooling applications where ambient air serves as heat sink. Typically air is used as cooling fluid which flows over the tubes and fins on air-side of the HX and cools the heat transfer fluid on tube-side. Since heat transfer in such HXs is constrained on air-side due to high thermal resistance, enhanced fin surfaces are typically utilized to increase fin-tube HX performance [Wang et al., 1999]. These extended surfaces are often incorporated with a series of flow interruptions such as louvers, off-strips and wavy fins that induce turbulent mixing of air flow and prevent growth of thermal boundary layer from leading edge [Webb and Jung, 1992; Chang and Wang, 1997]. Due to low manufacturing cost, louver or wavy fins are more commonly used to enhance heat transfer in fin tube HXs. However, at high ambient air-conditions finned round-tube HXs do not provide sufficient cooling capacity and higher condenser temperature reduces thermodynamic cycle efficiency by up to 1% for every degree increase in condensing temperature [Leidenfrost and Korenic, 1979]. In addition, further increase in fin density provides marginal increase in capacity at the cost of considerable increase in air-side pressure drop.

Any enhancement in condenser cooling efficiency especially at higher ambient temperatures could allow heat rejection either using smaller surface area or reduce condenser temperature for same HX area. This could reduce HX material cost, equipment footprint and energy required to produce the material. Secondly operating cost and energy consumption could be reduced due to lower pressure drop of process fluid flowing through

HX tubes. Thus, compressor work input could be reduced for refrigeration or air-conditioning applications, and power plant cycles could produce more power if condenser temperatures are lowered. Finally, with improved thermodynamic cycle efficiencies primary fuel and energy consumption could be reduced.

One way to enhance heat transfer in compact HXs is to utilize deluge or spray water evaporative cooling where a thin water film is applied over HX fins. As a result air-side heat transfer is enhanced through both forced convection on liquid film and latent heat of evaporation at the interface of flowing air and thin water film. Therefore, heat transfer could be significantly augmented even when $T_{amb} > T_c$. Compared to air-cooled condensers or fluid coolers, evaporative cooling could help reduce electric energy consumption of heat, ventilation and air-conditioning (HVAC) systems by 20-40%, while providing same cooling capacity obtained using water cooled units [Knebel, 1997]. However, lack of availability of sufficient wetting water, corrosion issues, and restriction on its use for industrial cooling limits the wide-spread application of evaporative cooling technology. This forms the objective of work presented in this Dissertation which experimentally evaluated round tube wavy-fin HX performance as hybrid cooler in dry conditions and wet conditions using deluge and spray cooling. Hybrid coolers/condensers utilize air cooling for a major portion of the year, and during ambient high temperature conditions spray or deluge cooling is employed to achieve desired capacity.

1.2 Methods of condenser cooling: Merits and Demerits

An overview condenser cooling technologies utilized by typical commercial and industrial systems is summarized in Figure 1.1.

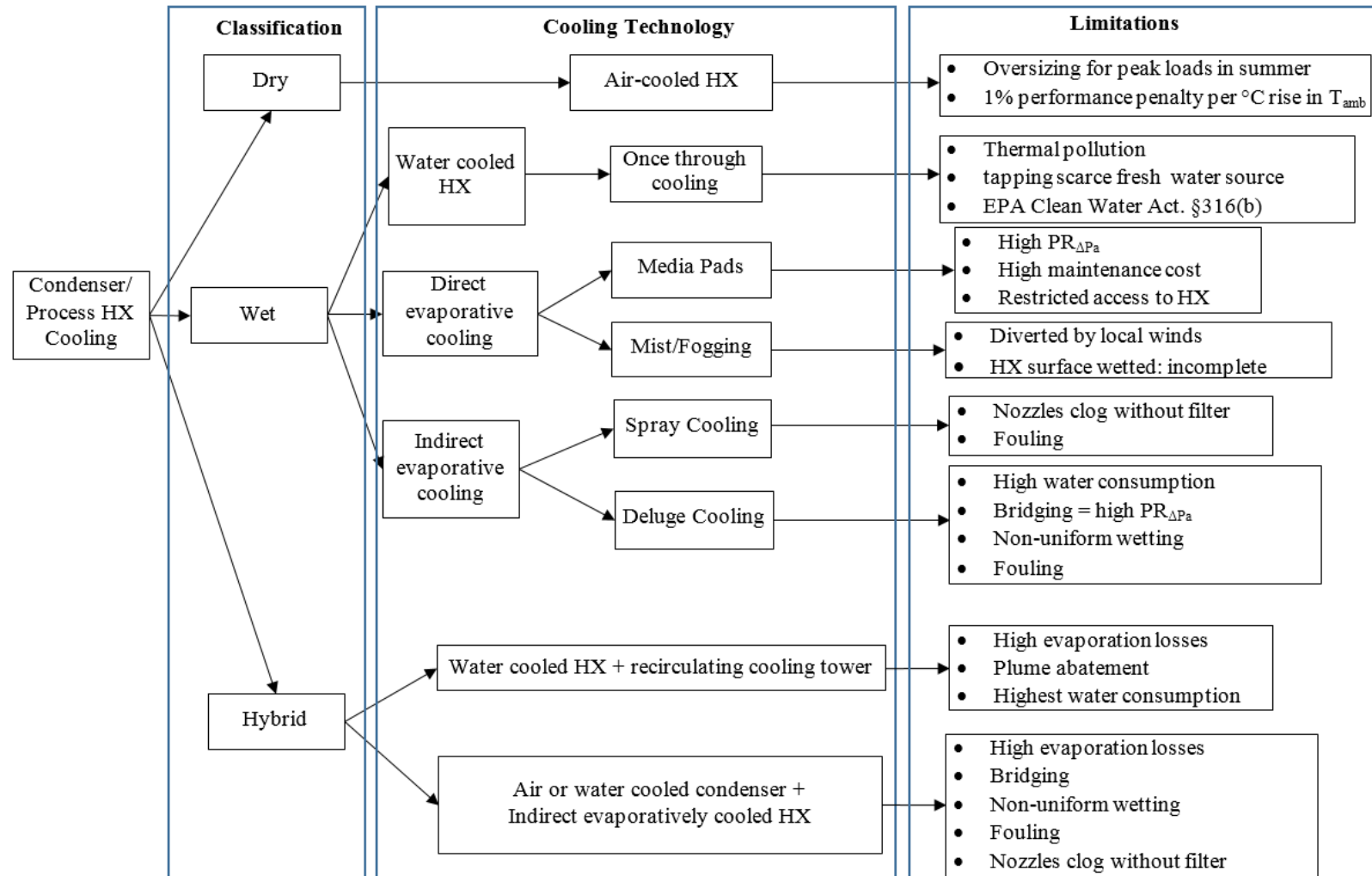


Figure 1.1: Overview of condenser or process HX cooling technologies utilized by typical commercial and industrial systems.

Condenser cooling technologies can be broadly classified into dry, wet and hybrid cooling technologies. *Dry cooling* uses air cooled HXs where air flows over the tubes and fins on air-side of the HX and condenses or cools the heat transfer fluid circulating through tube-side. However, due to poor heat transfer characteristics air cooled systems require much larger surface areas compared to water cooled units. Alternatively a surface condenser may be used to cool process fluid in a water cooled liquid to liquid HX and the heated water may then be cooled in an air cooled HX. The benefit of such a system is that it eliminates water evaporation losses, but additional components such as HX and pumps would be required which significantly enhance capital cost.

Wet cooling may involve utilization of a water cooled HX or evaporative cooled HX.

One of the cheapest and most commonly utilized method for power plant condenser cooling is a type of water cooled HX in a once through cooling scheme. The amount of cooling water required in a once through cooling system could be supplied by a local water body and is completely returned to the same water body acting as heat sink. Due to very high volume flow rate of water the rise in temperature is not significant. However, with time temperatures could rise and cause thermal pollution. Moreover as per EPA [2011] developed regulations under Clean Water Act §316 (b), it may be necessary for industrial cooling systems to utilize recirculation systems instead of once through systems. The latter adversely affects environment by pulling large number of fish or their eggs into plant's cooling systems. This kills the organisms due to heat, physical stress or chemical treatment used to clean the water.

Power plants are now moving towards recirculation based cooling towers where a portion of water which cools the condenser is evaporated in a cooling tower, thereby

reducing the temperature of the cooling water. Such recirculating or closed loop wet cooling towers reduce up to 90% of water withdrawal from freshwater or local sources.

Direct evaporative cooling technologies allow contact between cooling process stream and wetting water stream. Media evaporative pads and fogging are the most commonly used indirect evaporative cooling methods which precool inlet air by the evaporation of a small amount of water which absorbs a significant amount of heat from inlet air stream.

However, media pads cause massive air-side pressure drops due to dense filling material, have a very high maintenance cost and restrict access to coil surface. Fogging or mist cooling typically breaks droplets less than 50μ [Spray systems, 2013]. At this diameter droplets are highly prone to being diverted by local winds. Moreover, due to incomplete evaporation a portion of mist forms a thin water film on HX face and the initial purpose of avoiding water contact with fin surfaces is defeated. In addition at this droplet size range a significant carry over may occur downstream of HX, i.e. water droplets mass pass through the coil without impinging fin surface.

Indirect evaporatively cooled HXs solve the dual problem of water and fan power energy consumption by utilizing the large latent heat of evaporation of water (instead of sensible heat) to cool process fluid. Typically either deluge or spray water cooling is utilized for industrial and commercial applications especially to meet peak load requirements. *Deluge cooling* is easiest to install but causes significant increase in $PR_{\Delta Pa}$ due to severe bridging between fins, utilizes considerable amount of water compared to spray cooling, and has poor uniformity of wetting water distribution on fin surfaces.

Spray cooling utilizes least amount of water but may be prone to clogging of nozzles if water filters are not installed. If nozzle distance from HX is not optimum either spray would

fall before HX and could be diverted by local winds, or would cover a small HX face area which limits enhancement. If the HX is deep or fin spacing is high, then most water would be retrained by upstream tube banks. Thus uniform wetting is a major challenge. Also, both deluge and spray cooling cause fouling issues due to mineral build up on fin surfaces in the absence of water treatment systems. Fouling problem can be alleviated by not allowing wetting water to contact HX fin surface.

In order to reduce the energy and water consumption issues hybrid systems are often utilized (more commonly in HVAC industry). Two commonly utilized schemes are:

- 1) Water cooled HX + recirculating or closed-loop wet cooling tower
- 2) Wet/Dry hybrid evaporatively cooled HXs

In a recent study Bharathan [2013] presented a relative comparison of simple payback periods for each evaporative cooling technology. It was concluded that:

- 1) media pads and fogging had payback periods i.e. 9.4 and 6.1 years, respectively
- 2) Spray and deluge cooling had lower paybacks of 0.6 and 0.13 years, respectively

Thus in the light of the facts that, 1) wetting the HX surface produces significant enhancement and 2) contact of wetting water cannot be avoided due to local factors such as wind etc., spray and deluge cooling are often recommend as technologies of choice for evaporative cooling. It must be noted that simple water filtration systems would be sufficient to prolong HX life. Some studies have also shown that periodic dry and wet conditions cause fouling. Therefore, if the surface could be kept uniformly wet throughout the year, the corrosion issues could be entirely avoided. *Experimental investigation, quantification of capacity enhancements, and examination of merits and demerits of each of these technologies forms the focus of work presented in this Dissertation.*

1.3 Need for evaporative cooling

Evaporative cooling utilizes relatively low amount of water compared to water cooled HXs compared to deluge cooling. But water may be scarce or relatively expensive cooling medium compared to air depending on the location and therefore efforts must be made to minimize water consumption as much as possible.

For example power plants which typically utilize Rankine cycle for power generation need considerable condenser cooling for operation. Historically depending upon quantity and quality of cooling required, and cost of operation, local water bodies have been utilized as heat sinks. Figure 1.2 shows the condenser cooling technology and their water withdrawal rate within the power plant sector in US and Figure 1.3 presents the source of condenser cooling water utilized for power plants within US.



Figure 1.2: Condenser cooling technology and their water withdrawal rate within the power plant sector in US [Avery et al., 2011].

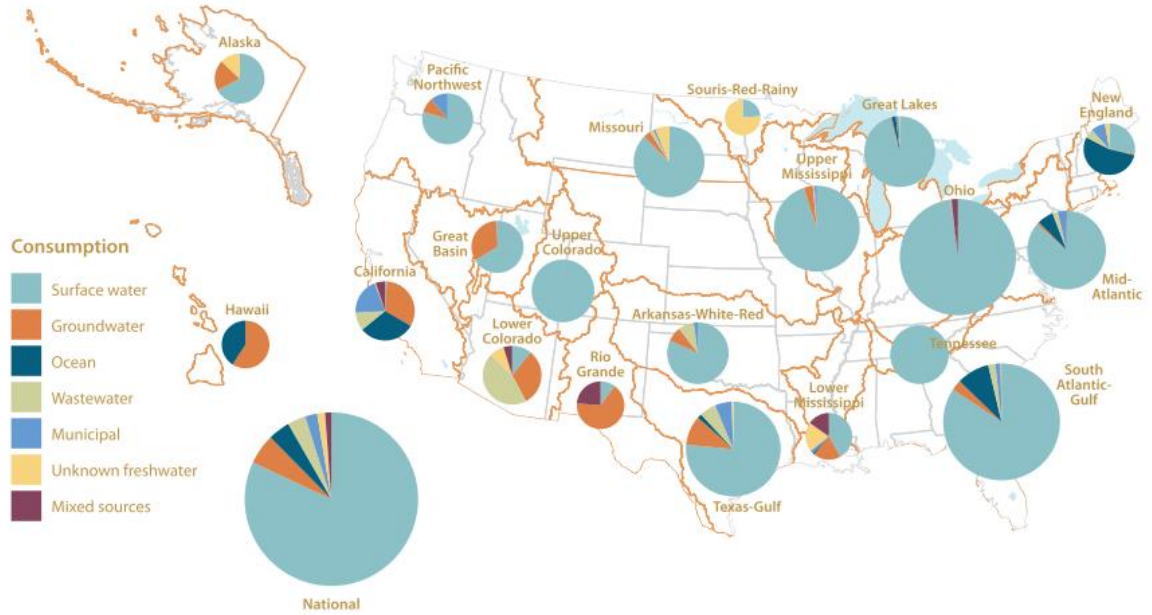


Figure 1.3: Source of condenser cooling water utilized for power plants within US [Avery et al., 2011].

It can be observed that approximately 84% of power plant cooling water consumption was met using surface freshwater sources such as lakes and rivers. This situation exists at a time when increasing water shortage is being felt within US and 2010-2013 droughts in southern US states serves as an indicator for the worsening situation. Unfortunately water shortage is not highlighted globally as much compared to energy shortage, but would enough proof exists to believe it would need to be dealt with more aggressively in the future. Another observation is the poor penetration of hybrid cooling technology in US energy sector as once through cooling technology is currently most widely utilized.

Hybrid systems utilize dry air cooling for a major portion of the year when ambient temperature is low and wetting water is applied to HX coils for meeting peak loads. In addition to significantly reducing operating cost compared to completely dry or wet cooling technologies, hybrid cooling also reduces oversizing of HX and auxiliary equipment.

Therefore there is a clear motivation for developing hybrid cooling technologies which combine the most optimum dry case design with best wetting strategy to cover peak load.

1.4 Thermodynamics of evaporative cooling

In order to evaluate the potential benefits of evaporative cooling and the maximum theoretical capacity enhancement it is important to understand psychrometric changes air undergoes as it passes through the HX coil. Figure 1.4 presents the humidity ratio and dry bulb temperature of air at different state points, and is also referred to as the Mollier diagram.

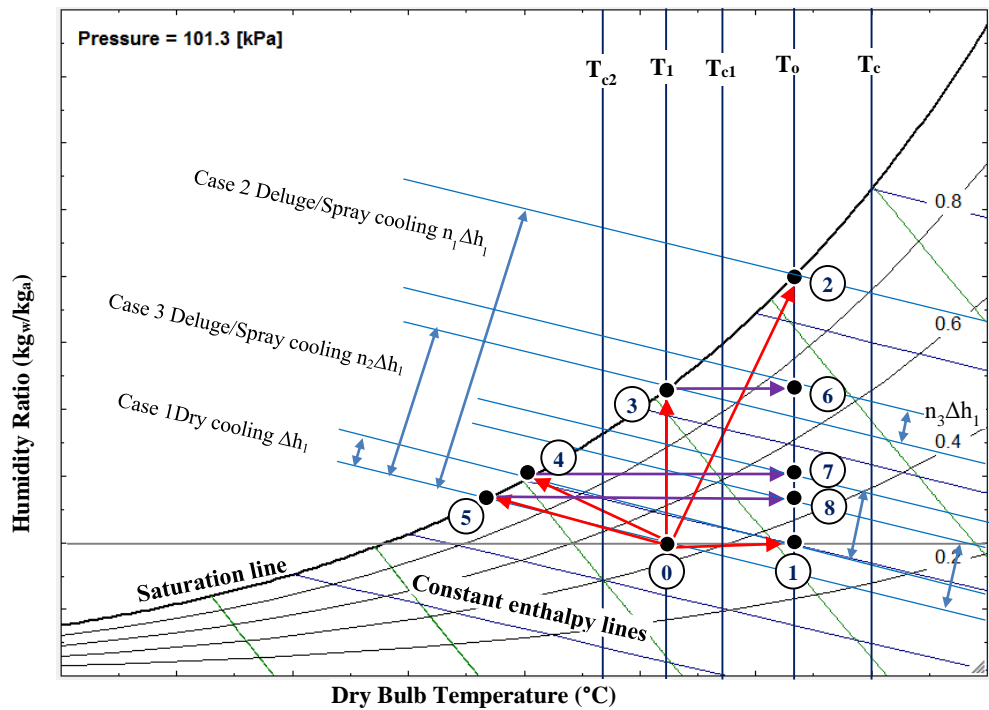


Figure 1.4: Humidity ratio and dry bulb temperature of air at different state points during dry and evaporative cooling (modified from Leidenfrost and Korenic, 1982).

We consider 5 different state point changes theoretically possible within a HX utilized as dry or evaporative cooler or condenser. Air at state point 0 represents the ambient air at HX inlet; T_c is condenser temperature and T_o is air outlet temperature.

Case 1 Baseline: Sensible heating (state point change 0 →1)

For dry case cooling air is only heated and while there would be no change in humidity ratio as HX surface is completely dry. The relative humidity at HX outlet would be lower due to heating of air. The heat transfer would be mass flow rate of air multiplied by enthalpy difference Δh_1 .

Case 2 Evaporative cooling and heating to saturation at T_o

(state point change 0 →2)

In this case simultaneous heat and mass transfer takes place between air and thin wetting water film on HX surface. The state change 2 represents a limiting case i.e. theoretical maximum where air exits at saturated condition and total heat transfer is $n_1 \Delta h_1$ which is significantly higher than dry cooling.

For a fixed load condenser/cooler this translates to reduction in either mass flow rate (fan energy savings) or heat transfer area (HX size could be reduced i.e. material savings).

Case 3 Isothermal saturation (state point change 0 →3)

In this case air is saturated at HX outlet but there is not increase in temperature as air passes through HX. Air mass flow rate and HX surface area could be reduced for this case too. It must also be observed that condensing temperature could be reduced to T_{c1} .

Case 6 Air-precooling + dry cooling (state point change 3 →6, 4→7 or 5→8)

During fogging or mist cooling and media evaporative cooling typically inlet air would be pre-cooled to saturation point. Three subcases could be considered here i.e. inlet air to HX would now be saturated and at state point 3, 4, or 5 as shown in Figure 1.4. This saturated stream then heats up as it passes through HX and could be at state points 6, 7 or 8.

In each of these cases i.e. state point change 3 →6, 4→7 or 5→8, the heat transfer rate is much lower compared to the Cases 2 to 4, where wetting water was allowed to be in direct contact with HX surface to be cooled. The main reason for this is because a significant portion of heat is removed from the air while air with poor heat transfer characteristics is still responsible for removing heat from HX surface. Therefore both media evaporative and fogging are not effective evaporative cooling technologies from a thermodynamic standpoint.

1.5 Evaporatively cooled hybrid HXs: Market overview

A brief overview of commercially available evaporatively cooled condenser/coolers is presented in Table 1.1.

Table 1.1: Overview of commercially available evaporatively cooled condenser/coolers.

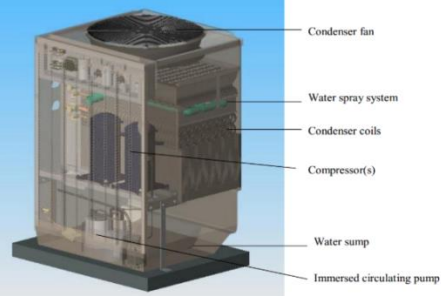
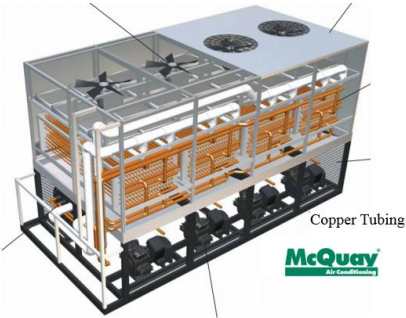
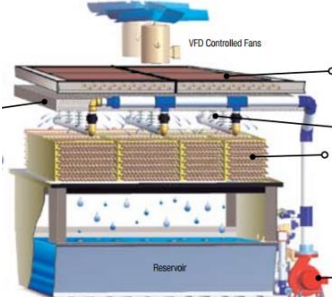
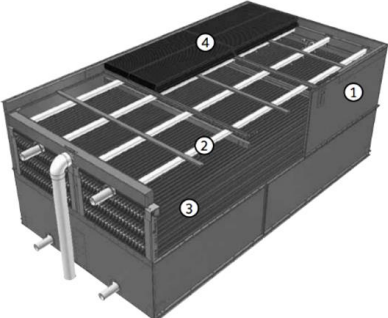
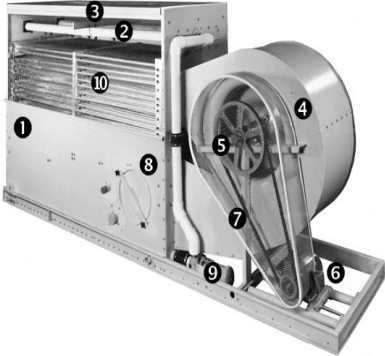
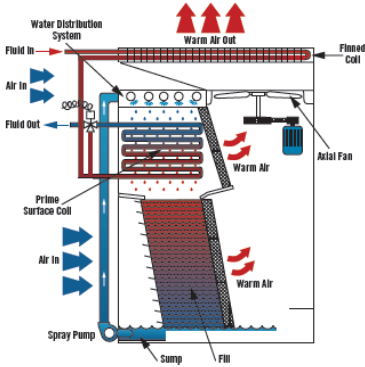

Manufacturer	Capacity (kW)	Refrigerant	Comments	
	[Freus, 2007]	19	R22	helical coil kept horizontally Nozzle
	[McQuay, 2013]	500		Horizontal coil Nozzle
	[AAON, 2013]	900	R410A	Horizontal coil Deluge
	[Frick/Johnson Control, 2013]	Up to 19000	R717, R134a,	Horizontal coil, Fin Spacing=5, Nozzle, 40 g/s/kW cooling

Table 1.1: Overview of evaporatively cooled condenser manufacturers (Cont'd).

Manufacturer	Capacity (kW)	Refrigerant	Comments
	Baltimore Air Company [BAC, 2013a]	6891	Horizontal coil Nozzle, 10 GPM/ft ²
		R717	
	Baltimore Air Company [BAC, 2013b]	900	Inclined coil for hybrid operation
	Recold/SPX [2013]	1500	R134a, R22, R404/507
			Horizontal coil Nozzle

Key observations in regard to these products are as follows:

1. Most manufacturers prefer horizontal coil arrangement.

The choice of horizontal and vertical arrangement of coil depends upon, 1) limitation on unit height, 2) HX geometry and 3) spray distribution. For example, horizontal finned coils have been observed to have issues with spray water retention downstream of coil. If air velocity is too high wetting water droplet carryover occurs, if it is too low air cannot blow excess wetting water out of coil and this excess water cannot flow down due to gravity as air pushes it into the coil. Therefore, typically circular fins with small height or un-finned coils are arranged horizontally. A vertical finned coil provides clear path for wetting water to flow down on fin surface due to gravity but increases unit height.

2. High fin spacing

Most commercially available products have not been designed for hybrid evaporative cooling operation. Due to low fin spacing they would not be efficient in dry conditions. Fin spacing used in most of the products is around 5-8 FPI while optimized compact HXs may have up to 12 FPI for wavy fin geometry.

3. Deluge versus spray cooling

There is a lack of clarity on pros and cons of the two technologies, and current capacity prediction capabilities are poor. This leads to oversized units with excess energy and water consumption in order to meet peak demand with evaporative cooling. There is no fixed set of standard parameters which takes into account overall operation of these technologies for objective comparison purposes.

1.6 Literature review: overview of experimental studies

In this section, experimental, numerical and analytical studies on evaporatively cooled HXs are summarized. Thermal hydraulic performance of both deluge and spray cooling technologies has been discussed at component and system levels.

A number of experimental studies have published performance data of air-cooled RTHX with different fin configurations and also presented correlations for predicting air-side heat transfer and pressure drop either in terms of Colburn j and f factors as a function of Reynolds number and HX geometry (Wang et al., 1998; Wang et al., 1999b; Wang et al., 1999c; Wang et al., 1999d).

In comparison to condenser performance data of RTHX in dry conditions, published experimental studies in wet conditions especially for wavy fin configuration are limited in the open literature. Table 1.2 presents an overview of experimental studies on evaporative cooling of finned HX coils utilized as condensers or fluid coolers. Evaporative cooling on 1) heated flat plates, 2) bare cylindrical tube surfaces of fluid coolers and cooling towers, and 3) falling film absorbers in heat driven pumps has been fairly well researched and is not included in this review. However, a similar operation on advanced compact finned HXs poses additional less understood problems such as identifying areas of uniform wetting, bridging, heat and mass transfer enhancement mechanisms etc. due to complex fin geometry. *Thus Table 1.2 mainly focusses on experimental studies where finned coils are evaporatively cooled.* Table 1.3 summarizes the major findings of experimental studies on evaporative cooling of finned HX coils utilized as condensers or fluid coolers.

Table 1.4 discusses the major findings of experimental studies on evaporatively cooled bare-tube HX coils utilized as condensers or fluid coolers.

Table 1.2: Summary of experimental studies on evaporative cooling of finned HX coils utilized as condensers or fluid coolers.

Author	Coil ¹	V _a (m/s)	M _{ww} (kg/m ² -h)	M _{ww} (g/m ³ -s)	CER	Max HTC Enhancement	EER% Improvement
Sen, 1973	Single row; Bare and circular fins (1 bank, 3 tubes), Fin height- 9.5 to 22.2 mm FPI 2 to 8	4.57-9.15	0-712	3114	Bare tube 20-16 Short fin 16-12.5 Long fin 4.1	15	
Simpson et al., 1974	Single tube bank ² circular fins	4.57-9.15	0-712	3114	5-16		
Yang and Clark, 1975	flat tube with plain ³ , louvered, and perforated fin; louver spacing 0.17 cm	1.5 to 13	41.3 ⁴ & 82.7 ⁴	164.3 ⁴ & 328.5 ⁴		1.5	
Tree <i>et al.</i> , 1978	12 FPI plain fin, 4 bank	0.8-2.3	6.5-19.5		1.4		
Kried <i>et al.</i> , 1979	plain slit fins (9 FPI)	0.9 to 4.87	609-1219	1128-2257	ITD 5°C 3-7 ITD 14°C 1.5-2.2		
Parry <i>et al.</i> , 1979	vertical flat tube HX, with partially cut horizontal fins	0.91-1.83	1116-1487	1771-2360	9.8		
Mori and Nakayama, 1980	bare/micro-finned	1 to 3	50-400	74-588	N	1.7	
Guinn and Novell, 1981	Plain fin; flat tube	-	97.7	-	1.087	-	19
Hauser <i>et al.</i> , 1982	circular fin	0.91-1.83	454-1135	993-2482	6.53		
Hauser and Kreid, 1982	wavy fin	0.91-4.57	680-907	1657-2210	5		
Trela, 1983	one row square fin HX	1.0-20.0	-	-	4	-	-
Blanco and Bird, 1984	single vertical tube evaporative cooler	up to 10	48-287	224-1344	17		
Simpson <i>et al.</i> , 1984	Three banks, circular fin	2 to 10	up to 820	255	1.3		

Note: ¹ Round tube coil and vertical HX with horizontal airflow unless otherwise stated.

² Bank refers to number of columns (or vertical rows) and rows refers to horizontal rows in fair flow direction

³ Plain refers to flat plate/strip of fins

⁴ Both water and ethylene glycol sprayed onto coils.

Table 1.2: Summary of experimental studies on evaporative cooling of HX coils utilized as condensers or fluid coolers (contd.).

Author	Coil	V _a (m/s)	M _{ww} (kg/m ² -hr)	M _{ww} (g/m ³ -s)	Max CER	Max HTC Enhancement	EER% Improvement
Nakayama <i>et al.</i> , 1987	plain and micro-finned tubes; 4 bank (8-11 rows)	1 to 3	50-390	87-677	6		
Fischer and Sommer, 1988	plate fin HX	1 to 5	120	-			
Oshima <i>et al.</i> , 1992	6 row spiral fin tube HX	0.5-3	171-452	136-359	4		
Dreyer <i>et al.</i> , 1992	elliptical fins and tubes, vertical air flow	1.6-6.5	35-450	-	3.5		
Walczyk, 1993	1 to 4 row spiral fin	1.2-2.6	189-315	309-515	2.7- 1 row, 1.65 4 row		
Erens and Dreyer, 1993	elliptical fins	2.2-6.4	450		horizontal: 3.9 inclined: 4.5		
Faca and Olieveira, 2000	bare, horizontal air	0.7-2.1	1050-6950	188-1245			
Ettouney <i>et al.</i> , 2001	Plain fin, FPI 10	6	3168-6840	22000-47500	1.3		
Hasan and Siren, 2003	Bare, plain fin	1.5-3.6	7867-17482	8741-19424	2.4		
Sarker <i>et al.</i> , 2009	circular fin	1.6-3.1	upto 12266	1521	fin tube 1.67, bare tube 3.56**		
Wiksten and Assad, 2010	wavy fin, FPI 9.5; 10 banks (18 rows)	3.5	6000	5747			
Bell <i>et al.</i> , 2011	louver	1 to 3	1936			2.4	

Table 1.2: Summary of experimental studies on evaporative cooling of HX coils utilized as condensers or fluid coolers (contd.).

Author	Coil	V_a (m/s)	M_{ww} (kg/m ² -hr)	M_{ww} (g/m ³ -s)	Max CER	Max HTC Enhancement	EER% Improvement
Popli <i>et al.</i> , 2012a	flat tube louver fin	1.2-3.5	907-2448	5039-13600	3.5		
Popli <i>et al.</i> , 2012b	round tube slit fin	1.4-3.5	576	1600	2.8		
Zhang, 2012	flat tube louver	1.4-3.5	72-365	253-1267	deluge and precool + deluge 3; precool 1.8		
Chen <i>et al.</i> , 2013	flat tube, louver	0.8-5.3	12.4-62	181-907	4.1		

Table 1.3: Major findings of experimental studies on evaporative cooling of finned HX coils utilized as condensers or fluid coolers.

Author	Major Findings
Sen, 1973	<ul style="list-style-type: none"> • atomization spray nozzle to precool the inlet air but no droplet arrestors were installed so a significant portion of un-evaporated droplets carried by inlet air stream wetted HX • Capacity enhancements: Bare tube 20-16; Short fin HX 16-12.5; Long fin HX 4.1 • Capacity enhancement for shorter fins (0.375") with wide spacing (0.563") approximately four times (16 to 12.5) that obtained using longer fins (0.875") with short spacing (0.125") • Dry case capacity: <ul style="list-style-type: none"> • finned coil = 4.4 to 7.4 times bare tube • long fins, low Fp = 2 to 2.5 times short fins, high Fp • Dry out at lower spray rates, but disappeared at spray rates > 500 kg/m²-h • Low spray rate rear tube side remains dry, high spray rate water accumulated in rear side which also had maximum heat transfer • Empirical model proposed ; no accuracy reported
Simpson et al., 1974	<ul style="list-style-type: none"> • heat transfer coefficient (HTC) enhancement ratio 5 - 16 for different fin geometry, highest enhancement for wide fin spacing and low fin height
Yang and Clark, 1975	<ul style="list-style-type: none"> • spray cooling did not affect pressure drop • HTC enhanced by approximately 40% and 45% for air Re_a of 1,000 and 500, respectively • 12.7% HTC enhancement for Re_a=7000 due to break up of liquid film on fin surface • spraying water and ethylene glycol provided similar improvement
Tree et al., 1978	<ul style="list-style-type: none"> • spray rates between 10 to 30 g/s maximum capacity enhancement of 40% • at same spray rates and air velocity, when spray droplet size was increased from 64 to 440μ and 3300μ, capacity enhancement reduced by up to 15% and 20% respectively • direct evaporation due to increased coverage area and uniformity of spray was found to be a much more significant parameter in capacity enhancement
Kried et al., 1979	<ul style="list-style-type: none"> • capacity enhancements of approximately 3 to 7 for air velocities 0.9 to 1.8 m/s • Maximum enhancement was attained at lowest ITD (process fluid and air inlet temperature difference), which also corresponded to highest ambient temperature conditions when evaporative cooling would be most required. • Due to distributor design dry out regions were observed even at high deluge rates but since high enhancements were obtained authors concluded that uniform wetting was not essential
Parry et al., 1979	<ul style="list-style-type: none"> • CER between 2 and 7, at inlet air RH between 70% and 10% • Droplet carryover at Va > 1.83 m/s, and $\dot{m}_{ww} > 620$ g/s-m of HX tube length • no change in capacity when changing HX angle from 0° to 16° • addition of surfactants increased heat transfer by 20-30% and ΔPa by 100% due to bubble formation • deluge cooling provides rivulet flow not thin film on fins • HX performance increases at higher deluge flow rate, and lower ITD between inlet air and process fluid
Mori and Nakayama, 1980	<ul style="list-style-type: none"> • Micro-finned tube coils obtained 20% HTC compared to bare tubes • large amount of spray water retained by first tube bank and subsequent banks are dry • micro-grooving increased heat transfer by enhanced wetted area • thin film increased evaporation rates; bridging/thick film caused heat transfer resistance

Table 1.3: Major findings of experimental studies on evaporative cooling of finned HX coils utilized as condensers or fluid coolers (cont'd).

Author	Major Findings
Guinn and Novell, 1981	<ul style="list-style-type: none"> • spraying on front face of condenser in a 3-ton split AC unit with flat tubes • EER increased from 12 to 19% and compressor head pressure reduced from 9 to 17% • Condenser capacity increased by 4.5 to 8.7 % compared to dry case
Hauser <i>et al.</i> , 1982	<ul style="list-style-type: none"> • thermal performance of spiral wound finned HX 35% higher than plane fin HX, but at equal air-side pressure drop both fins had similar performance • air side pressure drop for spiral wound HX is up to 25 Pa higher than plate fin or wavy fin HX • spiral wound HX capacity reduces when core angle increased from 15 to 20, so not suitable for A-type coils • wavy-fin HX gives best heat transfer performance at similar fan power consumption in dry conditions • In wet conditions spiral wound HX has 40% higher heat flux at same fan power • at air velocity more than 1.37 m/s deluge cooling effect started to decrease as water blown out of HX • In dry conditions at 2.71 kg/s/m² air flow spiral fin HX has 45% higher pressure drop compared to slit fin and 30% higher to wavy fin HX • In wet conditions, at 1.35 kg/s/m² air flow rate pressure drop of spiral fin HX is more than that of wavy and slit fin HX by 50% and 100% respectively • analytical model for calculating heat transfer and evaporation rate from surface of wet finned HX • empirical correlation for predicting deluge HTC, based on which enthalpy difference driving potential based analytical model predicts deluge capacity • maximum enhancement ratio of 4.5 achieved for spiral fin HX
Hauser and Kreid, 1982	<ul style="list-style-type: none"> • capacity enhancement found to vary between 2 and 5 • CER of at ITD 50°F and 75%RH and CER of 5 at ITD 20°F and RH 25% • higher enhancement for same pressure drop for wavy fins (1.2 times) compared to spiral fin HX dues to higher pressure drop using spiral fins • droplet carryover at air velocity more than 1.8 to 2.4 m/s • Extended model to predict evaporation rates but 20% over predictions
Fisher <i>et al.</i> , 1983	<ul style="list-style-type: none"> • Tested vertical falling film evaporative condenser was tested • Hybrid cooler was found to increase thermal efficiency of power stations by reducing condenser temperature, and offer the possibility of reducing condenser size, fog elimination etc. • Tests under deluge cooling caused droplet carryover and authors recommended use of mist eliminators
Simpson <i>et al.</i> , 1984	<ul style="list-style-type: none"> • Capacity enhancement 1.3 • No increase in ΔP_a for spray cooling for high fin pitch and low fins • dry patches on fin for surface temperature exceeding air temperature by > 30°C • single and two phase empirical correlation for pressure drop (friction coefficient) and heat transfer (Nu number)

Table 1.3: Major findings of experimental studies on evaporative cooling of finned HX coils utilized as condensers or fluid coolers (cont'd).

Author	Major Findings
Nakayama <i>et al.</i> , 1987	<ul style="list-style-type: none"> • no increase in ΔP_a while CER = 4 to 6 for bare and micro-finned tubes • micro-grooving tubes increases HTC by 20-40% • empirical model to correlate wetted area to spray rate, evaporation potential, and V_a • identified four wetting zones based on tube surface measurement for each pass • largely downward flow of wetting water due to low air velocity
Fischer and Sommer, 1988	<ul style="list-style-type: none"> • HX tested in horizontal and vertical positions • bridging found to be a function of air flow rate only • vertical HX achieves lower enhancement than horizontal, but higher ratio of enhancement per unit pressure drop • max enhancement of up to 2
Oshima <i>et al.</i> , 1992	<ul style="list-style-type: none"> • presented simple design procedure for commercial finned-tube HX assuming 1) complete wetting of HX and 2) inlet saturated, and 3) saturated air within HX, model valid for spray density > 350 kg/m² h • air side heat transfer varied from 93 to 418 W/m²/h depending on amount of spray water • spray water temperature not as important as amount of spray in capacity enhancement
Dreyer <i>et al.</i> , 1992	<ul style="list-style-type: none"> • Horizontal coil arrangement; CER up to 1.5 to 3.5, CER function of spray density and RH of inlet air • spray cooling for less than 2.5 mm fin spacing greatly increases air side pressure drop • short thick fins at more than 3-4 mm spacing work better in wet conditions • severe water retention in 25% coil i.e. downstream tube for $1.1 V_{crit} < V_{max} < 1.4 V_{crit}$
Walczyk, 1993	<ul style="list-style-type: none"> • maximum enhancement ratio of approximately 2.7 • spray flow rate and not droplet size affects the HX capacity
Erens and Dreyer, 1993	<ul style="list-style-type: none"> • Horizontal coil arrangement • empirical correlations for mass transfer and ΔP_a developed for cross-flow evaporative cooler; accuracy within 10% • CER for horizontal tubes: 3.9; tubes inclined at 60° with horizontal: CER = 4.5
Ettouney <i>et al.</i> , 2001	<ul style="list-style-type: none"> • Horizontal coil arrangement • Condenser efficiency increased at lower M_{ww}/M_a ratio and higher ITD • Parallel condenser configuration allows maximum flow rate; series configuration allows maximum sub-cooling • Evaporative cooling CER up to 1.6; potential for reducing HX area and fan power compared to air cooled unit • Correlation for condenser capacity within 7% of experimental data
Hwang <i>et al.</i> , 2001	<ul style="list-style-type: none"> • The performance of an innovative evaporatively cooled condenser was compared with a conventional air-cooled condenser for a split heat pump system • System capacity improvement of 1.8 to 8.1%, COP improvement of 11.1 to 21.6%, and SEER improvement of up to 14.5% over the baseline air-cooled unit • Condensing temperature of evaporative cooler was found to be limited by wet bulb temperature of air

Table 1.3: Major findings of experimental studies on evaporative cooling of finned HX coils utilized as condensers or fluid coolers (cont'd).

Author	Major Findings
Hasan and Siren, 2003	<ul style="list-style-type: none"> • Horizontal coil arrangement • 92% to 140% increase in heat transfer rate with finned HX compared to bare HX • Lower fin efficiency for wetted coils due to overall higher mass transfer coefficient • Bridging may result in lower heat and mass transfer rate; larger resistance to heat transfer due to thick water film • No bridging at Fp 6.1 mm and 11 mm
Hasoz and Kilicarslan, 2004	<ul style="list-style-type: none"> • Horizontal coil arrangement • experimental investigation of air water and deluge evaporatively cooled condenser units coupled to refrigeration cycle • refrigeration capacity and COP of evaporatively cooled unit higher by 31 and 14.3% compared to air cooled • capacity and COP of water cooled higher than evaporatively cooled by 2.9 to 14.4% and COP by 1.5 to 10.2% • Although water cooled unit performs better in some operating conditions compared to evaporatively cooled unit, evaporatively cooled units use much less water and initial cost is lower due to less space requirement and components
Sarker <i>et al.</i> , 2009	<ul style="list-style-type: none"> • Horizontal coil arrangement • Finned HX capacity 22% and 260% higher than bare tubes in wet and dry conditions respectively • To achieve same capacity in wet conditions finned tube HX required 80% lower air mass flow rate and 39% lower wetting water • ΔP_a for finned coils twice that of bare coils
Wiksten and Assad, 2010	<ul style="list-style-type: none"> • numerical model of fully and partially wetted wavy fin HX with non-unity Lewis number with emphasis on heat and mass transfer in air flow direction through HX depth • defined wetting parameter (0 to 1) which was calculated and results validated based on experimental data (black box model, no measurements made in HX depth only inlet and outlet) • no enhancement results reported
Bell <i>et al.</i> , 2011	<ul style="list-style-type: none"> • In dry conditions air side particulate fouling increases pressure drop by 50% with 600 g of fouling, however thermal performance is not affected • In wet conditions fouling has not impact on HX capacity or pressure drop
Popli <i>et al.</i> , 2012a	<ul style="list-style-type: none"> • CER from 2.6 to 2.8 and $PR_{\Delta P_a}$ from 2.3 to 2.4 respectively • Increasing inclination angle of HX from 0° to 20° increases capacity by 8.6%, and ΔP_a is unaffected • Droplet carryover at $V_a > 2.5$ m/s (8.2 ft/s)
Popli <i>et al.</i> , 2012b	<ul style="list-style-type: none"> • CER from 2.7 to 3.5 and $PR_{\Delta P_a}$ from 7 to 14 • Increasing inclination angle of HX from 0° to 20° increases capacity from 23-47%, and ΔP_a by 100%
Zhang, 2012	<ul style="list-style-type: none"> • Amount of unevaporated water increases with increase in spray rate; drain or recirculation recommended at higher spray rates • No significant increase in $PR_{\Delta P_a}$ compared to dry case • At $V_a = 1.8$ m/s water drained on coil face; at $V_a = 3.2$ m/s water drained at back of HX; at $V_a = 2.3$ m/s equal drainage in front and back of coil • 4 to 12% higher heat transfer rate for spray nozzles oriented at 10 from horizontal compared to horizontal nozzles.

Table 1.4: Major findings of experimental studies on evaporatively cooled bare-tube HX coils utilized as condensers or fluid coolers.

Author	Major Findings
Chen <i>et al.</i> , 2013	<ul style="list-style-type: none"> • Enhancement ratios and pressure penalty of up to 4.1 and 1 respectively at 40% RH and 2.8 and 1.25 respectively at 80% RH • Water blockage observed at higher spray rates and low air velocities, which reduced capacity enhancement • At spray rate of 0.5 g/s, lower air velocity desired <ul style="list-style-type: none"> • at spray rate of 2.5 g/s, higher velocity required to clear blockages
Mizushima <i>et al.</i> , 1967	<ul style="list-style-type: none"> • Tested horizontal bare round tube HX with triangular pitch (0.0254 to 0.08 m) • water/air ratio = 0.008 to 0.027 • proposed empirical equations for HTC and MTC
Scherber <i>et al.</i> , 1972	<ul style="list-style-type: none"> • spray cooling studied on circular, elliptical and semi-circular composite tube geometry at 2.2 to 6.3 g/s spray rate • heat transfer increases with increase in ratio of spray water-flow to air-flow rate, but insensitive to Re number (air side) and between air and hot surface • Increase in capacity found to be a function of area covered by liquid film
Dreyer and Erens, 1990	<ul style="list-style-type: none"> • Tested bare tube HX with 22 rows, tube OD/ID 38.1/34.9 mm steel tubes, triangular geometry • Spray rate: 41.6 to 166.6 g/s/ unit length of HX tube (up to 450 kg/m²/hr) • determined mass transfer and pressure drop correlations experimentally for crossflow evaporative cooler
Knebel, 1997	<ul style="list-style-type: none"> • compared the system level electrical energy demand for air, water, evaporative cooled HX • evaporative cooling reduced electrical energy demand and consumption of HVAC systems by 20-40% at same condenser capacity obtained using water cooled condenser • Furthermore evaporative cooling reduces recirculating water consumption from 3 GPM/ton for water
Costenaro, 2001 and Kutscher and Costenaro, 2002	<ul style="list-style-type: none"> • total consumption of 230 g/s to 880 g/s for a 1 MW geothermal plant • Evaluated one direct evaporative cooling method i.e. deluge cooling, and three indirect evaporative cooling, i.e. muntners cooling media pads, spray cooling inlet air to wet bulb temperature, and a combination of muntners and spray cooling • spray and hybrid cooling payback period evaluated as 10 and 11 years respectively • deluge cooling with maximum enhancement rates of 5 to 7 • scaling in deluge cooling minimized by rinsing with pure water • Muntners cooling not a viable enhancement option
Wang <i>et al.</i> , 2014	<ul style="list-style-type: none"> • COP increase from 6.1% to 18%, compressor power reduction of 14.3% for an AC system with evaporatively media cooled condenser • 2.4 C to 6.6 C saturation temperature drop through condenser

Table 1.4: Major findings of experimental studies on evaporatively cooled bare-tube HX coils utilized as condensers or fluid coolers (cont'd).

Author	Major Findings
Kim and Kang, 2003	<ul style="list-style-type: none"> • investigated effect of hydrophilic plasma treatment on evaporative heat transfer of plain, spiral, corrugated, and low finned copper tubes • refrigerant sprayed on tubes • hydrophilic coating induces film flow on tubes, whereas uncoated tubes have sessile drops • When the tubes were surface-treated, the UA values were enhanced by 40–77% for a plain tube, 6–11% for a spiral tube, 5–12% for a corrugated tube, and 7–23% for a low-finned tube • large drops introduced from the spray sit on a non-wetting tube for a certain time while providing a heat transfer path having relatively high thermal resistance, until they leave the surface due to disturbance of other drops sprayed from the nozzle near themselves.
Hosoz and Kilicarslan, 2004	<ul style="list-style-type: none"> • bare copper tubes used as air and evaporatively cooled condenser, and packed column used for indirect water cooled unit • experimental investigation of air water and evaporatively cooled condenser units coupled to refrigeration cycle • refrigeration capacity and COP of evaporatively cooled unit higher by 31 and 14.3% compared to air cooled • capacity and COP of water cooled higher than evaporatively cooled by 2.9 to 14.4% and COP by 1.5 to 10.2% • Although water cooled unit performs better in some operating conditions compared to evaporatively cooled unit, but evaporatively cooled units use much less water and initial cost is lower due to less space requirement and components
Silk et al., 2006	<ul style="list-style-type: none"> • straight, cubic and pyramid type microfins machined on the top surface of heated copper blocks with 2.0 cm² cross-sectional areas • 75% enhancement for straight fins at 30 angle when compared to flat surface at 0 angle, but 11% increase compared to straight fin surface at 0 angle
Liu, 2009	<ul style="list-style-type: none"> • The authors reported static contact angles, critical sliding angles, droplet aspect ratios, etc. for several topographical surfaces. • It was recommended that smaller groove spacing, larger depth and steeper sidewalls are favorable for drainage enhancement. • It was found that drainage performance of two different surfaces by comparing their critical sliding angles than by analyzing advancing and receding angle values.
Heyns and Kroger, 2010	<ul style="list-style-type: none"> • Spray cooling of bare tube HX at 0.7 to 3.6 m/s air velocity and 1.8 to 4.7 kg/m²/s spray rate • film HTC found to be a function of air mass velocity, deluge rate, and deluge temp; air MTC and ΔP_a

Table 1.5 presents major findings of experimental studies on air cooled HX coils utilized as condensers or fluid coolers where air is evaporatively precooled. It must be noted that Table 1.5 only summarizes a few important studies on air cooled HX where air itself is precooled using evaporative cooling and is not an exhaustive review. However, it gives an idea of the enhancements obtained through evaporative cooling technologies such as media pads and mist cooling where the wetting water does not directly contact the HX surface.

Table 1.5: Major findings of experimental studies on air cooled HX coils utilized as condensers or fluid coolers where air is evaporatively precooled.

Author	Major Findings
Hirasawa et al., 1983	<ul style="list-style-type: none"> • optimization study of mist cooled condensers for Rankine cycle geothermal power plants using box method • optimum HX geometry was found to be one with 3 rows, 4 passes, triangular tube pitch 50 mm, and operating conditions of $V_a = 2.2$ m/s, mist flow rate = 0.08 kg/m²/s
Hamlin et al., 1998	<ul style="list-style-type: none"> • Evaporative cooling used to enhance performance of HX in air cycle. Air-assisted atomizers perform better compared to pressure atomizers, and externally mixed air assisted atomizers are found to perform better than internally mixed.
Hwang et al., 2001	<ul style="list-style-type: none"> • bare tubes submerged in water, rotating disks carry thin film of water which evaporates in air stream, thus cools down water in which tubes are submerged • innovative evaporatively cooled condenser design has 1.8 to 8.1% higher capacity, 11.1 to 21.6% higher COP, higher SEER by 14.5% compared to air-cooled condenser • Performance of evaporatively cooled condenser compared with conventional air cooled condenser for a split heat pump system
Masri and Therkelsen, 2003	<ul style="list-style-type: none"> • Tested A - type coils, pre-evaporation of sprayed water into air stream before hitting air cooled HX condensing steam • Total wetting water flow 2 to 20 GPM (Flow per nozzle, 0.18 to 0.36 gpm) • Study presents a field testing of spray evaporative cooling • cooling effect was a strong function of ambient wet bulb depression and spray flow rate • Recommended (ambient temperature > 90° F and relative humidity < 40 percent) as most beneficial conditions for using spray cooling, where cooling of up to 80% or more of wet bulb depression was achieved • pintle type nozzles produce uneven droplets compared to swirl type nozzles
Hajidavalloo and Eghtedari, 2010	<ul style="list-style-type: none"> • 1.5 Ton Mitsubishi split-air conditioner retrofitted with cellulose media pad sprayed with 60g/s water to precool condenser air • power consumption can be reduced by 20% and COP improved by 50%

Although it is known that capacity enhancements would be lower, the technologies discussed in Table 1.5 are used mainly to avoid potential corrosion issues on HX metal surface.

Although limited in number, published experimental studies have established that evaporative cooling could significantly enhance heat transfer capacity of bare and finned-tube HXs. This could enhance power plant efficiency, refrigeration cycle COPs and offer substantial energy savings. Currently, 1) lack of availability of wetting water, 2) corrosion/fouling issues, and 3) lack of acceptable theory for predicting enhancement ratio, limits the wide-spread application of evaporative cooling technology. In addition to avoid the problems with water cooled systems, manufacturers want to move towards air cooled dry systems which may be oversized to take care of peak load in summer months. However, corrosion issues can be mitigated or reduced using reverse osmosis, ionic exchange etc. which have become cheaper in the last few years.

Table 1.6 Overview of Simulation/Modeling studies on direct evaporative cooling of heat exchangers.

Study	HX	Complete Wetting Assumption	Model Type	Fouling	Validation (%)
Mizushima et al 1967; 1968	Bare tube	Yes	• Empirical	No	
Kreid et al , 1979	Finned tube, vertical	Yes	• analytical	No	20-25%
Leidenfrost and Korenic (1982)	Bare tube	Yes	• analytical	No	-
Webb, 1984	Bare tube, Evaporative cooler and condenser; horizontal	Yes	• Correlation • NTU based approximate method	No	-
Erens and Dreyer, 1988			•		
Peterson et al 1988	Bare Tube	Yes	• 1-D numerical	No	30
Dreyer, 1993	Bare tube	No	• analytical	No	20
Zalewski 1993, 1997	Evaporative Condenser, bare tube	Yes	• Segmented Numerical	No	8-33
Alonso et al. 1998	Evaporative cooler	Yes	• Segmented	No	
Ho Song and Lee 2003	Evaporative cooler	Yes	• Segmented • Porous media • 2D Numerical	No	-
Hasan and Siren, 2003	Bare and fin tube HXs	Yes	• Segmented • Analytical	No	

Table 1.6 Overview of Simulation/Modeling studies on direct evaporative cooling of heat exchangers (cont'd).

Study	HX	Complete Wetting Assumption	• Model Type	Fouling	Validation (%)
Stabat and Marchio, 2004	Bare tube and fin tube, horizontal	Yes	• ϵ -NTU method	No	10%
Qureshi et al. 2006, 2011	Evaporative Condenser	Yes	• Segmented • numerical	Growth model	5.6
Ren and Yang, 2006	Bare tube, horizontal	No	• ϵ -NTU method	No	
Youbi et al. 2007	Fin tube	Yes	• Segmented • Correlation	No	
Wiksten & Assad 2009	Fin Tube	No		No	
Mehrabian and Samadi 2010	Bare tube HX, horizontal	Yes	• Numerical	No	5
Heyns and Kroger, 2010	Bare, Horizontal	Yes	• Analytical + empirical heat & mass transfer correlations	No	-
Jahangeer, et al, 2011	Single bare tube, horizontal	Yes	• numerical	No	-
Papaefthimiou, et al, 2012	Bare tube, sprayed , horizontal	Yes	• numerical	No	5.39
Zheng et al. 2012	Bare tube	Yes	• Segmented	No	6
Zhang et al. 2014	Flat tube louver fin	No	• Segmented • Correlation	No	20

Note: Conduction neglected for all studies.

1.7 Summary of literature review and research gaps

The following general conclusions could be drawn from experimental studies on wetted HXs:

- Higher CER obtained at lower air velocities
- Deluge cooling droplet carryover at HX frontal air velocity > 1.8 to 2.5 m/s
- $PR_{\Delta Pa}$ is a function of receding not advancing contact angle
- Spray droplets sized $< 50\mu$ have higher potential for being carried downstream without wetting HX. Also they have a higher chance of evaporatively cooling air stream than HX coil surface.
- CER is a function of baseline dry case capacity. CER could be lower for HXs optimized for dry cases even when no bridging occurs.
- Addition of surfactants to wetting water causes foaming and may not be suitable method for reducing water/metal surface tension to enhance droplet spread ability/wetting
- After certain flow rate, further addition of wetting water to HX causes negligible increase in capacity enhancement
- CER is a strong function of ITD and inlet air evaporation potential (in measurable parameters higher temperature difference between inlet air and process stream, and RH of inlet air)
- Even a small amount of wetting water is enough to cause significant CER
- Spray cooling water temperature does not affect HX performance, but for deluge cooling water temperature is a significant parameter
- Spray cooling droplet size does not affect HX performance more than 10-15%
- Spray droplets injected in the direction of air flow causes larger enhancement than injected counter to air flow direction

- Control of inlet air RH is critical to obtain accurate experimental data, furthermore this RH should be maintained at same constant value for both dry and wet cooling cases

The following research gaps were identified from experimental studies on wetted HXs:

- **No information on spray droplet size**

Most experimental studies do not typically provide any information on spray droplet size and therefore conclusion from Tree *et al.*, 1978 that spray droplet size does not affect HX capacity significantly, i.e. 10-15% for a very wide droplet size ranging from 64 to 3300 μ cannot be cross-verified. Furthermore retention of wetting water in upstream section of HX has been reported by Mori and Nakayama (1980), Dreyer et al., (1992) and Popli et al. (2012a) and (2012b).

- **No information on wetted water quality**

It is well understood that higher dissolved salt concentration or water hardness causes fouling. The mineral build-up on fin surface adds to thermal resistance and reduces HX capacity. However no author reports water quality parameters such as alkalinity and hardness.

- **Limited or no studies on HXs with wavy fins**

Breakup of published experimental studies on wetted HXs based on fin geometry is presented in Table 1.6.

Table 1.6: Breakup of published experimental studies on wetted HXs based on fin geometry.

Fin geometry	Number of studies
circular, elliptical or spiral	10
louver	5
plain	8
Micro-finned	2
Wavy	1

It is important to note that among the various fin geometries studied under wet conditions, louver and wavy fin geometry are most widely utilized for condenser and cooler applications. Also wavy-fin configuration is preferred over louver fins, as unlike louvers, wavy fins do not retain sprayed water and reduces potential bridging conditions.

However, except one experimental study by Hauser and Kreid (1982) there is no published work in open literature on evaporative cooling of wavy fin HXs. Moreover Hauser and Kreid (1982) studied deluge cooling while spray cooling of wavy fins has not yet been investigated and experimental work is required to enhance understanding of wavy fin performance in wet conditions and to provide data for improving HX capacity prediction capability.

- **Effect of hydrophilic coating of HX fins**

The magnitude of capacity enhancement obtained using evaporative cooling is directly related to uniform wetting of fin surfaces among other parameters. Some of the authors have therefore attributed a lower capacity enhancement ratios (Hauser et al., 1982; Hauser and Kreid,1982; Kreid et al.,1979a) for complex fin geometries and HXs with longer depth in direction of air flow to non-uniform water distribution. Ideally a thin layer of wetting

water should be maintained over the cooling surface, but such a layer is often not formed on the entire fin area i.e., uniformly in depth of coil. This limits overall heat transfer augmentation as a significant portion of coil may remain dry.

In a recent study, Lee et al. (2005) experimentally tested evaporative cooling enhancement on untreated and hydrophilic porous layer coated inclined surfaces, and found that latent heat transfer could be enhanced by approximately 80% for hydrophilic coated surfaces. Ma et al. (2007) tested effect of hydrophilic coating on air side heat transfer and friction factors on wavy fin and tube HXs under dehumidifying conditions (HX used as evaporator) and found that hydrophilic coatings could reduce air-side pressure drop by up to 44% and improve heat transfer by up to 35%. The authors attributed improved performance to thin film of condensate water on hydrophilic coated fins compared to droplets of condensate on uncoated fins. Kim and Kang (2003) observed similar heat transfer enhancement for hydrophilic coated tubes in the evaporator of absorption chiller due to higher heat transfer area of thin films compared to sessile drops on untreated tubes. Thus, hydrophilic coatings could offer a potential solution for non-uniform wetting of HXs but, to the best of author's knowledge no study on deluge or spray evaporative cooling performance of hydrophilic coated wavy-fins was found in published literature and was identified as a research gap.

- **Visualization of wetted coils**

The amount of area wetted using deluge or spray cooling is a critical parameter that decided CER obtained. Moreover, lack of qualitative or quantitative information of this parameter is largely responsible for incorrect wet case capacity predictions using analytical or numerical models.

Most of the studies assume $Le = 1$ or completely wetted HX fins, which is well known to be an incorrect assumption especially for deeper coils with compact fin spacing. Yet, neither studies on improving visualization of wetted fin areas nor any quantifying the amount of HX that may be wetted could be found in the literature. *This is a significant research gap which would significantly further the current body of knowledge on wetted coils and would be partly addressed in this Dissertation along with identification of challenges in visualization studies.*

1.8 Research objectives

The overall goal of this study is to measure the thermo-hydraulic performance of RTHX with herringbone wavy fins utilized as hybrid wet/dry HX using different evaporative cooling methods and to develop means to improve its performance.

The following tasks were defined for the work presented in this Dissertation:

Experimental construction and measurements

- Design and construct test setup capable of testing HXs as process fluid coolers for up to 17 kW cooling capacity. The tests facility would be designed to closely follow standard ASHRAE 41.2 and have features for wetting water visualization and varying HX inclination angle with the vertical from 0° to 60° .
- Measure HX capacity and air-side pressure drop of three RTHX with herringbone wavy fins in hybrid wet-dry conditions.
- Quantify effect of fin spacing and hydrophilic coating on wavy fin RTHX performance under conventionally utilized deluge and front spray evaporative cooling technologies.

Understand wetting water flow mechanisms and distribution in HX volume

- Develop enhanced air-side visualization approach to both quantitatively and qualitatively study HX air-side wetting water flow profile and understand wetting mechanisms for wetting water distribution approaches as a function of HX air velocity and wetting water flow rate.

Develop and test novel wetting water distribution methods

- Determine maximum theoretical HX capacity enhancement
- Develop and test novel methods of wetting HX coils to achieve the maximum theoretical capacity enhancement ratios at $PR_{\Delta Pa}$ of 1
- Establish performance parameters to understand and compare evaporative cooling technologies

1.9 Dissertation outline

This work presented in this Dissertation is structured as follows:

Chapter 1 describes the need for studying hybrid operation of HX coils utilized as coolers or condensers and summarized published experimental studies on the topic. Research gaps were identified which helped formulate the objectives of work presented in this Dissertation.

Chapter 2 describes the details of experimental setup design, construction, measuring instrumentation, operational capabilities and uncertainty analysis.

Chapter 3 presents experimental results for dry cooling of HXs which serve as baseline values for studying magnitude of capacity enhancement using various methods of wetting fin surfaces.

Chapter 4 discusses designs of wetting water distributors and experimental results of deluge cooling performance enhancement on wavy fin HX. Preliminary methodology to enhance visualization of wetted coils is also presented which could be utilized for bulk validation of CFD studies.

Chapter 5 describes selection criteria for spray nozzles, experimental results of spray cooled wavy fin HXs, effect of spray configuration, fin spacing, inlet air temperature and hydrophilic coating on wavy fins. Performance comparison of spray, deluge and air cooled HXs is also presented along with discussion on bottlenecks for further capacity enhancement at $PR_{\Delta Pa}$ of 1.

Chapter 6 presents the technology: brainstorming, development and implementation of a novel internal jet spray cooling method proposed in this Dissertation. It also reports the performance comparison of continuous and intermittent internal jet spray technology for evaporatively cooled wavy fin HXs, and their comparison with conventional evaporative cooling technologies.

Chapter 7 focuses on difficulty associated with visualization of wetting water distribution in HX depth and the need for enhanced air-side visualization methods which had been identified as a major research gap in published literature. A novel visualization method is proposed and implemented, which consisted of borescope assisted flow mapping of deluge and front spray cooling as a function of air velocities and wetting water flow rates. In addition a quantitative method to support visualization results is also presented for which a partitioned tray was utilized to separately record mass flow rate of wetting water flowing at HX bottom outlet. Furthermore a comparison of obtained HX wetting profiles is made with measured performance data presented in Chapters 3 to 6.

Conclusions on the major findings of this Dissertation are outlined in Chapter 8.

Chapter 2 Experimental test facility

2.1 Introduction

The experimental setup mainly consists of air-side, process-fluid and wetting-water loop described in Sections 2.2, 2.3 and 2.4, respectively. All experiments were conducted within an environmental chamber which simulates and controls desired HX inlet temperature and RH conditions. Temperature was controlled within an uncertainty of ± 0.5 °C and RH within $\pm 2\%$. Environmental chamber was equipped with a 35 kW vapor compression system which provided cooling or heating while RH was controlled using a PI controlled steam humidifier and silica solid desiccant wheel. An overview of experimental setup for testing wavy fin HXs in dry and wet conditions is shown in Figure 2.1.



Figure 2.1: Overview of the experimental setup placed in environmental chamber.

Each round tube test HX was placed in the test section and then leveled up as shown in Figures 2.2 (a) and (b), to ensure even distribution of wetting water on HX in evaporative cooling test cases.



(a)



(b)

Figure 2.2: Leveling the HX in test section.

A plastic sheet was used to ensure collection of wetting water into the wetting water tank through the drain hole as shown in Figure 2.3.



Figure 2.3: Plastic sheet is used to ensure collection of wetting water into the wetting water tank.

2.2 Air-side loop

The schematic of air-side loop in test facility which is a typical calorimetric wind-tunnel consisting of an axial fan, nozzles, air-mixer, guide vanes, visualization section, and HX is presented in Figure 2.4.

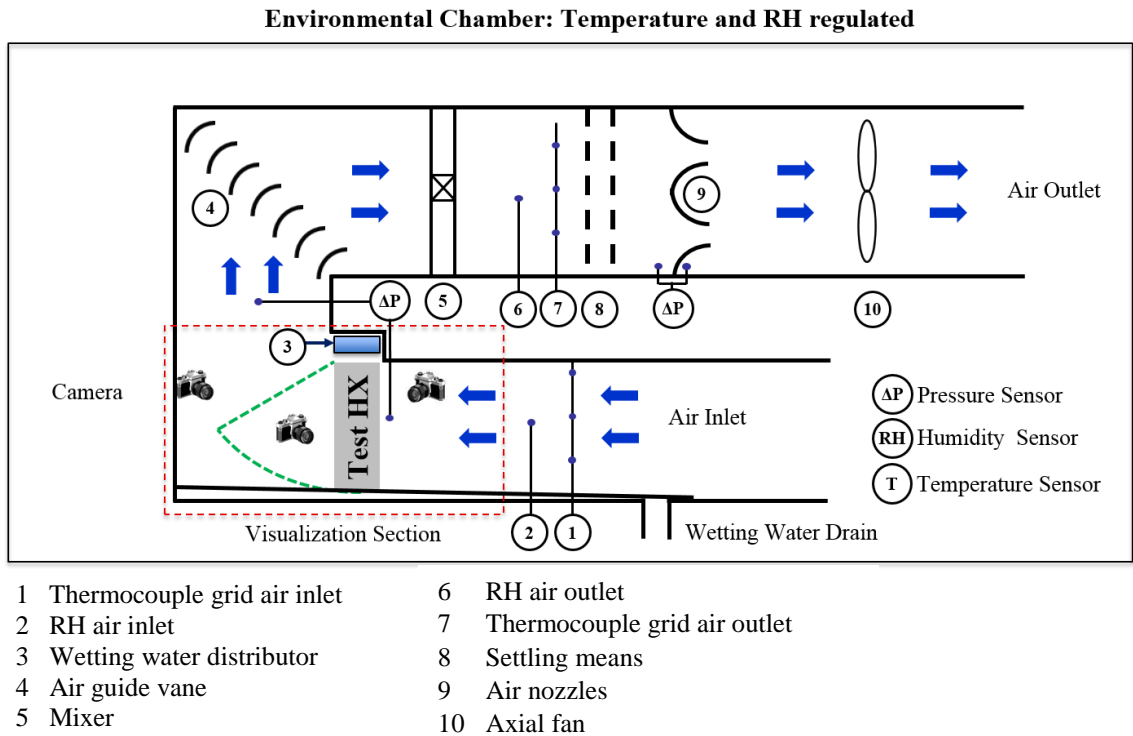


Figure 2.4: Schematic of air-side loop in test setup.

Variable frequency drive (VFD) controlled the speed of axial fan, which drives the air-flow through wind tunnel at the desired test case velocity. Each RTHX was installed in the wind-tunnel with a provision of varying angle of inclination of HX with vertical from approximately 0° to 60° as shown in Figure 2.4. Relative humidity (RH) and temperature of air were recorded at inlet and outlet of HX using a capacitive RH sensor and a 3x3 T-type thermocouple grid, respectively. Air mixer, guide vane and settling means were installed to ensure uniform flow and accurate measurement of RH and temperature measurement at the outlet. The differential

pressures across the HX and nozzles were measured using differential static pressure transducers in accordance with ASHRAE Standard 41.2 (1987). The differential pressure across nozzles was also measured and then used to calculate air velocity at HX face and volume flow rate through the wind tunnel. Gaps between heat exchanger frame and walls of test section were sealed to prevent bypass of air-flow.

2.2.1 Air-side instrumentation

Air side temperature and relative humidity (RH) was measured at the inlet and outlet of HX using a 3x3 thermocouple grid and a Pt-100 RH sensor, respectively. Figure 2.5 shows the thermocouple grid and RH sensor installed at air outlet in test duct.

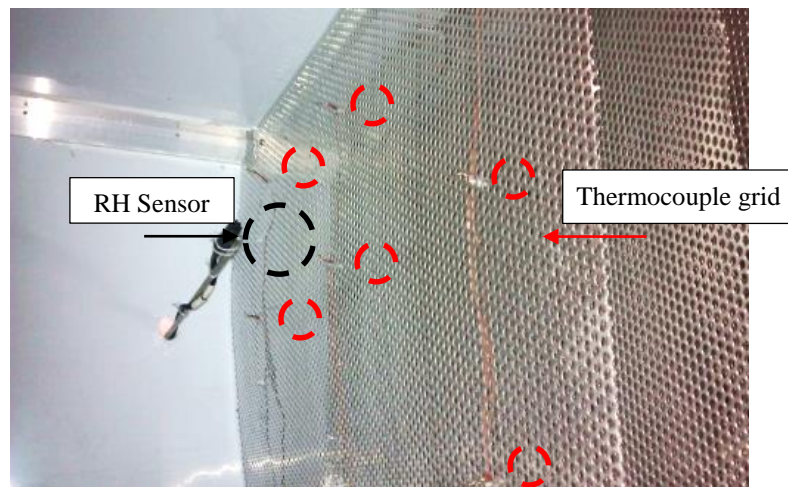


Figure 2.5: Thermocouple grid and RH sensor installed at air outlet in test duct.

The RH sensors are installed in the center most point of the duct to ensure accurate measurement of average RH value as shown in Figure 2.6.

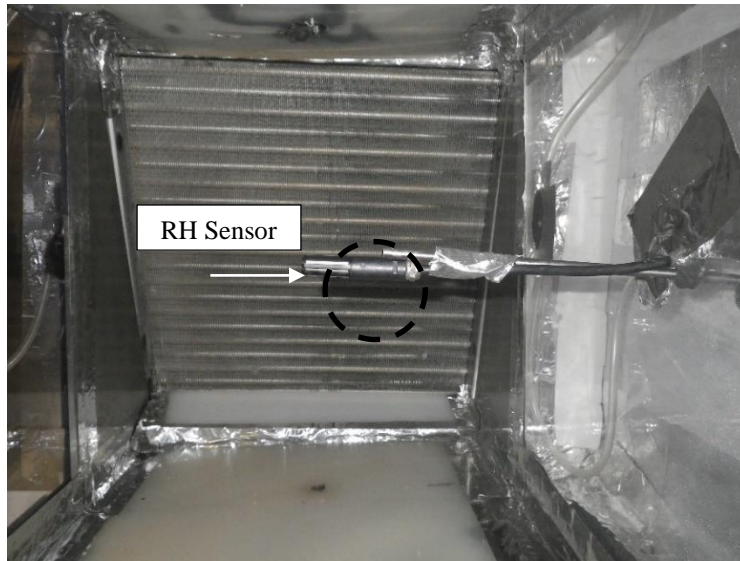


Figure 2.6: RH sensor installed in air duct.

Differential pressure drop across the air-side of HX was measured using static differential pressure transducers installed as per ASHRAE Standard 41.2. A three point measurement was taken across before the HX and a 4-point measurement after the HX as shown in Figure 2.7. Due to wetting water drain a 4-point measurement was not possible at HX inlet section.

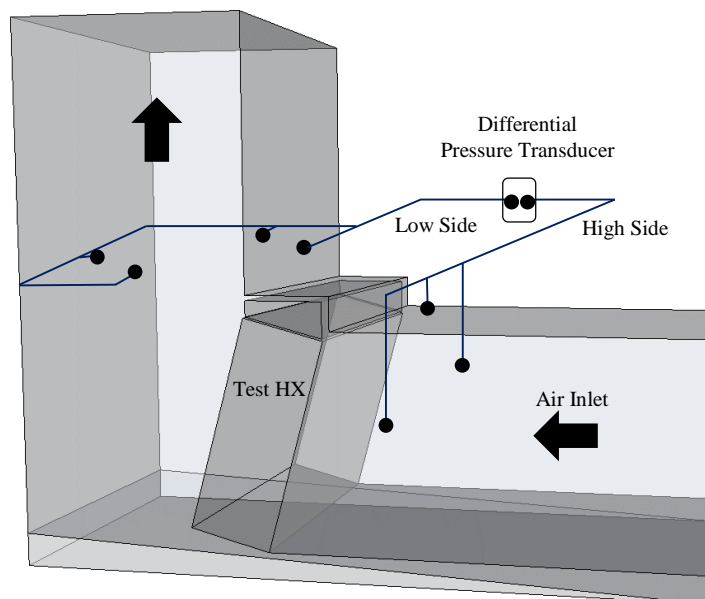


Figure 2.7: Differential pressure measurement across test HX.

Wetting water after wetting the HX flows to the drain as shown in Figure 2.8. This wetting water accumulates at the air inlet section and may cause fluctuations or incorrect measurement of RH. This part is therefore separated using a plate which seals the drain.

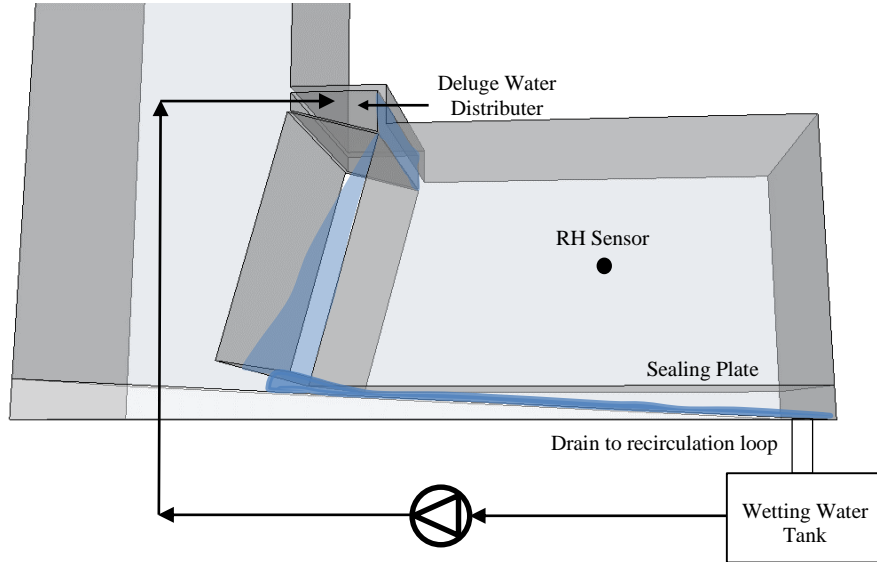


Figure 2.8: Flow path of wetting water to drain.

2.2.2 Air nozzle sizing

The HX frontal air velocity was varied between 1.5 m/s to 3.0 m/s which was decided in a way that it included the range of air velocities typically used for such coils in dry and hybrid operation. Based on the HX frontal area of 0.246 m², we obtain volumetric air flow rate, $\dot{v}_{a, low} = 0.369$ $\dot{v}_{a, high} = 0.738$ m³/s was obtained. ASHRAE Standard 41.2 (1987) states that air velocity through the nozzles should be maintained between 15 m/s to 35 m/s. Since one single nozzle would not cover the desired range of air flow rate, two 5” nozzles were chosen. Thus, cross-sectional area of each nozzle throat could thus be calculated using Equation 2.1 as 0.01266 m².

$$A_{n,th} = \frac{\pi D_n^2}{4} \quad (2.1)$$

$$V_{n, low} = \frac{\dot{v}_{a, low}}{N_n A_{n,th}} = \frac{0.369}{0.01266} = 29.14 \text{ m/s}$$

$$V_{n, high} = \frac{\dot{v}_{a, high}}{N_n A_{n,th}} = \frac{0.738}{2 * 0.01266} = 29.14 \text{ m/s}$$

Thus, nozzles throat velocity remains in the ASHRAE specified range for range of air flow rates to be tested.

2.2.3 Axial fan sizing

The axial fan drives the air-side loop by drawing air out of the test duct. Fan sizing is mainly done based on desired volumetric flow rate at expected pressure drop.

Test HX, duct geometry (90° turns), air mixer, and settling means are the main sources of air-side pressure drop and their expected contribution to total ΔP_{duct} is summarized in Table 2.1.

Table 2.1: Main sources of air-side pressure drop and their expected contribution to total ΔP_{duct} .

Source	ΔP_{duct} (Pa)
Test HX	250
Duct geometry	50
Air mixer	50
Settling means	240
Air-nozzles	486.5
Total ΔP_{duct}	1076.5

Thus, a Hartzell axial fan (Model 52-225TA-STFCL2) which could supply approximately 1.42 m³/s of air at 1245 Pa air-side pressure drop was installed in the test facility.

2.2.4 Air mixer and settling means

As per ASHRAE Standard 41.2 air mixer and settling means are required to be installed before the air nozzle. Air mixers are typically sized based on desired air flow rate. The air mixer shown in Figure 2.9 with volumetric flow rate range from 1.26 m³/s to 0.19 m³/s was selected.



Figure 2.9: Air-mixer attached to polypropylene sheet, ready to be mounted in test section.

Three settling means in the form of three meshes with 5 mm diameter holes are also mounted after the mixer and prior to nozzles as shown in Figure 2.10.

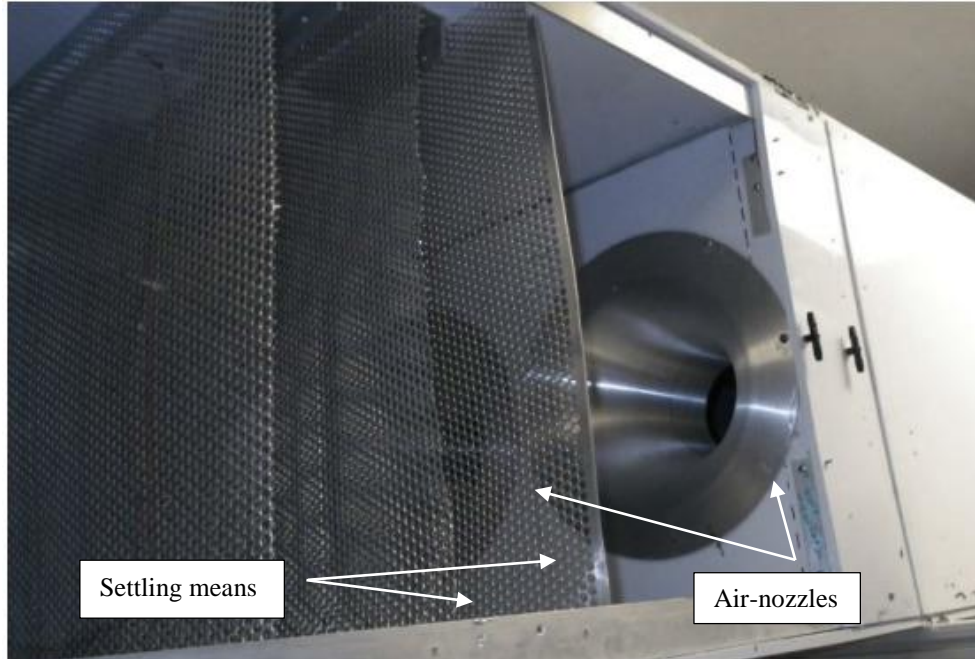


Figure 2.10: Settling means mounted prior to air nozzles.

2.3 Process fluid loop

Schematic of heat transfer fluid-side loop of experimental facility is presented in Figure 2.11.

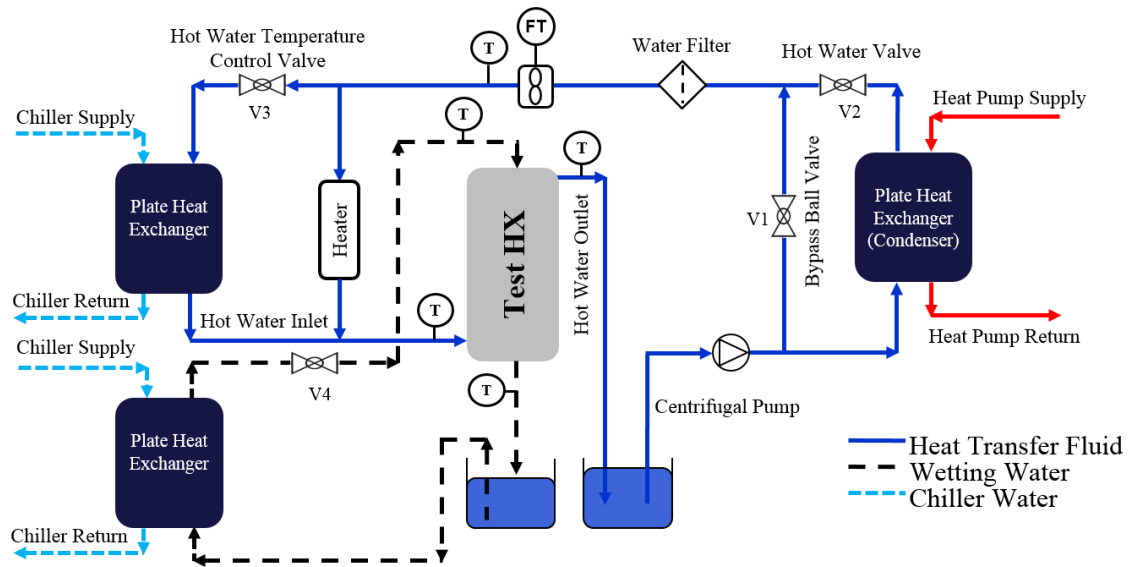


Figure 2.11: Schematic of process fluid and wetting water loop in test facility.

RO water used as process fluid enters the test HX at desired set point and cools down due to air flowing through wavy fins-and-tubes in dry case tests. Since process fluid was not expected to exceed 50°C, process fluid loop is constructed using schedule-40 plastic tubes which are rated for temperatures up to 60°C. When wetting water was used, air and wetting water flow in cross-flow pattern to cool the process fluid flowing through cooler tubes. Temperature of process fluid was measured at inlet and outlet of test HX using high precision resistance temperature detectors (RTD). Valve V2 provided water used for priming the centrifugal pump prior to start. A 0.75kW variable frequency drive (VFD) controlled centrifugal pump flow through heat transfer fluid loop which consisted of a water filter placed before turbine flow meter as a protection for turbine flow meter. The desired temperature at test HX inlet was maintained using heat supplied by a typical R-22 heat pump cycle using 4 kW fixed speed scroll compressor, and a 4 kW auxiliary heater. Therefore, the designed facility could test HX capacities up to 18 kW depending on test conditions. A 15 kW water chiller was utilized to cool overheated water and serve as additional temperature control along with bypass and temperature control valves. Thus process fluid temperature at HX inlet could be maintained within ± 0.05 °C of setpoint.

2.4 Wetting water loop

Schematic of process fluid and wetting water loop in experimental facility is presented in Figure 2.11. This Dissertation focuses on testing the conventional wetting water distribution methods such as deluge and front spray cooling and proposed methods which improve HX evaporative cooling performance. Figure 2.12 presents a summary of conventional and proposed wetting water distribution methods tested as part of this Dissertation. Deluge water required for testing cooler performance in wet conditions was

distributed evenly over the leading edge of RTHX using an overflow-type distributor attached on top of HX as shown in Figure 2.13.

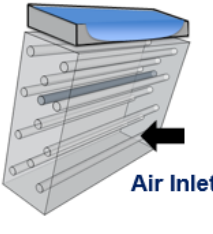
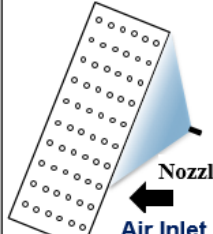
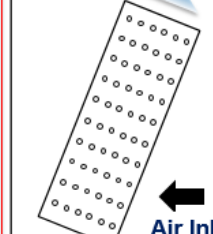
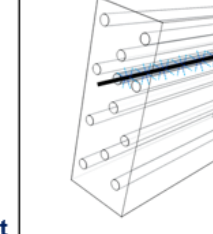
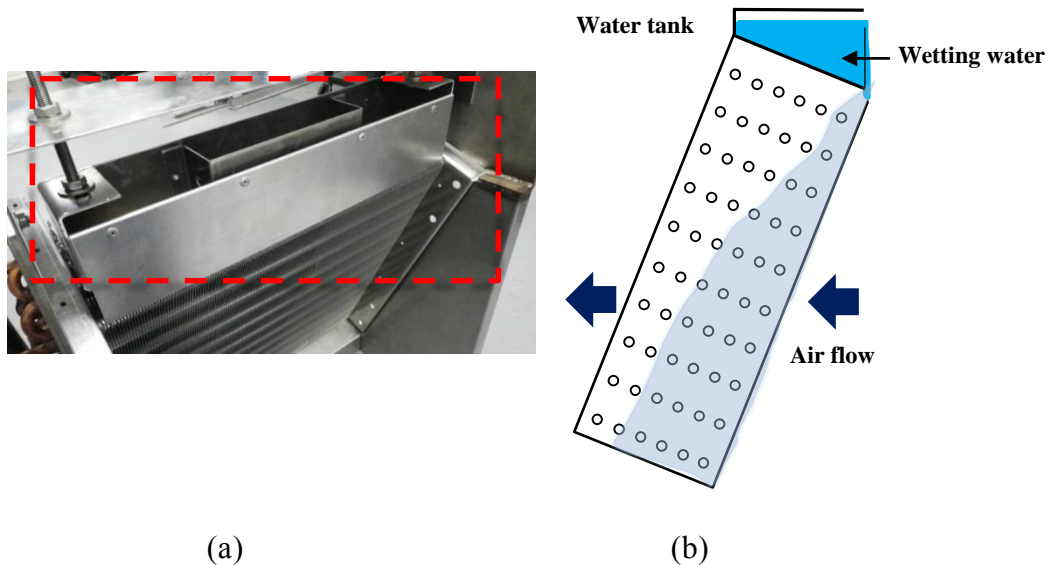
	Deluge Cooling	Front Spray	Top Spray	Internal Jet Spray
Wetting Method				
Features	<ul style="list-style-type: none"> • Water poured onto HX • Easy to install and operate 	<ul style="list-style-type: none"> • Nozzle spray water on HX face 	<ul style="list-style-type: none"> • Spray on HX top improves wetting in HX depth 	<ul style="list-style-type: none"> • Spraying within HX coil • Minimum dry region • Targeted wetting <p>Prov. Patent # 61/782,825</p>
	Conventional technology		Proposed methods	

Figure 2.12: Summary of conventional and proposed wetting water distribution methods tested for evaporatively cooled wavy fin HXs .



Note: Wetting zone shown Figure (b) is based on expected wetted zone.

Figure 2.13: Deluge evaporative cooling (a) top view (b) side view.

Spray cooling experiments were performed with nozzles placed in two configurations, i.e. in front of the HX and on top of the HX as shown in Figures 2.14 and 2.15, respectively.

Tap water supply was treated using a reverse osmosis (RO) system and water quality parameters measured using a photometer before and after treatment are listed in Table 2.2.

Table 2.2: Water quality parameters before and after reverse osmosis (RO) treatment.

Parameter	Reverse osmosis treated water	Tap water supply
Alkalinity (CaCO ₃ mg/l)	20	40-55
Hardness (CaCO ₃ mg/l)	25	60

Treated RO water was used as both heat transfer fluid within the tubes and as evaporative cooling fluid on air-side. Reduced salt content reduces potential scaling issues and facilitates consistent test conditions. Valve V6 provided water used for priming the gear pump prior to start-up. Temperature of wetting water was measured at inlet and outlet of test exchanger using high precision RTD. A 0.5 HP VFD controlled gear pump drove flow through wetting-water loop which also consists of a Coriolis flow meter. Wetting water can be cooled or kept at a constant inlet temperature using a 15 kW vapor compression water chiller.

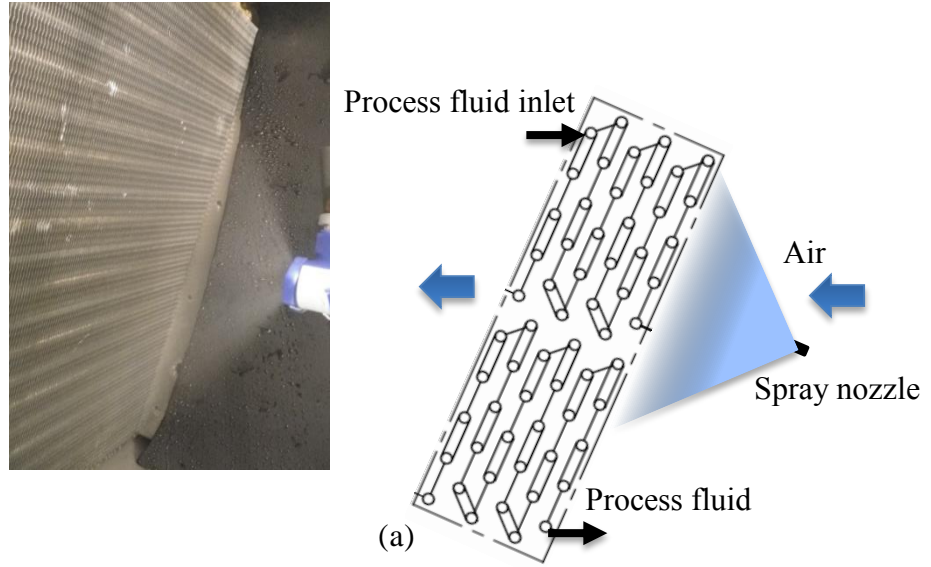
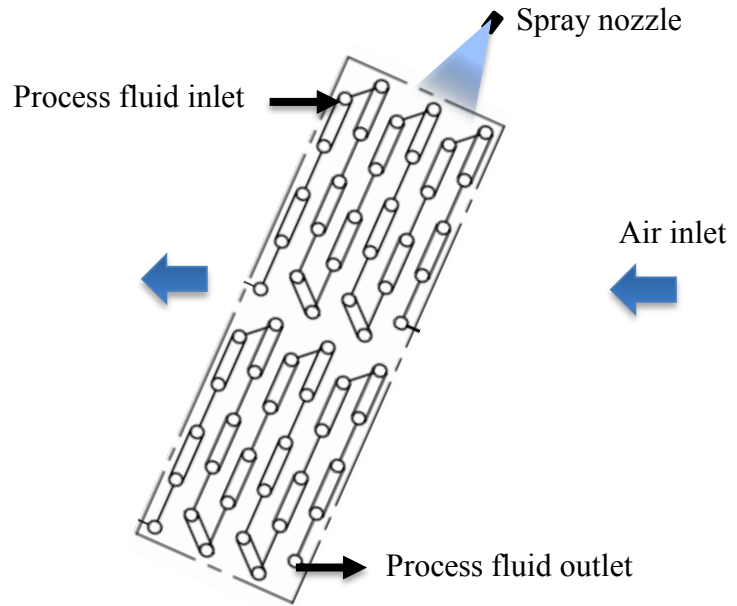
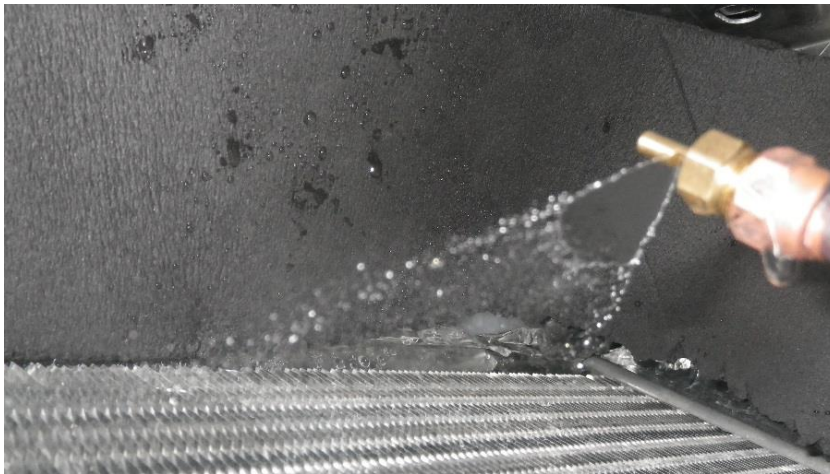


Figure 2.14: Front spray evaporative cooling (a) side view (b) top view.



(a)



(b)

Figure 2.15: Top spray evaporative cooling (a) side view (b) top view.

2.5 Heat pump loop

Process fluid must be maintained at the desired temperature at HX inlet, which requires a heat source. Typically a heater may be used to accomplish this however the experimental setup was designed to incorporate a heat pump water heater which would provide higher energy efficiency. The condenser of heat pump is a plate HX which cools refrigerant by heating process-fluid. The evaporator is kept at outlet of air-duct, thus same axial fan which drives air side loop was utilized to provide air-flow across the evaporator as shown in Figure 2.16.

Although the heat pump operating parameters are not of interest for the experiment, safe and efficient operation of heat pump requires monitoring of main parameters such as superheat, sub-cooling, compressor outlet temperature etc. Superheat is measured using suction line temperature and pressure measurement (before compressor inlet), while sub-cooling is measured using liquid line temperature and pressure (after condenser outlet).



Figure 2.16: Overview of heat pump loop of experimental test setup.

Heat pump cycle utilized HCFC-22 as working fluid with a fixed speed 4 kW Copeland scroll compressor (Model ZS38K4E-TF5). It was also incorporated with a hot-gas bypass valve between the compressor outlet and evaporator outlet, which enabled reducing the capacity of test HX without changing the speed of the compressor by allowing certain amount of refrigerant to bypass from the compressor discharge line back to suction line.

2.6 Measuring instrumentation and equipment sizing

As discussed in Section 1.6, the current data set for wetted HX performance available in published literature may not be reliable due to missing parameters which authors have failed to report such as energy balances, instrumental errors and experimental uncertainties. In many cases it is not reported how RH of air was maintained constant at the inlet air section of test HXs, while other do not even report a constant value of RH.

Thus, one of the main objectives of the Dissertation was also to provide accurate experimental data for evaporatively cooled test HXs wetted using both spray and deluge cooling. The test facility was well instrumented and systematic error of each measuring instrument is presented in Table 2.3.

Table 2.3: Systematic errors of measuring instruments.

Instrument	Manufacturer	Type	Range	Systematic uncertainty
Air-side				
Thermocouple	Omega	T-type	-250°C to 350°C	±0.3°C
Relative humidity sensor	Vaisala	PT 100	0% RH to 90% RH	±2%RH
ΔP transducer (Nozzle)	Setra	Strain	0”WC to 5”WC	±1.0% full scale
ΔP transducer (HX)	Setra	Strain	0”WC to 1”WC	±1.0% full scale
Process fluid and wetting water side				
RTD	Omega	PT 100	-100°C to 400°C	±0.06°C
Wetting water flow meter	Micro-motion	Coriolis	0 g/s to 200 g/s	±0.1% reading
VFD	Frenic		0.75 kW	
Process fluid flow meter	Hoffer	Turbine	157 g/s to 1840 g/s	±0.02% full scale

2.6.1 Process fluid and wetting water-side measuring instrumentation

The measuring instruments required for process and hot-water loop mainly consist of RTD sensors and flow meters. Inline PT-100 RTD sensors were used for measuring the HX inlet and outlet temperatures. The sensor tip is fixed at a depth equal to radius of the tube. Similarly, wetting water temperatures before being added to HX and after draining through HX, were measured with Inline PT-100 RTD sensors.

Wetting water passes through drain before temperature is measured at outlet as shown in Figure 2.14. This ensures the water collects and mixes well before a value of temperature is recorded.

Using RTD sensors is recommended especially for wetting water temperature measurements as the difference in inlet and outlet values is not more than 1- 2°C in most experimental cases. Thus systematic uncertainty in wetting water sensible heat transfer rate is considerably reduced to 0.05 °C, compared to 0.5°C systematic uncertainty for inline-thermocouples.

A turbine flow meter was used to measure process fluid volume flow rate through the loop. To ensure accurate measurement, flow meter is installed with up to 10D length of tubing on each side, where D is the tube diameter.

In order to calculate water side heat transfer rate, mass flow rate or density of water must be known. Since auxiliary water heater was installed after the flow meter, an additional inline RTD was installed immediately after the volume flow meter for water density calculation.

Wetting water flow rate was measured using micro-motion Coriolis mass flow meter which is calibrated in the range 0-200 g/s. This flow rate range is based on typical deluge and spray rates used in commercial hybrid evaporatively cooled condensers/coolers.

2.7 Test HX geometry and test matrix

Geometric specifications of three herringbone wavy-fin HXs tested as part of this Dissertation are presented in Table 2.4.

Table 2.4: Geometric specifications of herringbone wavy-fin HXs.

Parameter	Coil-1	Coil-2	Coil-3
Hydrophilic coating	No	Yes	No
Number of tube banks	6	6	6
Number of tubes per bank	10	10	10
Tube outer diameter (mm)	12.7	12.7	12.7
Tube horizontal spacing (mm)	24.9	24.9	24.9
Tube vertical spacing (mm)	50.0	50.0	50.0
(Fp) Fin pitch (mm)	2.4	2.4	3.0
(δf) Fin thickness (mm)	0.14	0.14	0.14
HX length (mm)	492.0	492.0	492.0
HX depth (mm)	150.0	150.0	150.0
HX height (mm)	500.0	500.0	500.0
Fin wave length (mm)	3	3	3
Fin wave height (mm)	1	1	1

Coils and 1 and 2 were geometrically similar i.e. fin spacing ($F_p=2.4\text{mm}$) but Coil 1 had untreated aluminum fins and Coil 2 had a hydrophilic plasma coating on aluminum wavy fins. Coil 3 had a slightly larger $F_p=3\text{mm}$. Therefore, effects of both fin spacing and

hydrophilic coating on HX capacity and ΔP_a were studied in both dry and deluge cooled conditions. RTHX set at 21° angle from vertical placed in test section and herringbone wavy-fin structure are shown in Figure 2.17.

Dry case tests were performed at air velocities varying from 1.5 m/s to 3.0 m/s, with process fluid inlet temperature 43°C , air inlet temperature 28°C , air inlet RH approximately 45%. Wet case tests were conducted under similar conditions with the addition of deluge wetting water flow rates at 0.015, 0.08, and 0.16 kg/s. Deluged cooling water is kept at constant inlet temperature of 28°C .



(a)



(b)



(c)



(d)



(e)



(f)

Figure 2.17: Wavy-fin RTHX (a) and (b) side view of test HX, (c) coil circuitry, (d) wavy-fins, (e) deluge cooling wetting water distributor, (f) wavy-fin RTHX placed in experimental test section.

Experimental test matrix for testing wavy fin RTHXs is summarized in Table 2.5.

Table 2.5: Experimental test matrix for three wavy-fin RTHXs.

Case	HX frontal air velocity (m/s)	Wetting water flow rates (g/s)	Inlet air temperature (°C)	Number of cases
Dry	1.5, 2.0, 2.5, 3.0	-	28, 37	24
Deluge	1.5, 2.0, 2.5, 3.0	15, 80, 166	28	34 ¹
Front Spray		2.2, 3.8, 8.0		72
Top Spray	1.5, 2.0, 2.5, 3.0		28, 37	72
Internal Jet Spray		2.2, 3.7		48

Note:

¹ Fp= 2.4, 3.0 mm (uncoated), Fp=2.4 mm hydrophilic coated

² No experimental data could be recorded at $V_a = 3.0$ m/s in deluge conditions due to excessive wetting water carryover from test HX.

Air, process fluid and wetting water parameters for testing herringbone wavy-fin RTHXs are summarized in Tables 2.6.

Table 2.6: Air, refrigerant and wetting water parameters for testing wavy-fin RTHXs.

Parameter	Average Value	Unit
Air Parameters		
Inlet temperature	28.0	°C
Inlet RH	45.0	%
Refrigerant Parameters		
Inlet temperature	43.0	°C
Flow rate	0.35	kg/s
Wetting-Water Parameters		
Inlet temperature	28.0	°C
Deluge flow rate	0.015, 0.080, 0.16	kg/s
Spray flow rate	0.0022, 0.0038, 0.008,	kg/s

2.8 Data acquisition system

Data acquisition program written in LabVIEW was used to record experimental data at frequency of 1 second. For each test case steady state was obtained and maintained for at least 15 minutes upon which data was recorded for 20 minutes. If energy balance was found to be more than 5%, data was discarded and test case repeated. The front panel of LabVIEW Visual Interface (VI) is shown in Figure 2.18.

PID controller for process fluid and wetting water loop in LabVIEW VI is shown in Figure 2.19.

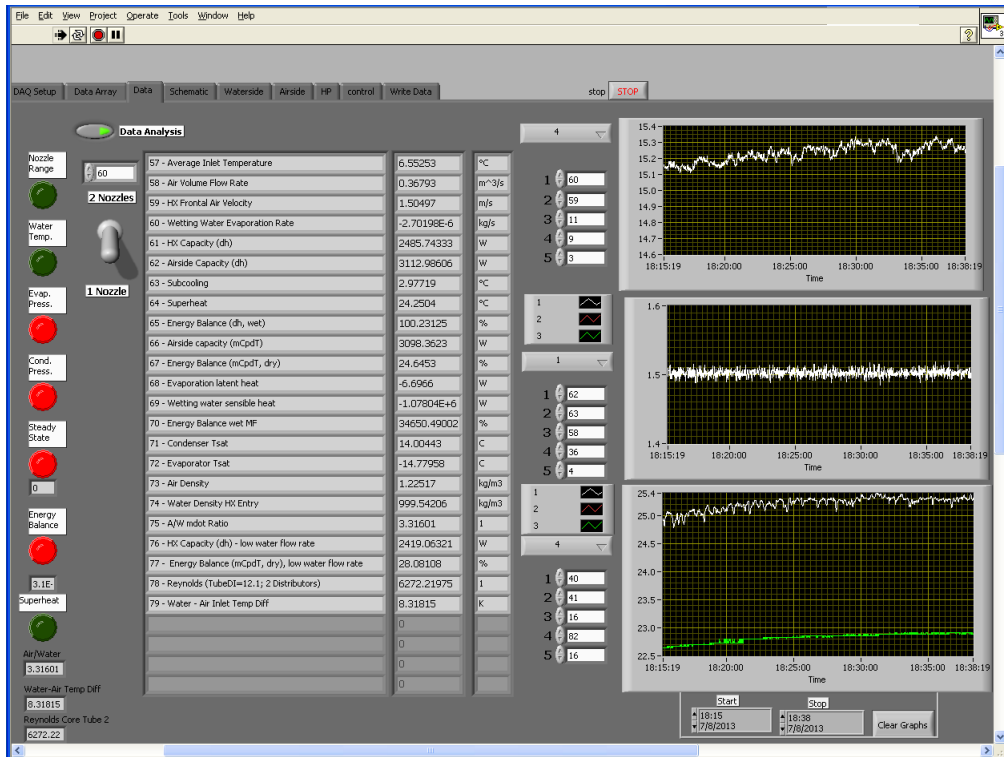


Figure 2.18: Front panel of LabVIEW graphical user interface (GUI).

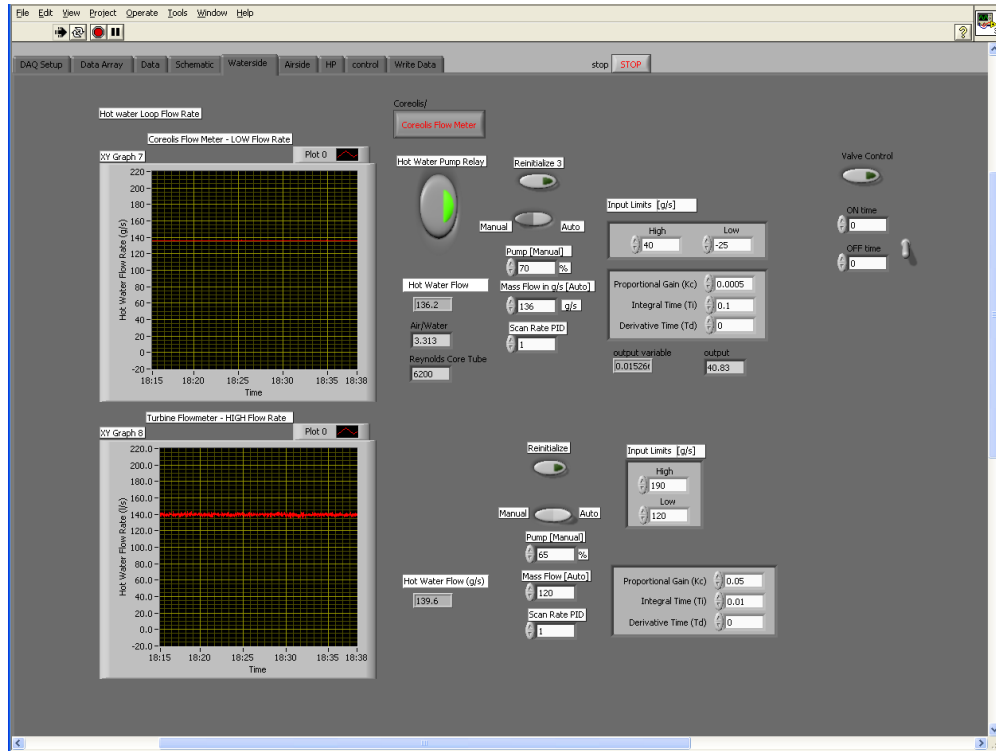


Figure 2.19: PID controller for process fluid and wetting water loop in LabVIEW

GUI.

Heat pump operating conditions were monitored to ensure its safe operation. Figure 2.20 shows the heat pump operating parameters displayed in LabVIEW VI.

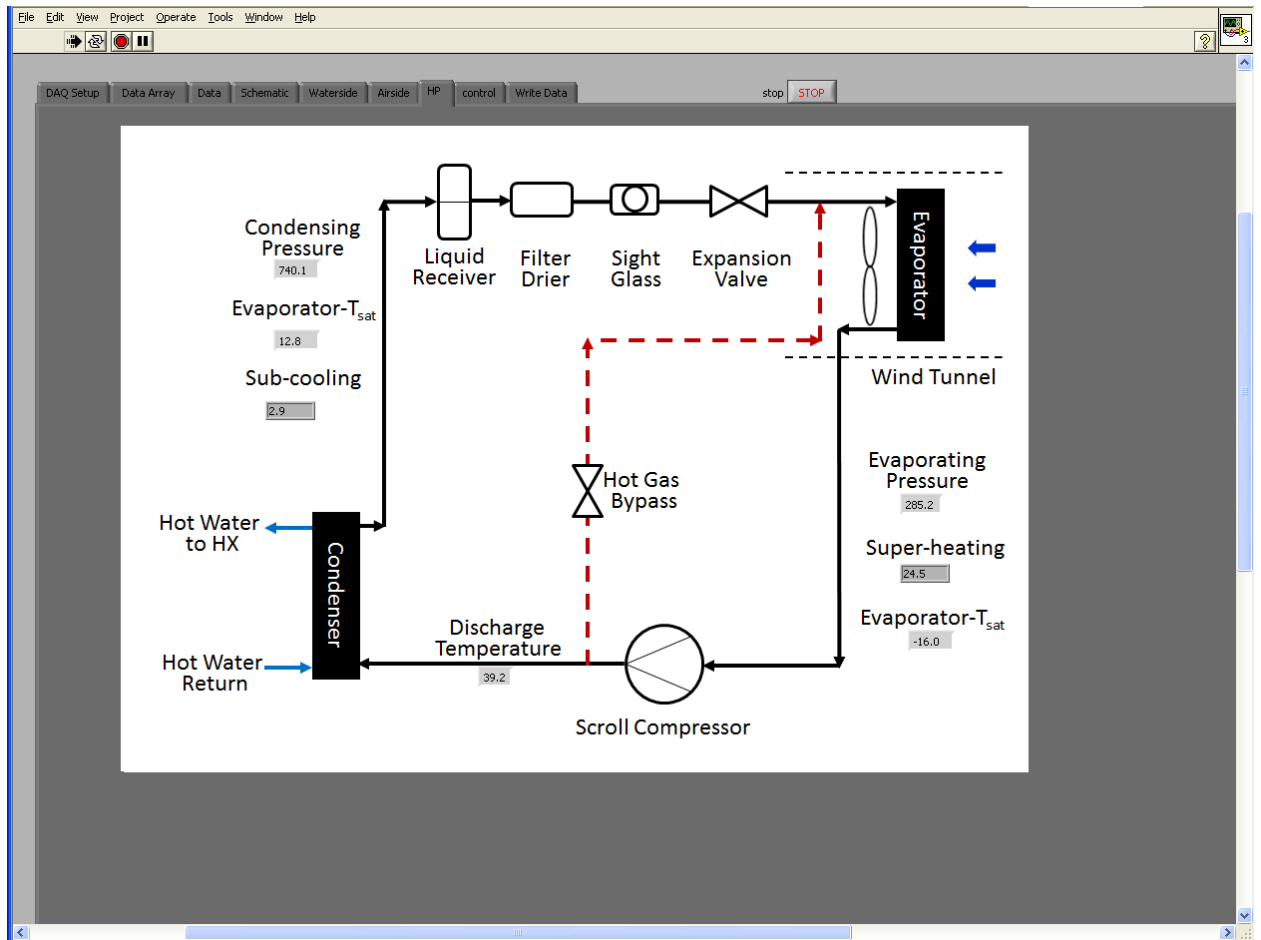


Figure 2.20: Heat pump operating parameters displayed in LabVIEW GUI.

Since the test HX capacity was expected to be within a wide range, an electronic expansion valve (EEV) rated for operation between 3 kW to 18 kW was installed. The EEV was controlled using a PI controller in LabVIEW which allowed maintaining the desired superheat. Increasing the super heat value reduced the process fluid temperature at the HX inlet and vice-versa. Figure 2.21 shows the PID controller for electronic expansion valve in heat pump loop.

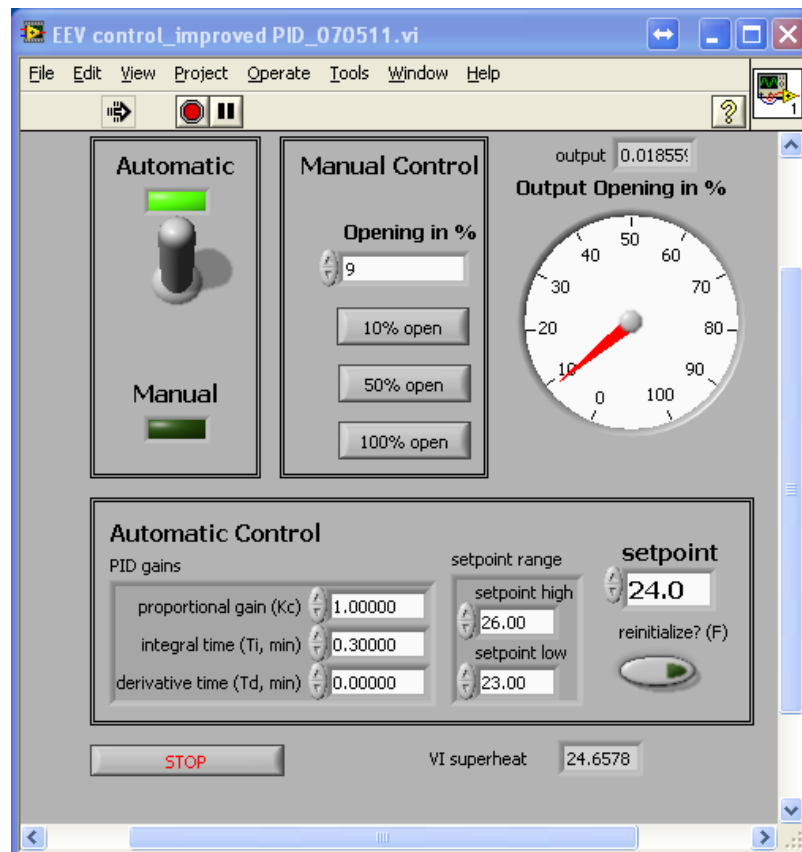


Figure 2.21: PID controller for electronic expansion valve (EEV) in heat pump loop.

2.9 Uncertainty analysis

The total uncertainty of measured variables such as air-side pressure drop was calculated using the sum of systematic error of each measuring instrument and random error which is the standard deviation of measured variable in respective test case.

In case of variables which were indirectly calculated (using other measured variables), propagated uncertainty is calculated using “determine propagation of uncertainty” functionality available in EES shown in Figure 2.22 which required the systematic uncertainty of directly measured variables as an input.

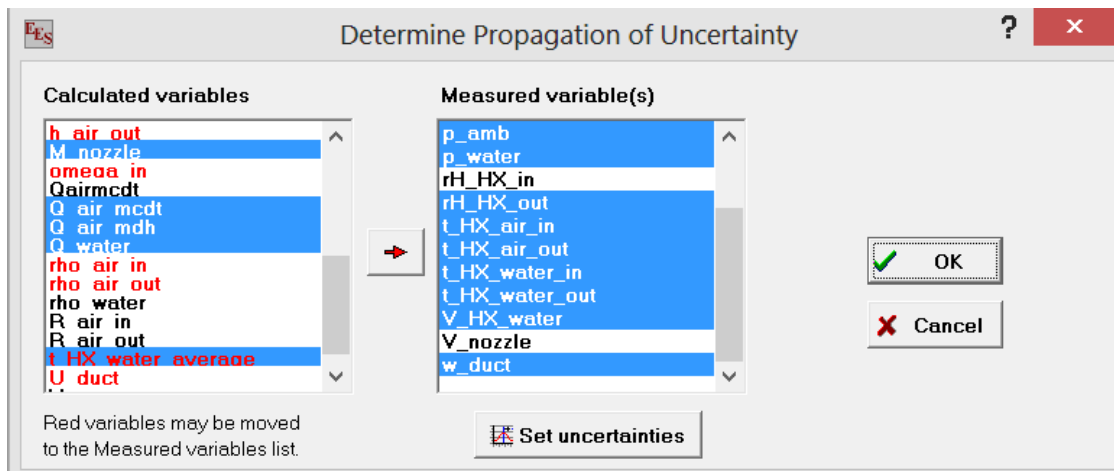


Figure 2.22: Calculated propagated uncertainty of each calculated variable in EES.

The uncertainty in a calculated parameter was calculated using Equation 2.2 specified by NIST [Taylor and Kuyatt, 1994].

$$U_y = \sqrt{\sum_i \left(\frac{\partial Y}{\partial X_i}\right)^2 U_x^2} \quad (2.2)$$

Where, U represents the uncertainty of variable, Y the calculated variable, and X the

measured variable.

Table 2.7 summarizes minimum and maximum total uncertainty in experimental measurement of key calculated variables.

Table 2.7: Minimum and maximum total uncertainty in experimental measurement of key calculated variables.

Parameter	Minimum Uncertainty	Maximum Uncertainty
HX air-side ΔP (Pa)	2.73	3.39
HX capacity (kW)	0.172	0.405
Energy Balance (%)	4.4	8.9
Capacity Enhancement Ratio (-)	0.03	0.056
$PR_{\Delta P}$ (-)	0.13	0.3

Note: Minimum and Maximum uncertainties vary due to change in air-velocity and wetting water flow rates.

2.10 Data reduction

Experimentally measured air, process-fluid and wetting-water parameters such as flow rate, temperature and relative humidity were used to calculate HX capacity, energy balances and enhancement ratios in both dry and wet conditions.

Dry case air-side capacity, $\dot{Q}_{a,dry}$, is calculated using Equation (2.1).

$$\dot{Q}_{a,dry} = \rho_a * \dot{v}_a * Cp_a * (T_{a,out} - T_{a,in}) \quad (2.1)$$

Both dry and wet case heat transfer fluid-side capacity, \dot{Q}_{pf} , is calculated using Equation (2.2).

$$\dot{Q}_{pf} = \dot{m}_{pf} * (h_{in} - h_{out}) \quad (2.2)$$

Equation (2.3) is used to calculate dry case energy balance error in %, $E_{eb,dry}$,

$$E_{eb,dry} = 100 * \left(1 - \frac{Q_{pf}}{Q_{a,dry}}\right) \quad (2.3)$$

Wet case air-side capacity, $\dot{Q}_{a,wet}$, is calculated using Equation (2.4).

$$\dot{Q}_{a,wet} = \rho_a * \dot{v}_a * [h_{out} - h_{in}\{1 - (w_{out} - w_{in})\}] \quad (2.4)$$

Wetting-water capacity, \dot{Q}_{ww} , is calculated using Equation (2.5).

$$\begin{aligned} \dot{Q}_{ww} = Cp_{ww} * [T_{ww,out}\{m_{ww} - (w_{out} - w_{in})m_{a,out}\} - (T_{ww,in} \\ * m_{ww,in})] \end{aligned} \quad (2.5)$$

Equation (2.6) is used to calculate wet case energy balance error in %, $E_{eb,wet}$.

$$E_{eb,wet} = 100 * \left(1 - \frac{Q_{pf}}{Q_{a,wet} + Q_{ww}}\right) \quad (2.6)$$

Several performance parameters are defined to compare the effect of spray and deluge cooling and the effect of hydrophilic coating and fin spacing.

$$1) \quad HX \text{ Capacity Enhancement Ratio} = \frac{\text{Wetted surface HX capacity}}{\text{Dry surface HX capacity}} \quad (2.7)$$

$$2) \quad HX \text{ Airside } \Delta P \text{ Penalty Ratio} = \frac{\text{Wetted surface HX } \Delta P}{\text{Dry surface HX } \Delta P} \quad (2.8)$$

$$3) \quad \text{Spray Efficiency} = \frac{\text{Evaporation rate}}{\text{Spray water flow rate}} \quad (2.9)$$

where, evaporation rate (ER) is calculated using Equation 2.10 as the difference in humidity ratios at the HX air outlet and inlet

$$\text{Evaporation Rate (ER)} = X_{air,out} - X_{air,in} \quad (2.10)$$

Also ratio of $\frac{\text{HX Capacity Enhancement Ratio}}{\text{HX Airside } \Delta P \text{ Penalty Ratio}}$ would provide useful information for comparison purpose.

Chapter 3 Experimental results: dry cooling

3.1 Introduction

This Chapter describes the dry cooling performance of the three wavy fin HXs set at 20° from the vertical. The effect of fin spacing and hydrophilic coating on the hydraulic performance of HX was investigated at different air flow rates, and air inlet temperatures. Thus, when dry case baseline performance of each HX was known, comparison was made with wet case operation and capacity enhancements can be obtained. Tests were performed at two values of air inlet temperature, i.e. high ambient air temperature $T_{a,in} = 37^\circ\text{C}$ and low ambient air temperatures $T_{a,in} = 28^\circ\text{C}$. The experimental values obtained were checked for energy balance within 5%, any data point outside this range was scrapped and test repeated. Table 3.1 and 3.2 present the test results for performance of wavy-fin HXs set at 20° from vertical in dry cooling conditions at $T_{a,in} = 28^\circ\text{C}$ and 37°C respectively.

3.2 Effect of hydrophilic coating

Capacities and ΔP_a of coated and uncoated wavy-fin HXs are plotted as a function of HX frontal air velocity in dry conditions in Figures 3.1 and 3.2 respectively and summarized in Tables 3.1 and 3.2.

Table 3.1: Performance of three wavy-fin HXs set at 20° from vertical in dry cooling conditions at approximately $T_{a,in}=28^{\circ}\text{C}$, $\text{RH}_{a,in} = 45\%$ and $\omega_{a,in}= 0.0106 \text{ kg}_w/\text{kg}_a$.

Parameter	Uncoated 2.4 mm fin spacing				Coated 2.4 mm fin spacing				Uncoated 3.0 mm fin spacing			
	Hot water parameters											
Volume flow rate (L/s)	0.35	0.35	0.35	0.35	0.35	0.35	0.35	0.35	0.35	0.35	0.35	0.35
Inlet temperature (°C)	42.98	42.94	43.02	43.09	43.07	43.03	43.12	43.07	43.02	43.00	43.15	43.08
Outlet temperature (°C)	39.49	38.70	38.07	37.51	39.82	38.98	38.55	37.84	40.18	39.50	39.01	38.27
Capacity (kW)	5.07	6.16	7.19	8.09	4.72	5.88	6.58	7.58	4.12	5.08	6.01	6.97
Air-side parameters												
Velocity (m/s)	1.50	2.00	2.50	3.00	1.50	2.00	2.50	3.00	1.50	1.99	2.51	3.00
Inlet temperature (°C)	27.95	27.96	27.95	28.05	27.94	27.90	28.17	27.83	27.94	27.99	28.03	28.13
Outlet temperature (°C)	39.37	38.68	38.10	37.66	38.62	37.95	37.16	36.80	37.41	36.88	36.29	36.01
Inlet RH (%)	43.97	44.03	44.43	44.69	44.32	43.47	43.20	43.47	43.42	43.16	42.64	44.77
Outlet RH (%)	23.86	24.71	25.58	26.48	24.66	24.93	26.35	26.26	25.95	26.58	27.04	28.52
HX air side pressure drop (Pa)	25.30	42.16	61.83	83.14	23.68	39.60	57.04	78.98	16.76	28.06	42.70	58.65
Air volume flow rate (m ³ /s)	0.37	0.49	0.62	0.74	0.3675	0.4972	0.6122	0.7	0.3677	0.4911	0.6127	0.7417

Table 3.2: Performance of three wavy-fin HXs set at 20° from vertical in dry cooling conditions at $T_{a,in} = 37^\circ\text{C}$.

Parameter	Uncoated 2.4 mm fin spacing				Coated 2.4 mm fin spacing			
	Hot water parameters							
Volume flow rate (L/s)	0.35	0.35	0.35	0.35	0.35	0.35	0.35	0.35
Inlet temperature ($^\circ\text{C}$)	43.1	43.06	43.07	43.09	43.17	43.06	43.15	43.14
Outlet temperature ($^\circ\text{C}$)	41.79	41.39	41.10	40.91	41.85	41.48	41.30	41.00
Capacity (kW)	1.9	2.42	2.86	3.15	1.91	2.29	2.67	3.10
Air-side parameters								
Velocity (m/s)	1.52	2.02	2.52	3.03	1.50	2.00	2.50	3.00
Inlet temperature ($^\circ\text{C}$)	36.88	36.66	36.62	36.72	36.89	36.89	36.90	36.85
Outlet temperature ($^\circ\text{C}$)	41.48	41.13	40.87	40.7	41.14	40.84	40.66	40.41
Inlet RH (%)	41.8	41.4	41.27	40.95	43.56	43.54	43.52	43.43
Outlet RH (%)	32.42	32.33	32.68	32.87	34.01	34.47	34.85	35.37
HX air side pressure drop (Pa)	24.41	39.62	58.68	79.06	24.96	38.68	55.76	76.4
Air volume flow rate (m^3/s)	0.37	0.49	0.62	0.74	0.38	0.49	0.61	0.7

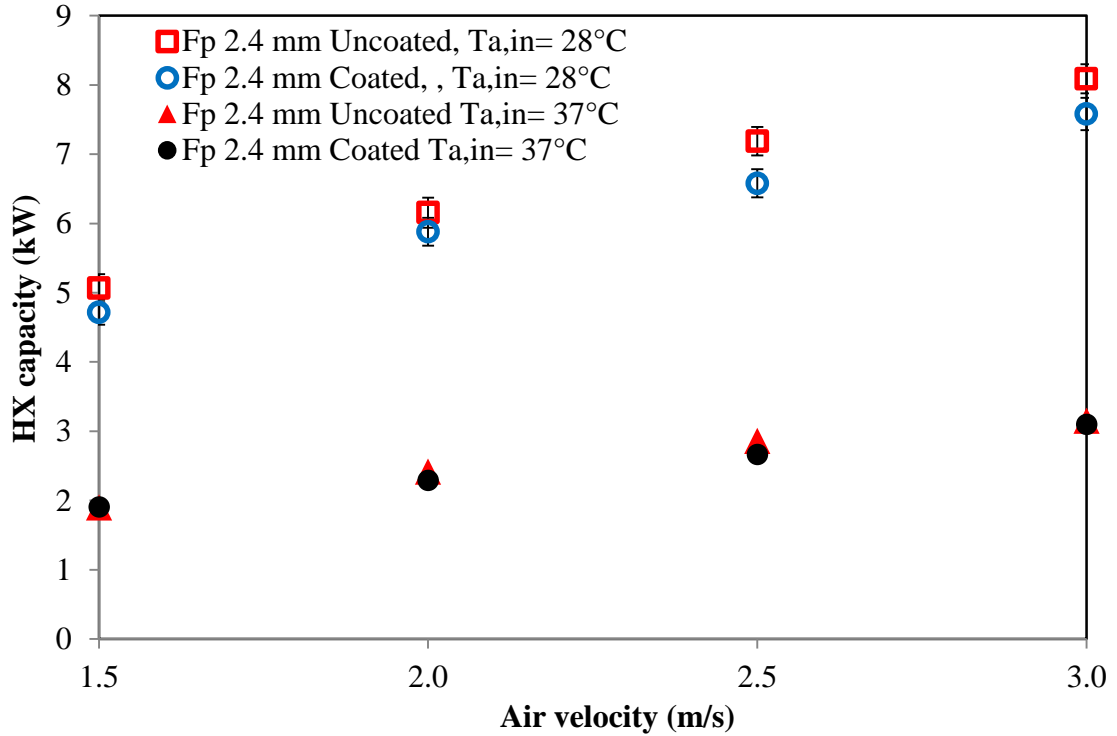


Figure 3.1: Capacity of coated and uncoated wavy-fin HX as a function of HX frontal air velocity in dry conditions at $RH_{a,in} = 45 \pm 2\%$, and $T_{a,in} = 28^\circ\text{C}$ and 37°C .

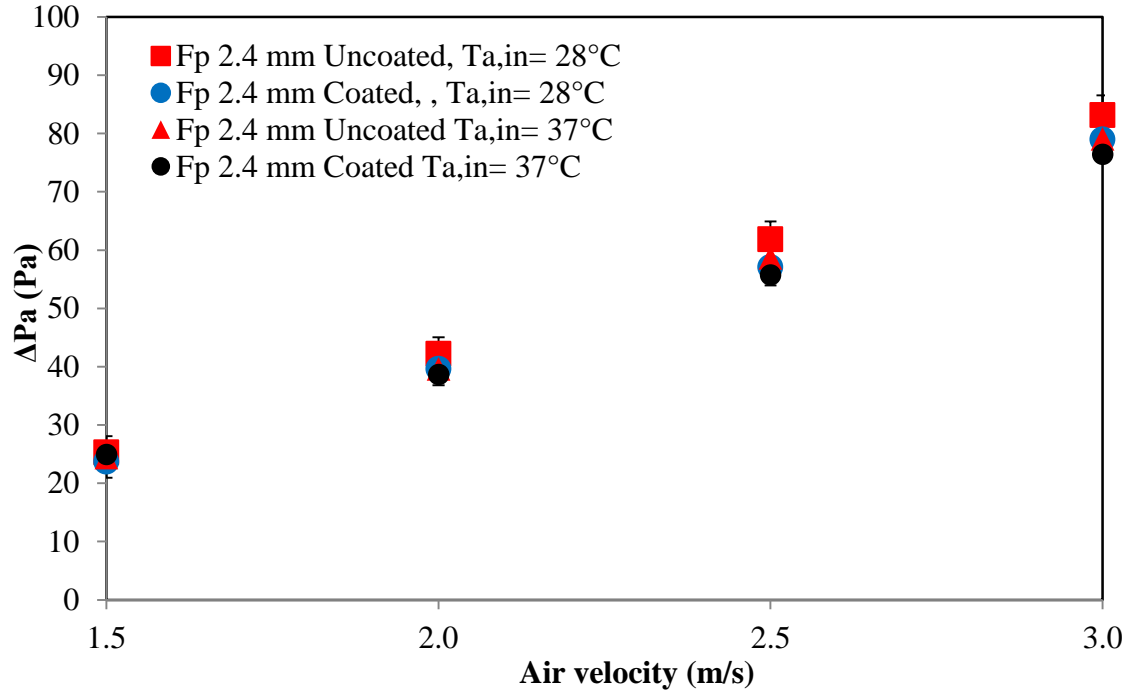


Figure 3.2: ΔP_a of coated and uncoated wavy-fin HX as a function of HX frontal air velocity in dry conditions at $RH_{a,in} = 45\%$, and $T_{a,in} = 28^\circ\text{C}$ and 37°C .

It was observed that, both capacity and ΔP_a are observed to increase linearly with increase in air velocity. Also, it was observed that compared to uncoated HX, both capacity and ΔP_a are reduced by up to 8% for HX with hydrophilic coating. Since the difference is almost within measurement uncertainty range for most cases it is difficult to conclude if hydrophilic coating is affecting capacity and ΔP_a , which is in line with previous dry case studies published in literature (Hong and Webb, 1999; Liu, 2011).

3.3 Effect of fin spacing

Capacities and ΔP_a of uncoated wavy-fin HXs with Fp 2.4 mm and 3.0 mm as a function of HX frontal air velocity in dry conditions at $RH_{a,in} = 45 \pm 2\%$, and $T_{a,in} = 28^\circ\text{C}$, in Figures 3.3 and 3.4 respectively.

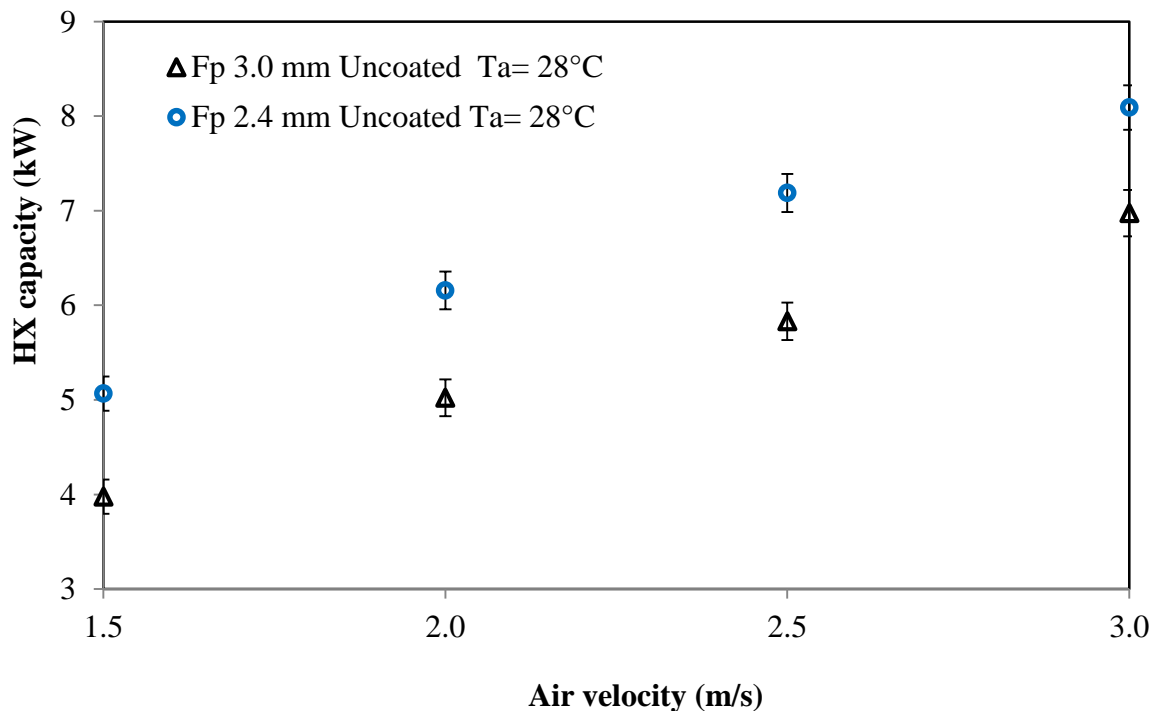


Figure 3.3: Capacities of uncoated wavy-fin HXs with Fp 2.4 mm and 3.0 mm as a function of HX frontal air velocity in dry conditions at $RH_{a,in} = 45\%$, and $T_{a,in} = 28^\circ\text{C}$.

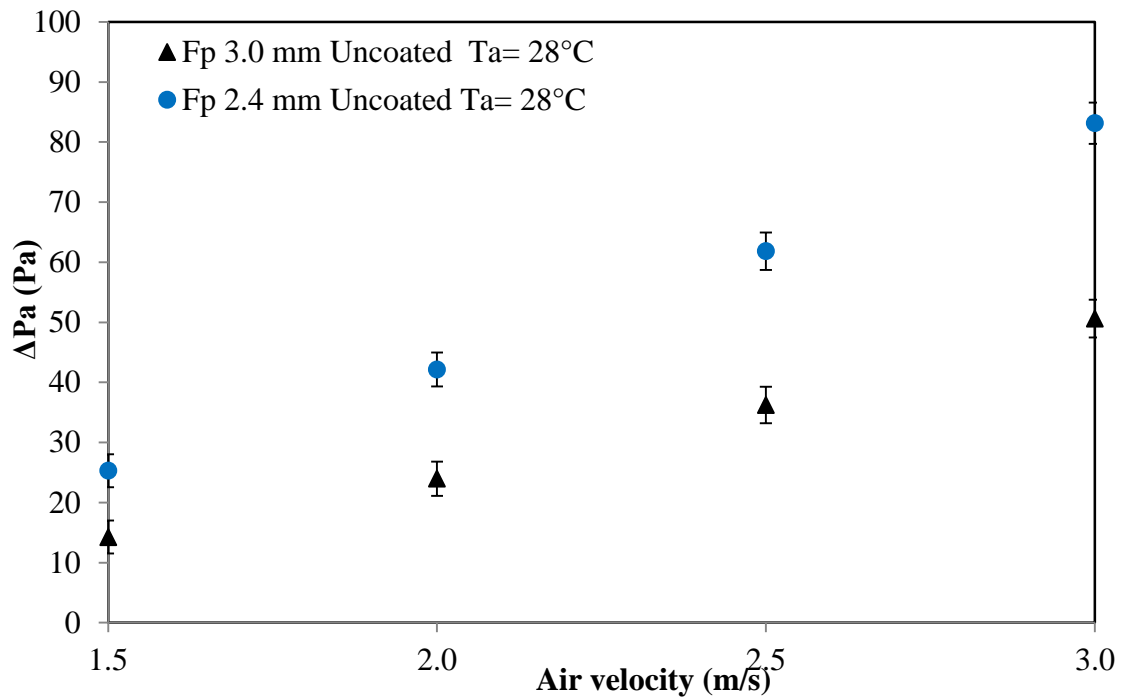


Figure 3.4: ΔP_a of uncoated wavy-fin HXs with Fp 2.4 mm and 3.0 mm as a function of HX frontal air velocity in dry conditions at $RH_{a,in} = 45\%$, and $T_{a,in} = 28^\circ C$.

Main observations summarizing effect of increasing Fp from 2.4 mm to 3 mm for a wavy-fin HX in dry conditions are as follows:

- Both HX capacity and airside pressure drop decreased
- Capacity reduction was approximately 14 to 21%
 - This was mainly due to 23.7% increase in HX surface area as Fp is reduced from 3.0 mm to 2.4 mm
- ΔP_a reduction is approximately 39 to 44%
- This is due to 25% increase in flow passage area through wavy fins

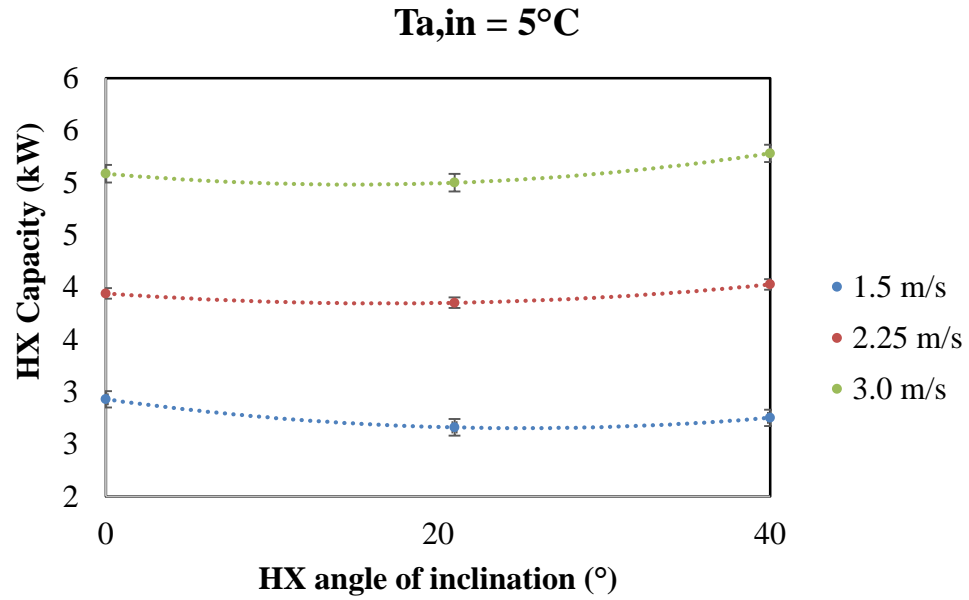
3.4 Effect of Inclination Angle

In this Section experimental data is reported for a separate test matrix specifically designed to study the effect of inlet air temperature and inclination angle on HX capacity. The test-matrix for studying effect of HX angle of inclination on heat transfer rate is presented in Table 3.3.

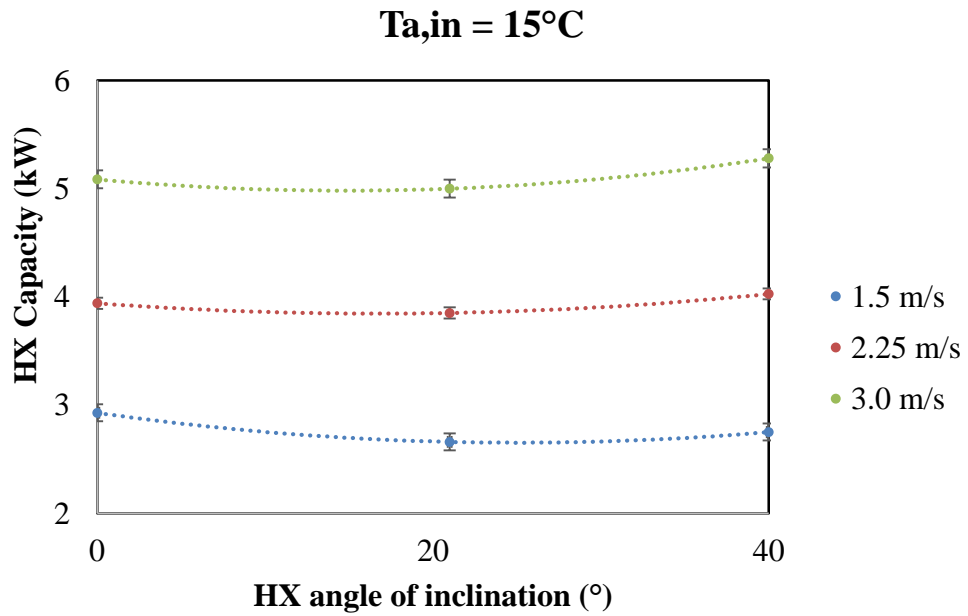
Table 3.3 Test-matrix for studying effect of HX angle of inclination on heat transfer rate.

Parameter	Unit	Value
Air-Side		
Inlet Temperature	°C	5, 15, 25, 35, 45
Inlet Relative Humidity	%	40
Frontal Air Velocity	m/s	1.5, 2.25, 3.0
HX Inclination Angle	° with vertical	0, 21, 40
Water-Side parameters fixed to maintain following:		
ITD	K	10
Air/Water-Mass-Flow-Ratio	(-)	4.1

Figures 3.5 (a to e) present the effect of HX capacity on HX angle of inclination at different air velocities and $T_{a,in}$ varying from 5°C to 45°C at 10°C fluid inlet temperature difference (ITD).

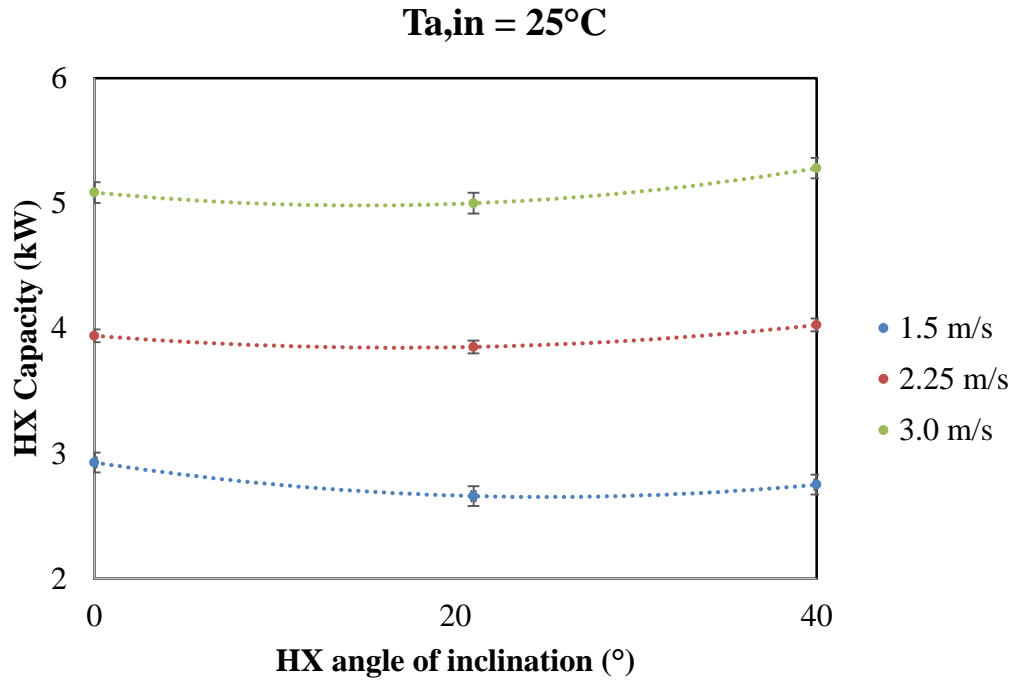


(a)

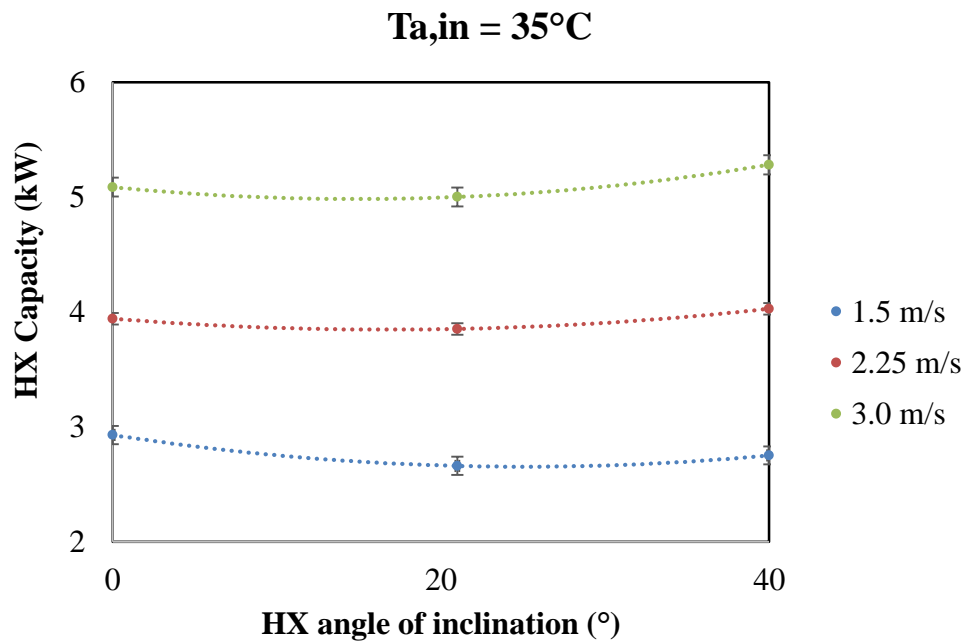


(b)

Figure 3.5 Effect of HX capacity on HX angle of inclination at different air velocities and T_{a,in} varying from 5°C to 45°C at 10°C fluid inlet temperature difference (ITD).

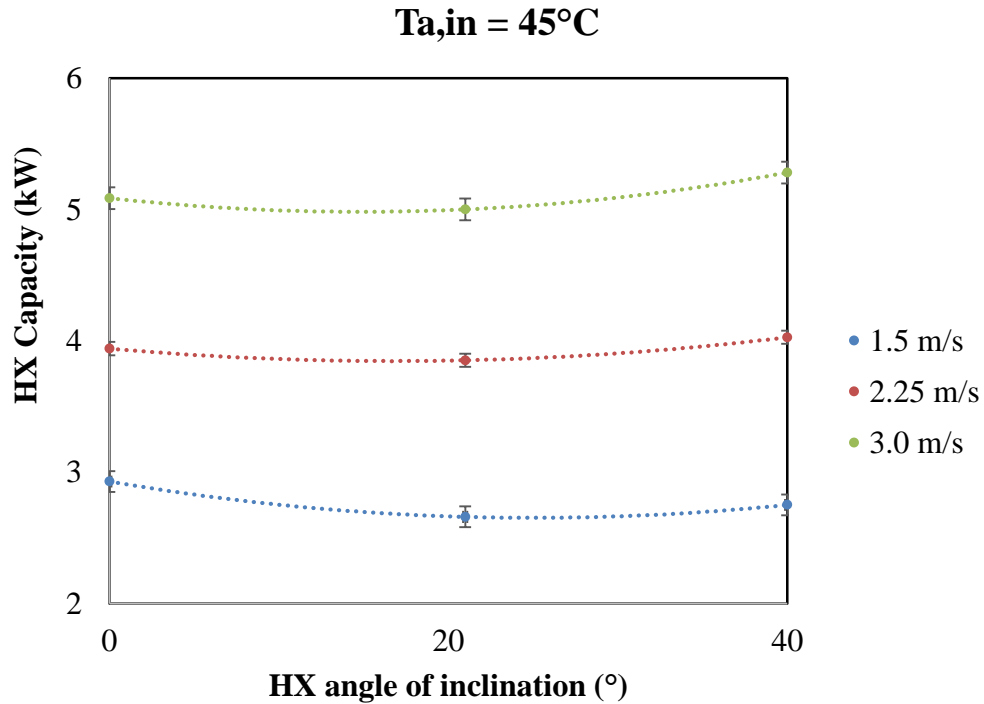


(c)



(d)

Figure 3.5 Effect of HX capacity on HX angle of inclination at different air velocities and T_{a,in} varying from 5°C to 45°C at 10°C fluid inlet temperature difference (ITD) (cont'd).



(e)

Figure 3.5 Effect of HX capacity on HX angle of inclination at different air velocities and T_{a,in} varying from 5°C to 45°C at 10°C fluid inlet temperature difference (ITD) (cont'd).

The key observations are as follows:

- 1) Less than $\pm 7\%$ difference in HX capacity with change in HX angle from 0° to 40°.
 - Up to 7% capacity reduction for 21° angle compared to 0° angle with vertical
 - Up to 4% capacity increase for 40° angle compared to 0° angle with vertical

It must be noted that there is approximately $\pm 5\%$ experimental measurement uncertainty associated with dry case measurements. Therefore results are reflective of the direction of trend but change in value compared to baseline is not significant.

- 2) Air-side pressure drop reduces by 7% when HX angle increased from 0° to 21°, but no further change in air-side pressure drop when HX angle further increased from 21° to 40°.

The difference in capacity could be better understood using a CFD study using commercial FLUENT software for predicting air flow path through the duct for varying HX angle of inclinations.

Figure 3.6 presents CFD Fluent predicted HX frontal velocity profile and air-side pressure drop for an empty duct.

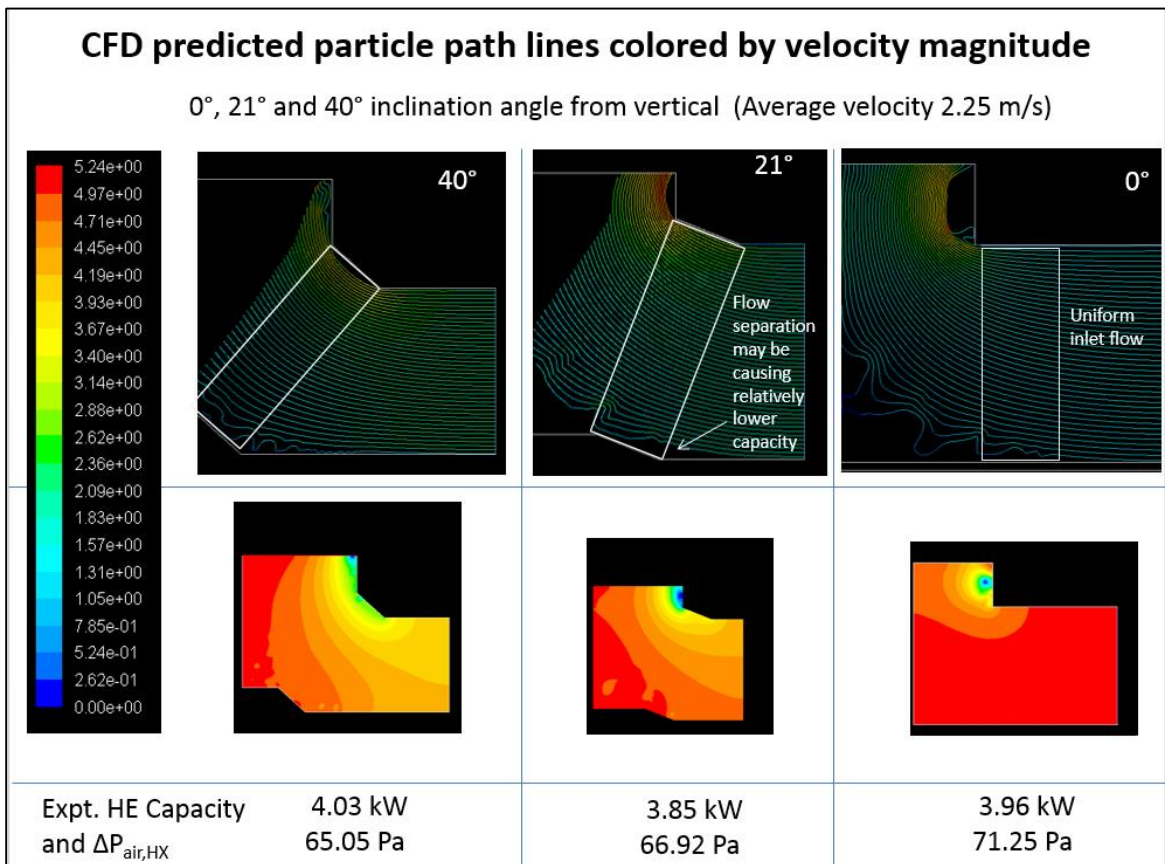


Figure 3.6 CFD Fluent predicted HX frontal velocity profile and air-side pressure drop for an empty duct.

Using CFD results the velocity profile was obtained for different HX angle of inclinations to study the non-uniformity in HX frontal air flow pattern as shown in Figures 3.7 to 3.9.

The key observations are as follows:

- 1) Flow is most uniform for 0° angle of inclination.
- 2) Bottom 20% of HX at 21° angle indicates significantly reduced air velocity which drops suddenly to 0.5 m/s.
- 3) This change is also visible for HX at 40° angle but only approximately bottom 10% of the area experiences air velocities lower than 0.5 m/s.

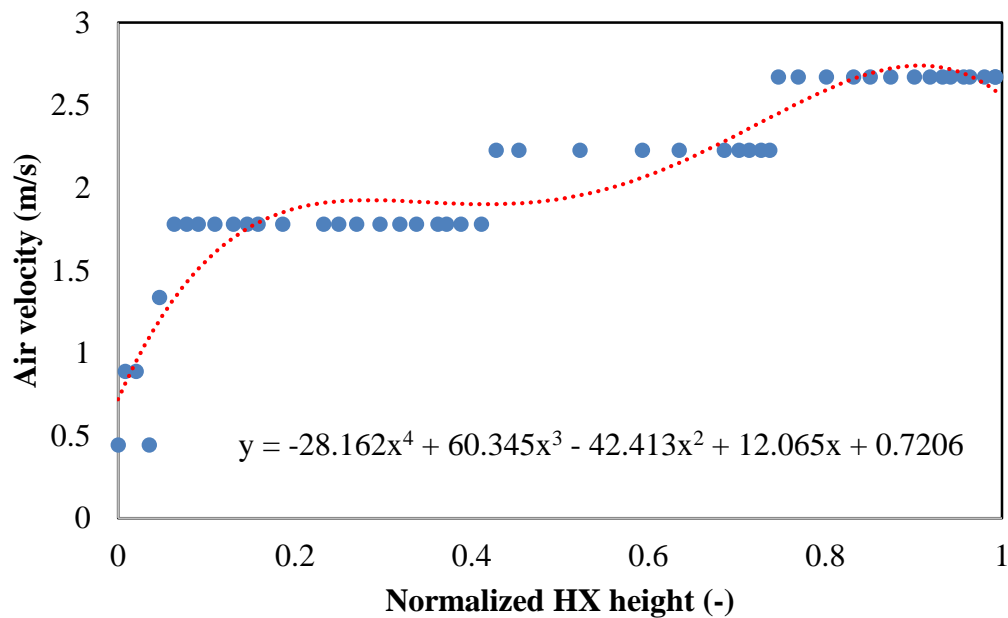


Figure 3.7 CFD predicted velocity profile at $v_A = 2.25$ m/s at 0° HX inclination with vertical.

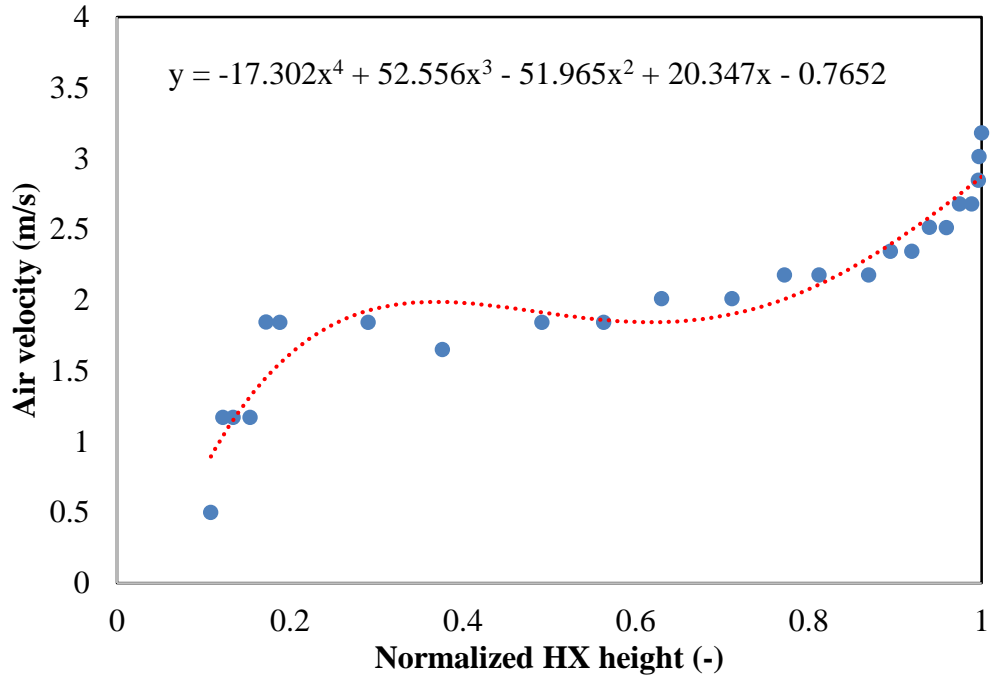


Figure 3.8 CFD predicted velocity profile at $V_a = 2.25$ m/s at 21° HX inclination with vertical.

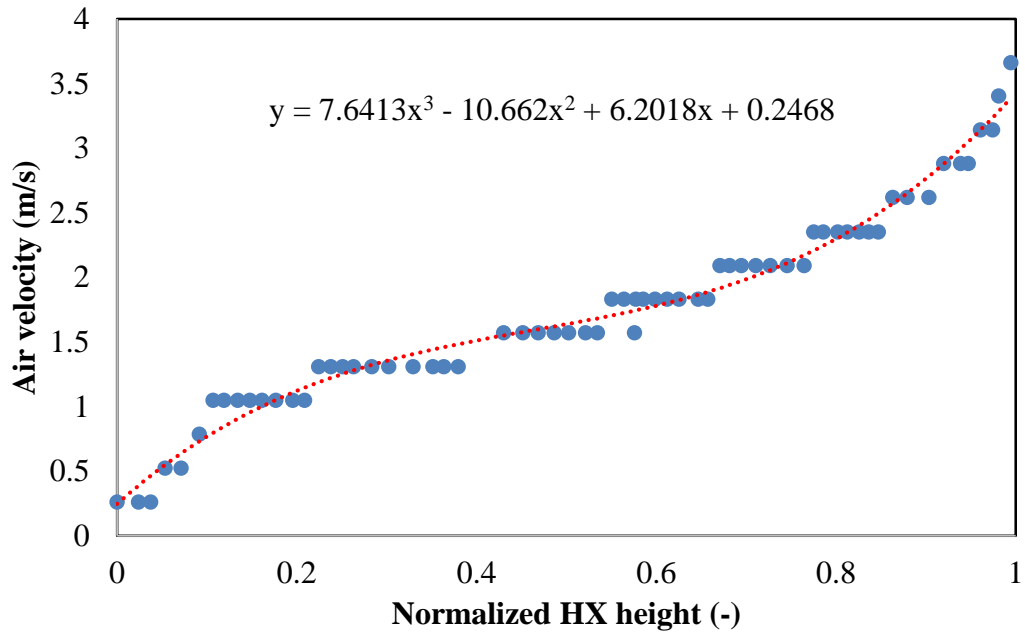


Figure 3.9 CFD predicted velocity profile at $V_a = 2.25$ m/s at 40° HX inclination with vertical.

3.5 Summary

Dry case performance of three wavy-fin HXs was experimentally measured in the designed test facility. The effect of fin spacing and hydrophilic coating was investigated at HX frontal air velocity from 1.5 m/s to 3.0 m/s. The following key observations were made:

- Hydrophilic coating reduced wavy fin HX dry case capacity and ΔP_a by up to 8%, however this is within experimental uncertainty and therefore this reduction cannot be attributed to coating alone.
- Increasing F_p from 2.4 mm to 3.0 mm, reduces wavy fin HX capacity by approximately 14 to 21% and ΔP_a by up to 39 to 44%. , but there was a 21% reduction in fin area due to increased fin spacing. Therefore, per unit air-side heat transfer area capacity would be similar. However, compact heat exchangers may be desirable for best airside performance in dry conditions under which HX may run for a major part of the year if the coil would be utilized as a hybrid wet-dry HX. It therefore is difficult to recommend one coil over the other as it may be application dependent. For example hydrophilic coating may reduce HX capacity for dry case operation and
- Less than $\pm 7\%$ difference in HX capacity with change in HX angle from 0° to 40° .
 - Up to 7% capacity reduction for 21° angle compared to 0° angle with vertical
 - Up to 4% capacity increase for 40° angle compared to 0° angle with vertical

- Air-side pressure drop reduces by 7% when HX angle increased from 0° to 21° , but no further change in air-side pressure drop when HX angle further increased from 21° to 40° .
- Increasing HX angle of inclination greater than 40° does not significantly affect improvement in heat transfer rates and no further benefit could be obtained through air-side pressure drop reduction. The experimental measurements summarized in this Chapter serve as baseline performance data for wet case capacity enhancement measurements described in Chapters 4 and 5.

Chapter 4 Experimental results: deluge cooling

4.1 Introduction

This Chapter describes the deluge wet cooling performance of the three wavy fin HXs set at 20° from the vertical. The effect of fin spacing and hydrophilic coating on the hydraulic performance of HX was investigated at different air and wetting water flow rates. The inlet air temperature was set at 28 °C.

4.2 Wetting water distributor design

The most critical aspect of evaporative cooling of finned HX is the method of applying wetting water on the HX fins. A good distributor design should be:

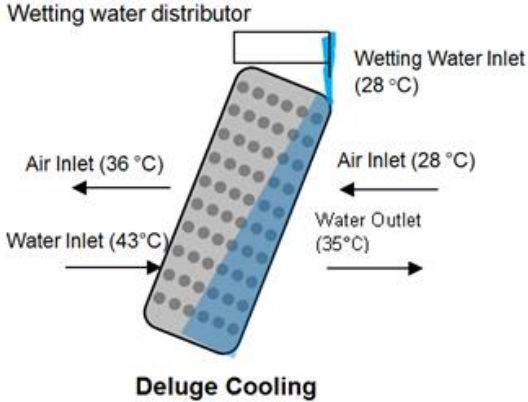
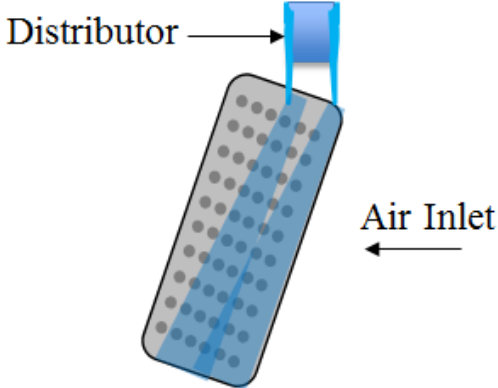
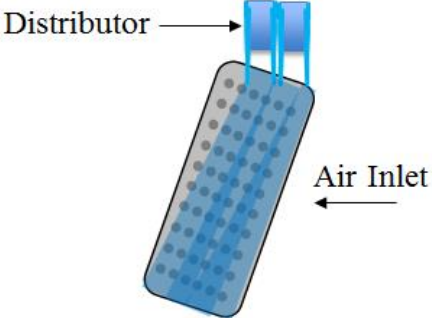
- 1) Simple to operate and must not clog easily
- 2) Easy to drain (especially for winter months to prevent freezing)
- 3) Able to distribute water evenly within HX core without obstructing air flow
- 4) Able to prevent droplet carryover into downstream of air. This is critical droplets corrode fan blades and may also form a plume.

With this in mind the wetting water distributor designs considered for this Study are summarized in Table 4.1 along with their advantages and disadvantages.

Wetting water installed in the current setup distributed water by overflowing onto the leading edge of fins as shown in Figure 4.1. Alternative configurations involving two-way or multiple overflow points shown in Figures 4.2 and 4.3, respectively, or a perforated bottom type distributor could also be employed.

However, the design shown Figure 4.1 is typically used for commercial deluge cooling applications; therefore it was selected for the experimental study.

Table 4.1: Wetting water distributor designs considered for this study along with their advantages and disadvantages.

Wetting Water Distributor Design	Comments
 <p>Figure 4.1 Wetting water distributor-Design 1</p>	<p>Advantages</p> <ol style="list-style-type: none"> 1) Reduced chance of wetting water droplet carryover 2) Better performance in co-flow configuration <p>Disadvantages</p> <ol style="list-style-type: none"> 1) High $PR_{\Delta Pa}$; increases linearly with wetting water flow rate 2) Poor distribution at low flow rate 3) Poor performance for deeper coils
 <p>Figure 4.2 Two-way overflow distributor</p>	<p>Advantages</p> <ol style="list-style-type: none"> 1) Good performance for deeper coils 2) Better distribution at lower flow rates
 <p>Figure 4.3 Multiple two-way overflow distributor</p>	<p>Disadvantages</p> <ol style="list-style-type: none"> 1) Higher chance of wetting water droplet carryover 2) Alignment important for equal flow on both sides 3) Over-lapping wetted regions due to HX inclination angle

4.3 Performance comparison of deluge and dry cooling

The experimental values obtained were checked for energy balance within 5%. Tables 4.2 and 4.3 provide experimental test summary for deluge cooled RTHX with uncoated and hydrophilic coated wavy fins, respectively, with F_p 2.4 mm each. Table 4.4 provides experimental test summary for deluge cooled RTHX with uncoated wavy fins with F_p 3.0 mm each.

Figure 4.4 presents the HX capacities as a function of ΔP_a for wavy-fin HXs under dry and deluge cooling.

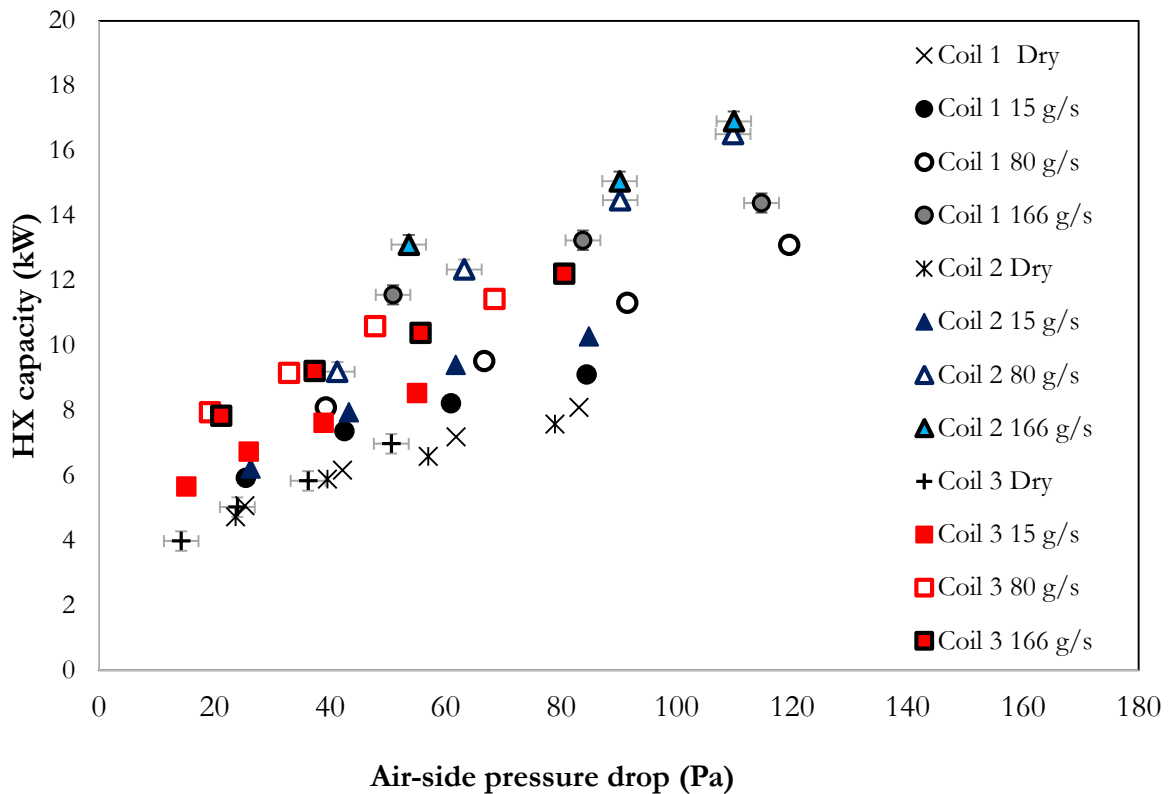


Figure 4.4: Wavy fin HX capacity as a function of ΔP_a under dry and deluge evaporative cooling at approximately $T_{a,in} = 28^\circ\text{C}$, $RH_{a,in} = 45\%$ and $\omega_{a,in} = 0.0106 \text{ kgw/kg}_a$.

Table 4.2: Test summary for deluge cooled uncoated wavy fin RTHX with 2.4 mm fin spacing at approximately $T_{a,in}=28^{\circ}\text{C}$, $\text{RH}_{a,in} = 45\%$ and $\omega_{a,in}= 0.0106 \text{ kg}_w/\text{kg}_a$.

Parameter	Deluge Cooling (15 g/s)				Deluge Cooling (80 g/s)				Deluge Cooling (166 g/s)			
Hot Water Side												
Flow Rate (l/s)	0.35	0.35	0.35	0.35	0.35	0.35	0.35	0.35	0.35	0.35	0.35	
Inlet Temperature ($^{\circ}\text{C}$)	42.99	43.07	43.08	43.11	43.16	43.02	43.01	43	43.1	43.0	43.0	
Outlet Temperature ($^{\circ}\text{C}$)	38.91	38	37.42	36.84	37.59	36.47	35.22	33.97	35.1	33.9	33.0	
Capacity and Uncertainty (kW)	5.9 ± 0.1 7	7.3 ± 0.19	8.2 ± 0.2	9.1 ± 0.2	8 ± 0.19	9.5 ± 0.2	11.3 ± 0.2	13.1 ± 0.3	11.5 ± 0.27	13.3 ± 0.28	14.4 ± 0.29	
Air Side												
Velocity (m/s)	1.5	2.0	2.5	3.0	1.5	2.0	2.5	3.0	1.5	2.0	2.5	
Inlet Temperature ($^{\circ}\text{C}$)	28.1	27.7	28.2	28.0	28.2	28.1	28.1	28.1	27.8	27.9	27.8	
Outlet Temperature ($^{\circ}\text{C}$)	38.6	38.0	37.5	36.9	38.2	37.4	36.4	35.1	36.7	35.5	34.3	
Inlet RH (%)	45.0	44.2	46.0	46.6	45.1	44.9	44.9	44.8	45.3	45.2	45.4	
Outlet RH (%)	28.2	27.6	37.5	30.5	34.3	34.3	36.5	39.9	39.1	41.7	45.4	
Capacity (kW)	5.9	7.6	8.6	9.7	8.1	9.8	11.7	13.6	8.6	10.7	13.1	
Nozzle Pressure Drop (Pa)	422.5	762.8	283.0	406.2	417	750	282	403.4	424.7	756.7	285.6	
HE Air Side Pressure Drop (Pa)	25.4	42.5	60.9	84.4	39.3	66.7	91.5	119.5	50.9	83.8	114.7	
Air Flow Rate (m^3/s)	0.37	0.49	0.61	0.74	0.37	0.49	0.61	0.74	0.37	0.49	0.61	
Deluge Side												
Flow Rate (g/s)	15	15	15	15	80	80	80	80	167.5	166.3	164.3	
Inlet Temperature ($^{\circ}\text{C}$)	29.3	29.3	28.5	29.0	32.1	31.3	30.7	29.6	28.8	27.9	28.2	
Outlet Temperature ($^{\circ}\text{C}$)	24.9	24.3	26.6	25.3	32.1	31.4	31.0	29.6	32.5	31.0	29.8	
Capacity (kW)	0.28	0.31	0.11	0.23	-	-	-	-	2.3	1.8	0.5	
Evaporation Rate (g/s)	0.6	0.7	0.8	0.8	1.5	1.7	2.3	2.9	1.9	2.6	3.4	
Energy Balance and Uncertainty (%)	3.82 ± 17	0.14 ± 17	3.4 ± 20	4.0 ± 21	0.23 ± 13	3.9 ± 14	4.5 ± 14	4.0 ± 14	1.9 ± 8	0.2 ± 9	0.5 ± 11	

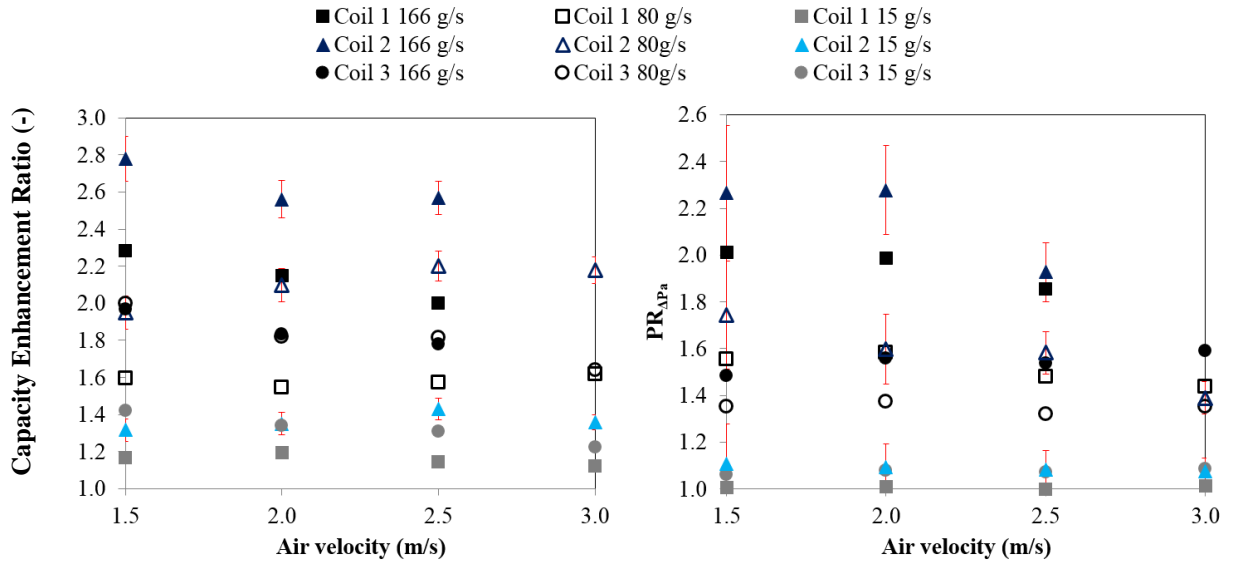
Table 4.3: Test summary for deluge cooled hydrophilic coated wavy fin RTHX with 2.4 mm fin spacing at approximately $T_{a,in} = 28^{\circ}\text{C}$, $\text{RH}_{a,in} = 45\%$ and $\omega_{a,in} = 0.0106 \text{ kg}_w/\text{kg}_a$.

Parameter	Deluge Cooling (15 g/s)				Deluge Cooling (80 g/s)				Deluge Cooling (166 g/s)			
Hot Water Side												
Flow Rate (l/s)	0.35	0.35	0.35	0.35	0.35	0.35	0.35	0.35	0.35	0.35	0.35	
Inlet Temperature ($^{\circ}\text{C}$)	43.1	43.1	43.1	43.1	43.2	43.1	43.1	43.2	43.1	43.0	43.1	
Outlet Temperature ($^{\circ}\text{C}$)	38.9	37.6	36.7	36.0	36.8	34.6	33.2	31.8	34.1	32.7	31.5	
Capacity and Uncertainty (kW)					9.1 \pm 0.2	12.3 \pm 0.2	14.4 \pm 0.2	16.5 \pm 0.3	13.1 \pm 0.3	15 \pm 0.3	16.9 \pm 0.3	
Air-Side												
Velocity (m/s)	1.5	2.0	2.5	3.0	1.5	2.0	2.5	3.0	1.51	2.0	2.5	
Inlet Temperature ($^{\circ}\text{C}$)	27.9	27.8	27.8	27.7	27.8	27.8	27.8	27.7	27.77	28.1	28.1	
Outlet Temperature ($^{\circ}\text{C}$)	38.3	37.4	36.5	35.7	37.5	35.5	33.2	32.1	35.66	33.0	31.9	
Inlet RH (%)	45.0	45.0	45.8	46.8	45.9	46.3	46.1	46.6	46.02	46.3	47.3	
Outlet RH (%)	28.5	30.3	32.6	34.4	35.3	43.4	51.3	55.7	48.46	57.8	63.7	
Capacity (kW)	6.1	8.3		10.8	8.0	11.8	14.3	16.9	10780.46	13696.0	16796.0	
Nozzle Pressure Drop (Pa)	431.0	781.5	294.0	420.4	425.7	773.9	294.2	408.6	425.25	759.4	285.0	
HE Air Side Pressure Drop (Pa)	26.2	43.3	61.8	84.9	41.3	63.2	90.3	109.8	53.6	90.2	109.9	
Air Flow Rate (m^3/s)	0.4	0.5	0.6	0.7	0.4	0.5	0.6	0.7	0.4	0.5	0.6	
Wetting Water-Side												
Flow Rate (g/s)	15.5	15.7	15.7	15.6	82.4	82.1	84.1	83.6	166.4	161.3	163.4	
Inlet Temperature ($^{\circ}\text{C}$)	27.83	27.1	27.6	27.3	28.4	27.3	27.2	27.2	28.5	28.7	29.0	
Outlet Temperature ($^{\circ}\text{C}$)	30.04	28.8	28.4	27.6	32.7	30.59	29.64	28.62	32.0	31.8	30.3	
Capacity (W)	60	18	101	150	1278	766	353	116	2056	1519	300	
Evaporation Rate (g/s)	0.63	1	1.27	1.465	1.48	2.84	4	5.09	3	4.22	5.5	
Energy Balance and Uncertainty (%)	4.2 \pm 17	3.4 \pm 17.4	1.2 \pm 17	4.7 \pm 18	3.0 \pm 12	4.7 \pm 10	4.8 \pm 11	3.8 \pm 11.2	3.5 \pm 7.7	4.7 \pm 8.3	4.7 \pm 8.9	

Table 4.4: Test summary for deluge cooled uncoated wavy fin RTHX with 3.0 mm fin spacing at approximately $T_{a,in}=28^{\circ}\text{C}$, $\text{RH}_{a,in} = 45\%$ and $\omega_{a,in}= 0.0106 \text{ kg}_w/\text{kg}_a$.

Parameter	Deluge Cooling (15 g/s)				Deluge Cooling (80 g/s)				Deluge Cooling (166 g/s)			
Hot Water Side												
Flow Rate (l/s)	0.35	0.35	0.35	0.35	0.35	0.35	0.35	0.35	0.3	0.4	0.3	0.3
Inlet Temperature ($^{\circ}\text{C}$)	43.15	43.09	43.07	43.05	43.10	43.09	43.14	43.17	43.1	43.1	43.1	43.1
Outlet Temperature ($^{\circ}\text{C}$)	39.25	38.45	37.82	37.17	37.63	36.79	35.85	35.30	37.7	36.8	36.0	34.8
Capacity and Uncertainty (kW)	5.661	6.73	7.624	8.54	7.943	9.15	10.59	11.43	7.8	9.2	10.3	12.2
Air-Side												
Velocity (m/s)	1.5	2.0	2.5	3.0	1.5	2.0	2.5	3.0	1.5	2.0	2.5	3.0
Inlet Temperature ($^{\circ}\text{C}$)	28.3	28.2	28.1	28.1	28.0	28.1	28.0	28.0	28.1	28.1	5.6	27.9
Outlet Temperature ($^{\circ}\text{C}$)	37.2	36.7	36.1	35.6	36.6	36.0	35.2	34.6	36.7	36.2	7.1	34.2
Inlet RH (%)	44.3	43.9	43.9	43.7	46.1	45.9	46.0	45.6	44.7	44.9	9.0	45.6
Outlet RH (%)	30.8	30.7	30.9	31.4	35.7	36.3	37.7	37.9	31.8	32.8	6.9	38.7
Capacity (kW)	5.6	6.9	7.9	8.9	6.8	8.5	10.0	11.0	5.5	7.0	8.6	10.7
Nozzle Pressure Drop (Pa)	427.3	758.8	288.6	416.6	434.3	765.9	287.7	418.7	427.7	750.9	286.7	416.2
HE Air Side Pressure Drop (Pa)	15.1	25.9	38.9	55.1	19.3	33.0	47.9	68.5	21.2	37.4	55.7	80.6
Air Flow Rate (m^3/s)	0.4	0.5	0.6	0.7	0.4	0.5	0.6	0.7	0.4	0.5	0.6	0.7
Wetting Water Side												
Flow Rate (g/s)	15.4	15.1	15.0	14.8	80.4	79.4	80.0	79.8	160	165	167	169
Inlet Temperature ($^{\circ}\text{C}$)	28.4	28.1	27.9	27.6	28.5	28.6	27.6	27.3	29	28	28	28
Outlet Temperature ($^{\circ}\text{C}$)	30.2	29.3	28.7	28.1	32.8	31.9	30.9	30.1	33	32	31	31
Capacity (kW)	0.02	0.02	0.05	0.07	1.3	0.9	0.9	0.7	2.406	2.409	2.021	1.88
Evaporation Rate (g/s)	0.68	0.76	0.81	0.91	1.2	1.49	1.849	2	0.697	0.929	1.263	2.007
Energy Balance and Uncertainty (%)	2.6±17	0.6±19.4	2.4±20	4.4±22	3.8±12	4.6±14	4.6±14.8	4.6±16	2±12.4	3.7±13.9	3.5±15	4.3±14.5

Deluge evaporative cooling tests were conducted with wetting water and air flowing in cross-flow configuration through the HX. CER and $PR_{\Delta P_a}$ of wavy-fin RTHXs using deluge evaporative cooling are presented in Figure 4.5.



Note: Values are relative to dry case capacities or ΔP_a at respective air velocities for each HX.

Figure 4.5: CER and $PR_{\Delta P_a}$ of wavy-fin RTHXs using deluge evaporative cooling at approximately $T_{a,in} = 28^\circ\text{C}$, $RH_{a,in} = 45\%$ and $\omega_{a,in} = 0.0106 \text{ kg}_w/\text{kg}_a$.

The main observations were as follows:

- Both capacities and $PR_{\Delta P_a}$ increased proportionately with deluge water flow rate as shown in Figure 4.5.
- The range of highest CER values for the 3 HXs was found to be within 1.97 to 2.78 at 166 g/s deluge flow rate. Although $PR_{\Delta P_a}$ was close to 1 for low deluge flow rates (15 g/s), it also corresponded to lowest CER values. Therefore, deluge cooling could not achieve CER higher than 2 without significantly increasing $PR_{\Delta P_a}$.
- Higher values of $PR_{\Delta P_a}$ may be caused by water bridging between adjacent fin surfaces.

4.4 Effect of hydrophilic coating

Hydrophilic coated coil achieves CER and $PR_{\Delta P_a}$ of 1.32 to 2.78 and 1.07 to 2.28, respectively and untreated coil with same fin spacing achieves lower CER and $PR_{\Delta P_a}$ values from 1.13 to 2.28 and 1.0 to 2.0, respectively. Therefore, compared to untreated coil, hydrophilic coated coil CER is approximately 21.7% higher which may be due to improved surface wetting. This is also evident from Figure 4.6 which shows the contribution of deluge water evaporation to overall HX capacity. The trends for ratio of Q_{evap}/Q_{total} are in line with the CERs in Figure 4.5, and so heat transfer enhancement is attributed to enhanced evaporation rates.

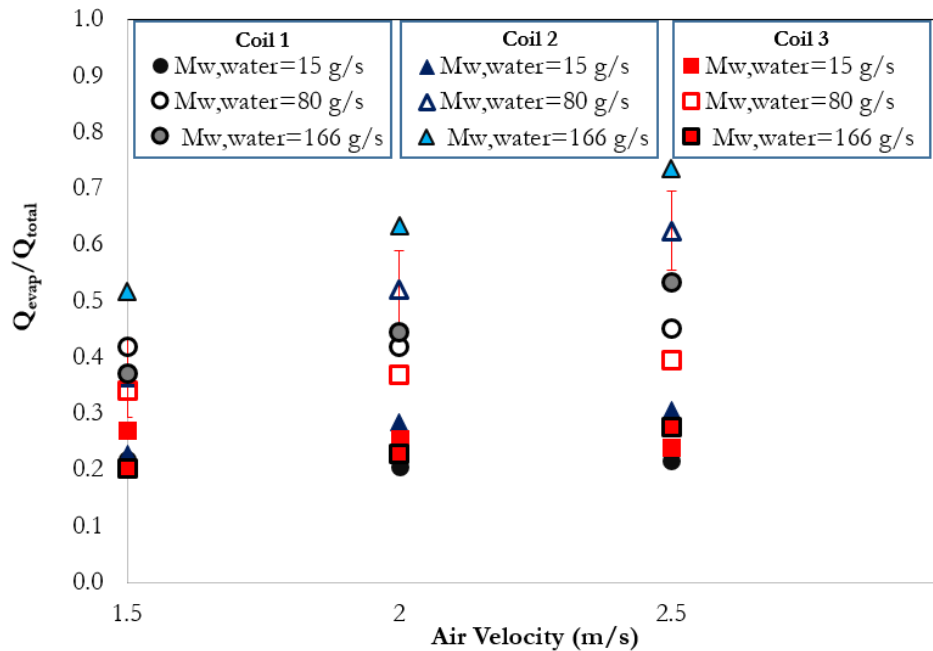
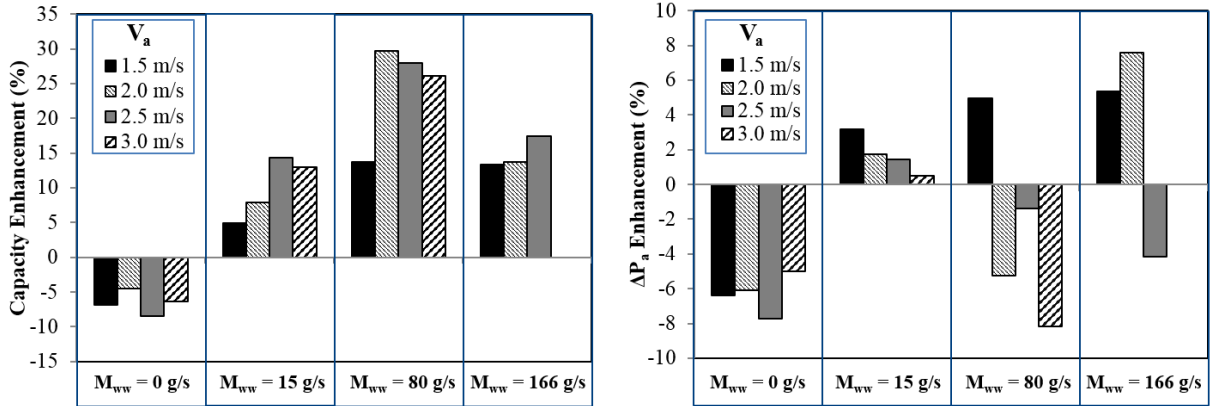


Figure 4.6: Contribution of deluge water evaporation to overall wavy fin HX capacity at approximately $T_{a,in} = 28^\circ\text{C}$, $RH_{a,in} = 45\%$ and $\omega_{a,in} = 0.0106 \text{ kg}_w/\text{kg}_a$.

In addition, percentage enhancements in HX capacity and ΔP_a relative to each dry and wet case of uncoated HX with same $F_p=2.4\text{mm}$ are plotted in Figure 4.7.



Note: Enhancements relative to capacity or ΔP_a of uncoated HX ($F_p = 2.4\text{mm}$).

- (a) % capacity enhancement at different deluge rates (b) % PA enhancement at different deluge rates

Figure 4.7: Effect of hydrophilic coating on capacity enhancement and ΔP_a enhancement of deluged wavy-fin RTHX at approximately $T_{a,in} = 28^\circ\text{C}$, $\text{RH}_{a,in} = 45\%$ and $\omega_{a,in} = 0.0106 \text{ kg}_w/\text{kg}_a$.

It is interesting to note that compared to the uncoated coil with same F_p , heat transfer was enhanced by 5 to 30% when deluge cooling was applied to hydrophilic coated coils but ΔP_a was not enhanced in most cases.

Although highest CERs were obtained for coated coil at $m_{ww}=166\text{g/s}$ (Figure 4.5), it is also observed that, relative to uncoated HX, highest capacity enhancement was obtained at $m_{ww}=80\text{g/s}$ as shown in Figure 4.7 (a). This reduction in enhancement may be due to droplet carryover which was observed for Coil 2 at $v_a \geq 2 \text{ m/s}$.

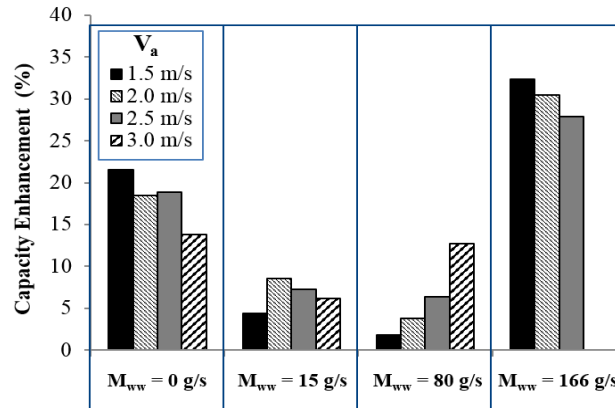
It can also be noted that at constant ΔP_a values, hydrophilic coated HX achieved higher capacity compared to uncoated coil at approximately half the deluge flow rates for same fin spacing, thereby offering substantial potential for wetting water savings.

4.5 Effect of fin spacing

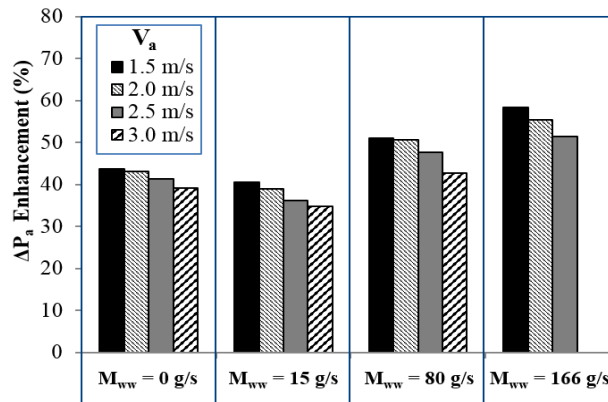
CER and $PR_{\Delta P_a}$ of 1.22 to 2.0 and 1.06 to 1.59, respectively, were obtained for HX with $F_p=3.0\text{mm}$ as shown in Figure 4.5. Although compared to HX with $F_p=3.0\text{ mm}$ (uncoated), CER of HX with $F_p = 3.0\text{ mm}$ were 35.4% lower, heat transfer enhancement was also lower by approximately 16%. HX with $F_p 3\text{ mm}$ achieved lowest contribution of deluge water evaporation to overall heat transfer rates compared to other test coils, as observed from Figure 4.6. To compare the effect of fin spacing, percentage enhancements in HX capacity and ΔP_a relative to each dry and wet case of uncoated HX with same $F_p=2.4\text{mm}$ are plotted in Figure 4.8.

It was found that compared to the coil with $F_p 3.0\text{ mm}$, heat transfer was enhanced by 2 to 30% when deluge cooling was applied to HX with $F_p 2.4\text{ mm}$ and ΔP_a increased by 33 to 58%. Even in dry cooling, reducing fin spacing enhances ΔP_a by 44% while heat transfer improves by 21%. The highest enhancement in both capacity and ΔP_a was obtained at highest deluge flow rate of $m_{ww}=166\text{g/s}$, and at lower flow rates $m_{ww}=15\text{g/s}$ and 80g/s there is no substantial difference in capacities obtained from Coil 1 or 3 but ΔP_a increases considerably.

Although ΔP_a values are higher for Coil 1, in both dry and deluge cooling, it may be recommended to use smaller fin spacings due to the fact that in many cases such HXs are utilized as hybrid fluid coolers or condensers. Therefore, a compact fin spacing helps obtain higher HX capacity not only for the major portion for the year in dry operation mode but also when deluge evaporative cooling is required in high ambient air temperature conditions.



(a) Capacity enhancement at different deluge rates



(b) ΔP_a enhancement at different deluge rates

Note: Enhancements relative to capacity or ΔP_a of uncoated HX ($F_p = 3.0$ mm).

Figure 4.8: Effect of decreasing fin spacing from 2.4 mm to 3 mm on capacity enhancement and ΔP_a enhancement of deluged wavy-fin RTHXs at approximately $T_{a,in} = 28^\circ\text{C}$, $RH_{a,in} = 45\%$ and $\omega_{a,in} = 0.0106$ kgw/kg.

Main observations summarizing effect of increasing F_p from 2.4 mm to 3 mm for a wavy-fin HX in deluge cooling conditions are as follows:

- Both HX capacity and airside pressure drop decreased
- Capacity and ΔP_a reduction was approximately 4-32% and 35-58%, respectively. This was due to 25% increase in flow passage area through wavy fins and 23.7% increase in HX surface area

- At approximately same ΔP_a and wetting water flow rates, HX with F_p 3 mm reached up to 8.5 to 16.76% lower capacity

4.6 Effect of flow-configuration

Dry cooled HXs are typically operated in counter-current configuration as shown in Figure X. However due to low penetration of wetting water in HX depth the hottest section of water in the tubes is not wetted. Therefore by changing to a co-current configuration the hottest stream of water would be cooled by wetting water directly. A few experiments were conducted to quantify the benefits of this configuration for deluge evaporatively cooled wavy-fin HX.

Figures 4.9, 4.10 and 4.11 present the effect of flow configuration on HX capacity, capacity enhancement ratio, and evaporation rate, respectively on deluged uncoated wavy-fin RTHX with $F_p = 2.4$ mm at approximately $T_{a,in} = 28^\circ\text{C}$, $RH_{a,in} = 45\%$ and $\omega_{a,in} = 0.0106$ kg_w/kg_a .

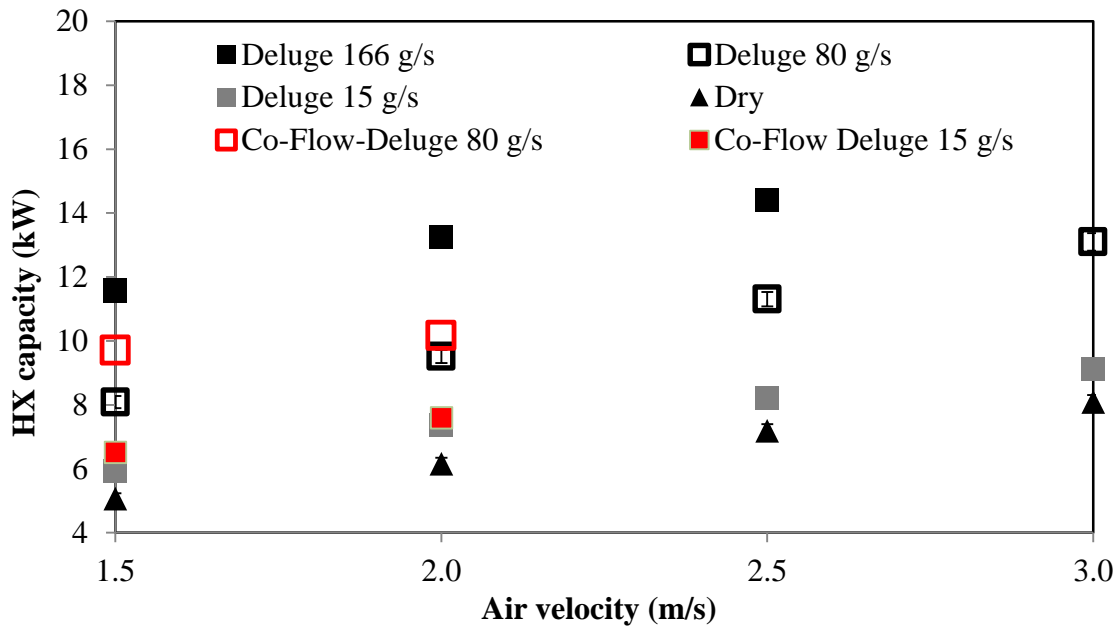


Figure 4.9 Effect of flow configuration on HX capacity of deluged uncoated wavy-fin RTHX with $F_p = 2.4$ mm at approximately $T_{a,in} = 28^\circ\text{C}$, $RH_{a,in} = 45\%$ and $\omega_{a,in} = 0.0106$ kg_w/kg_a .

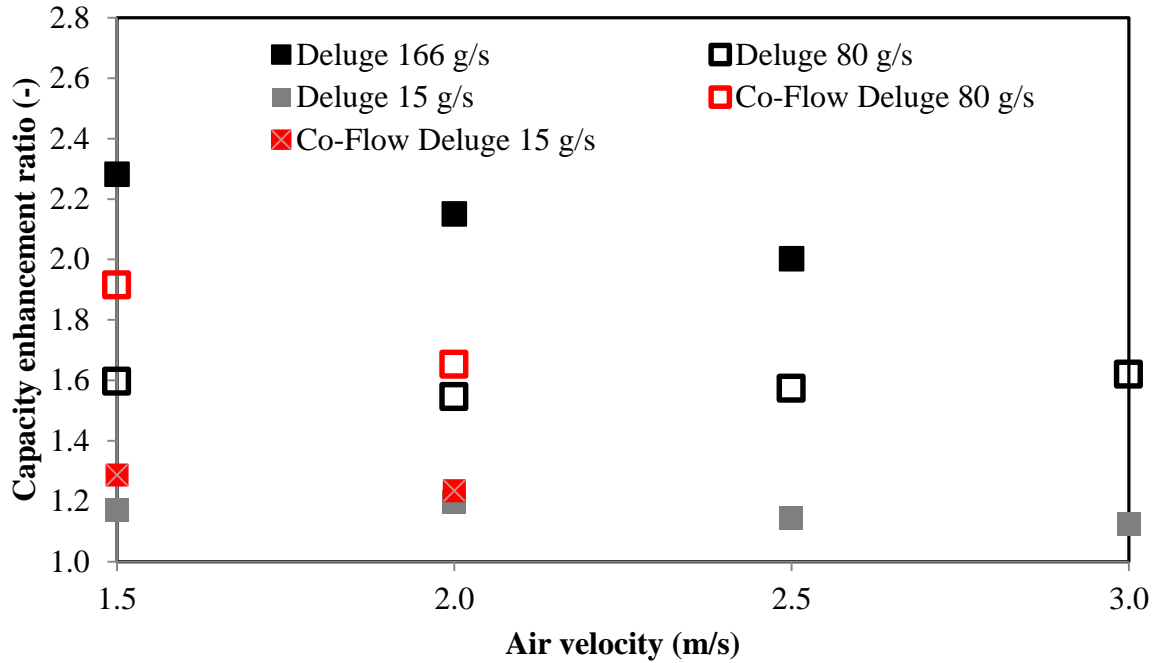


Figure 4.10 Effect of flow configuration on HX capacity enhancement ratio of deluged uncoated wavy-fin RTHX with $F_p = 2.4$ mm at approximately $T_{a,in} = 28^\circ\text{C}$, $RH_{a,in} = 45\%$ and $\omega_{a,in} = 0.0106$ kg_w/kg_a.

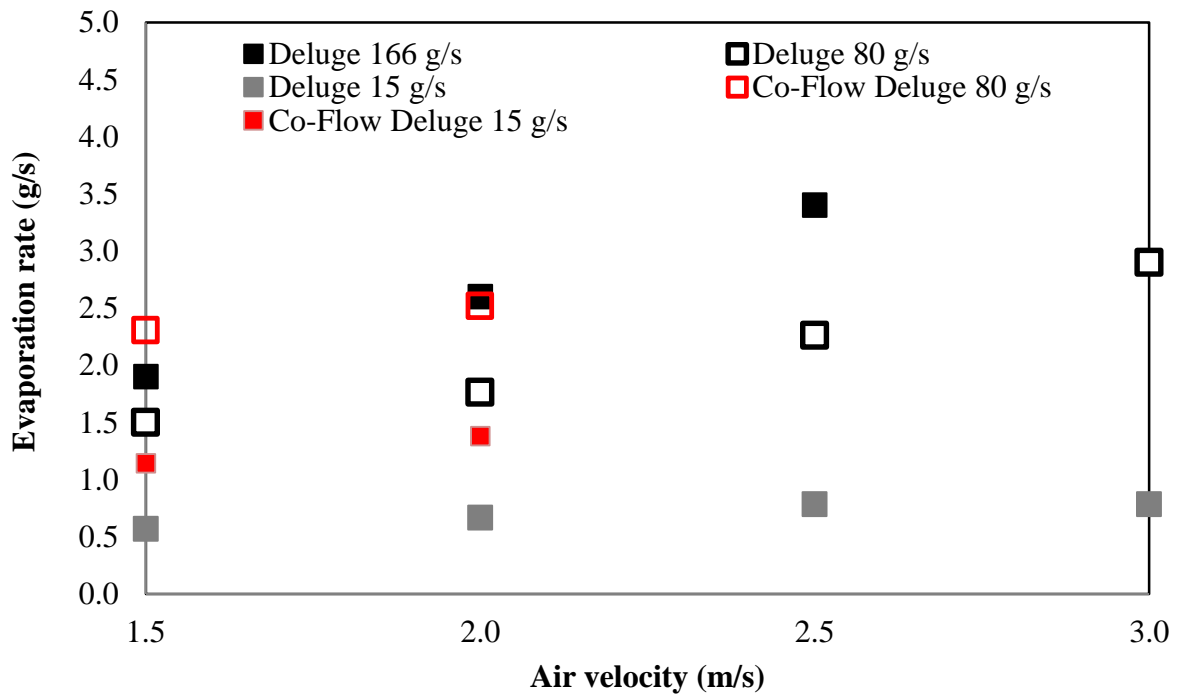


Figure 4.11 Effect of flow configuration on evaporation rate of deluged uncoated wavy-fin RTHX with $F_p = 2.4$ mm at approximately $T_{a,in} = 28^\circ\text{C}$, $RH_{a,in} = 45\%$ and $\omega_{a,in} = 0.0106$ kg_w/kg_a.

It was observed that HX capacity increased by up to 21% for deluge cooled HX with uncoated wavy fins at $F_p = 2.4$ mm, at same deluge flow rate of 80 g/s. However the benefit reduced substantially at higher air velocities, for example 2 m/s HX frontal air velocity the difference in HX capacity when operating in co-current instead of counter-current mode was only 7%. The benefit at lower deluge flow rates is even lower. Although it may be possible to change the flow configuration when switching to deluge cooling mode for the peak summer hours, if higher fan speeds are to be operated such a change in configuration may not be useful. But for a system designed for lower air velocities may benefit from this change in configuration.

4.7 Visualization of deluge wetting water distribution

One of the challenges in understanding capacity enhancement of HXs is the difficulty associated with visualization of distribution of wetting water in the depth of HX. With the amount of surface area of the HX which is being wetted unknown, one cannot understand the reason for high or low capacities of HXs in different conditions. Typical HX installation configuration in the air duct is shown in Figure 4.12 (a) and (b) with bottom and side frame of HX marked. Figure 4.13 shows HX installed with bottom frame removed to aid visualization.

By removing the bottom part of frame, a window access was obtained to visualize falling water at HX wetting water outlet. Figure 4.14 shows visualization of wetting water distribution in depth of RTHX (3.0 mm fin spacing) in deluge cooling conditions. There is no study which has focused on visualization of wetting water in deluge cooled HXs in the published literature. Therefore, it is envisaged that visualization improvement would

provide useful insight into the wetting of HX coils.

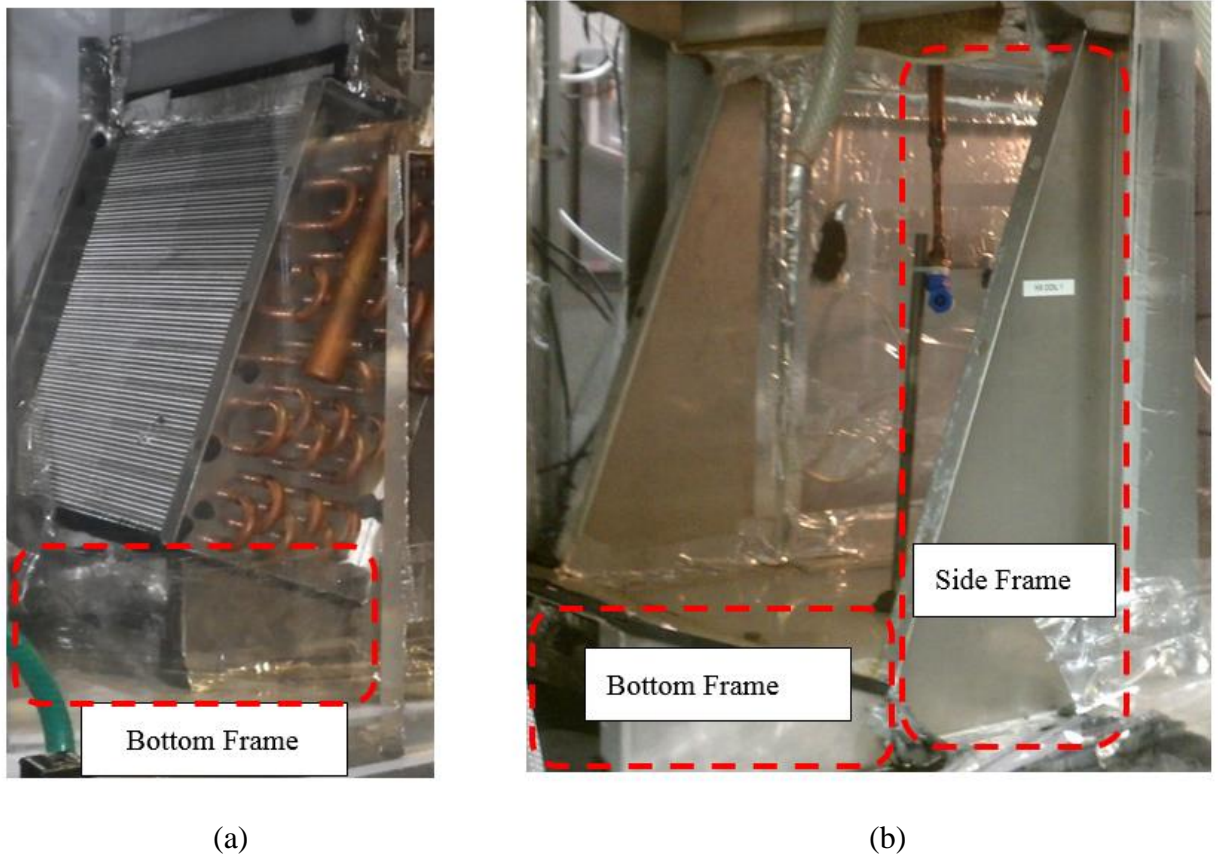


Figure 4.12: Typical HX installation configuration in the air duct with bottom and side frame of HX marked.

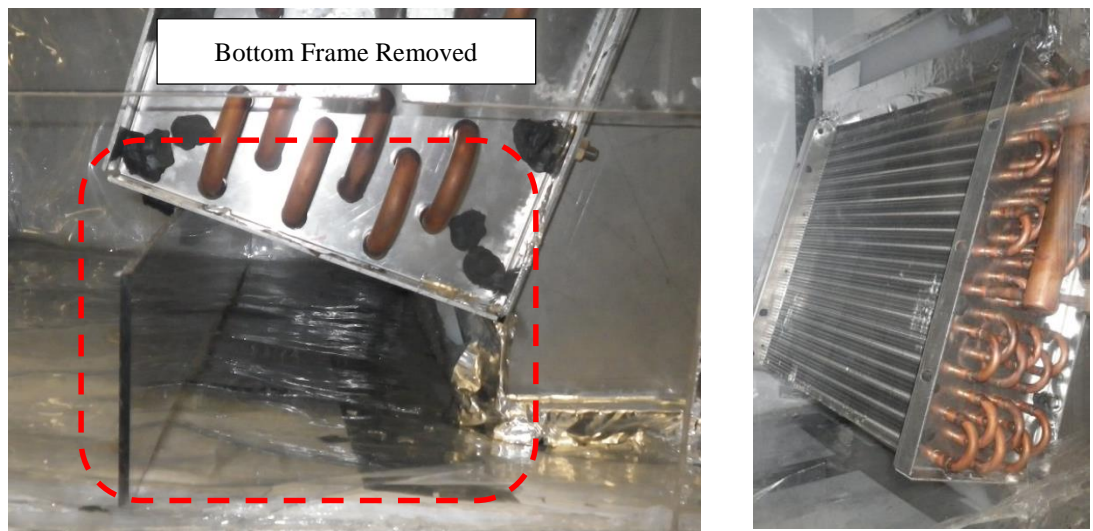


Figure 4.13: HX installed with bottom frame removed to aid visualization.

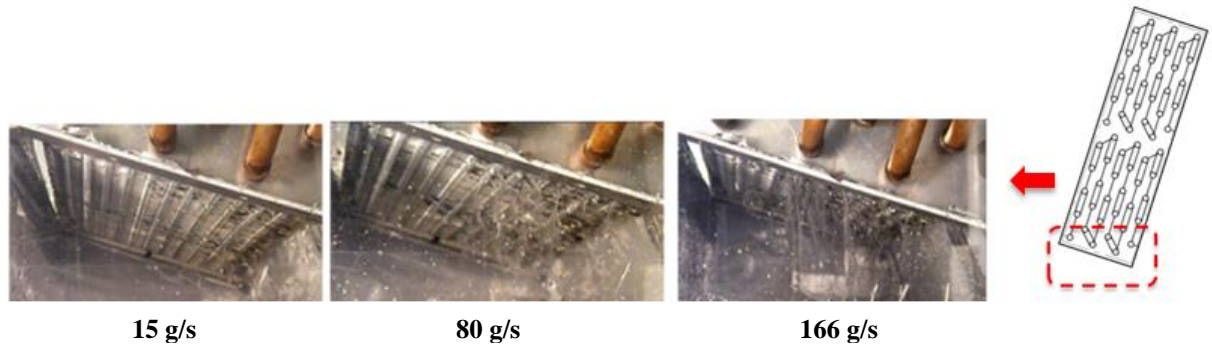


Figure 4.14: Visualization of wetting water distribution in depth of RTHX (3.0 mm fin spacing) in deluge cooling conditions.

HX is sealed at the edges before recording the videos of wetting water flow in different conditions. Furthermore, to ensure that removing the bottom plate does not affect capacity or air side ΔP considerably, the dry case data points were repeated for HX with 3 mm fin spacing. Table 4.5 summarizes the dry case capacity and ΔP_a of HX with Fp 3mm before and after removing bottom frame.

Table 4.5: Dry case capacity and ΔP_a of HX with Fp 3mm before and after removing bottom frame at approximately $T_{a,in} = 28^\circ\text{C}$, $RH_{a,in} = 45\%$ and $\omega_{a,in} = 0.0106 \text{ kg}_w/\text{kg}_a$.

Frontal Air Velocity (m/s)	1.5	2	2.5	3
Capacity (After) (kW)	4.1	5.2	6.1	6.9
Capacity Deviation from Baseline (%)	1.5	-1.7	-0.9	1.4
ΔP_a (Pa)	16.3	27.0	40.5	55.7
ΔP_a Deviation from Baseline (%)	2.9	3.9	5.4	5.4

Note: % deviation compared to HX capacity in similar conditions with bottom plate.

Since % deviation in capacity and ΔP_a was found to be less than 2% it was assumed that removing bottom plate does not cause significant changes to HX performance and videos obtained are representative of cases with bottom plate of frame not removed.

4.8 Summary

This Chapter reported the results of an experimental study conducted to evaluate the performance of three cross-flow herringbone wavy-fin HXs working as hybrid evaporative coolers set at 20° from vertical in both dry and wet conditions using deluge cooling. Effect of fin spacing and hydrophilic coating, on deluge cooling HX performance under varying air velocities and wetting water flow rates was presented in terms of capacity enhancement ratio and air-side pressure drop penalty ratios. It was found that in dry operation hydrophilic coating of coils reduces dry case HX capacity by 4 to 8% and increasing fin spacing reduces capacity by up to 21%.

Capacity enhancements due to deluge cooling were accompanied by significant increase in air-side pressure drops with maximum capacity enhancement ratio (CER) of 2.78 obtained for hydrophilic coated HX at $PR_{\Delta P_a}$ of up to 2.28. Furthermore, at a given ΔP_a values, hydrophilic coated HX achieved higher capacity compared to uncoated coil at approximately half the deluge flow rates for same fin spacing, thereby offering substantial potential for wetting water savings. Hydrophilic coated fins offer lower contact angles compared to uncoated coil, which spreads water film over larger area, increases wetting and evaporative cooling enhancement and reduces ΔP_a .

Also, it was found that compared to the coil with F_p 3.0 mm, heat transfer was enhanced by 2 to 30% when deluge cooling was applied to HX with F_p 2.4 mm and ΔP_a increased by 33 to 58%.

It was found that deluge cooling cannot provide CER higher than 2 without a significant increase in ΔP_a . Therefore, deluge cooling may not be a method of choice when applying evaporative cooling to finned coils and when fan energy consumption is a critical performance parameter. In addition, deluge cooling also utilizes a high amount of wetting water and is greatly affected by the distribution of wetting water within the coil volume, which makes the distributor design and placement on HX coils challenging. Based on experimental data, water bridging could also be suspected for HX coils with F_p 3 mm. Therefore, it is recommended that either much larger fin spacing or an HX with bare tubes should be used when deluge cooling is applied to HX coolers or condenser coils. Due to these drawbacks, deluge cooling was not investigated in the remaining part of this study.

Chapter 5 Experimental results: spray cooling

5.1 Introduction

This Chapter describes the spray wet cooling performance of the three wavy fin HXs set at 20° from the vertical. The effect of fin spacing and hydrophilic coating on the hydraulic performance of HX was investigated at different inlet air temperatures, and air and wetting water flow rates. Two modes of spray cooling were implemented i.e. front and top spray cooling. Front spraying is more conventionally utilized due to ease of installation and maintenance in larger size units. Top spraying is also more useful for vertical or inclined coils which may be deep (more tube banks) in the direction of air. Horizontal coils would typically utilize front spray configuration. The choice of horizontal and vertical arrangement of coil depends upon, 1) limitation on unit height, 2) HX geometry and 3) spray distribution as discussed in Chapter 1 of this Dissertation. The various commercially available spray cooling nozzles and the criteria for their selection in this Study are presented in Section 5.2. The experimental results of front spray cooling and effect of spray configuration on wavy fin HX performance are presented in Sections 5.3 and 5.4, respectively.

5.2 Spray nozzle selection

The effectiveness of evaporative cooling hot surfaces using spray nozzles depends on several factors such as spray droplet mean size, spray flow rate, nozzle discharge pressure, nozzle geometry, spray configuration and placement of nozzles. The typical spray rates utilized by experimental studies in published literature are summarized in Table 5.1. The spray rates are presented here in g/s per unit volume of HX coil, instead of typical spray

rate in g/s. This allows better comparison of HXs with different geometries and tubes banks.

Table 5.1: Spray rates utilized by experimental studies in published literature.

Study	Spray (g/m³-s)
Sen, 1973	3114.6
Simpson et al., 1974	3114.6
Yang and Clark, 1975	328.46
Kried et al., 1979	1128-2257
Kreid et al., 1979	1771-2360
Hauser et al., 1982	993-2482
Hauser and Kreid, 1982	1657-2210
Leidenfrost and Korenic, 1982	7865 - 11670
Nakayama et al., 1987	87-677
Oshima et al., 1992	136-359
Walczyk, 1993	309-515
Faca and Olieveira, 2000	188-1245
Hasan and Siren, 2003	8741-19424
Sarker et al., 2009	1521
Heyns, 2010	4500-11750
Wiksten and Assad, 2010	5747
Chen et al., 2013	181-907

The purpose of this work was to minimize the spray flow rate while obtaining highest CER value. With this in mind the following was considered before deciding a spray rate of 59-513 g/m³-s coil:

- Published studies utilized flow rates as high as approximately 19424 g/s/m³ coil and as low as 87 g/s/m³ coil sprayed onto the coils either in top or front spray configuration.
- None of the authors have reported spray droplet size used, effect of spray configuration, nozzle geometry etc.
- Based on preliminary results it was found that spray flow rates, less than approximately 25 g/s/m³ coil did enhance HX capacity appreciably (CER approximately 1.1).

Thus, spray flow rate was set at 2.2 g/s, 3.8 g/s and 8 g/s using three different nozzles.

To facilitate a parametric study on effect of spray flow rate on wavy fin HX performance, spray nozzles were chosen in a way that droplet size, discharge pressure, nozzle geometry, configuration and distance from HX coil would be kept constant.

Table 5.2 summarizes the commercially available spray nozzles, along with their geometry, spray pattern, droplet size range and minimum spray rates for water.

Table 5.2: Commercially available spray nozzles, along with their geometry, spray pattern, droplet size range and minimum spray rates for water. [Spray Systems, 2013].

Spray Nozzle	Droplet Size (μ)	Minimum Flow (g/s)
 <p data-bbox="386 632 558 663">Spiral Full Cone</p>	500-1000	30
 <p data-bbox="415 905 521 936">Full Cone</p>	500-1000	6.3
 <p data-bbox="350 1205 589 1236">Full Cone Wide Spray</p>	500-1000	88
 <p data-bbox="394 1503 557 1535">Flat Fan - Slit</p>	100-500	0.70
 <p data-bbox="370 1808 566 1839">Flat Fan Deflected</p>	100-500	2

Table 5.2: Commercially available spray nozzles, along with their geometry, spray pattern, droplet size range and minimum spray rates for water [Spray Systems, 2013] (Cont'd).

Spray Nozzle	Droplet Size (μ)	Minimum Flow (g/s)
 <p data-bbox="337 657 695 684">Flat Fan Deflected Narrow Angle</p>	500-1000	12
 <p data-bbox="391 1045 641 1073">Whirl Jet-Hollow Cone</p>	100-500	1.8
 <p data-bbox="337 1434 695 1461">Pintle Hollow Cone (Angle 80°)</p>	10-100	0.7
 <p data-bbox="337 1841 695 1869">Pintle Hollow Cone (Angle 60°)</p>	10-100	0.8

The hollow cone nozzle geometry is considered most effective for spray cooling of HXs. As shown in Figure 5.1, compared to full cone nozzle type, a hollow cone nozzle reduces overlapping wetted regions which reduces potential water bridging, improves spray efficiency and water economy.

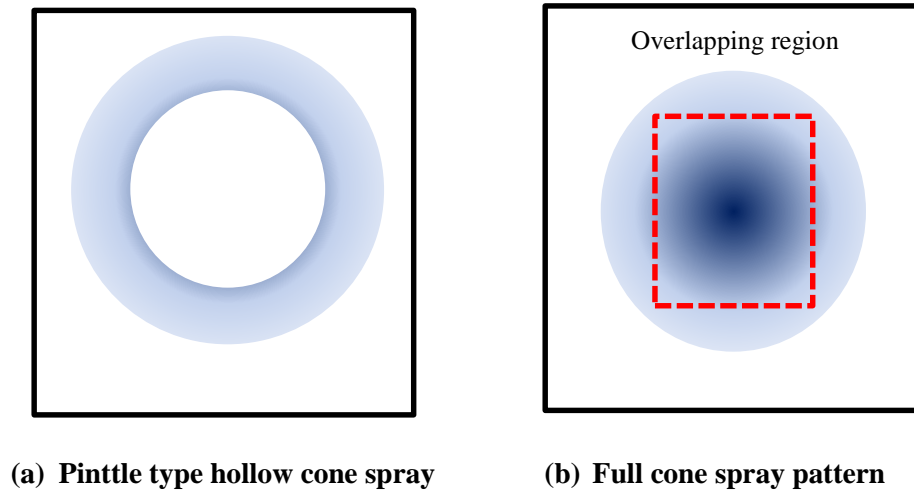


Figure 5.1: Projected spray pattern for hollow and full cone spray nozzles on HX face.

The limitation of using a hollow cone nozzle is that at lower flow rates the droplet momentum reduces much more than full cone nozzle spraying at same flow rate. Therefore there is a limitation on the spray angle using hollow cone nozzles. Commercially available hollow cone nozzles have a maximum spray angle of 80° compared to up to 140° for a full cone nozzle.

Lower spray angle would translate to reduced distance from HX before the droplets loose enough velocity that they fall short of HX as shown in Figure 5.2. On the other hand placing nozzle near the coil would reduce spray area. Thus for this Study the distance of nozzle

from HX (approximately 12-14 inches) was decided based upon the spray flow rate which in turn was a function of nozzle discharge pressure.

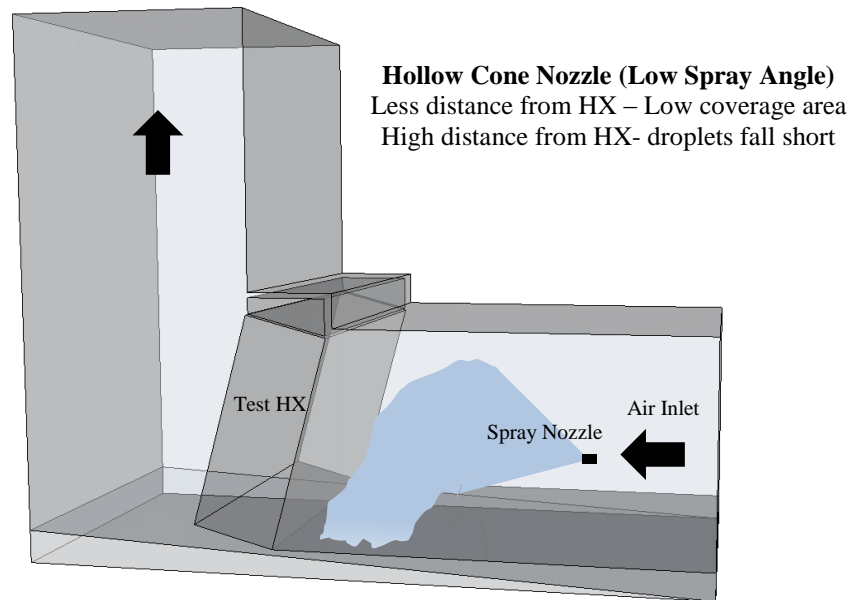


Figure 5.2: Low momentum droplets falling short of HX.

With nozzle type, configuration and flow rate decided a nozzle performance curve for pintle type spray nozzles shown in Figure 5.3 was used to select specific nozzles which could provide different flow rates at approximately same droplet size.

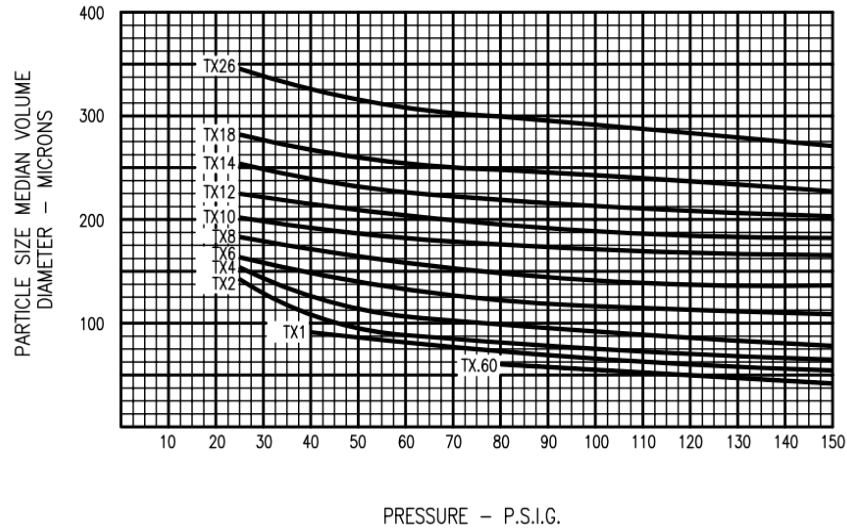


Figure 5.3: Spray droplet size as a function of pinttle type nozzle discharge pressure [Spray Systems, 2013].

Table 5.3: Spray nozzles selected for the current study along mean droplet size and flow rate range.

Nozzle Model Number	Drop Size (μ)	Flow Range (g/s)*
TX2	~90	2.0 to 2.8
TX3	~100	3.0 to 4.2
TX6	~125	6.0 to 8.5

Note: Flow range and droplet size for discharge pressure between 40 to 80 psi as per Figure 5.3.

Also as observed from Table 5.3 the droplet size varies between 90 to 125 μ for different nozzle types and flow rates. For the same type of nozzle it was found that droplet size could not be kept constant at varying flow rates especially when flow rates are very low, because droplet size increases as flow rate increase. The only way to achieve a higher flow rate with same droplet diameter would be to install two nozzles. But spray pattern and coverage area

would change on HX face. Thus nozzles presented in Table 5.3 were selected for current study.

Although, ideally a spray nozzle with smallest possible droplet size would be used but droplets below 50 μ have a higher chance of being carried downstream of air and require compressed air assisted atomization which adds to system complexity and energy consumption.

5.3 Front spray cooling

Experimental performance of three front spray cooled wavy-fin HX's is presented in this Section and effect of ambient temperature, fin spacing and hydrophilic coating are discussed in Sections 5.3.1 to 5.3.3, respectively.

Tables 5.4 and 5.5 provide experimental test summary for front spray cooled RTHX with uncoated and hydrophilic coated wavy fins, respectively, with Fp 2.4 mm each. Table 5.6 provides experimental test summary for front spray cooled RTHX with uncoated wavy fins with Fp 3.0 mm each.

Figure 5.4 presents the HX capacities as a function of ΔPa for wavy-fin HXs under dry and front spray cooling.

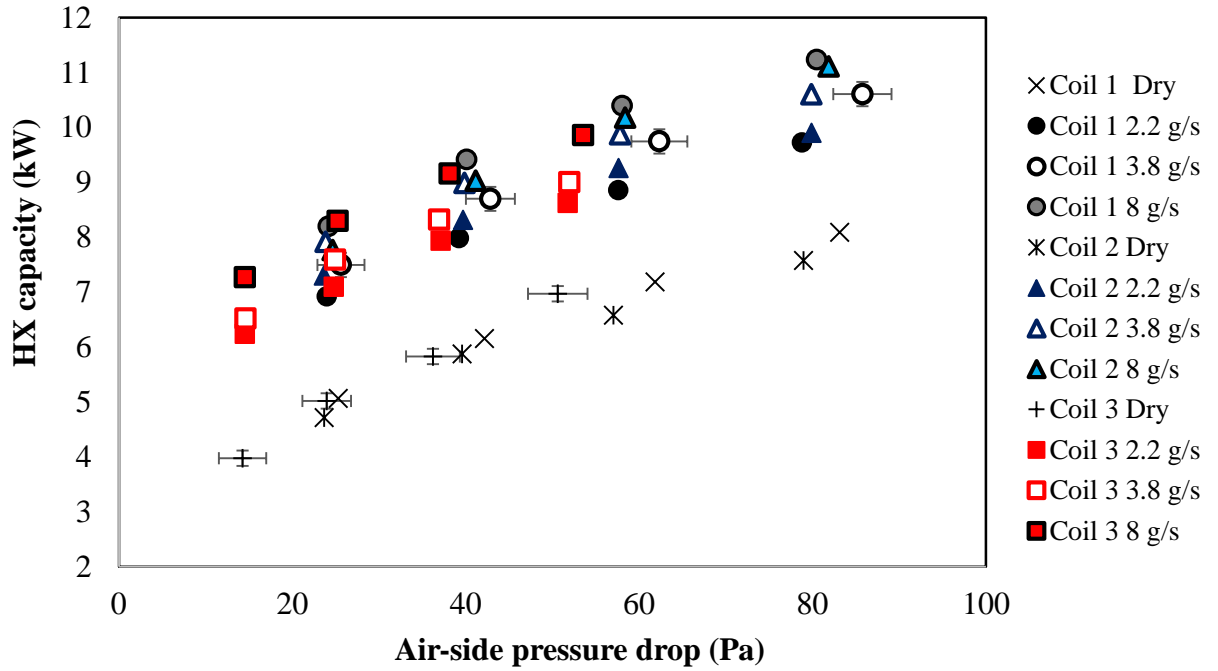


Figure 5.4: HX capacity as a function of ΔP_a under dry and front spray cooling conditions at approximately $T_{a,in}= 28^\circ\text{C}$, $\text{RH}_{a,in}= 45\%$ and $\omega_{a,in}= 0.0106 \text{ kg}_w/\text{kg}_a$.

Table 5.4: Test summary for front spray cooled uncoated wavy fin RTHX with $F_p=2.4$ mm at approximately $T_{a,in}=28^\circ\text{C}$, $RH_{a,in} = 45\%$ and $\omega_{a,in}= 0.0106$ kg_w/kg_a, and wetting water flow rate 8, 3.8 and 2.2 g/s .

Parameter	$M_{ww} = 8.0$ g/s				$M_{ww} = 3.8$ g/s				$M_{ww} = 2.2$ g/s			
Hot water side												
Flow rate (l/s)	0.35	0.35	0.35	0.35	0.35	0.35	0.35	0.35	0.35	0.35	0.35	0.35
Inlet temperature (°C)	42.96	43.07	42.96	42.95	43.0	43.1	43.1	43.1	43.02	43.05	42.99	43.21
Outlet temperature (°C)	37.31	36.58	35.8	35.21	37.8	37.1	36.3	35.7	38.25	37.55	36.89	36.51
Capacity and uncertainty (kW)	8.2±0.21	9.4±0.18	10.1±0.2	11.±0.2	7.5±0.1	8.7±0.1	9.7±0.2	10.6±0.1	6.9±0.1	7.9±0.1	8.8±0.2	9.5±0.2
Air-side												
Velocity (m/s)	1.50	2.00	2.50	3.00	1.5	2.0	2.5	3.0	1.5	2.0	2.5	3.0
Inlet temperature (°C)	28.07	28.2	28.25	28.26	27.7	27.8	27.8	27.9	28.3	28.4	28.1	28.2
Outlet temperature (°C)	38.23	37.65	37.07	36.44	38.7	38.1	37.4	36.8	38.5	37.9	37.3	36.8
Inlet RH (%)	45.32	45.1	45	45.1	45.2	43.6	43.8	44.1	45.3	45.2	44.7	45.2
Outlet RH (%)	34.82	33.8	33.6	34.1	30.7	29.5	29.7	30.6	31.9	31.3	30.6	31.0
Capacity (kW)	8.571	9.8	10.72	11.8	7.6	8.9	9.9	10.7	7.2	8.3	9.2	10.2
HX Air side pressure drop (Pa)	24.14	40.11	58.04	80.5	25.6	42.9	62.3	85.8	24.0	39.2	57.6	78.8
Air flow rate (m ³ /s)	0.37	0.49	0.6	0.74	0.37	0.50	0.62	0.74	0.37	0.49	0.6	0.7
Wetting water side												
Flow rate (g/s)	8	8	8	8	3.8	3.8	3.8	3.8	2.2	2.2	2.2	2.2
Inlet temperature (°C)	27.58	27.53	27.4	27.38	25.6	25.9	25.9	26.0	28.5	28.8	29.4	29.4
Outlet temperature (°C)	24.28	23.91	23.59	23.45	25.1	25.1	24.9	25.0	28.3	29.0	29.8	29.9
Capacity (kW)	0.11	0.124	0.127	0.131	0.1	0.1	0.1	0.1	-	-	-	-
Evaporation rate (g/s)	1.643	1.696	1.73	1.85	1.15	1.2	1.22	1.29	1.13	1.10	1.10	1.10
Energy balance and uncertainty (%)	3±12.8	2.6±14.5	4.4±16	4.0±17	2.1 ± 14	3.6 ± 16	2.8 ± 17	3.7 ± 18	4.5 ± 15	4.5 ± 17	4.6 ± 18	4.6 ± 20

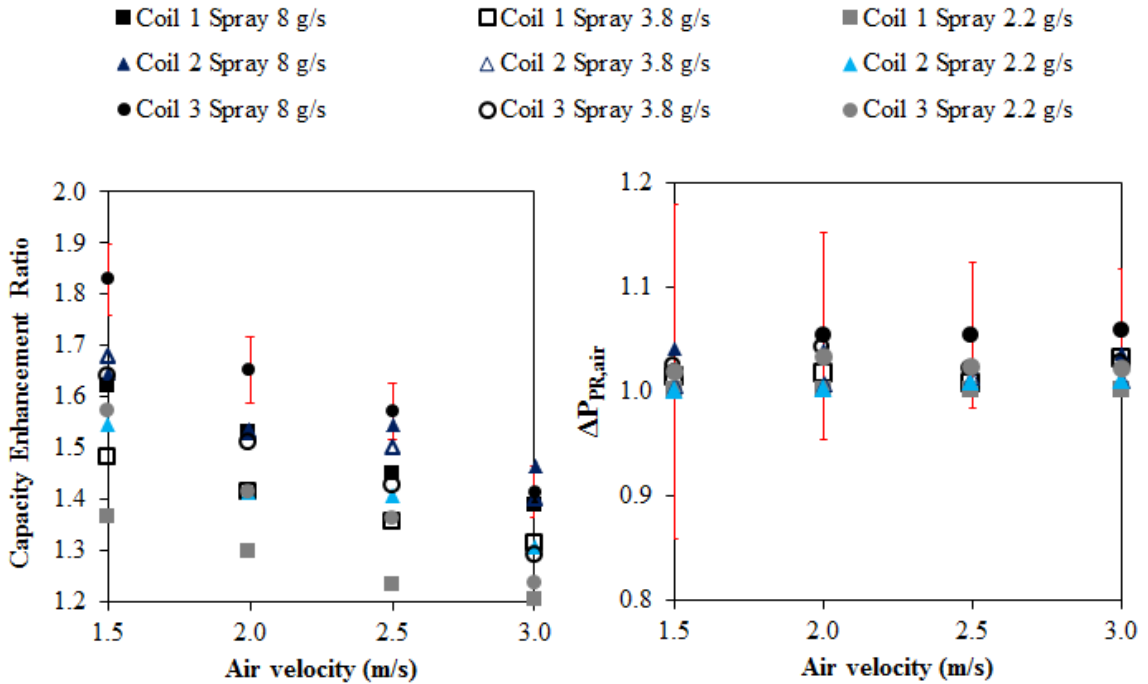
Table 5.5: Test summary for front spray cooled hydrophilic coated wavy fin RTHX with $F_p=2.4$ mm at approximately $T_{a,in}= 28^\circ\text{C}$, $\text{RH}_{a,in} = 45\%$ and $\omega_{a,in}= 0.0106$ kg_w/kg_a, wetting water flow rate 8, 3.8 and 2.2 g/s.

Parameter	$M_{ww} = 8.0$ g/s				$M_{ww} = 3.8$ g/s				$M_{ww} = 2.2$ g/s			
Hot Water Side												
Flow Rate (l/s)	0.35	0.35	0.35	0.35	0.35	0.35	0.35	0.35	0.35	0.35	0.35	0.35
Inlet Temperature (°C)	43.1	43.1	43.1	43.1	43.1	43.1	43.14	43.12	43.1	43.0	43.11	43.09
Outlet Temperature (°C)	37.8	36.8	36.0	35.5	37.7	36.9	36.34	35.82	38.1	37.3	36.73	36.27
Capacity and Uncertainty (kW)	7.7±0.1 4	9.0±0.1	10.1± 0.16	11.1±0. 16	7.9±0. 21	8.9±0.2 3	9.8±0. 26	10.6±0.2 5	7.3±0.1 9	8.3±0. 21	9.2±0.2 3	9.9±0.22
Air-Side												
Velocity (m/s)	1.5	2.0	2.5	3.05	1.5	2.0	2.5	3.05	1.5	2.0	2.5	3.05
Inlet Temperature (°C)	28.1	28.1	27.7	28.0	28.0	28.1	28.1	28.1	28.1	28.2	28.2	28.2
Outlet Temperature (°C)	38.1	37.4	36.6	35.9	38.1	37.4	36.8	36.2	38.2	37.5	36.7	36.3
Inlet RH (%)	45.2	46.0	44.6	44.9	43.8	43.6	43.8	44.9	43.8	43.5	44.7	45.3
Outlet RH (%)	33.6	33.6	33.1	34.2	32.5	31.7	31.9	32.7	31.2	30.5	32.0	32.4
Capacity (kW)	7.9	9.2	10.5	11.4	7.9	9.1	9.9	10.6	7.3	8.4	9.3	10.1
Nozzle Pressure Drop (Pa)	424.4	770.7	284.1	413.9	431.3	773.7	287.7	413.6	431.0	773.4	286.8	414.5
HX Air Side Pressure Drop (Pa)	24.7	41.2	58.4	81.9	23.8	39.9	57.8	79.9	23.7	39.7	57.6	79.9
Air Flow Rate (m ³ /s)	0.4	0.5	0.6	0.7	0.4	0.5	0.6	0.7	0.4	0.5	0.6	0.7
Wetting Water Side												
Inlet Temperature (°C)	27.8	27.7	28.6	28.4	28.6	28.3	28.4	28.3	28.5	28.5	26.6	27.7
Outlet Temperature (°C)	25.0	24.7	22.7	22.8	25.3	25.8	25.7	26.0	25.3	25.3	25.4	25.7
Capacity (kW)	0.24	0.25	0.35	0.35	0.180	0.182	0.190	0.181	0.134	0.147	0.141	0.148
Evaporation Rate (g/s)	1.4	1.47	1.64	1.76	1.37	1.38	1.41	1.38	1.13	1.11	1.2	1.19
Energy Balance and Uncertainty (%)	0.5±13	0.8±15	1.3±1 5	1.1±17	0.9±13	0.7±15	0.3±16	0.3±18.3	0.5±14	0.2±16	0.13±17	1.9±19.6

Table 5.6: Test summary for front spray cooled uncoated wavy fin RTHX with $F_p=3.0$ mm at approximately $T_{a,in}=28^\circ\text{C}$, $RH_{a,in} = 45\%$ and $\omega_{a,in}= 0.0106$ kg_w/kg_a, and wetting water flow rate 8, 3.8 and 2.2 g/s.

Parameter	$M_{ww} = 8.0$ g/s				$M_{ww} = 3.8$ g/s				$M_{ww} = 2.2$ g/s			
Hot Water Side												
Flow Rate (l/s)	0.35	0.35	0.35	0.35	0.35	0.35	0.35	0.35	0.35	0.35	0.35	0.35
Inlet Temperature (°C)	43.09	43.10	43.16	43.13	43.07	43.14	43.06	43.12	43.0	43.03	43.04	43.07
Outlet Temperature (°C)	38.08	37.38	36.85	36.34	38.58	37.91	37.33	36.92	38.7	38.15	37.57	37.13
Capacity and Uncertainty (kW)	7.27	8.3	9.164	9.86	6.51	7.59	8.32	9.0	6.2	7.09	7.94	8.62
Air-Side												
Velocity (m/s)	1.5	2.0	2.5	3.0	1.5	2.0	2.5	3.0	1.5	2.0	2.5	3.0
Inlet Temperature (°C)	28.0	28.2	28.1	28.0	27.8	27.8	27.7	28.1	28.2	28.2	28.2	28.3
Outlet Temperature (°C)	36.7	36.2	35.8	35.3	36.8	36.3	35.8	35.4	37.0	36.4	36.0	35.6
Inlet RH (%)	45.3	44.6	44.3	44.4	44.4	44.1	44.1	43.9	44.4	43.9	43.7	43.6
Outlet RH (%)	36.4	35.1	34.5	34.4	32.6	31.8	31.6	32.2	32.7	31.8	31.5	31.5
Capacity (kW)	7.4	8.5	9.5	10.4	6.4	7.6	8.3	8.9	6.2	7.2	7.9	8.6
HX Air Side Pressure Drop (Pa)	14.5	25.2	38.2	53.6	14.6	24.9	36.9	52.0	14.5	24.8	37.1	51.8
Air Flow Rate (m ³ /s)	0.4	0.5	0.6	0.8	0.4	0.5	0.6	0.7	0.4	0.5	0.6	0.7
Wetting Water Side												
Inlet Temperature (°C)	27.7	27.6	28.1	27.3	28.4	29.5	29.5	29.2	28.3	28.5	28.3	28.2
Outlet Temperature (°C)	24.6	24.1	24.0	23.7	24.3	24.0	23.9	23.9	24.4	24.0	23.9	23.6
Evaporation Rate (g/s)	1.4	1.47	1.52	1.54	0.99	0.99	0.99	0.99	0.93	0.9	0.88	0.84
Energy Balance and Uncertainty (%)	0.9±13	0.6±15	1.8±17	3.9±18	1.9±15	1.5±17	1.6±18	1.6±20	1.6±15	0.2±18	1.3±19	1.2±22

CER and $PR_{\Delta P_a}$ of wavy-fin RTHXs under front spray evaporative cooling are presented in Figure 5.5.



Note: Values are relative to dry case capacities or ΔP_a at respective air velocities for each HX.

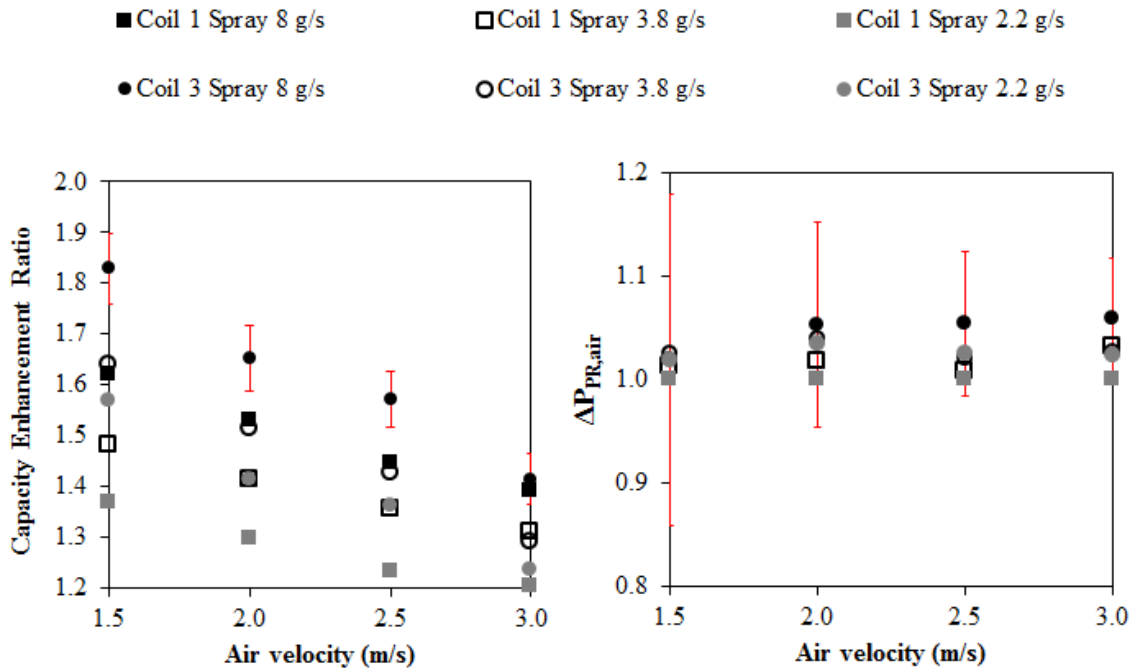
Figure 5.5: CER and $PR_{\Delta P_a}$ of wavy-fin RTHXs using front spray evaporative cooling at approximately $T_{a,in} = 28^\circ\text{C}$, $RH_{a,in} = 45\%$ and $\omega_{a,in} = 0.0106 \text{ kg}_w/\text{kg}_a$.

The main observations were as follows:

- Both capacities and $PR_{\Delta P_a}$ increased proportionately with spray flow rate as shown in Figure 5.5.
- The range of highest CER values for the 3 HXs was found to be within 1.62 to 1.83 at 8 g/s spray flow rate. Highest CER also corresponded to lowest air velocity.
- $PR_{\Delta P_a}$ was close to 1 for all spray rates, therefore spray cooling is a much better choice for wetting the coils compared to deluge cooling where massive $PR_{\Delta P_a}$ were reported.

5.3.1 Effect of fin spacing

Figure 5.6 presents comparison of spray cooling capacity enhancement ratios and air-side ΔP penalty ratios of uncoated wavy-fin RTHXs with fin spacing of 2.4 mm (Coil 1) and 3 mm (Coil 3), respectively.



11

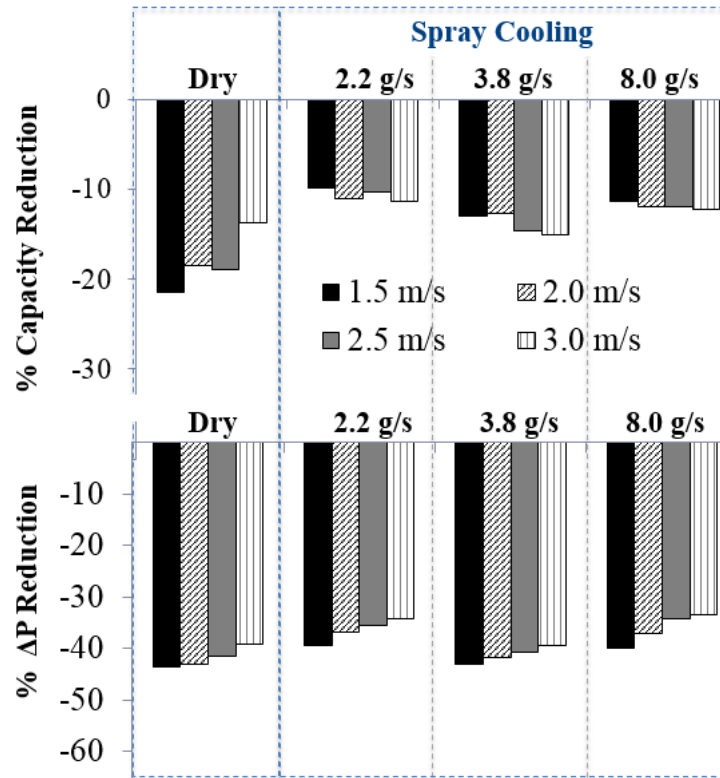
Note: Values are relative to dry case capacities or ΔP_a at respective air velocities for each HX.

Figure 5.6: Comparison of spray cooling capacity enhancement ratios and ΔP_a penalty ratios of uncoated wavy-fin RTHXs with fin spacing of 2.4 mm (Coil 1) and 3 mm (Coil 3) respectively at approximately $T_{a,in} = 28^\circ\text{C}$, $RH_{a,in} = 45\%$ and $\omega_{a,in} = 0.0106 \text{ kg}_w/\text{kg}_a$.

To further evaluate the effect of hydrophilic coating on HX performance, the capacity of each case is compared with the capacity obtained for the corresponding case of the uncoated wavy fin round tube HX with 2.4 mm fin spacing.

Figure 5.7 presents the effect of increasing fin spacing (from 2.4 mm to 3 mm) on HX

capacity and airside pressure drop.



Note: Comparison based on performance of uncoated HX with Fp 3.0 mm.

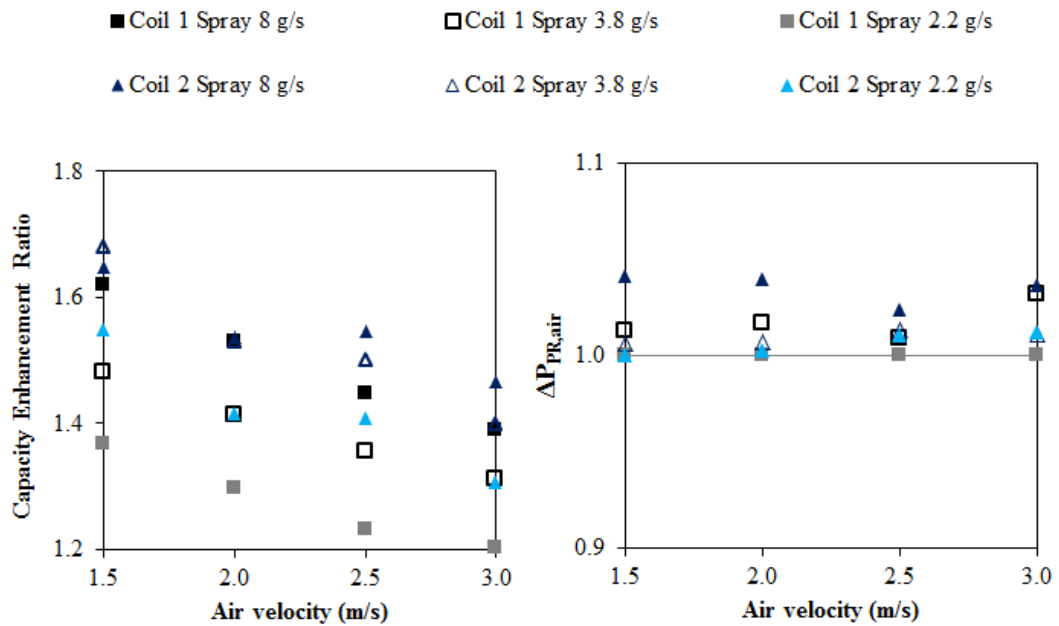
Figure 5.7: Effect of increasing fin spacing (from 2.4 mm to 3 mm) on HX capacity and airside pressure drop at approximately $T_{a,in} = 28^{\circ}\text{C}$, $\text{RH}_{a,in} = 45\%$ and $\omega_{a,in} = 0.0106 \text{ kg}_w/\text{kg}_a$.

Key points summarizing effect increasing fin spacing (from 2.4 mm to 3 mm) on HX performance are as follows:

- In all cases both HX capacity and airside pressure drop decreased
- Capacity reduction for dry and spray cooled cases was approximately 14 to 21%, and 10 to 15%, respectively.
- Pressure drop reduction for dry and spray cooled cases was approximately 39 to 44% and 33 to 43%, respectively.

5.3.2 Effect of hydrophilic coating

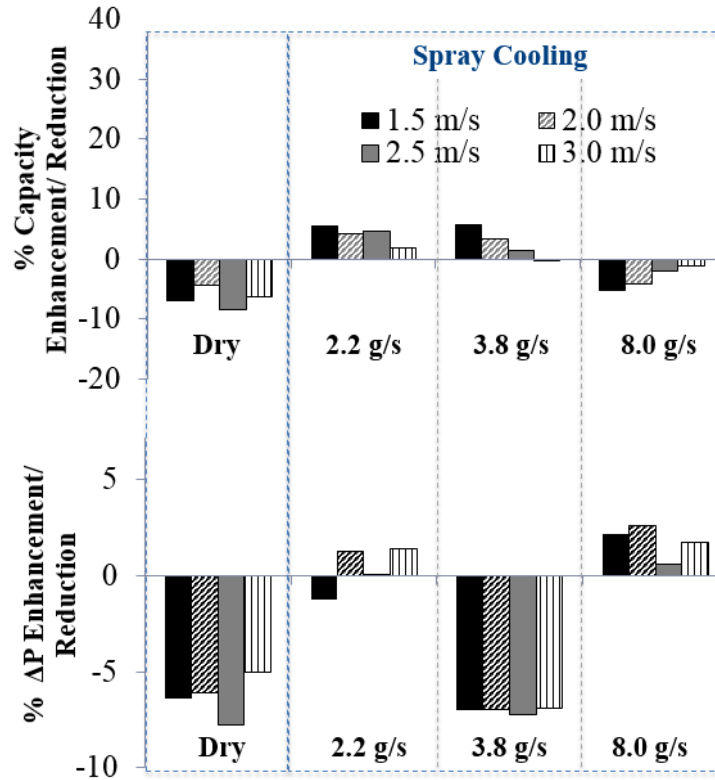
Hydrophilic coating helps achieve lower contact angles and improved wettability on fin surface. Figure 5.8 presents comparison of spray cooling capacity enhancement ratios and air-side ΔP penalty ratios of coated and uncoated wavy-fin RTHX with fin spacing of 2.4 mm.



Note: Values are relative to dry case capacities or ΔP_a at respective air velocities for each HX.

Figure 5.8: Comparison of spray cooling capacity enhancement ratios and air-side ΔP penalty ratios of coated and uncoated wavy-fin RTHX with fin spacing of 2.4 mm at approximately $T_{a,in} = 28^\circ\text{C}$, $RH_{a,in} = 45\%$ and $\omega_{a,in} = 0.0106 \text{ kg}_w/\text{kg}_a$.

Similarly, Figure 5.9 presents the effect of hydrophilic coating on HX capacity and airside pressure drop.



Note: Comparison based on performance of uncoated HX with Fp 2.4 mm.

Figure 5.9: Effect of hydrophilic coating on percentage capacity and airside ΔP enhancement/reduction at approximately $T_{a,in} = 28^\circ\text{C}$, $RH_{a,in} = 45\%$ and $\omega_{a,in} = 0.0106 \text{ kg}_w/\text{kg}_a$.

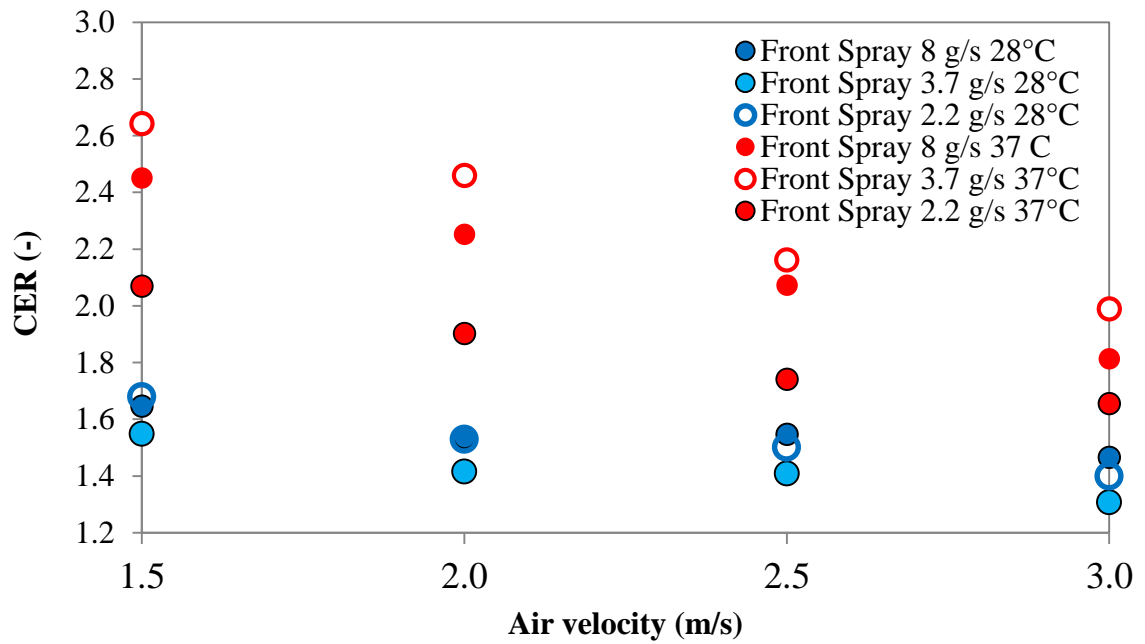
While there was a clear benefit of hydrophilic coated fins on HX performance enhancement in deluge cooling cases, a similar conclusion cannot be made about spray cooling as observations were too small (+4% to -6%) which was within uncertainty of measurement.

5.3.3 Effect of ambient air temperature

In previous sections inlet air temperature was set at 28°C . However to study the effect of inlet air temperature on HX performance additional tests were conducted with inlet air temperature set at 37°C .

Test summary for front spray cooled hydrophilic coated and uncoated wavy fin RTHX with $F_p=2.4$ mm at $T_{a,in}=37^\circ\text{C}$, wetting water flow rate 8, 3.8 and 2.2 g/s, are summarized in Tables 5.7 and 5.8, respectively.

Figure 5.10 presents the effect of inlet air temperature on capacity enhancement ratio of front spray cooled hydrophilic coated wavy- fin HX.



Note: For tests at $T_{a,in}=28^\circ\text{C}$, $RH_{a,in}=45\%$ and $\omega_{a,in}=0.0106$ kg_w/kg_a, and for tests at $T_{a,in}=37^\circ\text{C}$, $RH_{a,in}=45\%$ and $\omega_{a,in}=0.0179$ kg_w/kg_a.

Figure 5.10: Effect of inlet air temperature on capacity enhancement ratio of front spray cooled hydrophilic coated wavy- fin HX.

Table 5.7: Test summary for front spray cooled hydrophilic coated wavy fin RTHX with $F_p=2.4$ mm at approximately $T_{a,in}=37^\circ\text{C}$, $RH_{a,in} = 45\%$ and $\omega_{a,in}= 0.0179$ kg_w/kg_a, and wetting water flow rate 8, 3.8 and 2.2 g/s .

Parameter	$M_{ww} = 8.0$ g/s				$M_{ww} = 3.8$ g/s				$M_{ww} = 2.2$ g/s			
Hot water side												
Flow rate (l/s)	0.35	0.35	0.35	0.35	0.35	0.35	0.35	0.35	0.35	0.35	0.35	0.35
Inlet temperature ($^\circ\text{C}$)	43.1	43.0	43.0	43.1	43.1	43.0	43.1	43.1	43.1	43.1	43.1	43.0
Outlet temperature ($^\circ\text{C}$)	39.8	39.5	39.2	39.2	39.6	39.1	39.1	38.8	40.4	40.1	39.8	39.5
Capacity and uncertainty (kW)	4.67	5.15	5.53	5.62	5.03	5.63	5.7	6.16	3.95	4.36	4.64	5.13
Air-side												
Velocity (m/s)	1.50	2.00	2.50	3.00	1.5	2.0	2.5	3.0	1.5	2.0	2.5	3.0
Inlet temperature ($^\circ\text{C}$)	36.9	36.8	36.9	36.9	37.2	37.2	37.2	37.1	36.8	36.7	36.7	37.1
Outlet temperature ($^\circ\text{C}$)	40.3	39.9	39.6	39.5	40.0	39.7	39.4	39.1	40.6	40.3	40.0	39.8
Inlet RH (%)	43.9	43.8	43.6	43.2	42.2	41.8	41.6	41.2	41	41.5	42.3	41.8
Outlet RH (%)	41.7	41.3	41.3	40.6	43.3	42.1	41.2	40.6	38.0	37.1	37.5	37.6
HX Air side pressure drop (Pa)	24.7	39.9	58.2	76.4	22.3	36.7	54.2	74.1	24.6	39.0	56.2	75.5
Air flow rate (m ³ /s)	0.36	0.49	0.61	0.73	0.36	0.49	0.61	0.74	0.37	0.48	0.61	0.73
Wetting water side												
Flow rate (g/s)	8	8	8	8	3.8	3.8	3.8	3.8	2.2	2.2	2.2	2.2
Inlet temperature ($^\circ\text{C}$)	27.1	26.7	26.4	26.0	36.1	34.7	32.9	30.8	27.2	27.7	28.1	25.8
Outlet temperature ($^\circ\text{C}$)	29.3	29.0	29.0	29.2	29.3	29.0	29.4	28.7	30.6	30.5	29.3	28.6
Evaporation rate (g/s)					1.34	1.37	1.37	1.36	0.88	0.9	0.94	0.97
Energy balance (%)	2.5	3.5	4.2	3.6	4.4	3.5	2.9	4.7	1.9	2.8	4.5	3.9

Table 5.8: Test summary for front spray cooled uncoated wavy fin RTHX with $F_p=2.4$ mm at approximately $T_{a,in}=37^\circ\text{C}$, $RH_{a,in} = 45\%$ and $\omega_{a,in}= 0.0179$ kg_w/kg_a, and wetting water flow rate 8, 3.8 and 2.2 g/s.

Parameter	$M_{ww} = 8.0$ g/s				$M_{ww} = 3.8$ g/s				$M_{ww} = 2.2$ g/s			
Hot Water Side												
Flow Rate (l/s)	0.35	0.35	0.35	0.35	0.35	0.35	0.35	0.35	0.35	0.35	0.35	0.35
Inlet Temperature (°C)	43.1	43.0	43.0	43.0	43.10	42.93	42.95	43.03	43.09	42.97	43.06	43.09
Outlet Temperature (°C)	39.5	38.9	38.4	38.2	39.93	39.41	38.92	38.77	40.52	39.99	39.67	39.48
Capacity (kW)	5.19	5.93	6.57	6.97	4.59	5.1	5.83	6.18	3.73	4.32	4.9	5.2
Air-Side												
Velocity (m/s)	1.5	2.0	2.5	3.05	1.5	2.0	2.5	3.05	1.5	2.0	2.5	3.0
Inlet Temperature (°C)	36.8	36.8	36.8	36.80	36.8	36.8	36.8	36.9	36.93	36.96	36.90	36.93
Outlet Temperature (°C)	40.6	40.2	39.8	39.55	40.7	40.4	39.9	39.8	41.04	40.63	40.33	40.14
Inlet RH (%)	45.2	45.0	44.8	44.67	43.9	42.9	44.1	43.7	44.2	42.3	43.9	41.6
Outlet RH (%)	43.9	43.6	43.6	43.31	41.2	39.9	41.6	41.2	39.3	38.0	39.3	37.3
Capacity (kW)	5.2	5.99	6.52	7.02	4.55	5.04	5.76	6.2	3.73	4.31	4.68	4.99
HX Air Side Pressure Drop (Pa)	24.1	40.5	60.2	83.1	24.3	40.2	60.7	82.2	24.0	40.1	59.8	81.1
Air Flow Rate (m ³ /s)	0.4	0.5	0.6	0.7	0.369	0.491	0.613	0.736	0.4	0.5	0.6	0.7
Wetting Water Side												
Flow rate (g/s)	8	8	8	8	3.8	3.8	3.8	3.8	2.2	2.2	2.2	2.2
Inlet Temperature (°C)	37.4	37.5	37.4	37.4	31.8	32.0	33.8	36.5	40.6	39.5	35.2	37.5
Outlet Temperature (°C)	36.4	36.4	36.4	36.4	36.9	36.7	38.0	39.5	40.9	40.8	39.5	40.8
Evaporation Rate (g/s)	1.39	1.47	1.63	1.9	1.16	1.235	1.418	1.468	0.814	0.9	0.94	0.97
Energy Balance (%)	0.1	1	0.7	0.7	0.9	1.1	1.3	0.3	0.1	0.3	4.7	4.8

It was observed that:

- For air inlet at 1.5 m/s and 37°C, approximately 33.7%, 48.81% and 57.3% higher CER were obtained than that with inlet air at 28°C and at similar air velocity for spray rates 2.2, 3.8 and 8 g/s, respectively. This is due to higher evaporation potential for air at 37°C, which can pick up more moisture while flowing through HX.
- At a given spray rate, maximum enhancement is obtained at lowest air velocity.

5.4 Effect of spray configuration

One of the challenges in achieving maximum CER for wetted coils is completely wetting fin surface. However fin spacing is optimized to a smaller value which does not allow spray water to penetrate deeper into the coil when water is sprayed onto front face of HX. One of the ways to ensure water reaches in coil depth is to spray water on top of HX such that it is distributed on top edge of HX fins and flows down onto fin surface under gravity. Since surface area on top of HX was much less compared to frontal area, flat spray nozzles were utilized to spray water in top spray cooling mode. Top and front spray configuration schematic are presented in Figures 2.7 and 2.8, respectively.

Test summary for top spray cooled hydrophilic coated wavy fin RTHXs at wetting water flow rate 8, 3.8 and 2.2 g/s at $T_{a,in}=28^{\circ}\text{C}$ and $T_{a,in}=37^{\circ}\text{C}$, is presented in Tables 5.9 and Tables 5.10, respectively.

Table 5.9: Test summary for top spray cooled hydrophilic coated wavy fin RTHX with $F_p=2.4$ mm at approximately $T_{a,in}=28^\circ\text{C}$, $RH_{a,in} = 45\%$ and $\omega_{a,in}= 0.0106$ kg_w/kg_a, wetting water flow rate 8, 3.8 and 2.2 g/s.

Parameter	$M_{ww} = 8.0$ g/s				$M_{ww} = 3.8$ g/s				$M_{ww} = 2.2$ g/s			
Hot Water Side												
Flow Rate (l/s)	0.35	0.35	0.35	0.35	0.35	0.35	0.35	0.35	0.35	0.35	0.35	0.35
Inlet Temperature (°C)	43.1	43.1	43.0	43.1	43.0	43.1	43.1	43.2	43.0	43.1	43.0	43.1
Outlet Temperature (°C)	37.2	36.6	36.1	35.9	37.8	37.4	36.9	36.6	39.2	38.7	38.0	37.6
Capacity (kW)	8.61	9.39	10.03	10.40	7.54	8.27	9.03	9.47	5.53	6.33	7.23	7.91
Air-Side												
Velocity (m/s)	1.5	2.0	2.5	3.05	1.5	2.0	2.5	3.05	1.5	2.0	2.5	3.05
Inlet Temperature (°C)	28.0	28.0	28.0	28.0	28.1	28.1	28.0	28.1	28.0	28.1	28.1	28.1
Outlet Temperature (°C)	31.3	31.2	30.7	30.8	33.9	33.4	32.8	32.6	35.1	34.9	34.1	33.9
Inlet RH (%)	44.0	43.9	43.2	42.7	42.0	42.1	43.5	43.5	41.0	40.0	44.1	44.5
Outlet RH (%)	59.7	55.4	53.4	49.8	43.5	42.4	43.1	42.2	33.8	32.1	36.3	35.9
HX Air Side Pressure Drop (Pa)	20.5	32.9	48.5	65.7	21.5	33.3	48.9	65.0	19.8	31.4	47.8	64.4
Air Flow Rate (m ³ /s)	0.37	0.49	0.61	0.74	0.38	0.49	0.61	0.73	0.37	0.49	0.62	0.74
Wetting Water Side												
Flow rate (g/s)	8	8	8	8	3.8	3.8	3.8	3.8	2.2	2.2	2.2	2.2
Inlet Temperature (°C)	27.9	27.9	25.6	27.2	26.9	27.9	28.3	27.1	28.1	28.0	26.5	27.0
Outlet Temperature (°C)	27.9	27.9	27.9	27.9	28.1	28.0	28.1	28.1	28.0	28.0	28.1	28.1
Evaporation Rate (g/s)	2.84	3	3.21	3.22	1.9	2.07	2.2	2.24	0.93	0.1	0.17	0.12
Energy Balance and Uncertainty (%)	0.8	1.2	1.1	1.9	2.4	0.4	1.4	0.9	2.7	5.2	0.5	0.4

Table 5.10: Test summary for top spray cooled hydrophilic coated wavy fin RTHX with $F_p=2.4$ mm at approximately $T_{a,in}=37^\circ\text{C}$, $RH_{a,in} = 45\%$ and $\omega_{a,in}= 0.0179$ kg_w/kg_a, and wetting water flow rate 8, 3.8 and 2.2 g/s.

Parameter	$M_{ww} = 8.0$ g/s				$M_{ww} = 3.8$ g/s				$M_{ww} = 2.2$ g/s			
Hot Water Side												
Flow Rate (l/s)	0.35	0.35	0.35	0.35	0.35	0.35	0.35	0.35	0.35	0.35	0.35	0.35
Inlet Temperature ($^\circ\text{C}$)	43.1	43.2	43.1	43.2	43.1	43.0	43.1	43.1	43.1	43.1	43.1	43.1
Outlet Temperature ($^\circ\text{C}$)	38.0	37.7	37.4	37.2	39.2	38.8	38.7	38.5	40.6	40.0	39.8	39.8
Capacity (kW)	7.43	7.95	8.33	8.62	5.68	6.13	6.43	6.62	3.70	4.51	4.78	4.88
Air-Side												
Velocity (m/s)	1.5	2.0	2.5	3.05	1.5	2.0	2.5	3.05	1.5	2.0	2.5	3.05
Inlet Temperature ($^\circ\text{C}$)	37.3	37.2	37.1	37.0	37.3	37.2	37.2	37.2	37.3	37.3	37.3	37.3
Outlet Temperature ($^\circ\text{C}$)	35.7	35.5	35.1	35.1	37.8	37.3	37.0	36.9	39.6	39.2	38.9	38.8
Inlet RH (%)	41.8	42.8	43.0	42.5	44.4	43.4	43.4	41.8	41.6	42.2	42.6	42.2
Outlet RH (%)	65.1	63.5	62.1	59.6	53.7	51.5	50.8	48.4	41.3	41.8	42.3	41.5
HX Air Side Pressure Drop (Pa)	19.9	33.4	49.8	67.5	20.3	32.6	48.2	65.9	19.7	32.5	48.3	65.0
Air Flow Rate (m ³ /s)	0.36	0.49	0.61	0.74	0.37	0.49	0.61	0.74	0.37	0.49	0.62	0.74
Wetting Water Side												
Flow rate (g/s)	8	8	8	8	3.8	3.8	3.8	3.8	2.2	2.2	2.2	2.2
Inlet Temperature ($^\circ\text{C}$)	29.3	31.2	33.2	32.3	30.2	29.5	29.0	29.6	31.4	31.3	31.2	31.1
Outlet Temperature ($^\circ\text{C}$)	36.9	36.5	37.7	37.8	36.1	36.6	37.4	37.5	36.2	36.4	36.6	36.8
Evaporation Rate (g/s)	3.1	3.5	3.67	3.87	1.8	2.2	2.0	2.0	0.88	0.9	0.94	0.97
Energy Balance (%)	4.5	3.7	2.5	4.4	3.1	3.5	3.7	3.9	2.4	1.7	4.4	3.8

Figures 5.11 and 5.12 present the capacity enhancement ratio for front and top spray configurations at inlet air temperature of 37°C and 28°C respectively, for hydrophilic coated wavy- fin HX.

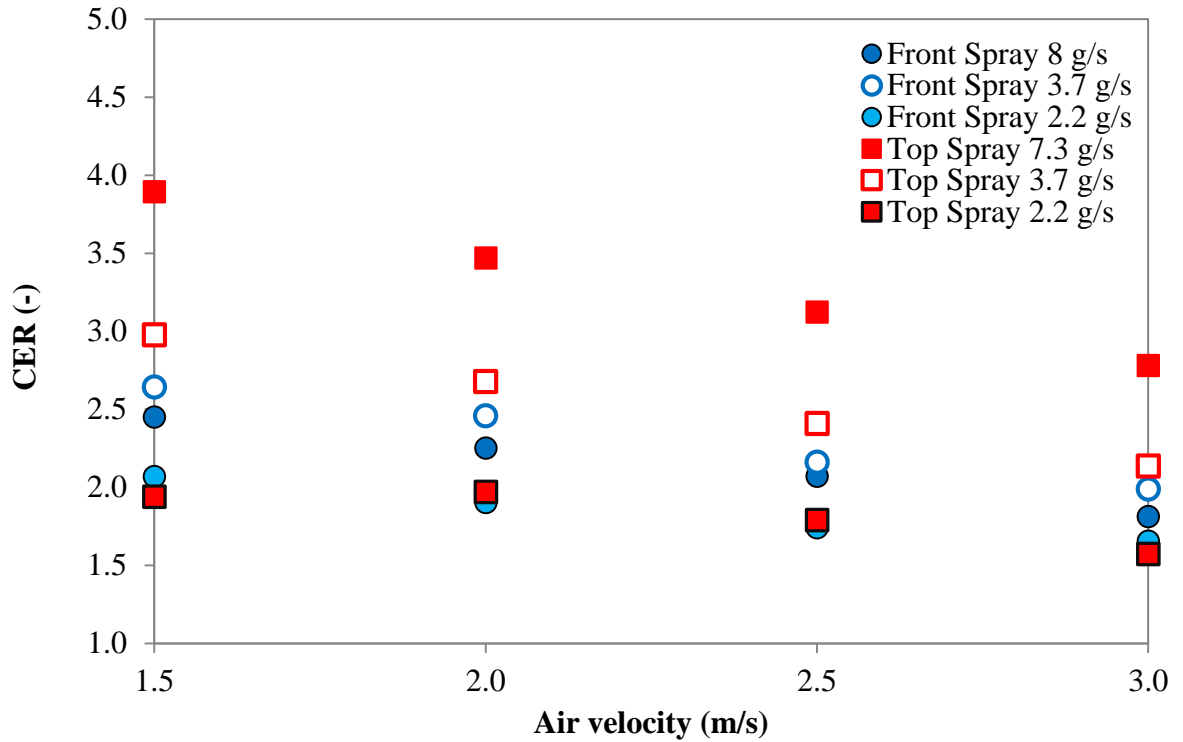


Figure 5.11: Capacity enhancement ratio for front and top spray configurations at approximately $T_{a,in}=37^{\circ}\text{C}$, $\text{RH}_{a,in} = 45\%$ and $\omega_{a,in}= 0.0179 \text{ kg}_w/\text{kg}_a$ for hydrophilic coated wavy- fin HX.

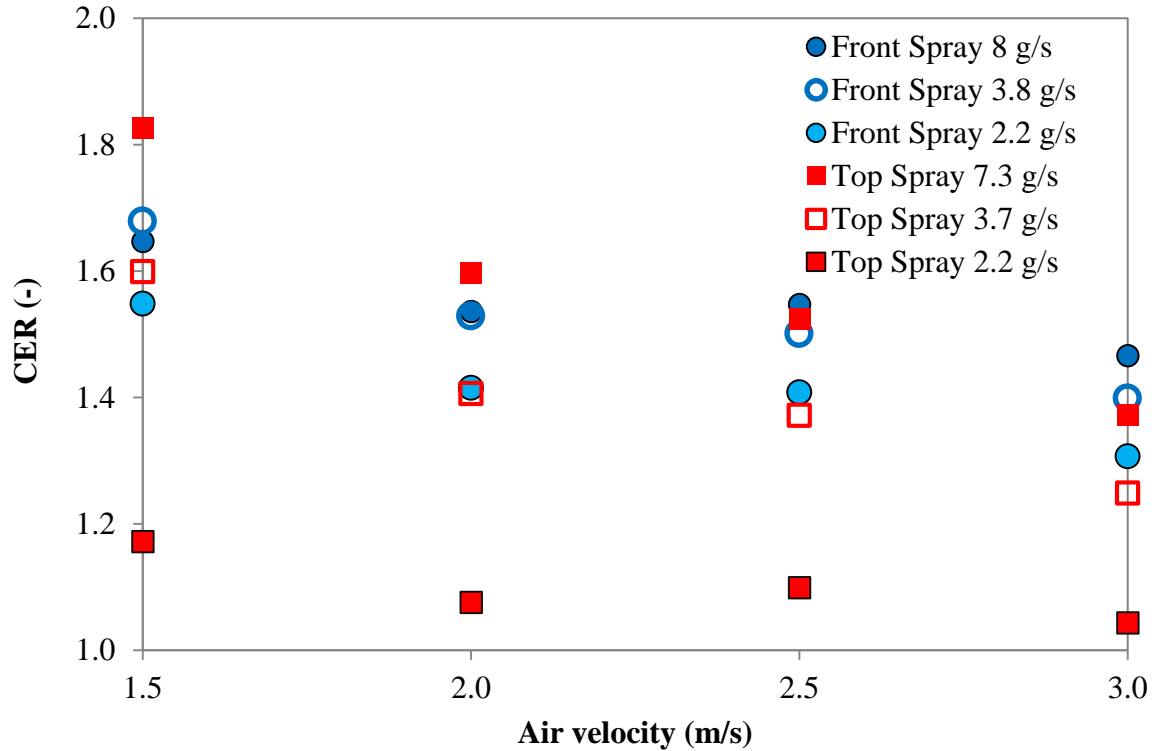
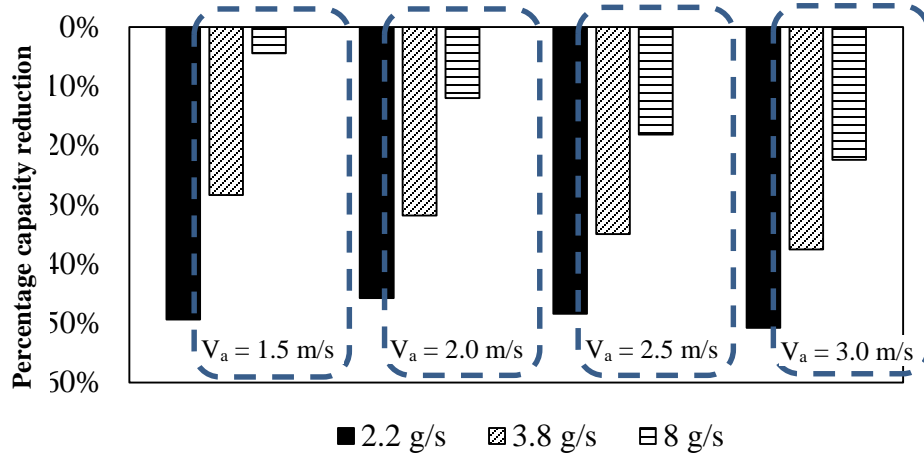


Figure 5.12: Capacity enhancement ratio for front and top spray configurations at approximately $T_{a,in}=28^{\circ}\text{C}$, $\text{RH}_{a,in} = 45\%$ and $\omega_{a,in}= 0.0106 \text{ kg}_w/\text{kg}_a$ for hydrophilic coated wavy- fin HX.

The following observations were made:

Spray configuration has significant effect on HX performance. However, it was very interesting to observe that this change was dependent on air inlet temperature. Figures 5.13 and 5.14 present the percentage reduction of wavy-fin HX capacity for top sprayed coils compared to front spraying in similar conditions at air inlet temperature 28°C and 37°C , respectively.



Note: Droplet carryover downstream of air in all cases.

Figure 5.13: Percentage reduction of wavy-fin HX capacity for top sprayed coils compared to front spraying in similar conditions at approximately $T_{a,in}=28^{\circ}\text{C}$, $\text{RH}_{a,in} = 45\%$ and $\omega_{a,in}= 0.0106 \text{ kg}_w/\text{kg}_a$.

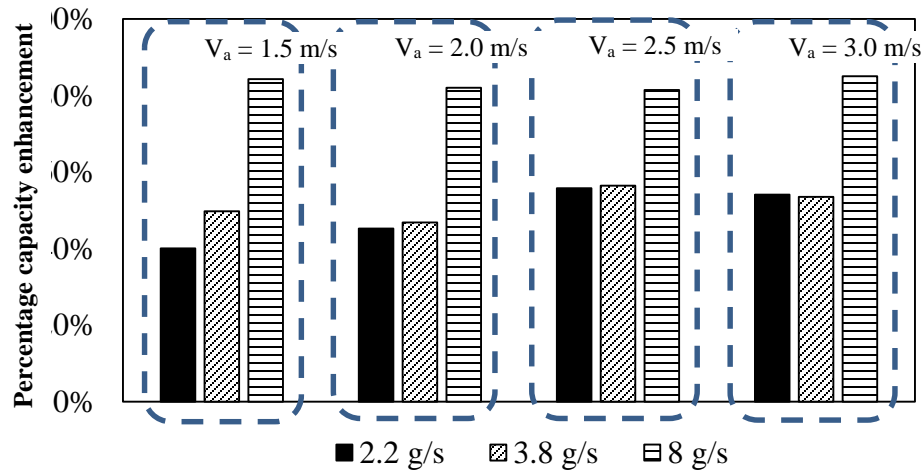


Figure 5.14: Percentage enhancement of wavy-fin HX capacity for top sprayed coils compared to front spraying in similar conditions at approximately $T_{a,in} = 37^{\circ}\text{C}$, $\text{RH}_{a,in} = 45\%$ and $\omega_{a,in}= 0.0179 \text{ kg}_w/\text{kg}_a$.

For air inlet at 28°C there changing to top spray configuration reduces HX capacity by up to 51% when spray rate was 2.2 g/s and 22% when spray rate was 8 g/s. The reduction rate increases for higher air velocity at a given spray rate and increases sharply for 8 g/s spray

rate.

However at air inlet temperature 37°C it was observed that HX capacity was enhanced by up to 85% for spray rate of 8 g/s and 56% for spray rate of 2.2 g/s. Also the enhancements were consistent with increase in air velocity.

The main reason for the poor performance of top spray cooling at 28°C was that unevaporated droplets of spray water were carried downstream of HX. Figure 5.15 shows spray unevaporated droplets deposited on visualization section plate at air outlet of experimental setup.



Figure 5.15: Unevaporated spray droplets deposited on visualization section plate at air outlet of experimental setup.

On the other hand no spray droplets were observed at air inlet 37°C when top spray cooling was applied at similar spray rates. Thus both evaporation potential and spray configuration play significant roles in enhancement ratios obtained for sprayed coils. This also highlights the fact that front spray cooling may not be wetting coil depth or hottest regions of HX.

5.5 Performance comparison of spray and deluge cooling

In this Section comparison of both spray cooling modes is made with results for deluge cooling discussed in Chapter 4 of this Dissertation. Discussion based on effectiveness and performance ratios would be made to determine the best technology for evaporative cooling of wavy-fin HXs.

a) *Fan power consumption is often a major concern for HX manufacturers and industrial or commercial consumers. Ideally the evaporative cooling should provide maximum heat transfer enhancement at minimum or no increase in ΔP_a . It was observed that spray cooling helped achieve this to the extent that ΔP_a remained approximately same as dry case baseline values, even when spray rates as high as 8 g/s were applied. Although deluge cooling achieved maximum CER at $T_a=28^\circ\text{C}$, it would be interesting to see how much enhancement it achieved per unit increase in ΔP_a . Figure 5.16 presents a comparison of CER and $\text{CER}/\text{PR}_{\Delta P}$ for front spray, top spray and deluge cooling of wavy fin HXs with $T_a = 28^\circ\text{C}$ and 37°C . Figure 5.17 presents a comparison of CER and $\text{PR}_{\Delta P}$ for front spray, top spray and deluge cooling of wavy fin HXs with $T_a = 28^\circ\text{C}$ and 37°C .*

b) Reducing wetting water consumption is also important to reduce operational costs and potential scaling or fouling on fin surfaces.

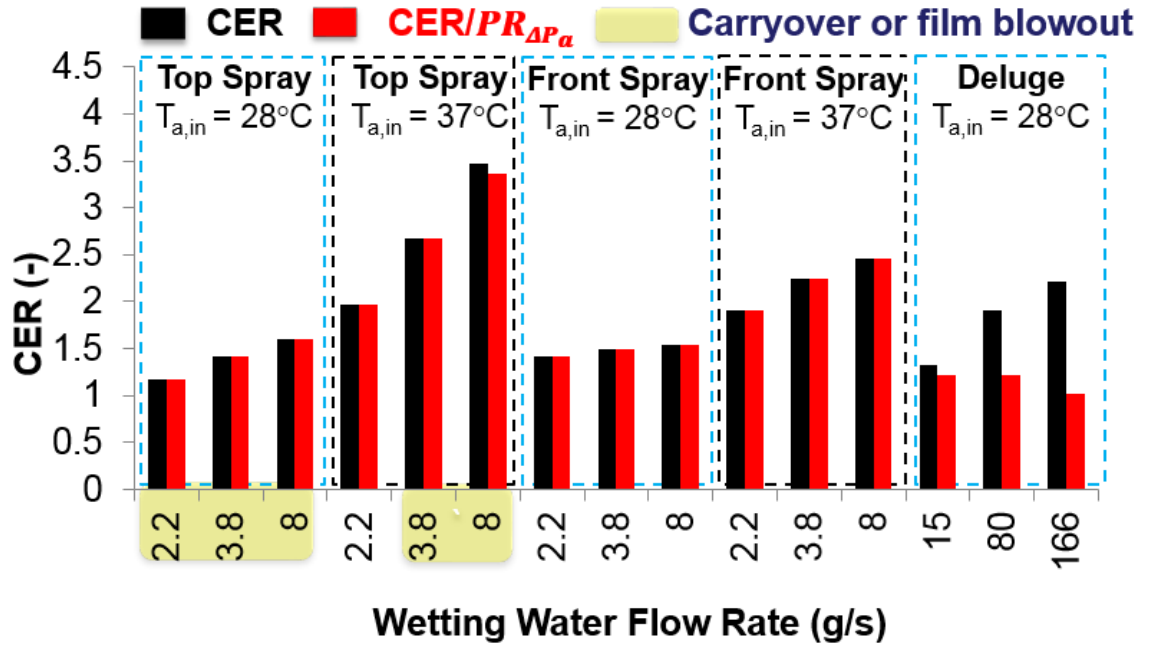


Figure 5.16: Comparison of CER and CER per unit PR_{ΔP} for front spray, top spray and deluge cooling of wavy fin HX with hydrophilic coating and F_p=2.4 mm at T_a = 28°C and 37°C.

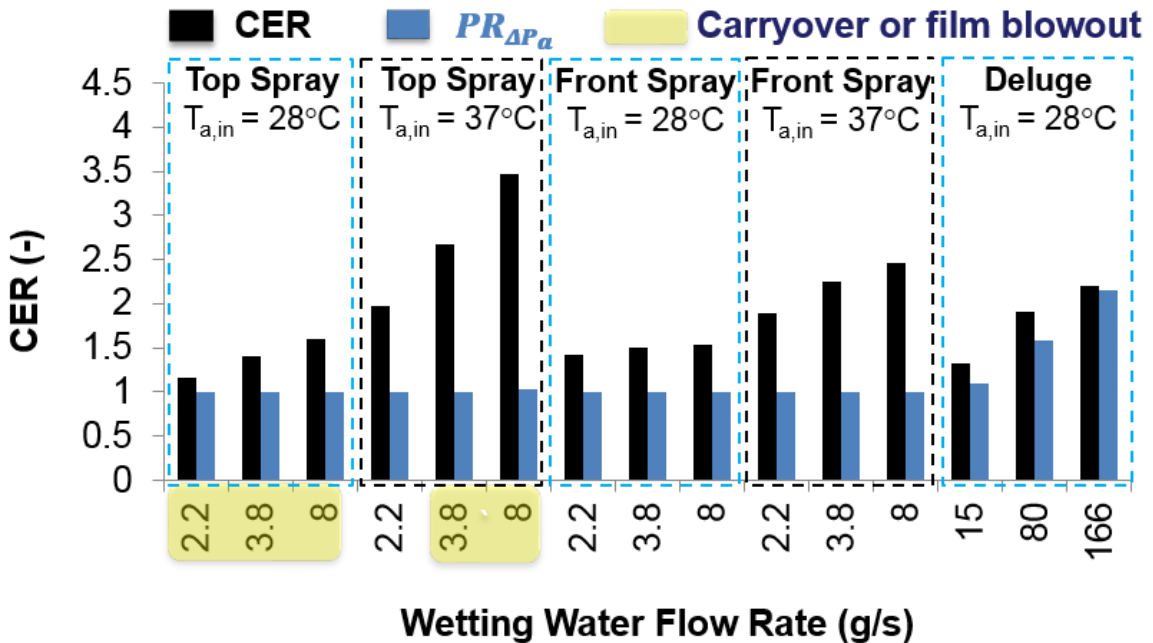
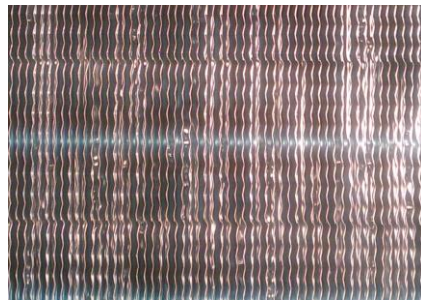


Figure 5.17: Comparison of CER and PR_{ΔP} for front spray, top spray and deluge cooling of wavy fin HX with hydrophilic coating and F_p=2.4 mm at T_a = 28°C and 37°C.

The following observations were made:

- **Front spray cooling (FSC) versus deluge cooling (DC) at $T_a=28^\circ\text{C}$**
 - FSC achieved 7.2 to 18.3 times higher CER per unit wetting water applied for uncoated coils and 9.2 to 16.9 times higher CER for coated coil. This could lead to substantial wetting water savings.
 - CER per unit $\text{PR}_{\Delta P}$ was 10-36% and 47-75% higher for FSC on uncoated and coated coils, respectively as compared to DC.
 - DC causes massive water bridging between fins as shown in Figure 5.18. Therefore, even with highest CER



(a) deluged coil



(b) dry coil

Figure 5.18: Deluged and dry coil showing bridging between fin surfaces.

- When deluge cooling water consumption was reduced to 15 g/s ΔP_a reduced however

there was a substantial capacity reduction as well, therefore DC fails to compete with spray cooling. For example front sprays cooling at $m_{ww}= 8$ g/s and 2.2 g/s is 2 and 7 times better than deluge cooling at 15 g/s.

- At the same time it is also observed that a minimum amount of water (2.2. g/s spray water) is enough to enhance capacity (especially when spray water cost is a concern). However instead of deluge cooling it would be beneficial to spray cool the HX coil. This is mainly due to higher surface area of wetting water droplets when being spray cooled.
- Although deluge cooling achieves enhancement ratios as high as 2.78 (166 g/s) while the spray cooling achieves 1.68 (3.8 g/s), deluge cooling wastes a substantial amount of water.

5.6 Summary

In this Chapter, experimental performance of front spray, top spray and deluged wavy fin coils was discussed. Several performance parameters were defined to compare the performance obtained using different evaporative cooling methods. The main results were as follows:

- **Even a small amount of wetting water (3.8 g/s) was enough to produce 48% capacity enhancement**, while 80 g/s wetting water produced 62% enhancement for uncoated coil (F_p 2.4 mm) in similar conditions. **Thus spray cooling was found to be better both in terms of wetting water and fan energy consumption.**
- At $T_a=28^\circ\text{C}$ CER per unit m_{ww} and $PR_{\Delta P}$ reduced from 13.9 to 48.5% when HX is sprayed from top instead of from the front due to unevaporated spray droplets downstream of HX. However, no droplets were observed at $T_a=37^\circ\text{C}$ CER and CER

improvement for top sprayed coil was 48 to 83% higher than that obtained with front sprayed coil.

- **Droplet carryover observed for top sprayed coil tests when $T_a=28^\circ\text{C}$ but no carryover was observed for $T_a=37^\circ\text{C}$.** This was due to much higher evaporation potential for latter case and could be confirmed using experimentally observed evaporation rates.
- Even with highest CER/ $PR_{\Delta P}$ and CER/ m_{ww} , **top spray cooling may not be suitable spray cooling technology due to potential for droplet carryover which could damage fan blades downstream of air.**
- **Higher enhancement ratios were obtained for lowest air-velocities** which could be due to droplet carryover at very high air velocities. Due to tortuous and compact wavy-fin structure wetting water could not be observed downstream of HX for front spray configuration, but based on experimental data rapid fall in CER was observed for $V_a > 2.5$ m/s. Thus at higher air velocity air side heat transfer coefficient takes dominates overall heat transfer rate.

5.7 Spray cooling capacity enhancement improvement constraints

- From the discussion presented in Section 5.5, it is clear that spray cooling is more efficient way to enhance HX capacity. Compared to deluge cooling it helps save both wetting water and fan energy power. However, several problems were identified which may need attention before theoretical maximum capacity enhancement could be achieved:
- Evaporative cooling is most efficient when there is uniform wetting water distribution

throughout the depth of RTHX coil. However, as shown in Figure 5.19, the droplets may not be penetrating uniformly in the HX depth and hottest part of HX remains dry.

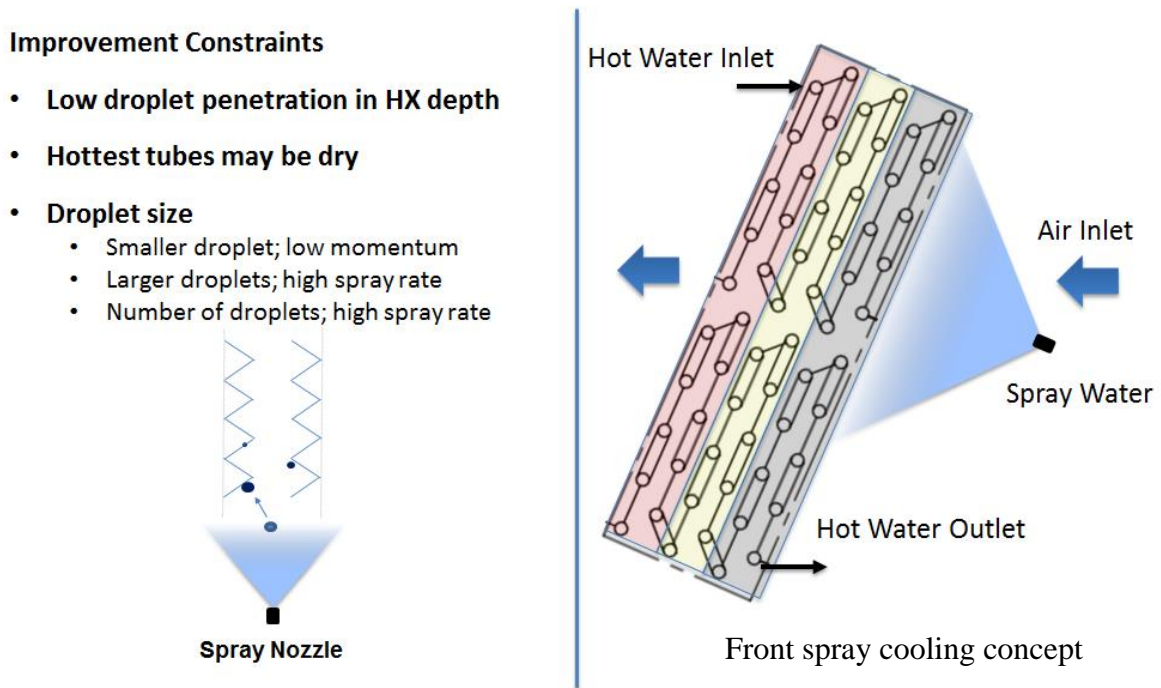
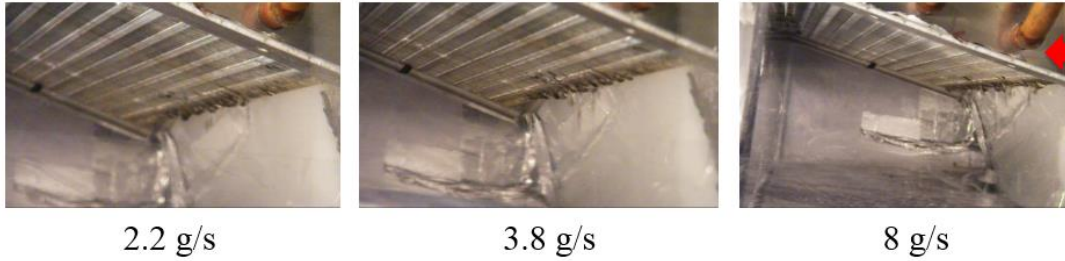


Figure 5.19: Spray cooling capacity enhancement improvement constraints.

It must be noted that due to compact and wavy fin structure it was not possible to visualize any fin surface in HX depth. For all front spray cooling cases no wetting water was observed on back face of coil. As explained in Section 4.6 the visualization point at bottom of HX was established by removing bottom frame plate. Wetting water distribution in depth of RTHX (3.0 mm fin spacing) in front spray and deluge conditions is presented in Figure 5.20. It was observed that for spray cooling water droplets mainly dropped on the bottom edge of fin near to air inlet section. Combined with the observation of a dry surface at back of HX this supports the theory that HX may not be wetted completely. However, it does not show the specific section of coil not being wetted.

Spray Cooling (3 m/s air velocity)



Deluge Cooling (3 m/s air velocity)

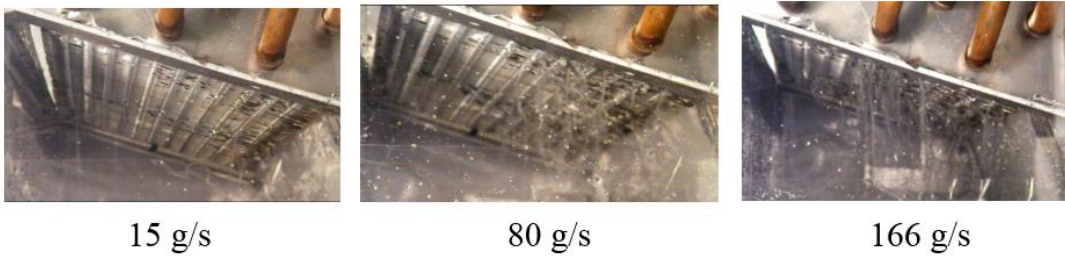


Figure 5.20: Wetting water distribution in depth of RTHX (3.0 mm fin spacing) in front spray and deluge conditions at approximately $T_{a,in}=28^{\circ}\text{C}$, $\text{RH}_{a,in} = 45\%$ and $\omega_{a,in}= 0.0106 \text{ kg}_w/\text{kg}_a$.

Chapter 6 Internal spray cooling technology development

6.1 Introduction and problem definition

Section 5.5 summarized the limitations of deluge and spray cooling in further in improvement of CER values though evaporative cooling. Spray cooling overcame a key challenge of capacity enhancement without penalizing air-side pressure drop. But due to a counter current configuration the hottest section of HX remained dry when spray cooling was applied to front face of HX as shown in configuration 1 of Figure 6.1. Placing the spray nozzle on top of HX as shown in configuration 2 (Figure 6.1) causes droplet carryover and is not a viable option. In order to spray water in hottest HX section spray nozzles could be placed in a way that they face the air outlet face of HX as shown in configuration 3 (Figure 6.1). But again this would cause droplet carryover and air would try to push spray droplets in opposite direction.

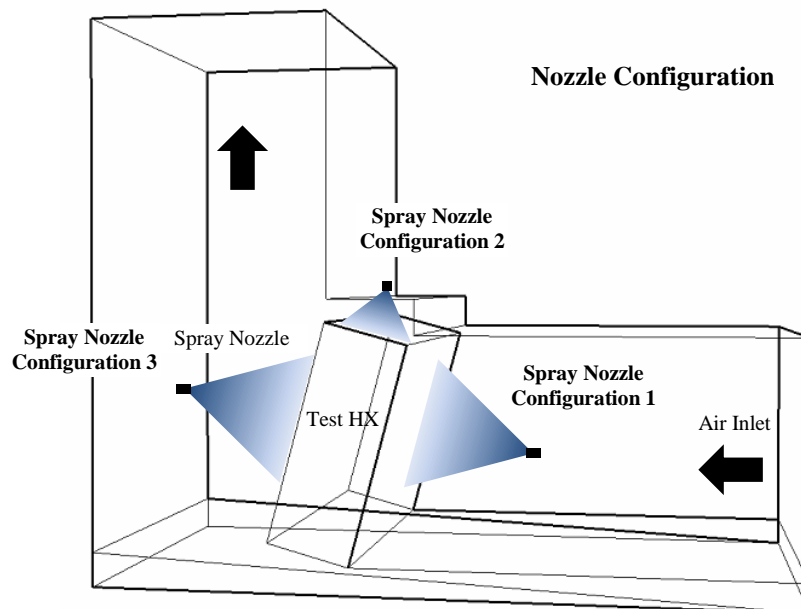


Figure 6.1: Different spray cooling nozzle configurations.

Therefore, the following objectives were defined for developing novel spray cooling ideas:

1) Improve wetting in HX depth, with no spray water carryover

(Hottest HX section must be evaporatively cooled)

2) Achieve a minimum CER of 3 or more at no increase in ΔP_a

(Maximum CER of 1.65 was obtained using front spray cooling)

3) Develop retrofit technology

(Novel technologies have a better chance of commercial success if no major change in current manufacturing technologies is required)

4) Obtain thinnest possible water film at spray rate less than 100 g/s-m³ of HX volume or 50 kg/hr-m² of HX frontal area

A brainstorming session was conducted within CEEE members and design ideas meeting above criteria were discussed. A comprehensive patent search was also conducted where approximately 1,700 US Patents in up to 15 sub-classes were searched. However no conflicting design ideas were found, and a provisional patent 61/782,825 [Popli et al., 2013] was filed with 7 design alternatives. One of these design ideas was selected for immediate implementation which would be discussed in Section 6.2.

6.2 Technology development process

The novel spray cooling design consisted of utilizing spray tubes (Figure 6.2) with regularly spaced holes for spraying water within the HX. Since the spray cooling occurs within the HX volume as shown in Figure 6.3 it was called internal spray cooling.

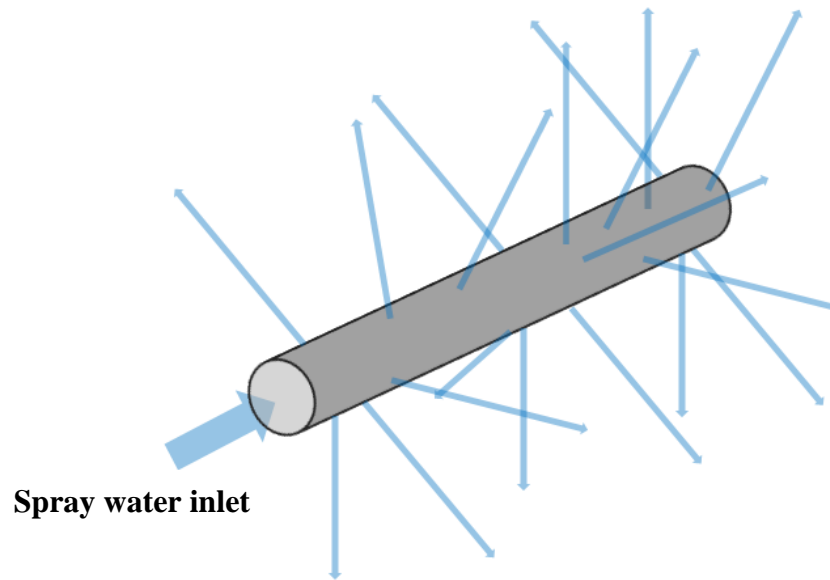


Figure 6.2: Schematic representation of permeable spray tubing (isometric view).

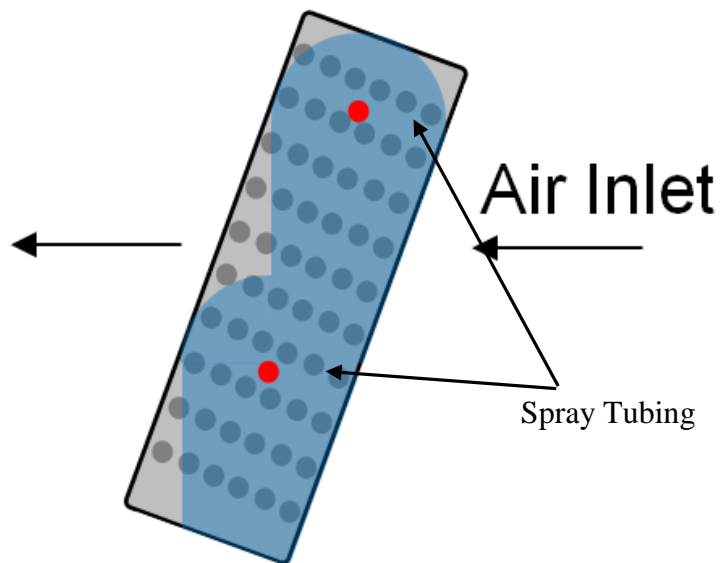


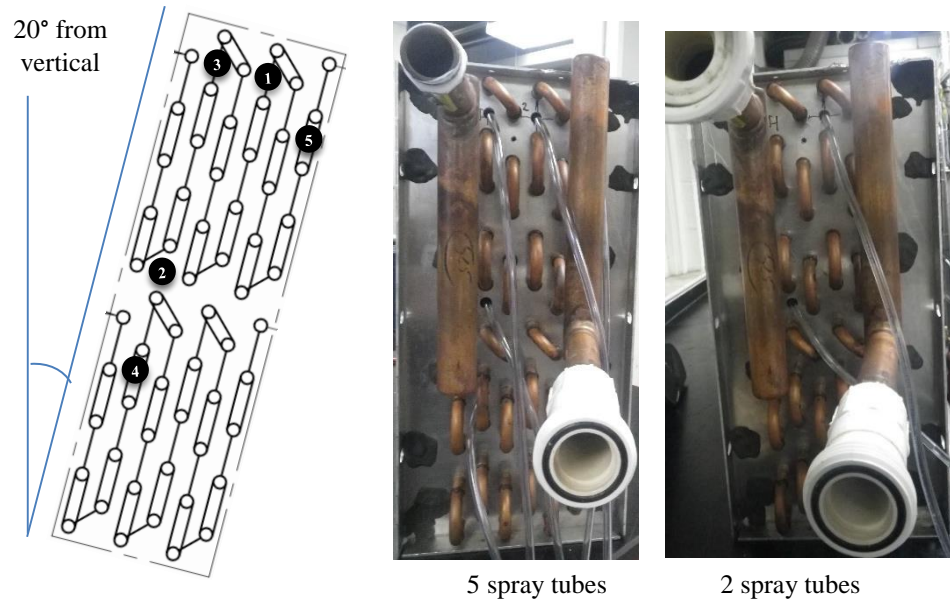
Figure 6.3: Novel method using two spray tubings which spray in a 360° radius along the length of the HX; red dots indicate example spray tube locations (side view).

There are several advantages to the proposed spraying method, with the main one being improved wetting coverage on the interior of the HX in all three dimensions. With respect to the depth of the HX, even with tight fin spacing the water will be able to penetrate the entire depth of the HX, whereas current exterior spraying methods struggle to wet the entire depth of the HX without using either a large number of nozzles or overly large droplet sizes and therefore flow rates. If the HX coil is particularly deep, or the fin spacing is particularly small, the interior method can be adapted to provide adequate coverage by adjusting the number and spacing of the wetting tubes.

Additionally, since the length of the tube runs along the entire length of the HX, there will be no distribution gaps along the length as there can be when using a bank of multiple cone shaped nozzles which don't fully overlap. Lastly, the position of the tube passes can be selected during the manufacturing process of the fins, and can thus be spaced to maximize coverage along the height of the HX regardless of the specific dimensions of the HX.

The second major advantage of the novel method is a reduced water consumption and water thickness layer when compared to other methods which can achieve full coverage, such as deluge wetting. This eliminates the need for a recirculation system, and the small droplets resulting from the spray will not significantly impede air flow. The elimination of a requirement for a recirculation system will reduce the initial cost of the system, and the operational energy cost will be reduced from the reduction in air side pressure drop and fan power consumption due to the smaller droplet sizes. If the spray flow rate required for adequate wetting is higher than the rate of evaporation, then intermittent spraying can be implemented. The intermittent spray can either be controlled through an on/off method, or by alternating the flow path between the banks or individual tubes as necessary.

Fin manufacturers typically punch these holes in all fin surfaces so HX manufacturers could build HXs with different tube circuitry. It was observed that if holes were drilled in HX side frame it could provide access to these holes. The spray tubes could then be fed through one of the sides up to a length equal to width of the coil as shown in Figure 6.4.



Note: Initial testing was performed using 2 spray tubes (holes marked 1 and 2). Number of spray tubes was later increased to 5 when holes marked 3, 4 and 5 were added.

Figure 6.4: Position of spray cooling spray tubes on HX frame (side view).

Next challenge was to produce even spray pattern inside HX. Since the hole size was approximately 12.5 mm spray nozzles could not be inserted to obtain fine spray. Drilling holes in a copper tube would produce much larger holes. Therefore, syringes were used to poke several holes in a clear plastic flexible hose approximately 12.5 mm diameter. Prior to this several attempts were made which failed to produce the spray pattern shown in Figure 6.5.



Figure 6.5: Uniform spray pattern obtained from plastic tube with holes in all directions.

The next part was to seal the flexible tube insert on other side. Several attempts were made to seal this using epoxy and also by fusing the tube end shut using heat.

But in both cases the discharge pressure caused the end to blow out. Finally another set of holes was made on the other side of HX frame and after feeding the spray tubes through the HX, tube ends were clamped shut using a copper tube plug (Figure 6.6).

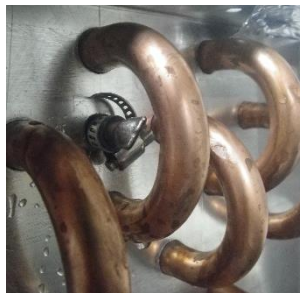


Figure 6.6: Sealed end of spray tubes using copper tube plug.

By utilizing the open passages through the HX fins proposed in the main design to spray a very narrow angle cone of water droplets through the width of the HX, such that the air flowing across the HX distributes the water droplets through the fins. The main issue with this method is that it may be difficult to scale for very long HXs, but for smaller HXs it

may be easier to implement. This problem may be reduced by combining internal spray with intermittent cooling at regular intervals controlled using a solenoid valve. In the next section, experimental results and performance comparison of internal spray cooling with conventional evaporative cooling methods would be discussed.

6.3 Comparison of novel and conventional evaporative cooling technologies

6.3.1 Internal spray cooling - 2 spray tubes

The novel internal spray cooling method was applied to hydrophilic coated coil and its performance was compared with conventional evaporative cooling technologies. Detailed performance of internal continuous and intermittent jet spray cooled hydrophilic coated wavy fin RTHX with $F_p=2.4$ mm using 2 spray tubes is presented in Appendix 1.

Figure 6.7 presents hydrophilic coated HX capacity enhancement using deluge, front spray and internal spray cooling with 2 spray tubes at approximately $T_{a,in}=28^\circ\text{C}$, $RH_{a,in} = 45\%$ and $\omega_{a,in}= 0.0106$ kg_w/kg_a.

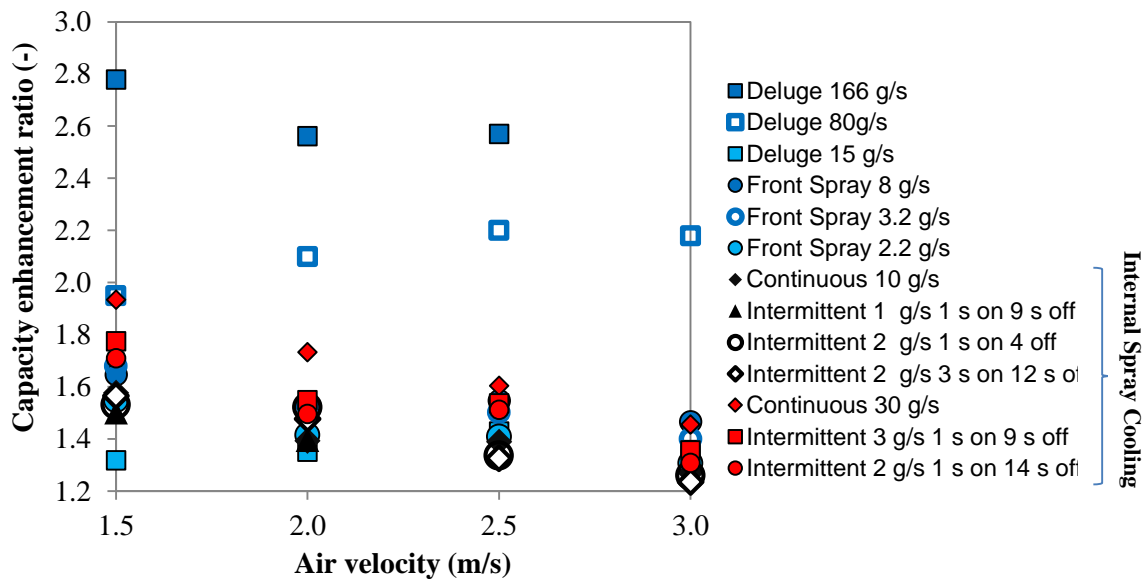


Figure 6.7: Hydrophilic coated HX capacity enhancement using deluge, front spray and internal spray cooling with 2 spray tubes at approximately $T_{a,in}=28^\circ\text{C}$, $RH_{a,in} = 45\%$ and $\omega_{a,in}= 0.0106$ kg_w/kg_a.

Both continuous and intermittent internal spray cooling was used and it was observed that:

- 1) Intermittent internal spray cooling with 2 spray tubes at 30 g/s achieved similar HX capacity that was obtained using deluge cooling at 80 g/s. There are two more points to be noted here, firstly internal spray cooling even at 30 g/s does not affect air side pressure drop. Secondly, internal spray cooling offers a unique solution for wetting water mal-distribution compared to deluge cooling where wetting water is distributed better using multiple spray points.
- 2) Interestingly, internal spray cooling at 10 g/s performed poorly even compared to very low spray rates in front spray configuration (2.2 g/s). This could be due to location of first two spray tubes shown in Figure 6.4.
- 3) When compared to conventional front spray cooling:
 - i. At 2 g/s spray rate internal spray is up to 11% better than front spray
 - ii. At approximately 3 g/s internal spray is up to 5.7 % better than front spray

More as observed in Figure 6.8, the benefit of internal spray cooling nearly diminishes to zero at higher air velocities.

- 4) The difference in HX performance due to different intermittent cooling cycles but same average spray rate was also investigated. Figure 6.9 presents the HX capacities as a function of wetting water flow rate for continuous and intermittent internal spray cooled HX. Intermittent cycles were tested for a given on and off time at a particular flow rate at approximately $T_{a,in}=28^{\circ}\text{C}$, $\text{RH}_{a,in} = 45\%$ and $\omega_{a,in} = 0.0106 \text{ kg}_w/\text{kg}_a$.

For same average spray rate (i.e. 2 g/s) up to 12% higher capacity was obtained when 1 s on and 14 s off cycle with higher flow rate was used.

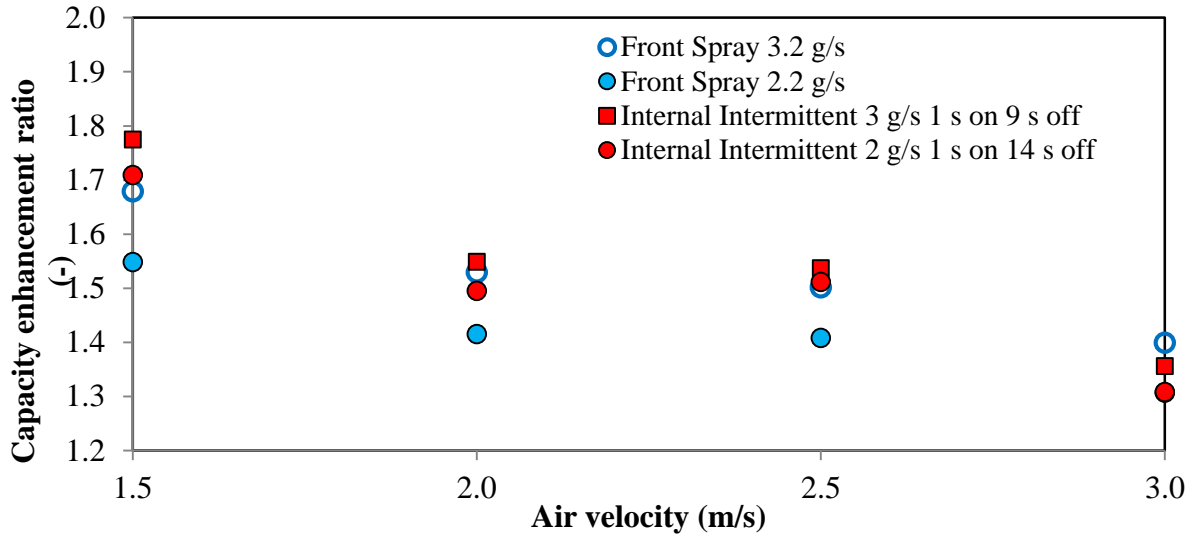


Figure 6.8: Hydrophilic coated HX capacity enhancement using front spray and internal spray cooling with 2 spray tubes at approximately $T_{a,in}=28^{\circ}\text{C}$, $\text{RH}_{a,in} = 45\%$ and $\omega_{a,in}= 0.0106 \text{ kg}_w/\text{kg}_a$.

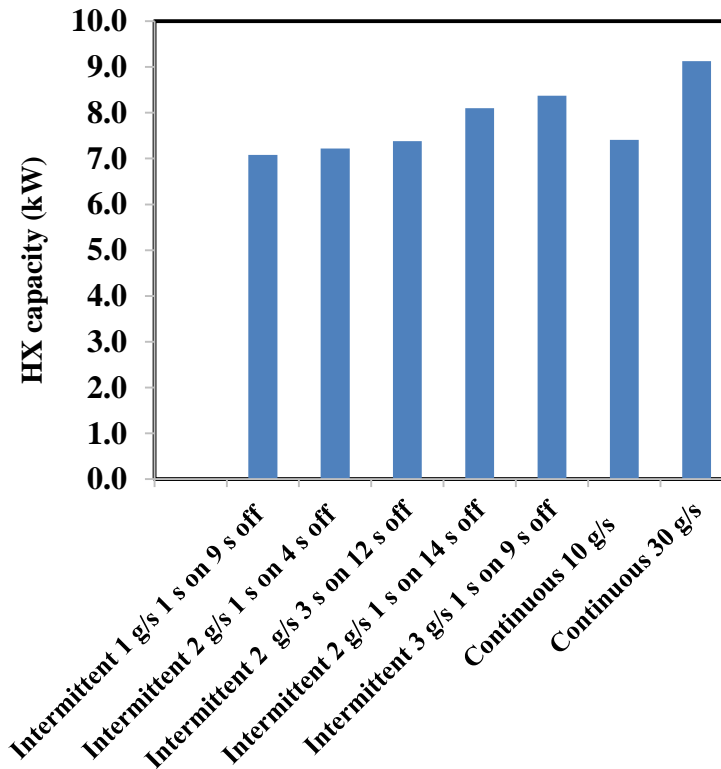


Figure 6.9: HX capacities as a function of wetting water flow rate for continuous and intermittent internal spray cooled HX ($V_a= 1.5 \text{ m/s}$; 2 spray tubes) at approximately $T_{a,in}=28^{\circ}\text{C}$, $\text{RH}_{a,in} = 45\%$ and $\omega_{a,in}= 0.0106 \text{ kg}_w/\text{kg}_a$.

5) It was also observed that evaporation rate and HX capacity were not affected during the part when wetting water was turned off. This may be the reason why continuous internal spraying at 10 g/s performs much worse compared to intermittent internal spraying at average spray rate of 2 g/s. However, it was not until the spray rate was increased to 30 g/s that the HX capacity was 12.65% higher than intermittent internal cooling at 2 g/s. This indicates that fundamental heat transfer mechanism is not the same for all these cases. Intermittent internal cooling promotes evaporative cooling where sprayed water is allowed to drain and resulting film on fin surface is much thinner compared to when continuous internal spraying was applied at 10 g/s. However, as in case of deluge cooling when wetting water rates are increased substantially a much larger area of fin surface is wetted and a thicker film forms on HX fins. In this case HX may be primarily water cooled while air is also being cooled down as it picks moisture while flowing over the water film. This cooled air stream then cools the HX tubes and fin area down stream of HX.

6.3.2 Internal spray cooling - 5 spray tubes

The benefit of internal spray cooling with 2 spray tubes was not significant, therefore HX capacity enhancement was investigated with 5 spray tubes. Figure 6.10 presents hydrophilic coated HX capacity enhancement using deluge, front spray and internal spray cooling with 5 spray tubes at approximately $T_{a,in}=28^{\circ}\text{C}$, $RH_{a,in} = 45\%$ and $\omega_{a,in}= 0.0106 \text{ kg}_w/\text{kg}_a$. Using 5 spray tubes in continuous internal spray cooling mode it was possible to achieve the same capacity that was achieved using deluge cooling at nearly twice the flow rate (166 g/s). The corresponding $PR_{\Delta P_a}$ for deluge and internal spraying case was 2.3 and 1.4, respectively (Figure 6.11).

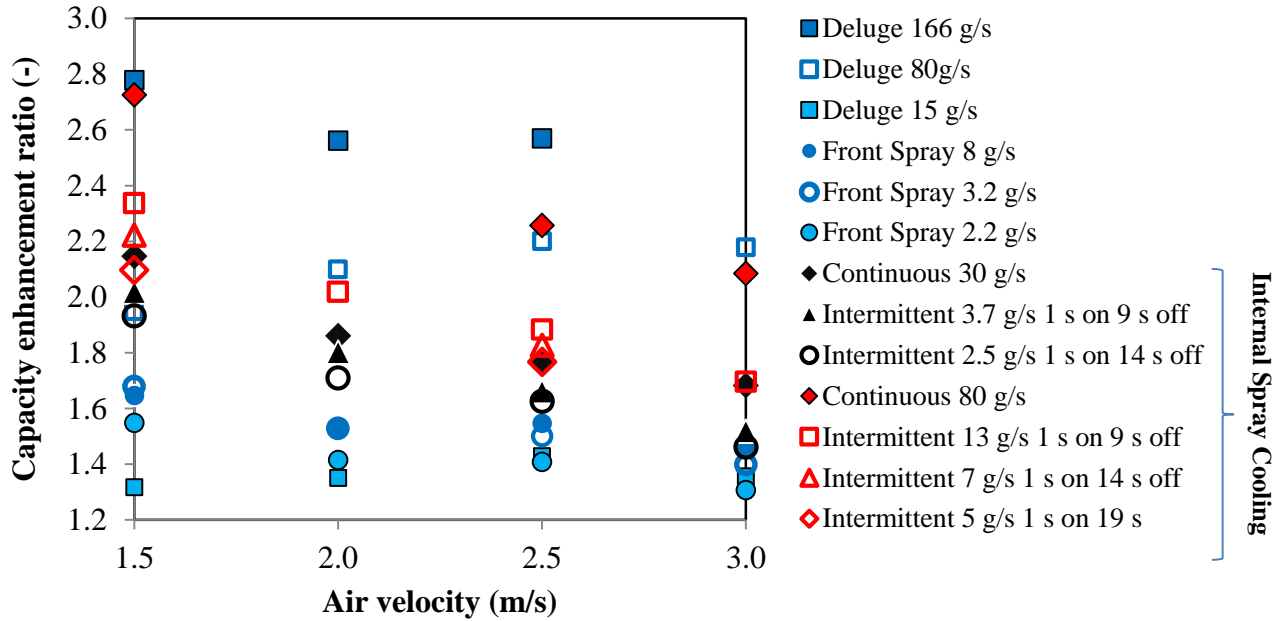


Figure 6.10: Hydrophilic coated HX ($F_p = 2.4$ mm) capacity enhancement using deluge, front spray and internal spray cooling with 5 spray tubes at approximately $T_{a,in}=28^\circ\text{C}$, $\text{RH}_{a,in} = 45\%$ and $\omega_{a,in}= 0.0106$ kg_w/kg_a.

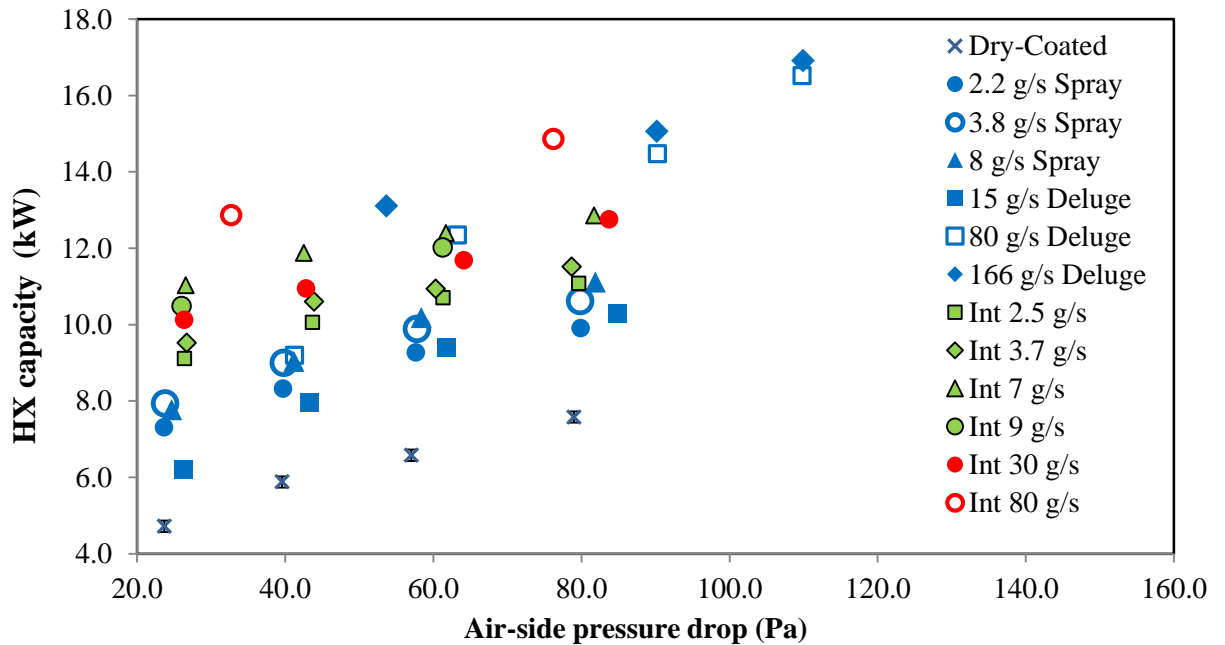


Figure 6.11: Hydrophilic coated HX capacity using deluge, front spray and internal spray cooling with 5 spray tubes at approximately $T_{a,in}=28^\circ\text{C}$, $\text{RH}_{a,in} = 45\%$ and $\omega_{a,in}= 0.0106$ kg_w/kg_a.

In all cases internal spray cooling with intermittent cooling obtained significantly higher HX capacity compared to front spray cooling at either equal or lower spray rates. Compared to front spray cooling intermittent internal spraying with 5 spray tubes could achieve up to 25%, 20%, and 35% higher capacity at approximately 2.5 g/s, 3.8 g/s and 8 g/s spray rates. Thus, compared to using 2 spray tubes for internal spray cooling, 5 spray tubes demonstrate a much better distribution of wetting water in HX depth as indicated from enhanced HX capacity. Figure 6.12 shows the wetting water falling from bottom edge of HX fins for front and internally sprayed coils at 3.7 g/s spray rate.

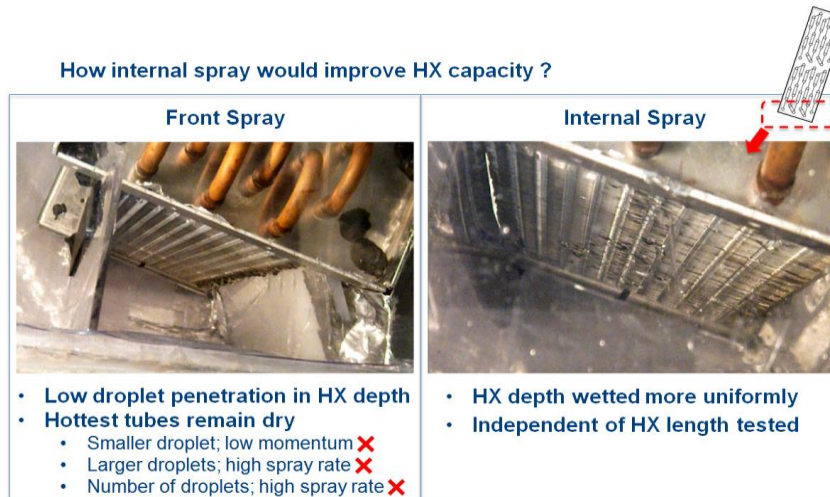
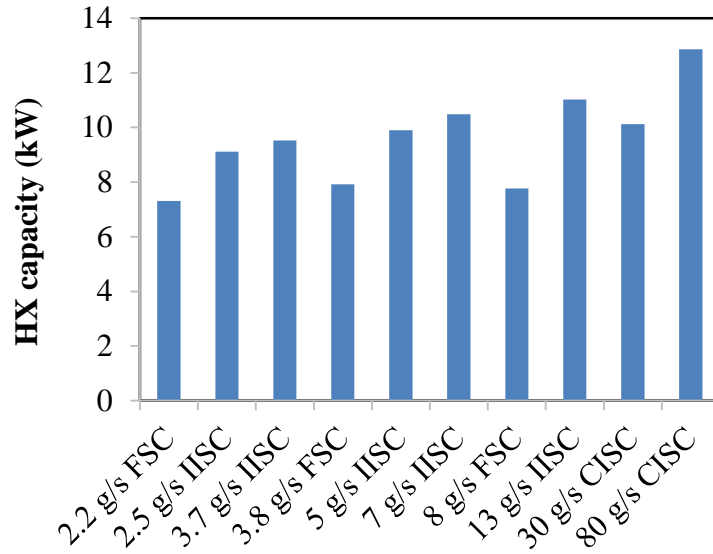


Figure 6.12: Comparison of front and internal spray cooling.

Figure 6.13 presents HX capacities as a function of wetting water flow rate for front spray cooling (FSC), continuous internal spray cooling (CISC) and intermittent internal spray cooling (IISC) ($V_a = 1.5$ m/s; 5 spray tubes).



Note: FSC-front spray cooling; CISC-continuous internal spray cooling; IISC-interment internal spray cooling

Figure 6.13: HX capacities as a function of wetting water flow rate for front spray, continuous and internal spray cooled HX ($V_a = 1.5$ m/s; 5 spray tubes) at approximately $T_{a,in} = 28^\circ\text{C}$, $RH_{a,in} = 45\%$ and $\omega_{a,in} = 0.0106$ kg_w/kg_a.

It can be observed that increasing spray rate from 5 to 30 g/s does not increase HX capacity, but a further spray rate increase to 80 g/s produced a 30% capacity enhancement. At such high flow rates the heat transfer is mainly due to forced convection between water film and fin surface than evaporative cooling. Furthermore, capacity increases almost linearly with increase in spray rate till 13 g/s, but a sharp drop is observed at 30 g/s where capacity enhancement due to thin film evaporation is overcome by a possible bridging and thickening of water film on hot HX surface. If the water film is thick enough only its top layer would be cooled due to evaporation.

Due to complexity of HX geometry and difficulty in visualization it is very difficult to predict the point at which this transition occurs.

Also, compared to front spray cooling, with internal spray cooling it is possible to get same cooling capacity at approximately three times lower air-side pressure drop. Alternatively, at $PR_{\Delta Pa} = 1$ for a given air-velocity, wetting water savings of up to 68% could be obtained. Similar fan energy consumption could be reduced by 2.3 times and wetting water savings from 68% to 96.75% could be achieved with internal spraying in comparison to deluge cooling.

Additional experiments were also conducted to study the effect of inlet air temperature on different spray cooling modes. Figures 6.14 and 6.15 present the hydrophilic coated HX capacity and CER using front, top and internal spray cooling with 5 spray tubes at approximately $T_{a,in}=37^{\circ}\text{C}$, $RH_{a,in} = 45\%$ and $\omega_{a,in} = 0.0179 \text{ kg}_w/\text{kg}_a$.

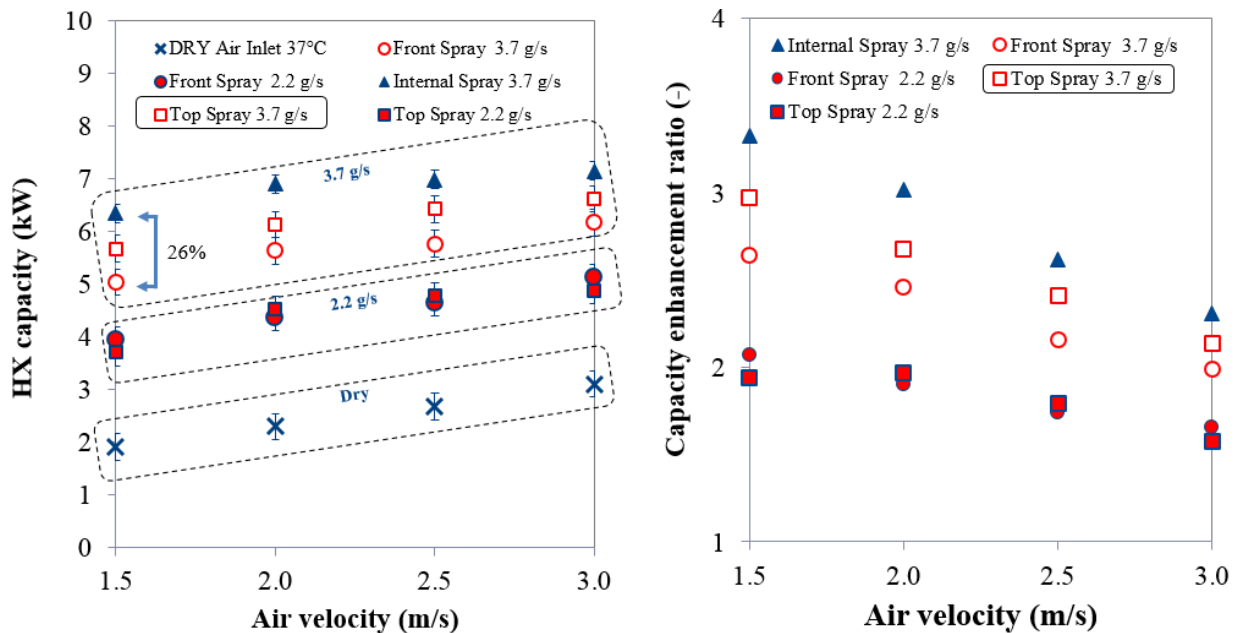


Figure 6.14: Hydrophilic coated HX capacity and CER using front, top and internal spray cooling with 5 spray tubes at approximately $T_{a,in}=37^{\circ}\text{C}$, $RH_{a,in} = 45\%$ and $\omega_{a,in} = 0.0179 \text{ kg}_w/\text{kg}_a$.

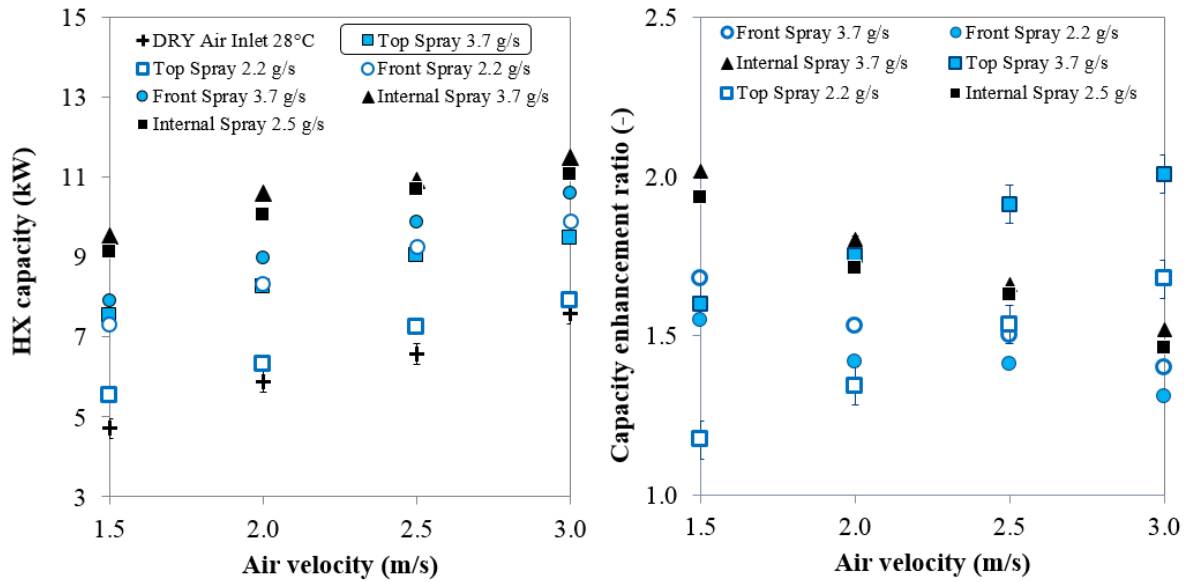


Figure 6.15: Hydrophilic coated HX capacity and CER using front, top and internal spray cooling with 5 spray tubes at approximately $T_{a,in}=28^{\circ}\text{C}$, $\text{RH}_{a,in} = 45\%$ and $\omega_{a,in}= 0.0106 \text{ kg}_w/\text{kg}_a$.

Due to much lower baseline HX capacities generally higher values of CERs were obtained for cases with higher inlet air temperature (37°C).

In comparison with front spray cooling internal spraying obtains up to 26% and 20% higher HX capacities at $T_{a,in}$ of 37°C and 28°C , respectively and humidity ratio of $0.0179 \text{ kg}_w/\text{kg}_a$ and $0.0106 \text{ kg}_w/\text{kg}_a$, respectively. Top spraying is not recommended as a considerable portion of spray water is blown out of HX.

Maximum CER of 3.2 was obtained for internal spray cooling at 3.7 g/s spray rate and 37°C air inlet. Thus for a hybrid cooler designed to operate at $T_{a,in} = 28^{\circ}\text{C}$ and $\omega_{a,in} = 0.0179 \text{ kg}_w/\text{kg}_a$, baseline dry case capacity could be obtained at 2.5 times lower air-side pressure drop with internal spray cooling when ambient air temperature rises to $T_{a,in} = 37^{\circ}\text{C}$ and $\omega_{a,in} = 0.0179 \text{ kg}_w/\text{kg}_a$. This could avoid equipment oversizing, associated material cost and energy required for their manufacturing, and fluid pumping costs due to lower pressure

drop in tube side.

6.4 Summary

In this Chapter a novel HX wetting spray cooling method was proposed with potential patenting and commercialization opportunity. The complete development process supported with experimental data was also described. Evaporative cooling performance enhancement potential of the novel method was experimentally investigated and compared to conventional spraying technologies such as front and top spray cooling and deluge cooling.

It was found that in comparison with front spray cooling internal spraying achieved up to 26% and 20% higher HX capacities at $T_{a,in}$ = of 37°C and 28°C, respectively and humidity ratio of 0.0179 kg_w/kg_a and 0.0106 kg_w/kg_a , respectively. Compared to front spray cooling intermittent internal spraying with 5 spray tubes could achieve up to 25%, 20%, and 35% higher capacity at approximately 2.5 g/s, 3.8 g/s and 8 g/s spray rates. Also, compared to deluge cooling, internal spray cooling could achieve same cooling capacity at approximately three times lower air-side pressure drop. This is due to higher HX capacity enhancement at lower air velocity, which may allow lowering the fan speed. Alternatively, at $PR_{\Delta Pa} = 1$ for a given air-velocity, wetting water savings of up to 68%-96.75% could be obtained.

The flexibility of novel spray cooling method developed could offer substantial further improvement opportunities. For example targeted cooling could be provided within deeper parts of HX volume without the problem of droplet carryover. This technology is not only retrofit but also overcomes several challenges faced by conventional evaporative cooling

technologies. Intermittent cooling combined with internal spray cooling reduces wetting water consumption as evaporative cooling sustains though the brief period when spray is turned off. Moreover, it opens up future research area for obtaining best cycle times and flow rates.

Chapter 7 Wetting water flow visualization

One of the challenges in understanding capacity enhancement of evaporatively cooled HXs lies in the difficulty associated with visualization of wetting water distribution in HX depth. With the amount of surface area of the HX wetted often unknown, one cannot understand the reason for varying capacities of HXs as air and spray flow rates or operating fluid temperatures vary. Due to difficulties in air-side visualization of compact HXs, these issues have not been sufficiently addressed in published literature.

7.1 Conventional visualization

Once installed in test section HX can be viewed in one of following directions/view angles as shown in Figure 7.1, (a, b) front/back view, (c) side view, (d) bottom side view.

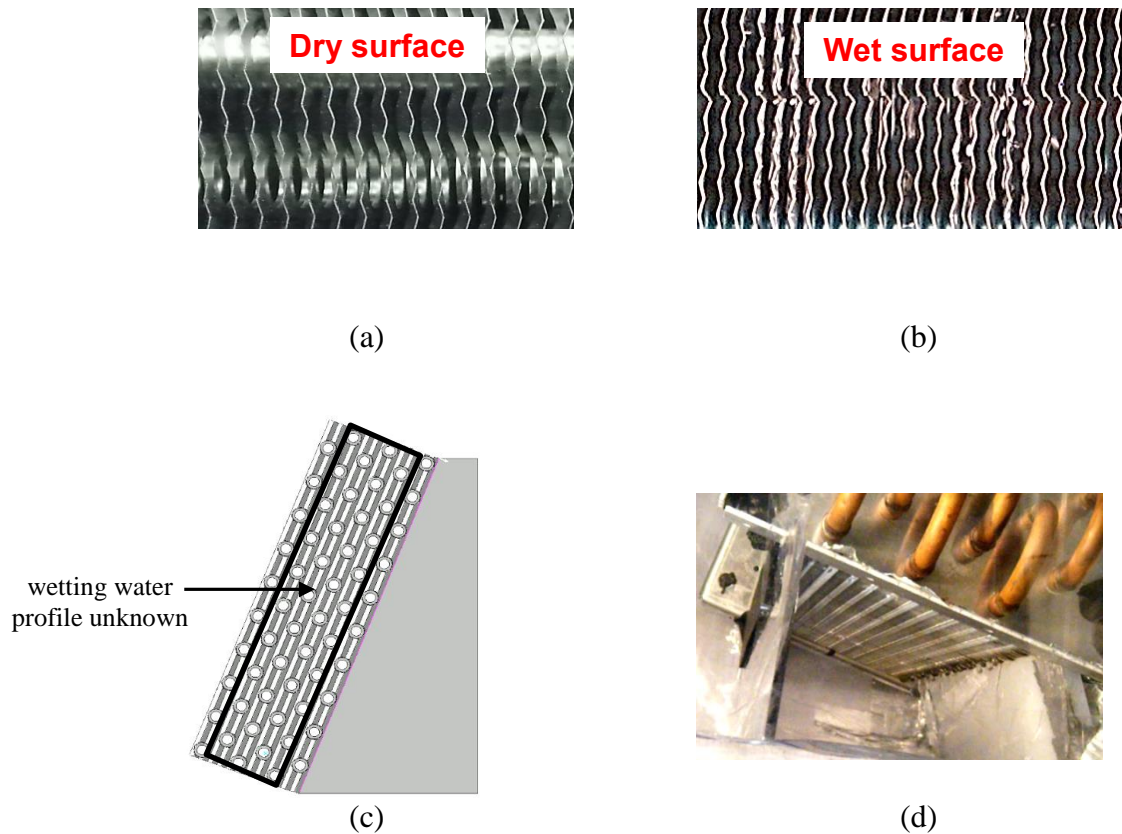


Figure 7.1: Conventional visualization; (a, b) front/back view, (c) side view, (d) bottom side view.

7.2 Need for better visualization methods

The following challenges limit application of typically utilized visualization view angles:

1) Deeper coils

Conventional methods work well for HXs one or two banks deep. However for visualizing of wetting on HXs such as the one being tested in the current work (Figure 3.2 c) i.e. 6 banks deep in the direction of air inlet alternate visualization methods are required.

2) Effect on air flow

In addition to issues related to accessing the center portion of HX, there is also a concern that air flow would be affected due to the camera placed in front of HX which may lead to reduced air velocity on the portion of HX being viewed thereby giving a false impression of how wetting actually occurs

3) Tight fin spacing

Due to hybrid wet dry operation the coils are optimized for dry cooling operation which leads to tight fin spacing (2 to 3 mm). This tight fin spacing further complicates visualization.

4) Fin geometry

Complex fin geometry such as wavy and louver, contributes further in reducing visual access to deeper portions of coil when viewed from front or back side of HX.

Looking underneath the HX from a side view helps understand the depth of wetting at the outlet of HX. But gives no information of wetted profile inside HX especially as a function of air velocity.

7.3 Novel visualization methods

A novel visualization strategy was implemented, as described in this Section. In addition a partitioned tray was also installed underneath HX to collect and separately measure wetting water falling from different sections.

7.3.1 Removal of bottom air flow guide plate

Typical HX installation configuration in the air duct is shown in Figure 7.2 (a) and (b) with bottom and side frame of HX marked, and Figure 7.3 shows bottom frame removed.

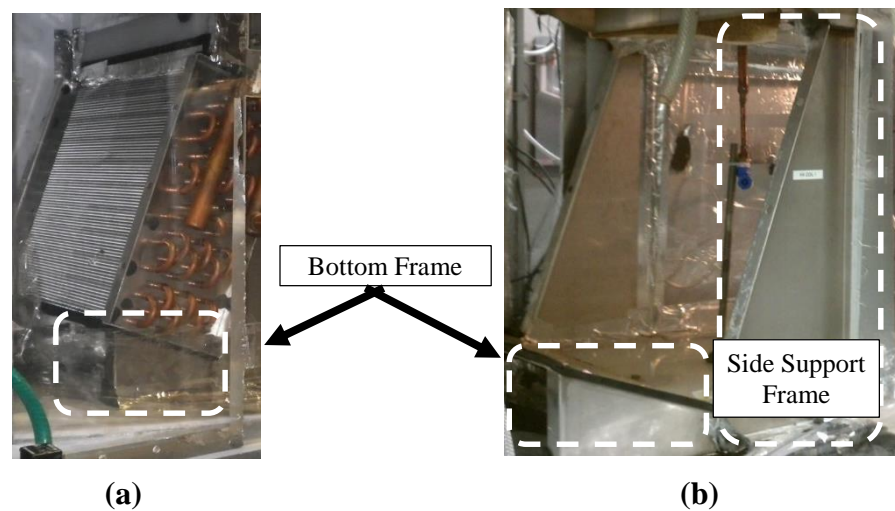


Figure 7.2: Typical HX installation in air duct with (a) bottom and (b) side support frame of HX.

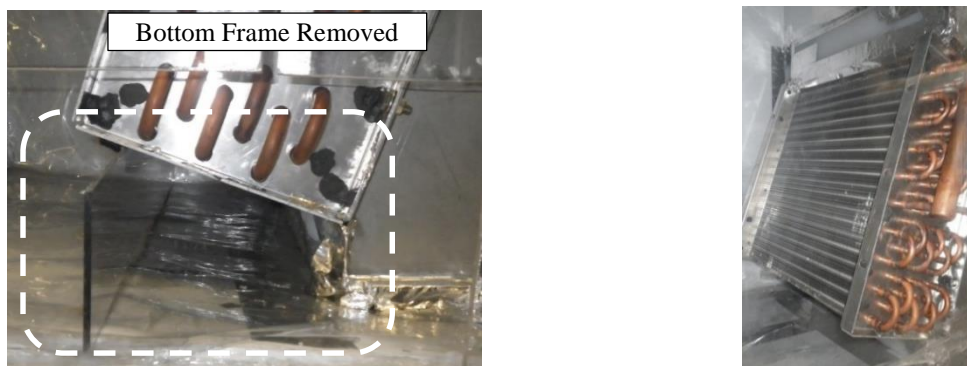


Figure 7.3: HX installed with bottom frame removed.

7.3.2 Partitioned water collection tray

A partitioned collection tray design concept in modified test setup is shown in Figure 7.4. The idea was to collect wetting water coming out of different HX tube banks. Ideally 6 partitions would be required but due to small distance between tube banks collection tray was designed to have three partitions, i.e. 2 banks per partition. Each section of tray would be connected to Coriolis flow meter to record respective water flow rates. It must be noted that this mass flow meter is in addition to the one already installed in the test setup which records the wetting water flow rate at spray/deluge inlet to HX. Therefore, the difference of two readings would provide amount of water evaporated in each experiment. After the flow meter at HX outlet the water returns to the bucket from where it is pumped back to the inlet to complete the wetting water loop cycle.

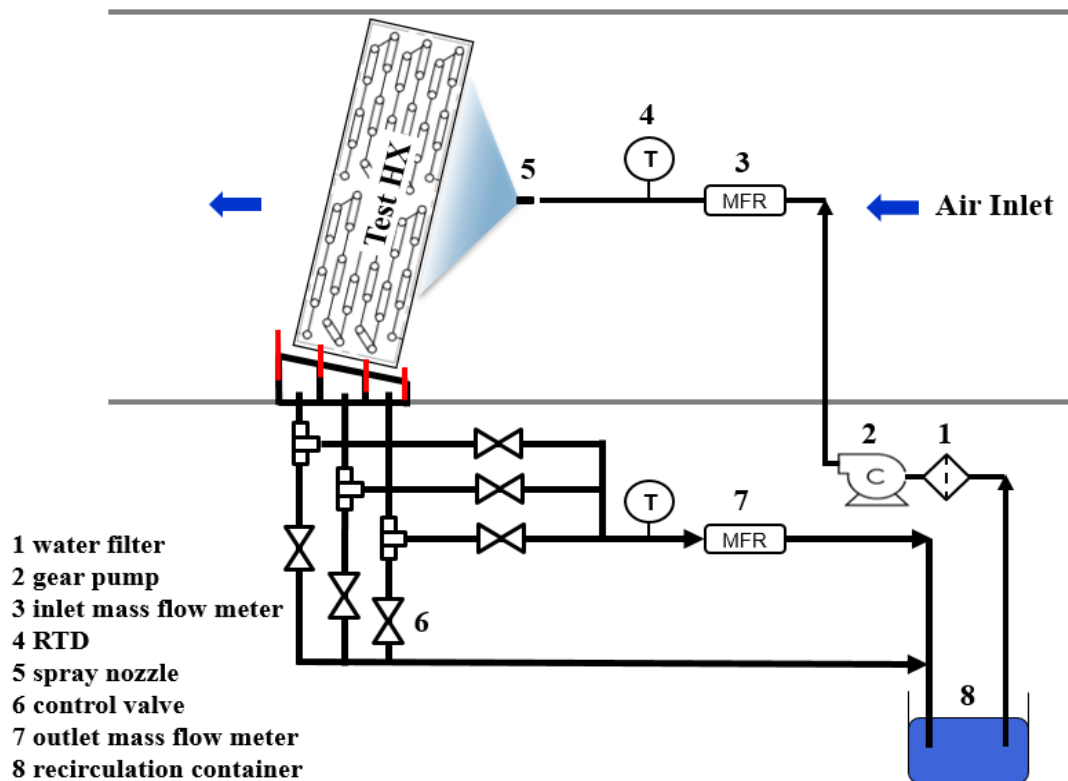


Figure 7.4: Partitioned collection tray design concept in modified test setup.

Figure 7.5 shows the partitioned collection tray placed underneath HX with each partition sealed to prevent air bypass between HX fins and flexible seal, and setup ready for visualization measurements.

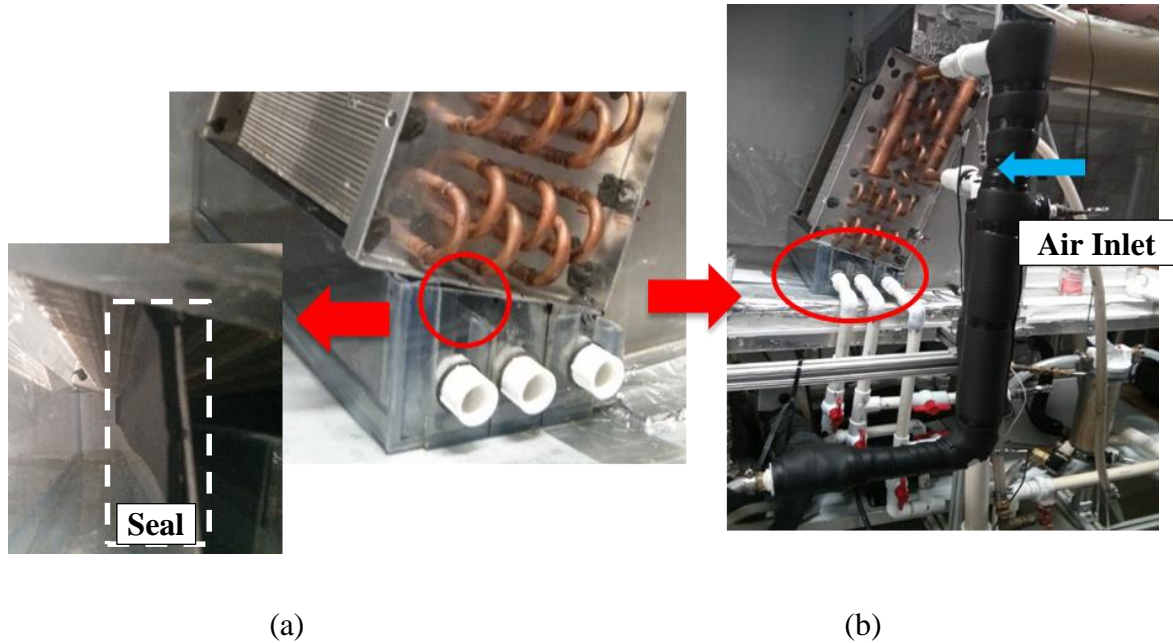
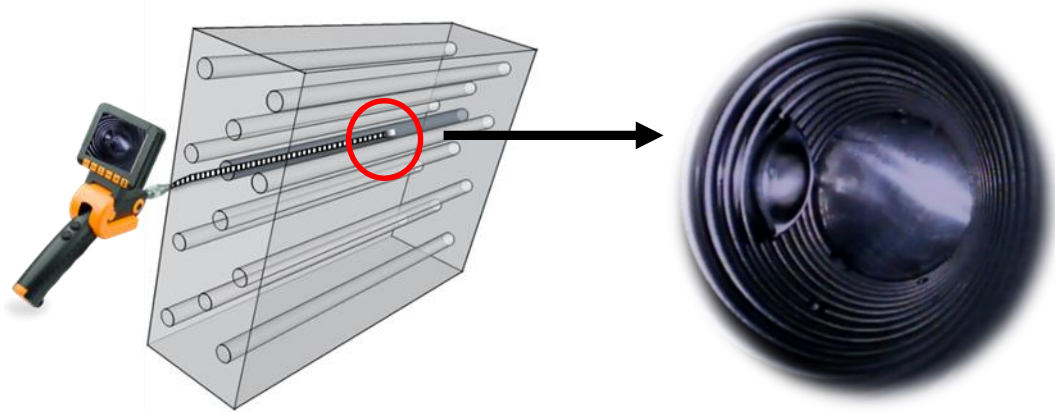


Figure 7.5: Partitioned collection tray placed underneath HX with each partition sealed to prevent air bypass between HX fins and flexible seal, (b) test setup ready for visualization measurements.

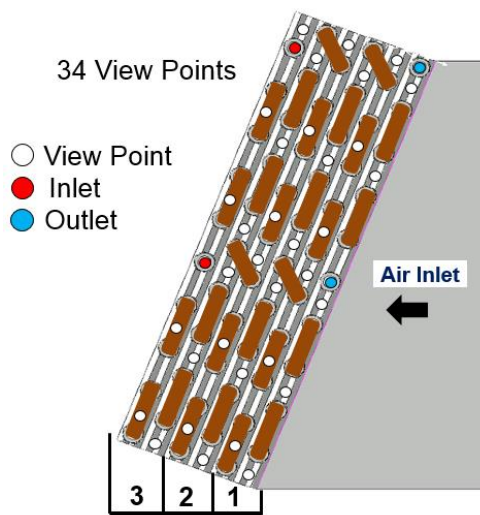
7.3.3 Borescope assisted visualization

A novel method of visualization was employed to gain access to deeper sections of the HX and is described in this Section. HX coil manufacturing process involves expanding copper tubes laid through the fins in a specific circuitry. However often the holes meant for tubes are left empty deliberately either because of the type of circuitry or as holes meant for support tubes for high width HXs (which prevents sagging in the center of the coil). These holes are not visible due to the side plate. However, drilling holes through the side plate gives access to these holes (Figure 7c) which run throughout HX width i.e. through each

fin. For the HX tested in current study, there were 6 holes each in 1st, 3rd and 5th tube bank. 17 out of these 18 holes were utilized for this study. The even numbered tube banks did not have any holes, so each visualization sub-case was repeated with the HX rotated such that odd numbered tube banks with the view-points became even numbered tube banks. Due to symmetry of HX nothing else changes when HX is rotated except the inlet and outlets ports are reversed. Therefore, 34 view-points are created and borescope inserted through each as shown in Figure 7.6. Deluge, and spray cooling tests were then repeated at representative wetting water flow rates and HX frontal air velocities to create a wetting profile for each case. In addition water collected in each section of bottom tray is reported as %mass of total wetting water flow rate.



(a)



(b)



(c)

**Figure 7.6: (a) Borescope inserted into HX through view point;
(b) and (c) view-points for visualization.**

7.4 Results and discussion

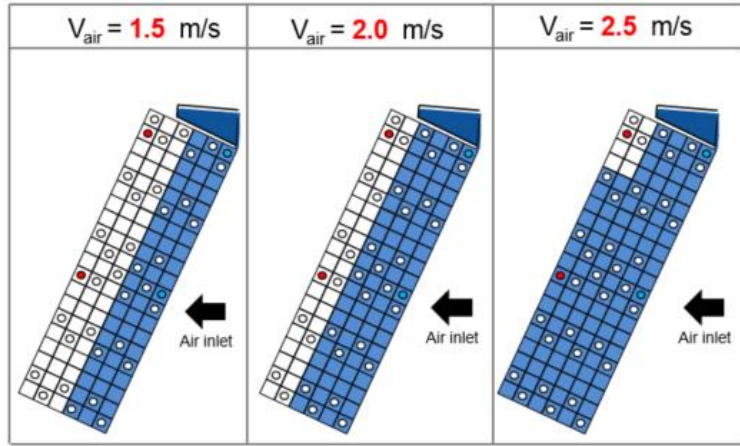
HX was divided into 6x20 grid and each grid was assigned wet or dry based on wetting observed through 34 viewpoints. Figure 7.7 presents the wetting profile for deluge cooling at wetting water flow rate 166, 80 and 15 g/s. Figure 7.8 presents the wetting profile for spray cooling at wetting water flow rate 8 and 3.8 g/s, and Figure 7.9 presents wetting profile for internal jet spray cooling at wetting water flow rate of 3.8 g/s.

Table 7.1 shows percentage mass fraction of wetting water in different tray sections and percentage wetted fin area, and HX capacity for deluge and spray cooling at 2.5 m/s air velocity.

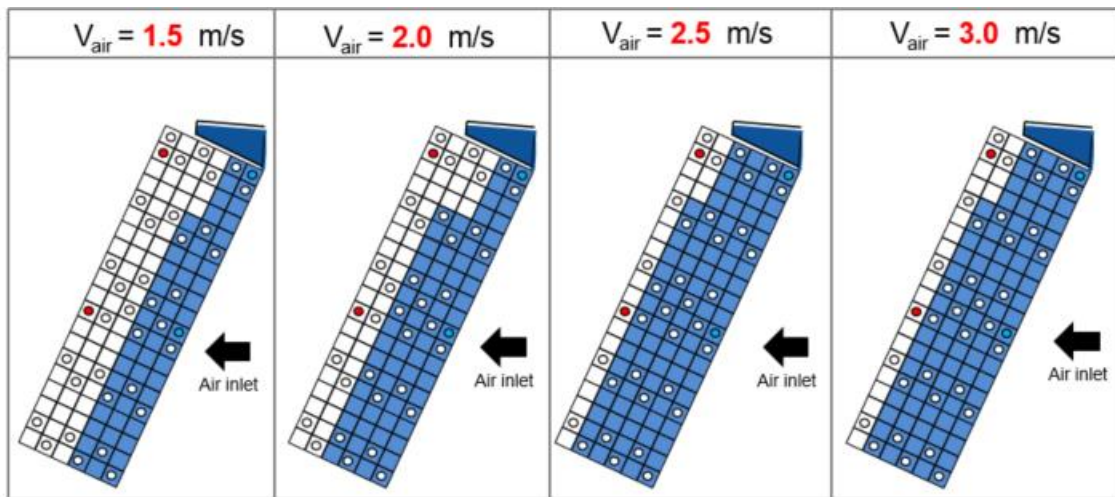
Table 7.1: Percentage mass fraction of wetting water in different tray sections and percentage wetted fin area, and HX capacity for deluge and front spray cooling at 2.5 m/s air velocity.

Test Case	Tray Section #			Wetted Fin Area (%)	HX Capacity ¹ (kW)
	1	2	3		
Front spray 3.8 g/s	72	0	0	13	9.9
Front spray 8 g/s	85	0	0	35	10.2
Deluge 15 g/s	85	12	0	45	9.4
Deluge 80 g/s	51	29	19	79	14.5
Deluge 166 g/s	74	24	0	83	16.9
Internal spray 3.8 g/s	82	4	10	85	10.9

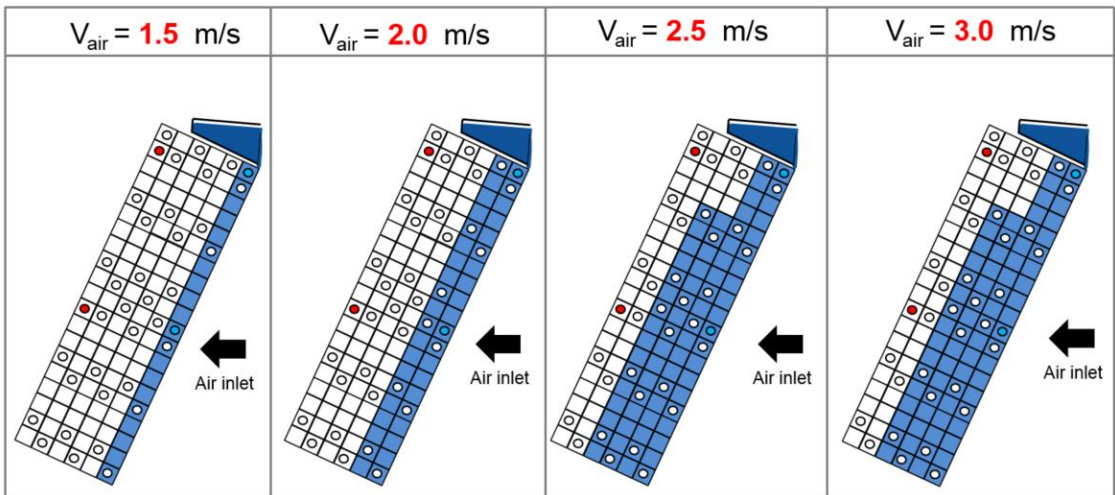
Note: ¹ measurement uncertainty ± 0.25 kW



(a)

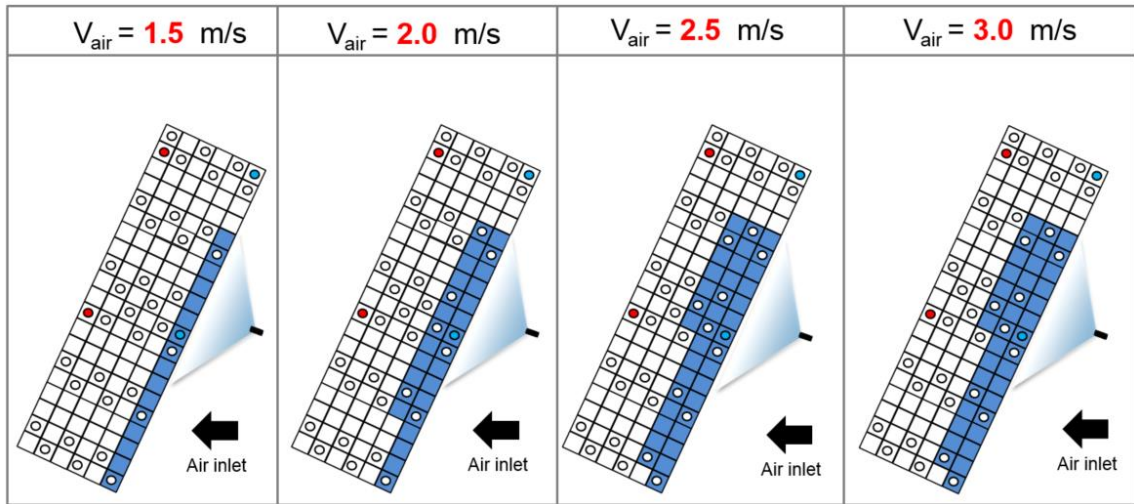


(b)

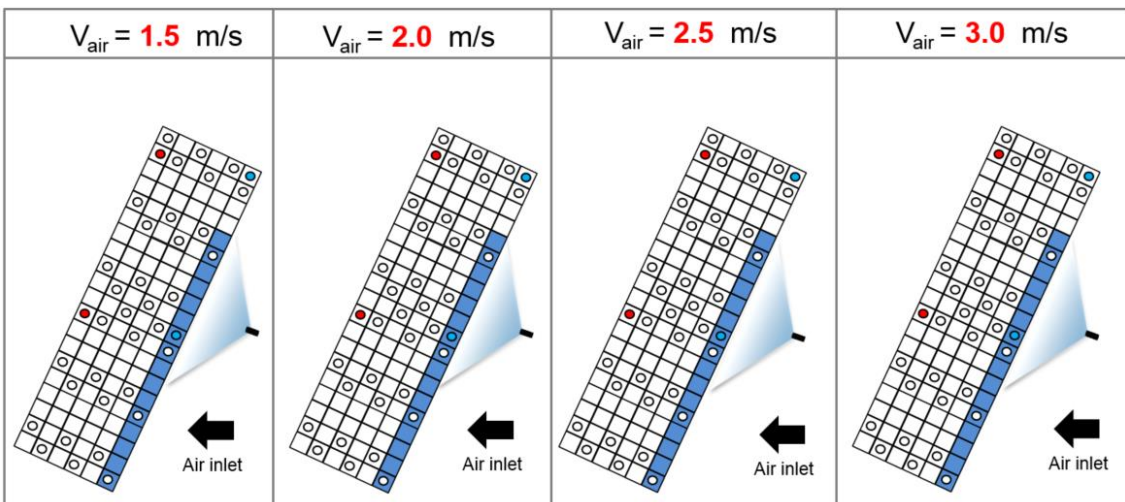


(c)

Figure 7.7: Wetting profile for deluge cooling at wetting water flow rate of (a) 166 g/s; (b) 80 g/s; (c) 15 g/s.



(a)



(b)

Figure 7.8: Wetting profile for front spray cooling flow rate (a) 8 g/s; (b) 3.8 g/s.

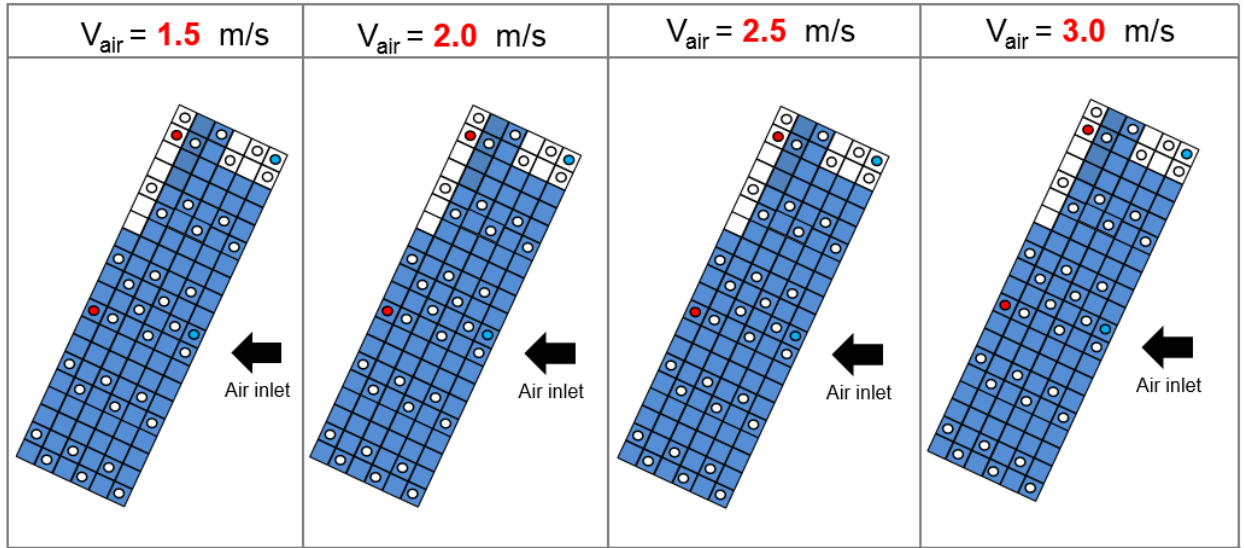


Figure 7.9: Wetting profile for internal spray cooling at wetting water flow rate 3.8 g/s.

Figure 7.10 shows the HX capacity as a function of fin area wetted for deluge, front spray and internal jet spray cooling at 2.5 m/s air velocity and Figure 7.11 presents the mass of wetting water measured in different sections of bottom split tray as a function of tray section number for deluge, front spray and internal jet spray cooling at 2.5 m/s air velocity.

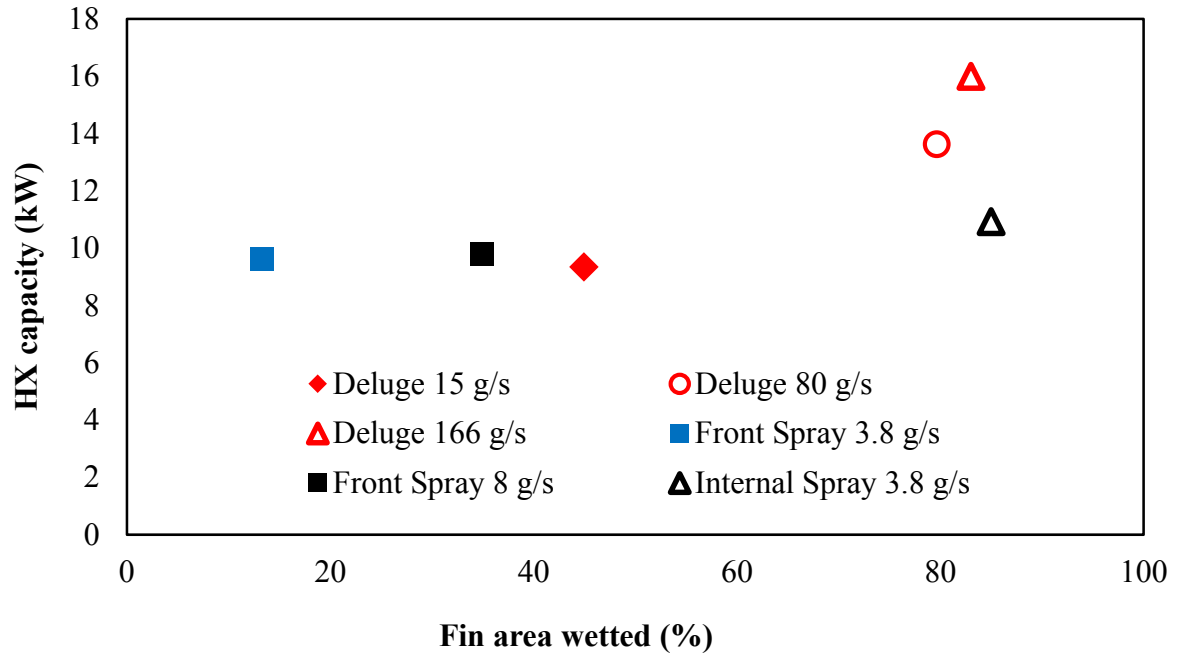


Figure 7.10: HX capacity as a function of fin area wetted for deluge, front spray and internal jet spray cooling at 2.5 m/s air velocity at approximately $T_{a,in}=28^{\circ}\text{C}$, $\text{RH}_{a,in} = 45\%$ and $\omega_{a,in}= 0.0106 \text{ kg}_w/\text{kg}_a$.

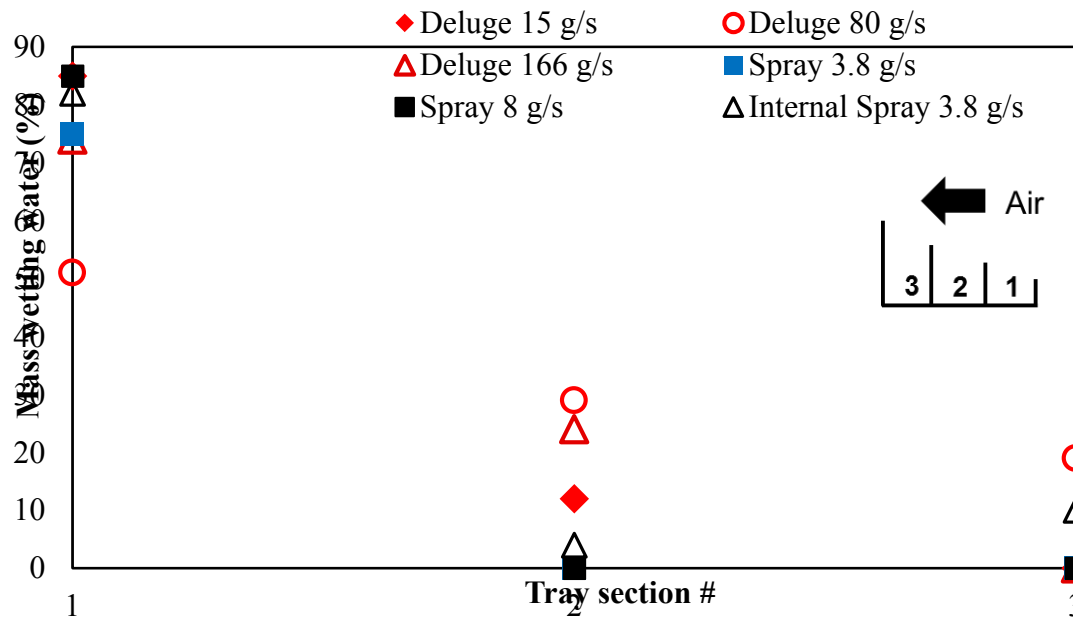


Figure 7.11: Mass of wetting water measured in sections of bottom split tray as function of tray section # for deluge, front spray and internal jet spray cooling at 2.5 m/s air velocity at approximately $T_{a,in}=28^{\circ}\text{C}$, $\text{RH}_{a,in} = 45\%$ and $\omega_{a,in}= 0.0106 \text{ kg}_w/\text{kg}_a$.

The following observations were made in regard to deluge and spray cooling:

Deluge cooling

- Conclusive proof of wetting in HX depth, up to 5th tube bank is wetted at higher flow rates.
- Increasing air flow rate increased the mass of water in partitioned collection tray sections #2 and 3, however it is not completely in line with the flow map obtained. This is due to inclination of HX with vertical due to which a significant portion of water ends up in section #1 although wetting profile shows much more water in tube bank 3 and 4. This further highlights additional information which proposed visualization setup provides compared to viewing HX from front or side view only.
- Approximately 45 to 83% of HX is wetted overall depending on deluge flow rate
- The study also highlighted a drawback of deluge cooling overflow distributors which are responsible for causing mal-distribution of wetting water over HX width. While a constant and evenly distributed water flows through the center portion of HX, the distribution towards the end was found to be uneven.

Front spray cooling

- Enhanced visualization method clearly shows that a significant portion (up to 87%) of HX remained dry when front spray cooling was applied to evaporatively enhance HX capacity
- Even when spray rate is increased to 8 g/s deeper tube banks 5 and 6 are not wetted. Thus, increasing the flow rate or adding more nozzles in front of HX would not be as beneficial since tube 1 and 2 only are wetted. It must be note that due to direction of

airflow having a spray nozzle on back side of HX may not be helpful

- Wetting profile was found to be parabolic in shape and closely follows the shape of spray pattern on HX face. Non-uniformity of spray pattern is visible through boroscope inserted at different depths in HX width.

It is interesting to observe that with approximately 13% wetted fin area front spray cooling achieves a higher capacity compared to deluge cooling at 15 g/s which wets approximately 45% of HX fin area. Therefore, wetted area alone does not determine HX capacity, spray droplet area to spray volume ratio may also be critical in determining capacity enhancement. To further analyze this, HX capacity was plotted as a function of evaporation rate for deluge, spray cooling at 2.5 m/s air velocity in Figure 7.12.

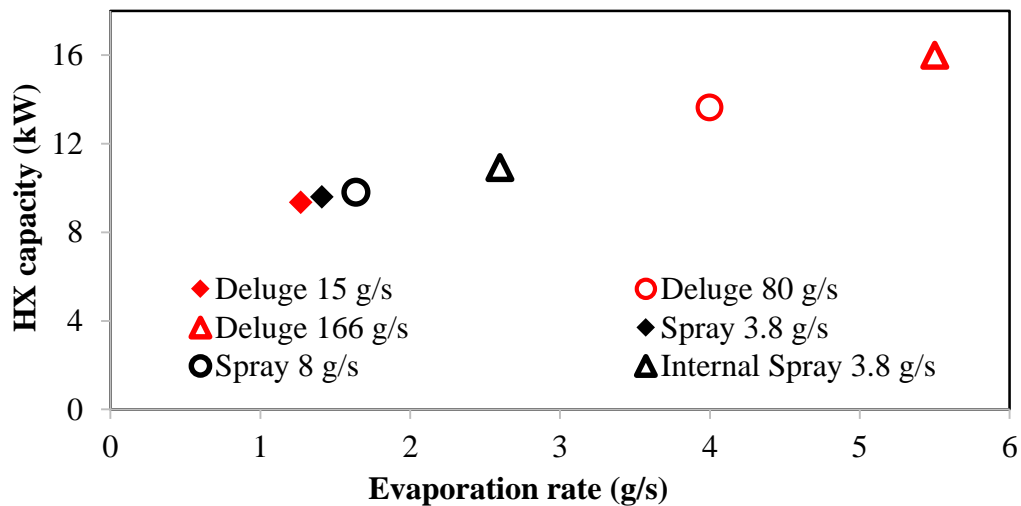


Figure 7.12: HX capacity as a function of evaporation rate for deluge, front spray and internal jet spray cooling at 2.5 m/s air velocity at approximately $T_{a,in}=28^{\circ}\text{C}$, $\text{RH}_{a,in} = 45\%$ and $\omega_{a,in} = 0.0106 \text{ kg}_w/\text{kg}_a$.

Thus, in addition for the coil to be completely wet sufficient evaporation must occur on HX fin surface to allow additional heat transfer due to latent heat removal.

Previous sections presented various types of method in the form of plots and tables to compare the performance of heat exchangers. The literature also lists several parameters including, capacity enhancement, are and volume goodness, droplet pechlet numbers etc. Each author not only uses different parameters but different plots to state the pros and cons of wet surface heat exchangers. Moreover these plots give no idea of the physical meaning and incremental development of wetting technologies. Therefore, the generic evaporative cooling performance plot presented in Figure 7.13 contributes to published literature by unifying the analysis in a single plot.

Quadrant 1 and 3 are regions of excessive wetting water and severe to moderate mal-distribution. The capacity enhancement may or may not be > 1 .

Quadrant 4 has high spray efficiency but, capacity enhancement is not high enough either due to high $PR_{\Delta P_a}$ penalty. This is a unique situation which may occur in very compact heat exchangers where water blockages or bridging increases ΔP_a in some areas, while a major portion of heat exchanger remains dry. So there is no capacity enhancement and/or high air-side pressure drop. Such a situation may occur in deluge cooled heat exchangers wetted at the leading edge of fins.

Quadrant 2, is the zone of most efficient water usage and maximum capacity enhancement to air-side pressure drop ratio. Ideally top right corner of Quadrant 2 is the best operation zone for evaporative coolers/condensers with maximum spray efficiency and HX CER.

Figure 7.14 shows, test data obtained for three wavy-fin HXs plotted on evaporative cooling performance plot.

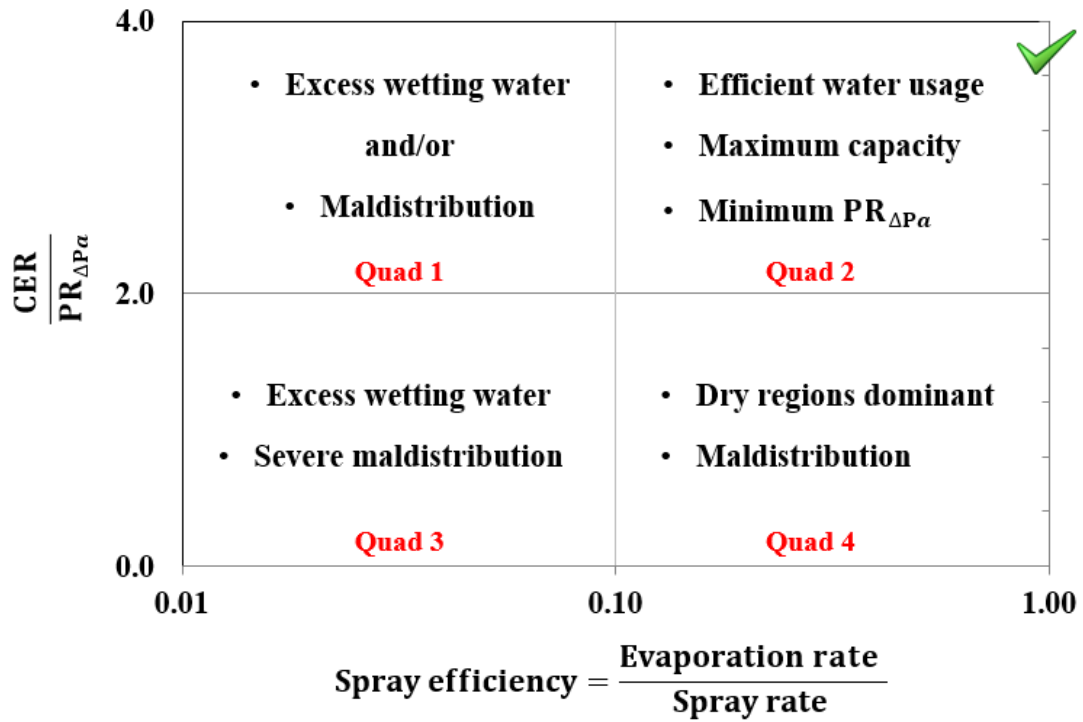


Figure 7.13: Generic evaporative cooling performance plot.

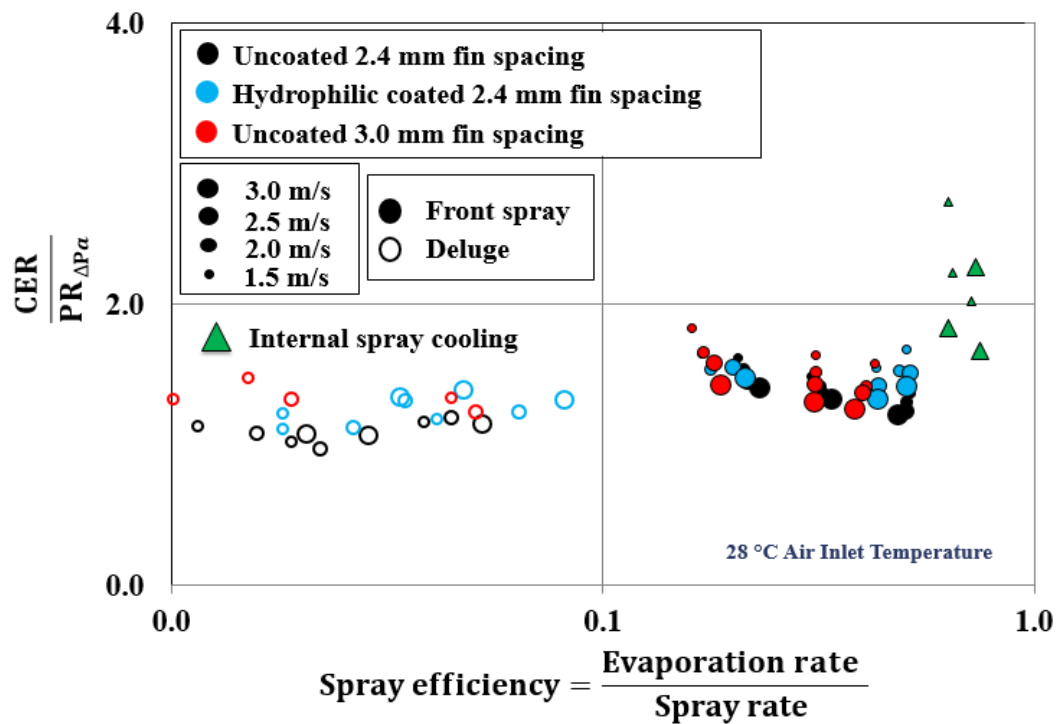


Figure 7.14: Test data obtained for three wavy-fin HXs plotted on evaporative cooling performance plot at approximately $T_{a,in}=28^{\circ}\text{C}$, $RH_{a,in} = 45\%$ and $\omega_{a,in}=0.0106 \text{ kg}_w/\text{kg}_a$.

The following are the key observations:

- Deluge cooling data points lie in quadrant 3 (i.e. zone of least efficient water usage and low CER to $PR_{\Delta Pa}$ ratio due to high air side pressure drop resulting due to bridging between fins.
- Spray cooling data points lie in quadrant 4, and are slightly higher than deluge cooling points (i.e. a shift towards Quad 2).
- Maximum CER to $PR_{\Delta Pa}$ ratio was observed at low air-velocities. This could lead to low fan energy consumption.
- Hydrophilic coating helps enhance wet case HX performance, especially for spray cooling cases
- Internal spray cooling offers the best combination of high CER to $PR_{\Delta Pa}$ ratio at high spray efficiency and lies partly within Quadrant 2 which is the target evaporative cooler performance zone.
- Maximum CER to $PR_{\Delta Pa}$ ratio for evaporative cooling achieved at lowest air flow rates

Another parameter is the Water Utilization Index (WUI) or the ratio of experimentally measured evaporation rate, $M_{evap,expt}$, to the amount of evaporation that contributes to useful latent heat transfer enhancement, $M_{evap,lat}$ and is defined in Equation 7.1.

$$Water\ utilization\ Index = \frac{M_{evap,expt}\ \text{obtained experimentally}}{M_{evap}\ \text{contributing to evaporative capacity enhancement}} \quad (7.1)$$

Table 7.2 presents evaporation rate and its contribution to HX capacity enhancement for deluge, front spray and internal jet spray cooling at 2.5 m/s air velocity, $T_{a,in} = 28 \pm 0.5^\circ\text{C}$, and $T_{a,RH} = 45 \pm 2\%$ or $\omega_{a,in} = 0.0106 \pm 0.0067\ \text{kg}_w/\text{kg}_a$.

Table 7.2: Evaporation rate and its contribution to HX capacity enhancement for deluge, front spray and internal jet spray cooling at 2.5 m/s air velocity, at approximately $T_{a,in}=28^{\circ}\text{C}$, $\text{RH}_{a,in} = 45\%$ and $\omega_{a,in}= 0.0106 \text{ kg}_w/\text{kg}_a$.

Parameter	$\dot{M}_{\text{evap,total}}$	\dot{Q}_{tot}	$\dot{Q}_{\text{tot}} - \dot{Q}_{\text{ww, sens}}$	\dot{Q}_{dry}	\dot{Q}_{evap}	$\dot{M}_{\text{evap, lat}}$	WUI
Unit	g/s	kW	kW	kW	kW	(g/s)	(-)
Front spray 3.8 g/s	1.41	9.9	9.9	6.6	3.3	1.46	1
Front spray 8.0 g/s	1.64	10.2	10.2	6.6	3.6	1.59	1
Deluge 15 g/s	1.27	9.4	9.4	6.6	2.7	1.23	1
Deluge 80 g/s	4	14.5	13.6	6.6	7.0	3.12	0.78
Deluge 166 g/s	5.5	16.9	16.0	6.6	9.4	4.17	0.76
Internal spray 3.8 g/s	2.6	10.9	10.9	6.6	4.3	1.9	0.73

It was observed that increasing wetting water flow rate alone was not sufficient to enhance the evaporation rate and therefore the HX capacity. For example in deluge cooling at 166 g/s (highest wetting water flow rate tested) and HX frontal air velocity of 2.5 m/s, approximately 16.9 kW cooling capacity was obtained. The corresponding baseline (dry case) value for 2.5 m/s air velocity was 6.58 kW. The additional 10.32 kW capacity was due to evaporative cooling and sensible cooling of deluge water. The sensible cooling was measured as difference between the inlet and outlet deluge water temperature, and found to be 0.9 kW. Therefore, 9.42 kW capacity comes due to evaporation of water on airside of HX tubes. Using the latent heat of water, this would require at least 4.17 g/s of deluge water to evaporate. However, the evaporation rate measured was approximately 5.5 ± 0.43 g/s. Thus approximately 31% of deluge water ended up not contributing to useful evaporative cooling enhancement.

Internal spray cooling offers high CER and $\text{PR}_{\Delta p_a} = 1$, while wetting the HX uniformly at

a lower wetting water flow rate. However, internal spray cooling WUI was found similar to that of deluge cooling as it consisted of spray jets that form a thicker film on HX fin surface area. The next generation of internal spray cooling technology would incorporate spray nozzles installed within HX volume which would further enhance HX CER and WUI of internal spray cooling. Results obtained for front, deluge and internal jet spray cooling, are further indicator of potential benefits of internal spray cooling.

7.5 Summary

A study was conducted to improve air-side visualization for compact HXs with wavy fin pattern and 6 tube bank HX. A novel visualization method was proposed and implemented, which consisted of borescope assisted flow mapping of deluge and front spray cooling as a function of air velocities and wetting water flow rates. In addition a quantitative method to support visualization results was also implemented for which a partitioned tray was utilized to separately record mass flow rate of wetting water flowing at HX bottom outlet.

- Visualization provided useful insight into how the HX capacities enhance because of % fin area wetted.
 - Wetted area was found to increase both with increase in air velocity and wetting water flow rate for deluge cooling.
 - For deluge cooling it was found that a maximum 83% wetted fin area at 166 g/s deluge flow rate and 2.5 m/s air velocity.
 - At 2 m/s air velocity, deluge cooling wetted approximately 33%, 59% and 66% of HX volume at 15 g/s, 80g/s and 166 g/s deluge flow rate, respectively. Thus increasing deluge flow rate beyond 80 g/s doesn't help increase wetted area significantly.

- At deluge flow rate 80 g/s increasing air velocity beyond 2.5 m/s did not increase wetted area.
- Wetted area did not increase significantly with increasing air velocity for front spray cooling and internal jet spray cooling
- A conclusive proof that up to 85% of HX volume remained dry when front spray cooling was applied to HX was also obtained.
- It was also observed that increasing the spray rate or number of nozzles would not address the issue since tight fin spacing and wavy fin geometry acts as droplet arrestor and prevents wetting in HX depth. Thus, the hottest section of HX remains completely dry for front spray cooling.
- Wetting the HX uniformly was found to be a critical parameter to enhance CER, and having a thin film of wetting water helps maximize the CER to $PR_{\Delta Pa}$ ratio. However, the evaporation rate is the index of latent evaporative cooling benefit. Furthermore, due to cost of wetting water its most efficient utilization is indicated by water utilization index that was found to be approximately 0.97 to 1 for front spray cooling, 0.75 to 0.96 for deluge cooling, and 0.7 for internal spray cooling. Thus, the mode of application affects this parameter significantly. It is interesting to observe that although WUI is lower for internal jet spray cooling compared to deluge cooling, internal cooling requires much less amount of initial water, offers potential for eliminating recirculation system, does not have any droplet carryover, and maintains $PR_{\Delta Pa} = 1$. With the application of spray nozzles to internal spray cooling WUI and evaporation rate is expected to increase as droplet surface area to volume ratio would increase.

Chapter 8 Conclusions

In this Dissertation, the thermo-hydraulic performance of herringbone wavy fin RTHXs was investigated, focusing on hybrid wet/dry operation under conventional and proposed evaporative cooling approaches. Wetting water distribution and flow through the HX volume was studied to understand their impact on HX capacity enhancement ratio, air-side pressure drop penalty ratio, water utilization index, and spray efficiency. The main findings of the Dissertation are summarized in this Chapter.

8.1 Dry case HX performance

- Dry case performance of three wavy-fin HXs was experimentally measured in the designed test facility. The effect of fin spacing and hydrophilic coating was investigated at HX frontal air velocity varying from 1.5 m/s to 3.0 m/s.
- **Effect of hydrophilic coating**
 - Hydrophilic coating reduced wavy fin HX dry case capacity and ΔP_a by up to 8%, however this was within experimental uncertainty.
- **Effect of increasing fin spacing**
 - Increasing F_p from 2.4 mm to 3.0 mm, reduced wavy fin HX capacity by approximately 14 to 21% and ΔP_a by up to 39 to 44% , but there was a 21% reduction in fin area due to increased fin spacing. Therefore, per unit air-side heat transfer area capacity would be similar. However, compact heat exchangers may be desirable for best airside performance in dry conditions under which HX may run for a major part of the year if the coil would be utilized as a hybrid wet-dry HX. It therefore is difficult to recommend one coil over the other as it may be application dependent.

- **Effect of HX inclination angle**

- Less than $\pm 7\%$ difference in HX capacity with change in HX angle from 0° to 40° .
 - Up to 7% capacity reduction for 21° angle compared to 0° angle with vertical
 - Up to 4% capacity increase for 40° angle compared to 0° angle with vertical
- Air-side pressure drop reduces by 7% when HX angle increased from 0° to 21° , but no further change in air-side pressure drop when HX angle further increased from 21° to 40° .
- Increasing HX angle of inclination greater than 40° did not significantly affect improvement in heat transfer rates and no further benefit could be obtained through air-side pressure drop reduction.
- The experimental measurements summarized in this Chapter serve as baseline performance data for wet case capacity enhancement measurements.

8.2 Deluge evaporative cooling

- Capacity enhancements due to deluge cooling were accompanied by significant increase in air-side pressure drops with maximum capacity enhancement ratio (CER) of 2.78 obtained for hydrophilic coated HX at $PR_{\Delta P_a}$ of up to 2.28. Furthermore, at a given ΔP_a values, hydrophilic coated HX achieved higher capacity compared to uncoated coil at approximately half the deluge flow rates for same fin spacing, thereby offering substantial potential for wetting water savings.

- Hydrophilic coated fins offer lower contact angles compared to uncoated coil, which spreads water film over larger area, increases wetting and evaporative cooling enhancement and reduces ΔP_a .
- Also, it was found that compared to the coil with Fp 3.0 mm, heat transfer was enhanced by 2 to 30% when deluge cooling was applied to HX with Fp 2.4 mm and ΔP_a increased by 33 to 58%.
- It was found that deluge cooling cannot provide CER higher than 2 without a significant increase in ΔP_a . Therefore, deluge cooling may not a method of choice when applying evaporative cooling to finned coils and when fan energy consumption is critical performance parameter.
- In addition deluge cooling also utilizes high amount of wetting water and is greatly affected by distribution of wetting water within the coil volume which makes the distributor design and placement on HX coil challenging.
- Water bridging between the fin occurs for all HXs tested (i.e. with Fp = 2.4 mm and Fp= 3.0 mm). This is confirmed based on test data and a novel qualitative visualization method developed as part of this Dissertation.
- Therefore, it is recommended that either much larger fin spacing or a HX with bare tubes should be used when deluge cooling is applied to HX cooler or condenser coils.

8.3 Front spray evaporative cooling

- **Even a small amount of wetting water (3.8 g/s) was enough to produce 48% capacity enhancement**, while 80 g/s wetting water produced 62% enhancement for uncoated coil (Fp 2.4 mm) in similar conditions. **Thus spray cooling was found to be better both in terms of wetting water and fan energy consumption.**

- At $T_a=28^\circ\text{C}$ CER per unit m_{ww} and $\text{PR}_{\Delta P}$ reduced from 13.9 to 48.5% when HX is sprayed from top instead of from the front due to unevaporated spray droplets downstream of HX. However, no droplets were observed at $T_a=37^\circ\text{C}$ CER and CER improvement for top sprayed coil was 48 to 83% higher than that obtained with front sprayed coil.
- **Wetting water droplet carryover observed for top sprayed coil tests when $T_a=28^\circ\text{C}$ but no carryover was observed for $T_a=37^\circ\text{C}$.** This was due to much higher evaporation potential for latter case and could be confirmed using experimentally observed evaporation rates.
- Even with highest CER/ $\text{PR}_{\Delta P}$, **top spray cooling may not be suitable spray cooling technology due to potential for carryover which could damage fan blades downstream of air.**
- **Higher enhancement ratios were obtained for lowest air-velocities** which could be due to droplet carryover at very high air velocities. Due to tortuous and compact wavy-fin structure wetting water could not be observed downstream of HX for front spray configuration, but based on experimental data rapid fall in CER was observed for $V_a > 2.5$ m/s. Thus at higher air velocity air side heat transfer coefficient takes dominates overall heat transfer rate.

8.4 Internal jet spray cooling

- A novel HX wetting spray cooling method was proposed with potential patenting and commercialization opportunity. The complete development process supported with experimental data was also described and as result of this effort a provisional patent (Prov. Patent # 61/782,825) was issued by the office of technological

commercialization at University of Maryland, College Park. Evaporative cooling performance enhancement potential of the novel method was experimentally investigated and compared to conventional spraying technologies such as front and top spray cooling and deluge cooling.

- Compared to front spray cooling intermittent internal spraying with 5 spray tubes could achieve up to 25%, 20%, and 35% higher capacity at approximately 2.5 g/s, 3.8 g/s and 8 g/s spray rates.
- Also, compared to deluge cooling, internal spray cooling could achieve same cooling capacity at approximately three times lower air-side pressure drop. Alternatively, at $PR_{\Delta Pa} = 1$ for a given air-velocity, wetting water savings of up to 68%-96.75% could be obtained.
- Critical parameters affecting HX performance during internal intermittent spray evaporative cooling are:
 - Cycle time (ON/OFF duration)
 - Flow rate during ON time
 - Number of spray tubes
 - Location of spray tubes (especially critical for inclined HXs)
 - The spray tubes should be placed within the top section of deeper tube banks which allows for water to distribute well as it falls under gravity
 - No insert must be placed within the last bank as it would lead a portion of spray droplets leaving HX volume and being carried downstream of air stream, unless spray direction is within HX volume only (unlike

spray tubes utilized for the current study which sprayed in a 360° direction).

- Due to inclination of HX it would be necessary to add one spray tubes towards the lower section of the penultimate tube bank. This would ensure uniform wetting of HX volume.
- Internal spraying combines advantages of conventional technologies and overcomes the drawbacks, by getting CEF approx. 3.8 without droplet carryover and increase in ΔPa while getting best wetting uniformity in HX depth
- The flexibility of novel spray cooling method developed could offer substantial further improvement opportunities. For example targeted cooling could be provided within deeper parts of HX volume without the problem of droplet carryover. This technology is not only retrofit but also overcomes several challenges faced by conventional evaporative cooling technologies. Intermittent cooling combined with internal spray cooling reduces wetting water consumption as evaporative cooling sustains though the brief period when spray is turned off. Moreover, it opens up future research area for obtaining best cycle times and flow rates.

8.5 Enhanced air-side visualization

- A novel visualization method was proposed and implemented, which consisted of borescope assisted flow mapping of deluge and front spray cooling as a function of air velocities and wetting water flow rates. In addition a quantitative method to support visualization results was also implemented for which a partitioned tray was utilized to separately record mass flow rate of wetting water flowing at HX bottom outlet.

- Visualization provided useful insight into how the HX capacities enhance because of % fin area wetted.
 - Wetted area was found to increase both with increase in air velocity and wetting water flow rate for deluge cooling.
 - For deluge cooling it was found that a maximum 83% wetted fin area at 166 g/s deluge flow rate and 2.5 m/s air velocity.
 - At 2 m/s air velocity, deluge cooling wetted approximately 33%, 59% and 66% of HX volume at 15 g/s, 80g/s and 166 g/s deluge flow rate, respectively. Thus increasing deluge flow rate beyond 80 g/s doesn't help increase wetted area significantly.
 - At deluge flow rate 80 g/s increasing air velocity beyond 2.5 m/s did not increase wetted area.
 - Wetted area did not increase significantly with increasing air velocity for front spray cooling below 3.8 g/s and for all cases internal jet spray cooling
 - A conclusive proof that up to 85% of HX volume remained dry when front spray cooling was applied to HX was also obtained.
 - It was also observed that increasing the spray rate or number of nozzles would not address the issue since tight fin spacing and wavy fin geometry acts as droplet arrestor and prevents wetting in HX depth. Thus, the hottest section of HX remains completely dry for front spray cooling.
- Wetting the HX uniformly was found to be a critical parameter to enhance CER, and having a thin film of wetting water helps maximize the CER to $PR_{\Delta Pa}$ ratio. However, the evaporation rate is the index of latent evaporative cooling benefit.

Furthermore, due to cost of wetting water its most efficient utilization is indicated by water utilization index that was found to be approximately 0.97 to 1 for front spray cooling, 0.75 to 0.96 for deluge cooling, and 0.7 for internal spray cooling. Thus, the mode of application affects this parameter significantly. It is interesting to observe that although WUI is lower for internal jet spray cooling compared to deluge cooling, internal cooling requires much less amount of initial water, offers potential for eliminating recirculation system, does not have any droplet carryover, and maintains $PR_{\Delta Pa} = 1$. With the application of spray nozzles to internal spray cooling WUI and evaporation rate is expected to increase as droplet surface area to volume ratio would increase.

Chapter 9 Major contributions and future work

9.1 Major contributions

The thermo-hydraulic performance of RTHX with herringbone wavy fins utilized as hybrid wet/dry HX were tested using different evaporative cooling methods. The following were the key research contributions of the work presented in this Dissertation:

1. Comprehensive literature review

- Comprehensive and most up to date summary of published literature on the experimental studies on evaporative cooling of finned HX coils utilized as condensers or fluid coolers.
- Summarized the range of technologies, operating parameters, technological limitations of spray and deluge evaporative cooling, and need for hybrid wet/dry systems

2. Experimental dataset (300+data points)

- Quantified the effect of hydrophilic coating, fin spacing, air velocity, wet flow rate, spray orientation on evaporative cooled wavy fin heat exchanger performance
- The range and number of parameters tested for different evaporative cooling methods is first comprehensive test data contribution for wavy-fin HXs utilized as coolers

3. Develop and test novel wetting water distribution methods

- Developed and experimentally tested a novel method of spray cooling: Internal intermittent spray cooling, As a result of the effort a provisional patent # 61/782,825) was issued by the office of technological commercialization at university of Maryland, College Park.

- Quantified the benefits of internal jet spray cooling compared to conventional wetting water distribution technologies utilized to evaporatively cool the HX cooler, in a retrofit proof of concept design.
- Further proposed intermittent internal jet spray cooling as a method of reducing wetting water spray rates, which helps form thin film on HX fins and enhances evaporation rates
- Established new performance parameters to understand and compare evaporative cooling technologies

4. Improved understanding of wetting water flow mechanisms and distribution in HX volume

- Enhanced air-side visualization approach to both quantitatively and qualitatively study HX air-side wetting water flow profile and understand wetting mechanisms for different wetting water distribution approaches as a function of HX air velocity and wetting water flow rate was developed and implemented.
- This is the first such a study in the published literature which makes an attempt to correlate HX cooler wetted fin area with HX capacity and air side pressure drop through direct visualization.
- Helped establish wetted fin area, method of wetting water distribution, film thickness, and wetting water droplet area to volume ratio as most important factors affecting evaporatively cooled HX performance.

9.2 List of Publications

Journal

1. Popli, S., Hwang, Y and Radermacher, R., Deluge evaporative cooling performance of wavy fin and tube inclined heat exchangers, ASHRAE Transactions, Vol. 121, Pt 1, 2014.
2. Freiherr, M., Popli, S., Hwang, Y., Radermacher, R., Summerer, F., and Cibis, D., Design, construction and shake-down of an experimental setup for performance testing of wetted heat exchanger cores, Ki Kälte Luft Klimatechnik, 04, 2012.
3. Effect of spray configuration on evaporative cooling performance of wavy-fin heat exchangers- Applied Energy/IJR (Planned)
4. Deluge and spray cooling of hydrophilic coated coils - Applied Energy/IJR (Planned)
5. Review of condenser cooling technologies: Experimental and Modelling studies- IJR (Planned).

Provisional patent (61/782,825)

1. Popli, S., Hwang, Y., Radermacher, Leighton, D., Eisele, M. Direct evaporative cooled heat exchanger wetting water distribution enhancement, (May 2013, second extension May 2014).

Peer-reviewed conference papers

1. Popli, S., Hwang, Y and Radermacher, R., Performance enhancement of herringbone wavy-fin round tube inclined heat exchangers with and without hydrophilic coating using spray and deluge cooling, In Proceedings of ASME 2013 International Mechanical Engineering Congress and Exposition, San Diego, CA, November 15-21, 2013.

2. Popli, S., Hwang, Y and Radermacher, R., Experimental investigation of flat tube-louver fin heat exchanger performance working as a condenser in dry and wet condition, ASME 2012 International Mechanical Engineering Congress and Exposition, Houston, Texas, November 9-15, 2012.
3. Popli, S., Hwang, Y and Radermacher, R., Enhancement of round tube heat exchanger performance using deluge water cooling, 14th International Refrigeration and Air Conditioning Conference, West Lafayette, Indiana, July 16-19, 2012.

9.3 Future work

The work presented in this Dissertation quantified the capacity enhancement of HX coolers using conventional and novel evaporative cooling schemes. It also provided a novel methodology of observing and quantifying HX wetted fin area, which helped improve the understanding of wetting mechanisms under different wetting water distribution methods.

However this work lays the foundation for the following future research topics:

- **Porous/wicking fins or porous coatings on HX fins**

One idea to test could involve a HX with porous or wicking fins, or metal fins coated with porous material. HX could then be placed in a pool of water and fin structure would wick the water into the HX fins from where it could be evaporated into the air stream. If the HX fins are porous coatings then spray cooling may be required and could be combined with internal jet spray cooling. The purpose of such coatings would be to create extremely hydrophilic surfaces which would allow a thin film formation which is most beneficial for evaporative cooling

enhancement. Furthermore coating helps reduce fouling by up to 50% compared to uncoated coils [Kukulka and Leising, 2009].

- **Internal spray nozzle assisted cooling**

Second generation of internal spray cooling technology would involve testing a HX with spray nozzles inserted within HX volume. This was not possible for the first generation prototype as current HXs had an access hole size which was limited by tube diameter (12 mm) and increasing this hole size was not possible without damaging the fins. If a HX could be assembled with up to 3 larger size holes (approximately 1 inch in diameter) for HX volume similar to those tested in this Dissertation, then spray tubes with nozzles mounted on them could be inserted into the HX. This would be helpful in increasing the spray water droplet area to volume ratio and lead to thinner film formation on fin surface which in turn would lead to higher evaporation rates and CER values closer to theoretical maximum.

- **Internal intermittent spray cooling tests**

One of the observation for wet case testing was that wetting water film takes time to drainage or flow through the HX length. Also in order to keep the HX wetted a certain minimum flow rate of wetting water is required. But intermittent cooling offered a solution where for the time the film drains through the HX, the spray could be switched off. While initial internal intermittent spray testing revealed that average spray rates could be reduced by cycling the wetting water spray time, further work could reveal optimum cycle times and further reduction of spray rates. While conducting such testes process fluid outlet temperature and evaporation rates

must be monitored for fluctuations which is usually a symptom of HX fin area dryout due to longer off time.

- **Testing evaporatively cooled condenser in a heat pump loop**

Testing of evaporatively cooled condenser of a heat pump cycle would allow quantification of system level benefits and compressor electric power savings.

- **Simulation studies for wet case capacity prediction**

The present study contributed to the knowledge of flow profiles obtained for evaporative cooling methods, and proposed and implemented a novel method for quantifying the wetted fin area. This work could be utilized for development of a segmented model with capability of dry and wet zone capacity prediction. This model could then be incorporated as an additional feature for CEEE's software package CoilDesigner.

- **Enhanced visualization through neutron imaging**

One of the drawbacks of the wetted fin area profiles obtained through the novel method discussed in this study was that a 3D profile could not be obtained, i.e. both front spray and deluge cooling had non uniformity of water distribution along HX length. The wetted area profile may therefore look parabolic and neutron imaging could be an option to address this issue.

Appendix 1- Internal jet spray cooling 2-spray tubes

Test summary for internal intermittent jet spray cooled hydrophilic coated wavy fin RTHX with $F_p=2.4$ mm at approximately $T_{a,in}=28^\circ\text{C}$, $RH_{a,in}$ 45% and $\omega_{a,in}=0.0106$ using 2 spray tubes at various combinations of cycle times is presented in Tables A1.1 and continuous internal jet spray performance summarized in Table A1.2.

Table A1.1: Test summary for internal intermittent jet spray cooled hydrophilic coated wavy fin RTHX with $F_p=2.4$ mm at approximately $T_{a,in}=28^\circ\text{C}$, $RH_{a,in}$ 45% and $\omega_{a,in}=0.0106$ using 2 spray tubes.

Spray rate (g/s)	0.5	1	2	0.67	1	1	1	1	2	2	2	2
On time (s)	2	2	2	1	1	1	1	1	1	1	1	1
Off time (s)	58	28	13	14	9	9	9	9	4	4	4	4
Test Case	Hot water parameters											
Flow Rate (l/s)	0.35	0.35	0.35	0.35	0.35	0.35	0.35	0.35	0.35	0.35	0.35	0.35
Inlet Temperature ($^\circ\text{C}$)	43.2	43.0	43.1	43.2	43.1	43.0	43.0	43.1	43.1	43.1	43.1	43.1
Outlet Temperature ($^\circ\text{C}$)	39.1	38.7	38.5	37.6	38.2	37.4	37.2	36.7	38.1	37.0	37.0	36.5
Capacity (kW)	5.9	6.2	6.3	8.0	7.08	8.2	8.5	9.3	7.2	8.9	8.8	9.6
	Air-side parameters											
Velocity (m/s)	1.5	1.5	1.5	1.5	1.5	2.0	2.5	3.0	1.5	2.0	2.5	3.0
Inlet Temperature ($^\circ\text{C}$)	28.0	28.0	27.9	28.0	28.0	28.0	28.1	28.0	28.1	28.0	28.1	28.0
Outlet Temperature ($^\circ\text{C}$)	35.8	35.7	35.7	36.5	36.9	36.3	35.7	35.2	36.8	35.9	35.6	35.1
Inlet RH (%)	43.9	43.9	43.9	43.3	43.0	43.7	43.1	42.5	43.1	44.6	43.2	42.6
Outlet RH (%)	34.2	35.1	36.2	36	33.2	33.3	32.4	32.2	34.1	36.2	33.1	32.9
HX Air-Side ΔP (Pa)	16.9	17.0	17.1	39.6	24.7	42	56.9	78	24.8	41	57.2	76.4

Table A1.1: Test summary for internal intermittent jet spray cooled hydrophilic coated wavy fin RTHX with $F_p=2.4$ mm at approximately $T_{a,in}=28^\circ\text{C}$, $RH_{a,in}$ 45% and $\omega_{a,in}=0.0106$ using 2 spray tubes (contd.).

Spray rate (g/s)	1.67	2	2	2	2	1	1	3	3	2	2
On time (s)	5	3	3	3	3	2	2	1	1	1	1
Off time (s)	25	12	12	12	12	18	18	9	9	14	14
	Hot water parameters										
Flow rate (l/s)	0.35	0.35	0.35	0.35	0.35	0.35	0.35	0.35	0.35	0.35	0.35
Inlet temperature ($^\circ\text{C}$)	43.1	43.2	43.0	43.1	43.1	43.1	43.0	43.1	43.1	43.1	43.1
Outlet temperature ($^\circ\text{C}$)	37.3	38.1	37.1	37.1	36.6	37.3	37.2	36.9	36.9	37.1	37.0
Capacity (kW)	8.5	7.4	8.7	8.7	9.4	8.4	8.4	8.8	9.1	8.7	8.8
	Air-side parameters										
Velocity (m/s)	2	1.5	2.0	2.5	3.0	2	2.5	1.5	2	1.5	2
Inlet temperature ($^\circ\text{C}$)	28	28.1	28.0	28.0	28.0	28.0	28.0	27.9	27.9	28.0	28.0
Outlet temperature ($^\circ\text{C}$)	35.9	36.8	35.9	35.6	35.15	36.1	35.7	35.8	35.6	35.9	35.7
Inlet RH (%)	44.6	43.5	43.5	43.2	42.7	43.5	42.7	43.5	42.9	43.5	42.9
Outlet RH (%)	36.2	34.7	35.3	32.7	32.6	33.8	32.2	41.7	36.8	40.7	35.6
HX air-side ΔP (Pa)	41.5	24.7	40.9	57.2	76.4	40.5	56.8	25.8	41.3	25.6	40.9

Table A1.1: Test summary for internal intermittent jet spray cooled hydrophilic coated wavy fin RTHX with $F_p=2.4$ mm at approximately $T_{a,in}=28^\circ\text{C}$, $RH_{a,in}$ 45% and $\omega_{a,in}= 0.0106$ using 2 spray tubes (contd.).

Spray rate (g/s)	3	3	3	3	2	2	2	2
On time (s)	1	1	1	1	1	1	1	1
Off time (s)	9	9	9	9	14	14	14	14
	Hot water parameters							
Flow rate (l/s)	0.35	0.35	0.35	0.35	0.35	0.35	0.35	0.35
Inlet temperature ($^\circ\text{C}$)	43.1	43.1	43.1	43.1	43.2	43.1	43.1	43.1
Outlet temperature ($^\circ\text{C}$)	37.3	36.9	36.1	36.0	37.6	37.0	36.3	36.3
Capacity (kW)	8.4	9.1	10.1	10.3	8.1	8.8	9.9	9.9
	Air-side parameters							
Velocity (m/s)	1.5	2	2.5	3.0	1.5	2	2.5	3.0
Inlet temperature ($^\circ\text{C}$)	27.8	27.9	27.9	27.9	27.9	28.0	27.9	27.9
Outlet temperature ($^\circ\text{C}$)	36.0	35.6	34.7	34.4	36.2	35.7	34.8	34.6
Inlet RH (%)	43.1	42.9	42.4	42.4	43.1	42.9	42.4	42.8
Outlet RH (%)	39.1	36.8	37.4	36.0	37.8	35.6	37.0	35.0
HX air-side ΔP (Pa)	24.76	41.34	59.39	79.1	24.71	40.93	59.18	78.5

Table A1.2: Test summary for internal continuous jet spray cooled hydrophilic coated wavy fin RTHX with $F_p=2.4$ mm at approximately $T_{a,in}=28^\circ\text{C}$, $RH_{a,in}$ 45% and $\omega_{a,in}=0.0106$ using 2 spray tubes.

Spray rate (g/s)	10	10	10	10	30	30	30	30
	Hot water parameters							
Flow rate (l/s)	0.35	0.35	0.35	0.35	0.35	0.35	0.35	0.35
Inlet temperature ($^\circ\text{C}$)	43.1	43.0	43.1	43.1	43.1	43.1	43.1	43.1
Outlet temperature ($^\circ\text{C}$)	38.0	37.4	36.8	36.5	36.8	36.0	35.8	35.5
Capacity (kW)	7.4	8.2	9.1	9.6	9.1	10.2	10.6	11.0
	Air-side parameters							
Velocity (m/s)	1.5	2	2.5	3.0	1.5	2	2.5	3.0
Inlet temperature ($^\circ\text{C}$)	28.0	28.1	28.0	28.0	27.9	27.9	27.9	27.9
Outlet temperature ($^\circ\text{C}$)	36.7	36.2	35.4	35.1	35.5	35.1	34.5	34.0
Inlet RH (%)	43.1	43.6	43.3	42.2	44.0	43.2	42.2	42.3
Outlet RH (%)	34.6	33.8	34.0	33.0	42.1	39.9	38.4	37.8
HX air-side ΔP (Pa)	25.3	41.6	57.8	76.9	25.5	44.2	61.1	81.9

Appendix 2- Internal jet spray cooling 5-spray tubes

Test summary for internal continuous jet spray cooled hydrophilic coated wavy fin RTHX with $F_p=2.4$ mm at approximately $T_{a,in}=28^\circ\text{C}$, $RH_{a,in}$ 45% and $\omega_{a,in}=0.0106$ using 5 spray tubes at various combinations of cycle times is presented in Tables A2.1 and internal intermittent jet spray performance summarized in Table A2.2.

Table A2.1: Test summary for internal continuous jet spray cooled hydrophilic coated wavy fin RTHX with $F_p=2.4$ mm approximately $T_{a,in}=28^\circ\text{C}$, $RH_{a,in}$ 45% and $\omega_{a,in}=0.0106$ using 5 spray tubes.

Spray rate (g/s)	30	30	30	30	80	80	80
	Hot water parameters						
Flow rate (l/s)	0.35	0.35	0.35	0.35	0.35	0.35	0.35
Inlet temperature ($^\circ\text{C}$)	43.14	43.11	43.09	43.13	42.8	43.1	43.0
Outlet temperature ($^\circ\text{C}$)	36.16	35.55	35.02	34.3	33.9	32.9	32.5
Capacity (kW)	10.13	10.94	11.69	12.75	12.8	14.8	15.3
	Air-side parameters						
Velocity (m/s)	1.5	2	2.5	3.0	1.5	2.5	3.0
Inlet temperature ($^\circ\text{C}$)	27.86	27.9	27.9	27.9	27.9	27.8	27.7
Outlet temperature ($^\circ\text{C}$)	34.37	33.7	32.8	32.4	33.2	31.0	30.3
Inlet RH (%)	43.19	43.4	43.6	44.0	42.8	45.0	50.3
Outlet RH (%)	47.62	46.5	46.5	46.3	58.5	61.6	62.7
HX air-side ΔP (Pa)	26.37	42.83	64.11	83.7	32.7	76.2	94.0

Table A2.2: Test summary for internal intermittent jet spray cooled hydrophilic coated wavy fin RTHX with $F_p=2.4$ mm at approximately $T_{a,in}=28^\circ\text{C}$, $RH_{a,in}$ 45% and $\omega_{a,in}=0.0106$ using 5 spray tubes.

Spray rate (g/s)	3.7	3.7	3.7	3.7	2.5	2.5	2.5	2.5
On time (s)	1	1	1	1	1	1	1	1
Off time (s)	9	9	9	9	14	14	14	14
	Hot water parameters							
Flow rate (l/s)	0.35	0.35	0.35	0.35	0.35	0.35	0.35	0.35
Inlet temperature ($^\circ\text{C}$)	43.0	43.1	43.1	43.1	43.1	43.1	43.1	43.0
Outlet temperature ($^\circ\text{C}$)	36.5	35.9	35.6	35.2	36.8	36.2	35.7	35.4
Capacity (kW)	9.5	10.6	10.9	11.5	9.1	10.1	10.7	11.1
	Air-side parameters							
Velocity (m/s)	1.5	2.0	2.5	3.0	1.5	2.0	2.5	3.0
Inlet temperature ($^\circ\text{C}$)	27.9	27.9	27.9	27.8	27.9	27.9	27.9	27.8
Outlet temperature ($^\circ\text{C}$)	34.8	34.1	33.6	33.0	35.0	34.4	33.8	33.3
Inlet RH (%)	43.0	43.6	45.4	42.9	43.0	43.0	42.1	42.2
Outlet RH (%)	47.0	44.5	44.7	42.9	44.8	42.5	41.1	40.7
HX air-side ΔP (Pa)	26.7	43.9	60.3	78.7	26.4	43.7	61.3	79.6

Table A2.2: Test summary for internal intermittent jet spray cooled hydrophilic coated wavy fin RTHX with $F_p=2.4$ mm at approximately $T_{a,in}=28^\circ\text{C}$, $RH_{a,in}$ 45% and $\omega_{a,in}=0.0106$ using 5 spray tubes (contd.).

Spray rate (g/s)	13	13	13	13	7	7	5	5
On time (s)	1	1	1	1	1	1	1	1
Off time (s)	9	9	9	9	14	14	19	19
	Hot water parameters							
Flow rate (l/s)	0.35	0.35	0.35	0.35	0.35	0.35	0.35	0.35
Inlet temperature ($^\circ\text{C}$)	43.1	43.1	43.1	43.2	43.1	43.1	43.1	43.1
Outlet temperature ($^\circ\text{C}$)	35.5	34.9	34.6	34.3	35.8	34.8	36.2	35.1
Capacity (kW)	11.0	11.9	12.4	12.9	10.5	12.0	9.9	11.6
	Air-side parameters							
Velocity (m/s)	1.5	2.0	2.5	3.0	1.5	2.5	1.5	2.5
Inlet temperature ($^\circ\text{C}$)	27.9	27.8	27.8	27.8	27.9	27.8	27.9	27.8
Outlet temperature ($^\circ\text{C}$)	34.2	33.3	32.6	32.2	34.6	33.0	34.9	33.3
Inlet RH (%)	42.5	43.8	43.9	43.7	42.2	43.8	42.0	43.2
Outlet RH (%)	52.3	51.3	50.2	48.8	49.1	47.8	46.5	45.3
HX air-side ΔP (Pa)	26.6	42.5	61.7	81.7	26	61.3	26.3	60.2

Table A2.2: Test summary for internal intermittent jet spray cooled hydrophilic coated wavy fin RTHX with $F_p=2.4$ mm at approximately $T_{a,in}=28^\circ\text{C}$, $RH_{a,in}$ 45% and $\omega_{a,in}= 0.0106$ using 5 spray tubes (contd.).

Spray rate (g/s)	4	3	3	3	2
On time (s)	1	1	1	1	1
Off time (s)	24	29	9	9	14
	Hot water parameters				
Flow rate (l/s)	0.35	0.35	0.35	0.35	0.35
Inlet temperature ($^\circ\text{C}$)	43.0	43.1	43.1	43.1	43.1
Outlet temperature ($^\circ\text{C}$)	35.3	35.7	35.5	36.0	35.7
Capacity (kW)	11.2	10.8	10.3	10.3	10.7
	Air-side parameters				
Velocity (m/s)	2.5	2.5	1.5	1.5	1.5
Inlet temperature ($^\circ\text{C}$)	27.9	27.9	27.9	27.8	27.9
Outlet temperature ($^\circ\text{C}$)	33.7	34.0	34.5	34.4	34.8
Inlet RH (%)	44.0	44.4	42.7	43.4	42.1
Outlet RH (%)	44.0	42.4	50.3	50.6	47.7
HX air-side ΔP (Pa)	59.8	59.5	26.6	27.0	25.9

Table A2.3: Test summary for internal intermittent jet spray cooled hydrophilic coated wavy fin RTHX with $F_p=2.4$ mm at approximately $T_{a,in}=37^\circ\text{C}$, $\text{RH}_{a,in}$ 45% and $\omega_{a,in}= 0.0179$ using 5 spray tubes (contd.).

Spray rate (g/s)	3.7	3.7	3.7	3.7
On time (s)	1	1	1	1
Off time (s)	9	9	9	9
	Hot water parameters			
Flow rate (l/s)	0.35	0.35	0.35	0.35
Inlet temperature ($^\circ\text{C}$)	43.1	43.2	43.1	43.0
Outlet temperature ($^\circ\text{C}$)	38.7	38.4	38.3	38.1
Capacity (kW)	6.3	6.9	7.0	7.2
	Air-side parameters			
Velocity (m/s)	1.5	2.0	2.5	3.0
Inlet temperature ($^\circ\text{C}$)	36.8	36.9	37.0	36.9
Outlet temperature ($^\circ\text{C}$)	38.1	37.8	37.5	37.1
Inlet RH (%)	43.0	43.5	43.0	43.1
Outlet RH (%)	51.5	51.0	50.0	49.9
HX air-side ΔP (Pa)	25.5	42.1	59.6	79.0

Appendix 3 – Review of simulation/modeling studies on direct evaporative cooling of HXs

Table A3.1: Major findings of simulation/modeling studies on direct evaporative cooling of heat exchangers.

Author	Major Findings
Mizushima et al., 1967; 1968	<ul style="list-style-type: none"> • Based on experimental data; deluge cooling of bare 19.05 mm bare tubes; empirical correlations obtained • thermal design of evaporative coolers based on his correlation
Kreid et al., 1978, 1979	<ul style="list-style-type: none"> • Extended the dry case finned HX analytical model to predict heat transfer rate in deluged conditions through transformation of dry case performance variables. Good validation was found with experimentally obtained heat transfer rates expect at low inlet air humidity values when model under predicts wet case HX capacity
Leidenfrost and Korenic, 1982	<ul style="list-style-type: none"> • Experimentally and analytically shown that complete wetting ensures maximum performance of evaporative condenser with bare tubes. • Increasing spray rate to level of deluge flow rates does not increase performance, but increases air and water side pumping power, water consumption and possible droplet carry over downstream of HX • Higher fan speed/power is undesirable when using evaporative cooling • Analytical procedure Based on graphical method initially developed by Bosnjakovic
Webb,	<ul style="list-style-type: none"> • Two major ways of calculating wetted capacity • Approximate methods: <ul style="list-style-type: none"> • NTU based + correlations for wetted surface heat and mass transfer coefficients • Rigorous methods: <ul style="list-style-type: none"> • Numerical solution based
Erens and Dreyer, 1988	<ul style="list-style-type: none"> • Presented the generalized Poppe and Merkel formulations for calculating the overall HX capacity. Although no validation was given, the two methods gave similar HX capacity within 0.2%.

Table A3.1: Major findings of simulation/modeling studies on direct evaporative cooling of heat exchangers (cont'd).

Author	Major Findings
Peterson et al., 1988	<ul style="list-style-type: none"> • modified Parker and Treybals’s model to predict performance of evaporative condensers. Using their own experimental data, the authors extended Parker and Treybal’s mass transfer coefficient correlation. However high errors up to 30% compared to experimental data were reported
Dreyers, 1992	<ul style="list-style-type: none"> • modified Bourillot and Poppe and Rogeners ‘s cooling tower theory to incorporate specific terms relating to wetness fraction and heat transfer between spray water film and process fluid. Complete wetting was not assumed, instead the wetness fraction was set based on experimental observation for a vertical air flow HX with spray water in counter flow configuration. Model predictions were within 10% of experimental data but errors upto 20% were observed for higher spray rates when possible flooding or water retention was suspected in the lower part of HX.
Erens and Dreyer 1993	<ul style="list-style-type: none"> • modified Dreyer et al., 1992, analytical model for a wetted horizontal finned HX to determine heat transfer rate for a spray cooled inclined finned HX. Model prediction were found to be within 10% of their experimental data. Although not explicitly, this study is the only study in the literature which takes into account effect of HX inclination angle.
Song et al., 2003	<ul style="list-style-type: none"> • Proposed an analytical solution for a 2-D heat and mass transfer process in finned channel modelled using porous medium approach and applied to predict the capacity of wetted flat tube heat exchanger. It was found that relatively higher fin thickness of approximately 0.05 to 1mm may be required to maintain fin efficiency of 0.8 to 0.9 for wetted coils compared to when they are in dry cooling mode. <ul style="list-style-type: none"> ○ $Le = 1$ ○ Higher Fin thickness beneficial for Evaporative cooler ○ Typically hybrid coolers have fin thickness optimized for sensible air cooling mode only. Therefore fin efficiency reduces when wetting water supplied to it. author proposes fin thickness of 0.05 to 1mm for fin efficiency of 0.8 to 0.9

Table A3.1: Major findings of simulation/modeling studies on direct evaporative cooling of heat exchangers (cont'd).

Author	Major Findings
Mehrabian and Samadi, 2004	<ul style="list-style-type: none"> • Authors presented a numerical model for counter parallel and counter flow wetted HX and model prediction as validated with experimental results of Hasan and Siren 2002, within 5%. They found that increasing mass flow rate of both air and spray water increased HX effectiveness. In counter flow arrangement as spray water passes through the HX, the spray water temperature was found to increase and then decrease, while an opposite trend was observed for parallel-flow arrangement
Stabat and Marchio, 2004	<ul style="list-style-type: none"> • Authors presented an ϵ-NTU based method to predict the capacity of closed cooling tower along with evaporation rates and deluge water temperature profile through the heat exchanger. Although simplistic, the model was based on determining internal and external heat transfer coefficients through experimental or manufacturer's operating data.
Ren and Yang, 2006	<ul style="list-style-type: none"> • presented an ϵ-NTU based spray cooled HX model for both parallel and counter flow configurations which took into account effects of spray water evaporation, spray water temperature variation and spray water enthalpy change along the heat exchanger surface. They found that HX performance could be enhanced using a small spray flow rate and enhanced surface wettability especially under counter current configuration. The authors took Le number as 0.87 for standard atmospheric conditions, and no calculation to determine its exact value was presented.
Youbi, 2007	<ul style="list-style-type: none"> • Precooling the inlet air and water also hits the fins • Identified parameters for spray cooled condenser capacity: spray rate, evaporation rate and wetting area • 55% COP improvement predicted • $Le = 1$ • Numerical model • Nakayama correlation used to predict: wetted area • Chang and Wang correlation used to predict air side heat transfer correlation • Model breaks down capacity prediction: sensible air side, evaporative airside, sensible water side

Table A3.1: Major findings of simulation/modeling studies on direct evaporative cooling of heat exchangers (cont'd).

Author	Major Findings
Heyns and Kroger, 2010	<ul style="list-style-type: none"> • presented an analytical model for wetted HX similar to the Poppe and Regener method, and simplified it with two main assumptions i.e. 1) compared to total deluge flow rate, amount of water lost due to evaporation was negligible and 2) $Le = 1$. Furthermore, based on experimental results, empirical correlations for heat and mass transfer coefficients were proposed as function of air and deluge water flow rates.
Jahangeer, et al., 2011	<ul style="list-style-type: none"> • carried out numerical simulation of single bare tube evaporatively spray cooled on the air-side. Water film thickness between 0.075 to 0.15 mm was simulated and it was found that the thinnest film (0.075 mm) provided maximum wall to air overall HTC of up to 2000 W/m²K.
Papaefthimiou, et al., 2012	<ul style="list-style-type: none"> • presented a numerical model of closed-wet cooling tower with serpentine bare tubes. It was found that at wetted HX performance is optimum at low inlet air humidity ratio when both HX effectiveness and spray water evaporation rate were high. It was also found that spray water temperature did not decrease more than 2°C for spray rates up to 1.85 kg/s/27m² (246 kg/m²/hr).
Zhang et al., 2014	<ul style="list-style-type: none"> • Wet case model built on top of correlation based dry model • Heat and mass transfer analogy used to calculate evaporation rate • Evaporation rate is critical parameter here. But the uncertainty of this parameter is not reported??? • Z – wetting parameter is not correctly defined (Z=1 does not ensure complete or partial wetting, just because evap rate is high) • HX face is assumed completely wet and partial wetting assumed thereafter in HX depth • Validation data is internal report and conf paper which reports no RH value (no environmental chamber so value may not be constant)

References

- 1 AAON, 2013, URL:
http://www.aaon.com/Documents/Featured/EvapCooled_Cond_071015.pdf, last accessed on 8/4/13.
- 2 Alonso, J.F., Martinez, F.J., Gomez, E.V., Plasencia, M.A. 1998. Simulation model of an indirect evaporative cooler. *Energy and Buildings*, Vol. 29, pp. 23–27.
- 3 ASHRAE. 1987. Standard Methods for Laboratory Airflow Measurement, ANSI/ASHRAE 41.2, ASHRAE, Atlanta, GA, USA.
- 4 Averyt, K., J. Fisher, A. Huber-Lee, A. Lewis, J. Macknick, N. Madden, J. Rogers, and S. Tellinghuisen. 2011. Freshwater use by U.S. power plants: Electricity’s thirst for a precious resource. A report of the energy and Water in a Warming World initiative. Cambridge, MA: Union of Concerned Scientists.
- 5 Baltimore Aircoil Company (BAC), 2013a, URL:
<http://www.baltimoreaircoil.com/english/products/evaporative-condensers/series-v>, last accessed on 8/4/13.
- 6 Baltimore Aircoil Company (BAC), 2013b, URL:
<http://www.baltimoreaircoil.com/english/resource-library/file/647>, last accessed on 8/4/13.
- 7 Bell, I.H., E.A. Groll, and H. Konig. 2011. Experimental Analysis of the Effects of Particulate Fouling on Heat Exchanger Heat Transfer and Air-Side Pressure Drop for a Hybrid Dry Cooler. *Heat Transfer Engineering*, Vol. 32, pp. 264–271.
- 8 Bharathan, D., 2013. Hybrid Cooling for Geothermal Power Plants Final ARRA Project Report. Technical Report NREL/TP-5500-58024.
- 9 Blanco, H.P. and Bird, W.A., 1984, Study of heat and Mass transfer in a vertical tube evaporative cooler, Vol. 106, pp. 210–215.
- 10 Chang, Y.J., and C.C. Wang. 1997. A generalized heat transfer correlation for louver fin geometry. *Int. J. Heat Mass Transfer*, Vol. 40, pp. 533–544.
- 11 Chen, C.W., Yang, C.Y., and Hu, Y.T., 2013, Heat Transfer Enhancement of Spray Cooling on Flat Aluminum Tube Heat Exchanger, Vol. 34(1), pp. 29–36.

- 12 Costenaro, D.M. 2001. Cost and Performance Analysis of Evaporative Cooling Enhancement for Condensers at Empire Energy Geothermal Plant. National Renewable Energy Laboratory Report.
- 13 David, E., 1997. Evaporative condensing minimizes system power requirements. Heating Piping Air Conditioning Engineering. Vol. 69 (4), pp. 75–84.
- 14 Dreyer, A., Kriel, D.E., Erens, P.J., 1992, Analysis of Spray-Cooled Finned-Tube Heat Exchangers, Vol. 13 (4), pp. 53–71.
- 15 Dreyer, A.A. and Erens, P.J. 1990. Heat and mass transfer coefficients and pressure drop correlations for a cross-flow evaporative cooler. International Heat Transfer Conference, pp. 223–238.
- 16 Erens, P.J. and Dreyer, A.A., 1988, An improved procedure for calculating the performance of evaporative closed circuit coolers, AIChE Symposium Series, Heat Transfer, Houston, TX.
- 17 Erens, P.J. and Dreyer, A.A., 1993, Enhancement of Inclined Heat Exchangers Performance by Spray Cooling, Experimental Heat Transfer, Fluid Mechanics, and Thermodynamics, pp. 400-407.
- 18 Frick/Johnson, 2013, URL: http://www.johnsoncontrols.com/content/dam/WWW/jci/be/industrial_refrigeration/downloads/140_920_sed_xlp2.pdf, last accessed on 8/4/13.
- 19 Facao, J. and Oliveira, A.C., 2000, Thermal behaviour of closed wet cooling towers for use with chilled ceilings, Applied Thermal Engg., Vol. 20, pp.1225–1236.
- 20 Fisher, U., Leidenfrost, W., Li, J. 1983. Hybrid evaporative-condenser cooling tower. Heat transfer Engineering, Vol. 4 (2), pp. 28–41.
- 21 Fischer, O., and Sommer, A., 1988, Experimental of Spray Enhanced Surface Tube and Plate Fin Heat exchangers, 6th IAHR Cooling Tower Workshop, Pisa, Italy.
- 22 Freus, 2007, URL: <http://www.freus.com/> last accessed on 8/4/13.
- 23 Guinn, G.R. and Novell, B.J., 1981. Operating performance of a water spray on an air-type condensing unit, Ashrae Transactions, Vol. 87, pp. 373–381.
- 24 Hasoz, M. and Kilicarslan, A., 2004, Performance evaluations of refrigeration systems

- with air-cooled, water-cooled and evaporative condensers, *International Journal of Energy Research*, Vol. 28 (8), pp. 683–696.
- 25 Hasan, A., Sirén, K., 2002. Theoretical and computational analysis of closed wet cooling-towers and its applications in cooling of buildings, *Energy and Buildings*, Vol. 34.
 - 26 Hasan, A., and K. Siren. 2003. Performance investigation of plain and finned tube evaporatively cooled heat exchangers. *Applied Thermal Engineering*, Vol. 23, pp. 325–340.
 - 27 Hauser, S.G., E.J. Eschbach, R.L. Gruel, B.M. Johnson, J.C. Huenefeld, and D.K. Kreid. 1982. A progress report on experimental evaluation of dry and wet air cooled HX. US Department of Energy Report, Richland, WA, USA.
 - 28 Hauser, S.G. and D.K. Kreid. 1982. Dry-Wet performance of a plate-fin air-cooled heat exchanger with continuous corrugated fins. US Environmental Protection Agency Report, Richland, WA, USA.
 - 29 Heyns, J.A., and D.G. Kröger. 2010. Experimental investigation into the thermal-flow performance characteristics of an evaporative cooler. *Applied Thermal Engineering*, Vol. 30, pp. 492–498.
 - 30 Hisham, M., Ettouney, Hisham T. El-Dessouky, Bouhamra, W., Bader Al-Azmi, 2001, Performance of Evaporative Condensers, *Heat Transfer Engineering*, Vol. 22 (4), pp. 41–55.
 - 31 Hirasawa, S., Kuwahara, H., Nakayama, W., and Mori, Y. 1983. Optimization of mist-cooled condensers for binary cycle plants. Vol. 2, *Proceedings of ASME Conference*.
 - 32 Hong, K., and R.L. Webb. 1999. Performance of Dehumidifying Heat Exchangers with and Without Wetting Coatings. *Journal of Heat Transfer*, Vol. 121, pp. 1018–1026.
 - 33 Hosoz, M., and A. Kilicarslan. 2004. Performance evaluations of refrigeration systems with air-cooled, water-cooled and evaporative condensers. *International Journal of Energy Research*, Vol. 28, pp. 683–696.
 - 34 Hamlin, S., Hunt, R., and Tassou, S.A. 1998. Enhancing the performance of

- evaporative spray cooling in air cycle refrigeration and air conditioning technology. Vol. 18 (11), pp. 1139–1148.
- 35 Hwang, Y., Haider, S.I., Markey, B., Kopko, W., and Radermacher, R. 2000. Evaporatively-cooled condenser with rotating disks, *Journal of Enhanced Heat Transfer*, Vol. 7 (1), pp. 273–287.
 - 36 Hwang, Y., Radermacher, R., and Kopko, W. 2001. An experimental evaluation of a residential-sized evaporatively cooled condenser, *International Journal of Refrigeration*, Vol. 24, pp. 238–249.
 - 37 Jahangeer, K.A., Tay, A.A.O., and Islam, M.R., 2011. Numerical investigation of transfer coefficients of an evaporatively-cooled condenser, *Applied Thermal Engineering*, Vol. 31(10), pp. 1655–1663.
 - 38 Kim, H.Y., and Kang, B.H. 2003. Effects of hydrophilic surface treatment on evaporation heat transfer at the outside wall of horizontal tubes. *Applied Thermal Engineering*, Vol. 23, pp. 449–458.
 - 39 Kreid, D.K., H.L. Parry, L.J. MacGowan, and B.M. Johnson. 1979. Performance of a plate fin air-cooled heat exchanger with deluged water augmentation. *Proceedings of American Society of Mechanical Engineers Winter Conference*, NY, USA, December 2-7.
 - 40 Kim, H.Y. and Kang, B.H., 2003, Effects of hydrophilic surface treatment on evaporation heat transfer at the outside wall of horizontal tubes, Vol. 23 (4), pp. 449–458.
 - 41 Knebel, D.E. 1997. Evaporative Condensing Minimizes, System Power Requirements. *Heating/Piping/Air Conditioning Engineering*, Vol. 69, pp. 5–23.
 - 42 Kutscher, C. and Costenaro, D. 2002. Assessment of Evaporative Cooling Enhancement Methods for Air-Cooled Geothermal Power Plants. *Geothermal Resources Council (GRC) Annual Meeting Reno, Nevada September 22– 25, 2002*.
 - 43 Kukulka, D.J., and Leising, P. 2009. Evaluation of surface coatings on heat exchangers. *Chemical Engineering Transactions*, Vol. 18.
 - 44 Hajidavalloo, E. and Eghtedari, H. 2010. Performance improvement of air-cooled

- refrigeration system by using evaporatively cooled air condenser. *International Journal of Refrigeration*, Vol. 33 (5), pp. 982–988.
- 45 Lee, D.Y., J.W. Lee, and B.H. Kang. 2005. Experimental Study on the Hydrophilic Porous Film Coating for Evaporative Cooling Enhancement. *Journal of Air-Conditioning and Refrigeration*, Vol. 13, pp. 99–106.
 - 46 Leidenfrost, W. and B. Korenic. 1979. Analysis of Evaporative Cooling and Enhancement of Condenser Efficiency and of Coefficient of Performance. *Wärme- und Stoffübertragung* Vol. 12, pp. 5–23.
 - 47 Leidenfrost, W. and B. Korenic. 1982. Evaporative Cooling and Heat Transfer Augmentation related to reduced condenser temperatures. *Heat Transfer Engineering*, Vol. 3, pp. 38–59.
 - 48 Liu, L. 2011. Effect of Air-Side Surface Wettability on the Performance of Dehumidifying Heat Exchangers. PhD Thesis, University of Illinois at Urbana-Champaign, IL, USA.
 - 49 Ma, X., Ding, G., Zhang, Y., and Wang, K. 2007. Effects of hydrophilic coating on air side heat transfer and friction characteristics of wavy fin and tube heat exchangers under dehumidifying conditions. *Energy Conversion and Management*, Vol. 48, pp. 2525–2532.
 - 50 Masri, M. and Therkelsen, R. 2003. Spray Enhancement of Air Cooled Condensers. Report number P500-03-109 - Electric Power Research Institute.
 - 51 McQuay, 2013,
URL:http://www.mcquay.com/mcquaybiz/literature/lit_aa_rah/Brochures/ASP31-791Finallo.pdf, last accessed on 8/4/13.
 - 52 Mehrabian, M.A. and Samadi, B. 2010. Heat-transfer characteristics of wet heat exchangers in parallel-flow and counter-flow arrangements. *International Journal of Low-Carbon Technologies*. Vol. 5 (4), pp. 256–263.
 - 53 Mizushima, T., Ito, R., and Miyashita, H. 1967. Experimental study of an evaporative cooler. *International Chemical Engineering*, Vol. 7 (4), pp. 727–732.

- 54 Mori, Y., and Nakayama, W., 1980. High-Performance Mist Cooled Condensers for Geothermal Binary Cycle Plants. Japan US Heat Transfer Joint Seminars, pp. 211–218.
- 55 Nakayama, W., Kuwahara, H., and Hirasawa, S., 1988, Heat transfer from tube banks to air-water mist flow, *Intl. Jour of Heat and Mass Transfer*, Vol. 31(2), pp. 449–460.
- 56 Oshima, T., Iuchi, S., Yoshida, A., and Takamatsu, K., 1972, Design calculation method of air-cooled heat exchangers with water spray, *Heat Transfer-Japanese Research*, Vol. 1, pp. 47–55.
- 57 Papaefthimiou, V.D., Rogdakis, E.D., Koronaki, I.P., Zannis, T.C. 2012 Thermodynamic study of the effects of ambient air conditions on the thermal performance characteristics of a closed wet cooling tower, *Applied Thermal Engineering*, Vol. 33-34, pp. 199–207.
- 58 Parry, L.E., MacGowan, L.J., Kreid, D.K., Wiles, L.E., Faletti, D.W., and Johnson, B.M., 1979. Augmented dry cooling surface test program: Analysis and Experimental Results. US Department of Energy Report, Richland, WA, USA.
- 59 Peterson, J.L. 1993. An effectiveness model for indirect evaporative coolers, *ASHRAE Transactions*, Vol. 99, Part II.
- 60 Popli, S., Y. Hwang, and R. Radermacher. 2012a. Enhancement of Round Tube Heat Exchanger Performance Using Deluge Water Cooling- Paper #2331. 14th International Refrigeration and Air Conditioning Conference, West Lafayette, IN, USA, July, pp. 16–19.
- 61 Popli, S., Y. Hwang, and R. Radermacher. 2012b. Experimental Investigation of Flat Tube-Louver Fin Heat Exchanger Performance Working as a Condenser in Dry and Wet Condition, Paper #85884. ASME 2012 International Mechanical Engineering Congress and Exposition, Houston, TX, November, pp. 9–15.
- 62 Qureshi, Bilal A., Zubair, Syed M. 2006. A comprehensive design and rating study of evaporative coolers and condensers. Part I. Performance evaluation, Vol. 29(4), pp. 645–658.
- 63 Qureshi, Bilal A., Zubair, Syed M. 2006. A comprehensive design and rating study of evaporative coolers and condensers. Part II. Sensitivity analysis. *International Journal of Refrigeration*, Vol. 29 (4), pp. 645–658.

- 64 Ren, C. and Yang, H. 2006. An analytical model for the heat and mass transfer processes in indirect evaporative cooling with parallel/counter flow configurations. *International Journal of Heat and Mass Transfer* 49 (2006) 617–627.
- 65 Sarker, M., Shim, G.J., Lee, H.S., Moon, C.G., Yoon, J.I., 2009, Enhancement of cooling capacity in a hybrid closed circuit cooling tower, Vol. 29, pp. 3328–3333.
- 66 Scherberg, M.G., Wright, H.E., Elrod, W.C. 1972. Heat transfer potential of liquid-gas spray flows. *Progr. Heat Mass Transfer*, Vol. 6, pp. 739–752.
- 67 Sen, G., 1973. Heat transfer during air-water mist flow across annular finned tube banks. University of Strathclyde, PhD Thesis.
- 68 Silk, E.A., Gollhofer, E.L., and Selvam, R.P. 2008. Spray cooling heat transfer: Technology overview and assessment of future challenges for micro-gravity application. *Energy Conversion and Management*, Vol. 49 (3), pp. 453–468.
- 69 Simpson, H.C., Beggs, G.C., and Sen, G.N., 1974. Heat transfer from extended surface tubes to an air-water mist. *Symposium Series*, Vol. 38, pp. 1–22.
- 70 Simpson, H.C., Beggs, G.C., and Raouf, M., 1984. Air-water mist flow over extended surface tube banks. *First UK National Conference on heat transfer*, University of Leeds, Vol.1, pp. 745–760.
- 71 Song, C.H., Lee, D.Y., and Ro, S.T. 2003. Cooling enhancement in an air-cooled finned heat exchanger by thin water film evaporation, *International Journal of Heat and Mass Transfer*, Vol. 46(7,) pp. 1241–1249.
- 72 Spraying Systems Co., 2013 URL: <http://www.spray.com/> last accessed on 8/4/13.
- 73 SPX Technologies, URL: <http://spxcooling.com/en/coolingtowers/list/cooling/evaporative-fluid-coolers/>, last accessed on 8/4/13.
- 74 Stabat, P., and Marchio, D., 2004, Simplified model for indirect-contact evaporative cooling-tower behavior, *Applied Energy*, Volume 78, Issue 4, August 2004, pp. 433–451.
- 75 Taylor, B.N., and Kuyatt, C.E., 1994, Guidelines for Evaluating and Expressing the Uncertainty of NIST Measurement Results, National Institute of Standards and

Technology Technical Note 1297.

- 76 Tree, D.R., Goldschmidt, V.W., Garrett, R.W., and Kach, E., 1978, Effect of water sprays on heat transfer of a fin and tube heat exchanger. 6th Intl. Heat Trans Conf., Toronto.
- 77 Trela, M., 1983, Heat and mass transfer in mist flow (in Polish). Rpt. Inst. of Fluid Machinery 154/1069/83.
- 78 Vrachopoulos, M.G., A.E. Filios, G.T. Kotsiovelos, and E.D. Kravvaritis. 2007. Incorporated evaporative condenser. *Applied Thermal Engineering*, Vol. 27, pp. 823–828.
- 79 United States Environmental Protection Agency, Cooling Water Intake Structures—Clean Water Act §316(b), 2011.
- 80 Walczyk, H., 1993, Enhancement of heat transfer from air-fin coolers, *Chem Engg and Processing*, Vol. 32, pp. 131–138.
- 81 Wang, C.C., Y.M. Tsi, and D.C. Lu. 1998. A comprehensive study of convex-louver and wavy fin-and-tube heat exchangers. *AIAA J of Thermophysics and Heat Transfer*, Vol. 12, pp. 423–430.
- 82 Wang, C.C., C.J. Lee, C.T. Chang, and S.P. Lin. 1999a. Heat transfer and friction correlation for compact louvered fin and tube heat exchangers. *Int. J. Heat Mass Transfer*, Vol. 42, pp. 1945–1956.
- 83 Wang C.C., Y.T. Lin, C.J. Lee, and Y.J. Chang. 1999b. An investigation of wavy fin-and-tube heat exchangers: a contribution to databank. *Experimental Heat Transfer*, Vol.12, pp. 73–89.
- 84 Wang C.C., J.Y. Jang, and N.F. Chiou. 1999c. Effect of waffle height on the air-side performance of wavy fin-and-tube heat exchangers. *Heat Transfer Engineering*, Vol. 20, pp. 45–56.
- 85 Wang C.C., J.Y. Jang, and N.F. Chiou. 1999d. A heat transfer and friction correlation for wavy fin-and-tube heat exchangers. *Int. J Heat and Mass Transfer*, Vol. 42, pp. 1919–1924.
- 86 Wang, T., Sheng, C., and Nnanna, A.G.A. 2014, Experimental investigation of air conditioning system using evaporative cooling condenser. *Energy and Buildings*, July

2014.

- 87 Webb, R.L. 1984. A unified theoretical treatment for thermal analysis of cooling towers, evaporative condensers and fluid coolers, ASHRAE Trans. 1984, pp. 398–415.
- 88 Webb, R.L., and S.H. Jung. 1992. Air-side performance of enhanced brazed aluminum heat exchangers. ASHRAE Trans., Vol. 98, pp. 391–401.
- 89 Wiksten, R., Assad, M.E.J., 2010, Heat and mass transfer analysis of a wavy fin-and-tube heat exchanger under fully and partially wet surface conditions, International Journal of Thermal Sciences, Vol. 49, pp. 349–355.
- 90 Yang, W.J., and D.W. Clark. 1975. Spray Cooling of Air-Cooled Compact Heat Exchangers. Int. J. Heat Mass Transfer, Vol. 18, pp. 311–317.
- 91 Youbbi-Idrissi, M., Macchi-Tejeda, H., Fournaison, L, and Guilpart, J. 2007. Numerical model of sprayed air cooled condenser coupled to refrigerating system, Energy Conversion and Management, Vol. 48 (7), pp. 1943–1951.
- 92 Zalewski, W., and Gryglaszeski, P.A. 1997 Mathematical model of heat and mass transfer processes in evaporative fluid coolers, Chemical Engineering and Processing, 36, pp. 271–280.
- 93 Zalewski, W. 1993. Mathematical model of heat and mass transfer processes in evaporative condensers. Rev Int Froid, Vol. 16(1), pp. 23–30.
- 94 Zhang, F., Bock, J., Jacobi, A.M., and Wu, H., 2012. Simultaneous heat and mass transfer in a wetted heat exchanger, part I: Experiments, International Refrigeration and Air Conditioning Conference at Purdue.
- 95 Zheng, W.Y., Zhu, D.S., Song, J., Zeng, L.D., Zhou, H.J. 2012. Experimental and computational analysis of thermal performance of the oval tube closed wet cooling tower, Applied Thermal Engineering 35, pp. 233–239.

Glossary of terminology

Air-side pressure drop penalty ratio	Ratio of HX air-side pressure drop in wet conditions to that obtained in dry air-cooled conditions under similar operating parameters
Carryover	the portion of wetting water droplets carried downstream of the air to the HX air outlet stream. This may occur at very high air velocities combined with high wetting water flow rates.
Bridging	Wetting water retained between adjacent fins either due to excessive wetting water applied on HX or if the fin spacing between the HX fins is too small
Capacity enhancement ratio	Ratio of HX capacity in wet conditions to that obtained in dry air-cooled conditions under similar operating parameters
Deluge cooling	A type of evaporative cooling method where the wetting water is poured on top of the HX in such a way that it falls down in cross-flow configuration with air.
Hybrid wet/dry cooler	Typical fluid coolers operate in dry air-cooled conditions for a major portion of the year when ambient temperature is low, and are evaporatively cooled during peak summer hours
Recirculation	If a significant portion of wetting water is unevaporated it could be collected at the bottom of HX and pumped back to the wetting water inlet at the top of the HX. Recirculation is typically utilized for deluge cooling.
Spray efficiency	Ratio of amount of wetting water evaporated to amount of wetting water added onto HX for evaporative cooling
Water utilization index	the ratio of experimentally measured evaporation rate, $M_{\text{evap,expt}}$, to the amount of evaporation that contributes to useful latent heat transfer enhancement, $M_{\text{evap,lat}}$